

Genetic Regulation of Vascular Development

- Building the Zebrafish Vascular Tree -

The research described in this thesis was performed at the Hubrecht Institute of the Royal Netherlands Academy of Arts and Sciences (KNAW), within the framework of the Graduate School of Cancer Genomics and Development Biology in Utrecht, in close collaboration with the department of Experimental Cardiology of the Erasmus University Medical Center, within the framework of the COEUR graduate school in Rotterdam, The Netherlands.

Cover: “Vascular tree” compiled of several names of genes involved in vascular development.

Printed by Digital Printing Partners, Houten.

ISBN: 978-90-9025220-9

Copyright © 2010 by Robert L.J.M. Herpers. Allrights reserved. No part of this book may be reproduced , stored in a retrieval system or transmitted in any for or by any means, without prior permission of the author.

Contact: robert.herpers@gmail.com

Genetic Regulation of Vascular Development

- Building the Zebrafish Vascular Tree -

De genetische regulatie van vasculaire ontwikkeling
- De groei van de zebravis vasculaire boom -

Proefschrift

ter verkrijging van de graad van doctor aan de Erasmus Universiteit
Rotterdam op gezag van de rector magnificus
Prof.dr. H.G. Schmidt
en volgens besluit van het College voor Promoties.

De openbare verdediging zal plaatsvinden op
woensdag 31 maart 2010 om 09.30 uur

door

Robert Leonie Johan Mery Herpers

geboren te Urmond



Promotiecommissie

Promotoren: Prof.dr. D.J.G.M. Duncker
Prof.dr. S. Schulte-Merker

Overige leden: Prof.dr. F.G. Grosveld
Prof.dr. C.L. Mummery
Dr. R. Willemsen

Copromotor: Dr. H.J. Duckers

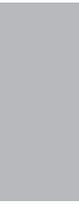
Financial support by the Netherlands Heart Foundation and J.E. Jurriaanse Foundation for the publication of this thesis is gratefully acknowledged.

Contents

Chapter 1	Introduction	7
Chapter 2	Cross-species identification and characterization of novel vascular-specific genes	23
Chapter 3	Redundant roles for <i>sox7</i> and <i>sox18</i> in arteriovenous specification in zebrafish	41
Chapter 4	The role of <i>agtr1b</i> during angiogenesis	55
Chapter 5	Role of Dll4/Notch in the formation and wiring of the lymphatic network in zebrafish	65
Chapter 6	Vegfc/Flt4 signalling is suppressed by Dll4 in developing zebrafish intersegmental arteries	93
Chapter 7	Summarizing discussion	111
	References	121
	Samenvatting in het Nederlands	131
	Dankwoord	134
	Curriculum Vitae	136
	List of publications	137
	PhD Portfolio	138

Introduction

1



The extensive networks of blood and lymphatic vessels within the vertebrate body are essential for the transport and delivery of fluids, gases, macromolecules and cells, and play important roles in facilitating immune responses. The development of the vascular tree requires a highly coordinated interplay of hierarchical genetic and environmental factors, ultimately leading to the formation of a functional network of interconnected tubules that efficiently perfuses tissues. Through the use of various *in vitro* and *in vivo* model systems many major interactors in vascular development have been identified in the past decade. The zebrafish (*Danio rerio*) system in particular offers several advantages for *in vivo* studies, and has played a pivotal role in new discoveries within the angiogenesis field (Lawson and Weinstein, 2002). Further understanding of the mechanisms whereby blood and lymphatic vessels form is an important question that could yield therapeutic options to alleviate vascular disorders, which are leading causes of mortality.

The vasculature is among the first organs to develop in vertebrate embryos. For the normal functioning of the complex vertebrate body architecture a continuous and efficient transport of liquids, gases, hormones, and circulating cells to tissues and organs is required. This requirement is met by two endothelial structures that form highly branched, tubular networks; the blood vessels and the lymphatic vessels. Although these two endothelial structures are intimately linked and even form functional connections, they fulfill different functions; whereas the main function of the blood vessels is to allow the transport of blood and to oxygenate distal tissues, the lymphatic vessels are key in draining fluids from the interstitium. Both endothelial networks are indispensable in maintaining homeostasis and their malformation or dysfunction is causative to the pathogenesis of many diseases (Cueni and Detmar, 2006; Alitalo et al., 2005). Insufficient delivery of oxygen by blood vessels causes tissue ischemia and might even lead to myocardial infarction. During cancer growth, stimulation of angiogenesis by the tumor tissue leads to improved supply of oxygen and nutrients to the tumor, which further stimulates tumor growth (Carmeliet, 2005; Ferrara, 2005). Cancer metastasis to distal tissues on the other hand, mainly occurs through spreading via the lymphatic vasculature (Aachen and Stacker, 2006). As cardiovascular diseases and cancer are the major causes of mortality in westernized societies (Lusis, 2000), the understanding of blood- and lymphatic vessel growth and the ability to control pathogenic vessel growth is of utmost importance to public health.

THE ASSEMBLY OF THE VASCULATURE

The growth of the vascular system is a highly coordinated process of cell proliferation, differentiation and migration during tissue morphogenesis. Blood vessels in the vertebrate embryo initially form through a process called *vasculogenesis* (Risau et al., 1995). During vasculogenesis, mesodermally derived precursor cells, termed angioblasts (Choi et al., 1998; Vogeli et al., 2006), differentiate to endothelial cells and subsequently proliferate *in situ* within a previously avascular tissue and coalesce to form a primitive tubular network (Fig. 1). During vasculogenesis, the major vessels in the embryo, including the dorsal aorta

and cardinal vein are formed (Drake et al., 2000). The primary network is then remodeled through *angiogenesis*, which includes the pruning, growth and sprouting of pre-existing vessels to form the interconnecting branching patterns that characterize the mature vasculature (Carmeliet, 2000; Adams and Alitalo, 2007) (Fig. 1). With the growing maturity of the vasculature, the endothelial cells also tightly integrate supporting cell types like vascular smooth muscle cells (vSMCs) and pericytes into the vessel wall, further enhancing the functionality of the vascular bed (Folkman and D'Amore, 1996; Armulik et al., 2005; Bergers et al., 2005). Exchange of fluids and gases is chiefly accomplished within the capillaries of the vascular system, which are almost completely composed of endothelial cells and only rarely covered with vascular smooth muscle cell-like pericytes (Yancopoulos, 1998). A further differentiation of the embryonic veins enables the sprouting of lymphatic

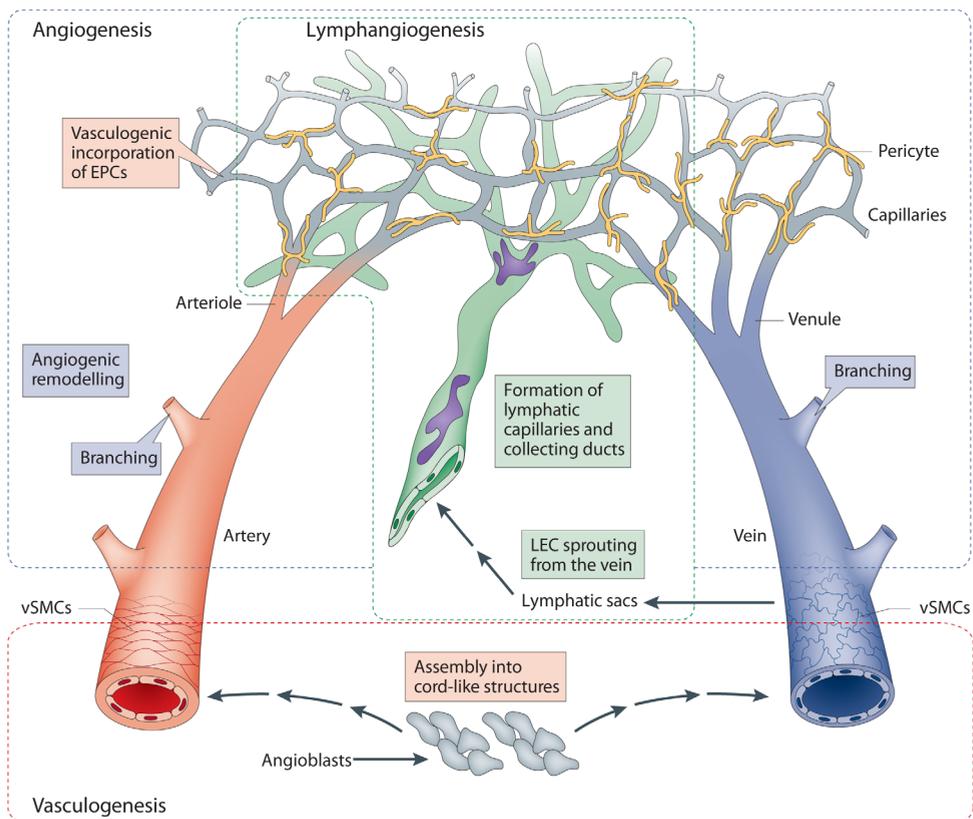


Fig. 1. The assembly of the vasculature. Mesodermally derived cells differentiate to angioblasts and coalesce to form cord-like structures, in a process called *vasculogenesis*. A further differentiation of the endothelial cells gives rise to arteries (red) and veins (blue), which are progressively remodeled into a hierarchical network of arterioles, capillaries, and venules during subsequent steps of *angiogenesis*. During angiogenesis, endothelial cells sprout and branch off from pre-existing vessels in response to environmental factors that stimulate vessel growth. After lumenization of the newly formed vessels, circulation is initiated, allowing for perfusion and oxygenation of distal tissues. A further maturation of the vascular tree is characterized by the coverage of arteries and veins with vascular smooth muscle cells or pericytes. Similarly, lymphatic endothelial cells differentiate and sprout from the venous compartment to give rise to the lymphatic system (green). *Adapted from Adams and Alitalo, 2007*

endothelial cells, which then migrate and proliferate to give rise to the lymphatic system (Francois et al., 2008) (Fig. 1).

In the zebrafish embryo, similar hemangiogenic features can be distinguished; first the major vessels including the dorsal aorta and the posterior cardinal vein are formed through vasculogenesis, followed by remodelling and growth of the vasculature through angiogenesis (Roman and Weinstein, 2000; Baldessari and Mione, 2008). As is the case in other vertebrates, angioblasts arise during early gastrulation in the mesoderm of zebrafish embryos (Jin et al., 2005). After consecutive processes of differentiation, proliferation and migration of the angioblasts towards the midline, a distinct cord of endothelial cells is formed that will lumenize (Blum et al., 2008; Kamei et al., 2006; Jin et al., 2005) and give rise to the axial vessels of the primary vascular network including the dorsal aorta (DA) and posterior cardinal vein (PCV) (Fouquet et al., 1997) (Fig. 2). Shortly thereafter, at 24-26 hours post fertilization, circulation is initiated through a simple single circulatory loop, making the cardiovascular system the first functional organ to arise. During subsequent developmental angiogenesis two distinct stages can be distinguished in the zebrafish embryo; primary sprouts form from the DA to give rise to intersegmental vessels (arterial angiogenesis) from approximately 22 hours post fertilisation (hpf) and then secondary sprouts form from the PCV to give rise to intersegmental veins and lymphatic vascular precursors (venous angiogenesis) from approximately 32 hpf (Isogai et al., 2003; Yaniv et al, 2006) (Fig. 3). Although primary sprouts will contribute to both functional arteries and veins after the later remodelling of the trunk vasculature based on flow (Isogai et al., 2003), primary sprouting is considered an arterial angiogenic process as sprouts derive exclusively from the dorsal aorta and express arterial markers (Siekman and Lawson, 2007), whilst secondary sprouting from the PCV is considered a venous angiogenic process.

The intersegmental arteries that sprout bilaterally from the DA (also referred to as primary sprouts) extend between the somites and the notochord and elongate dorsally. Pathfinding and patterning of these developing blood vessels is regulated by repulsive and attractive plexin cues, similarly to axonal pathfinding and neuronal patterning (Torrez-Vasques et al., 2004). During this elongation process numerous active filopodia can be seen extending and retracting near the leading tip of the extending sprout. At the time the extending sprouts reach the dorsal side of the embryo trunk, a "T" shaped branching of the intersegmental arteries is observed. These "T" shaped endothelial cells extend longitudinally and ultimately anastomose with neighbouring intersegmental arteries at approximately 28 hpf to form a right and left pair of dorsal longitudinal anastomotic vessels (DLAVs). Not long after the formation of the DLAVs, vessel lumenization takes place and active circulation in the intersegmental arteries and the DLAVs can be observed. At this timepoint, an intersegmental artery is composed of three linked endothelial cells (Childs et al., 2002); (1) one cell resides close to the dorsal side of the roof of the DA and forms the base of the intersegmental artery, (2) another cell sits at the junction of the intersegmental artery with the DLAV, while (3) a third cell is found at the midline connecting the other two cells. After the formation of the primary, aorta-derived ad-axial vascular network a

secondary wave of angiogenic sprouting from the PCV (referred to as secondary sprouting) is initiated at approximately 32 hpf.

Similar to primary sprouts the secondary sprouts emerge bilaterally near the somite boundaries and display active filopodic behaviour in the leading tip of the emerging sprout. The secondary sprouts extend dorsally towards the nearest primary vessel (Isogai et al., 2003). Approximately half of the secondary sprouts connect with the existing primary sprouts, remodelling the arterial connections to venous ones and linking the PCV to the primary vascular network. After circulation is established in the connecting secondary sprouts, the primary sprouts will regress and finally disappear. The remainder of the secondary sprouts that do not reconnect to the primary sprouts will further migrate up to the horizontal myoseptum from approximately 36 hpf onwards (Fig. 3). Between 48 and 72 hpf these cells remain in this region before migrating either dorsally or ventrally to contribute to the formation of the dorsal longitudinal lymphatic vessel (DLLV) or the thoracic duct respectively (Hogan et al., 2009).

Besides the formation of the axial vasculature, intensive vascularization of other tissues including the embryonic brain, gills and the intestine is accomplished through angiogenesis (Isogai et al., 2001). Zebrafish vascular development takes place in a temporally and spatially highly coordinated fashion. Alterations of flow characteristics, for instance by complete blockage of cardiac contraction, leads to little or no changes in the patterning and development of the vasculature (Isogai et al., 2003; Sehnert et al., 2002). The highly patterned and robust nature of the vasculature suggests a strong genetic control that drives the formation and growth of the vascular system.

GENETIC CONTROL OF VASCULAR DEVELOPMENT

With the discovery of the vascular endothelial growth factors (VEGFs) and their receptors as essential regulators of endothelial cell differentiation and blood vessel formation (Ferrara et al., 1997; Ferrara et al., 1999; Olsson et al., 2006) an initial step towards the identification of the genetic pathways controlling vascular development had been made. Since then, increasing knowledge of the mechanisms through which downstream target genes of the VEGF receptors and other factors involved in vascular development are regulated has been gained. As is the case for the basic development and architecture of the vascular system, the genetic programs that underlie both vasculogenesis and angiogenesis are evolutionary largely conserved across vertebrates (Thisse and Zon, 2002).

Vascular endothelial growth factor A (VEGF-A), also known as vascular permeability factor (VPF), is a major player in blood vessel development, controlling chemotaxis, EC differentiation and proliferation. Five different VEGF-A isoforms are generated as a result of the alternative splicing of a single VEGF-A gene (Ladomery et al., 2006), which is part of a large family of angiogenic regulators including placental growth factor PlGF, VEGF-B, VEGF-C and VEGF-D (Shibuya, 2006; Ferrara et al., 2003). The responses of endothelial cells to VEGF are strictly regulated by temporal and spatial differences in the expression of the different VEGF family members, but also by their different binding affinities to their respective receptors. In mammals, three signaling tyrosine-kinase receptors belonging to the VEGF-receptor family

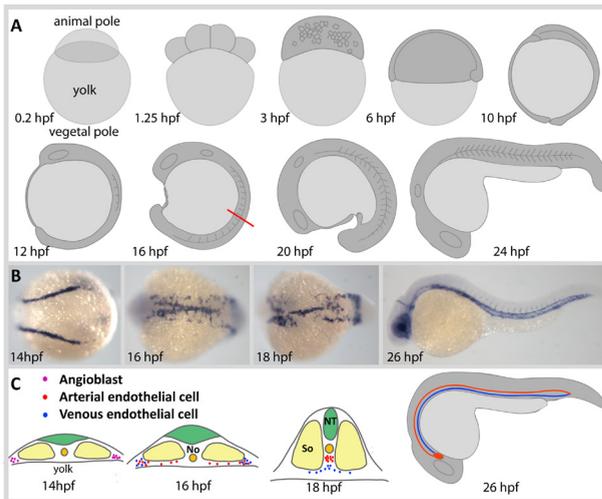


Fig. 2. Zebrafish vascular development.

A schematic overview of the early stages of the developing zebrafish embryo is displayed in (A). Following fertilization, the cytoplasm accumulates in a single cell at the animal pole of the embryo, on top of the yolk. After multiple rounds of cell division, morphogenic cell movements will commence in a process called gastrulation (>5hpf). Using *in situ* hybridization for *sox18*, the dynamic movements of the angioblasts during gastrulation can be visualized; during gastrulation (>10hpf), angioblasts arise in the lateral plate mesoderm (B, 14hpf), which will migrate towards the midline (B, 16hpf) to coalesce and form cord-like structures (B, 18hpf) that give rise to the dorsal aorta and posterior cardinal vein (B, 26hpf). In (C),

a schematic overview of a cross-section of an embryo at the level of the red bar in (B) is displayed; angioblasts that originally arise in the lateral plate mesoderm migrate towards the midline, where they will form a cord-like structure. The first cells to reach the midline will form the future dorsal aorta, dorsal to the notochord (No) and in between the somites (So), followed by the formation of the posterior cardinal vein (PCV). At 26hpf, a simple circulatory loop is established that allows the transport of blood from the anterior side of the embryo toward the posterior side via the dorsal aorta (red) and back to the heart through the PCV (blue). Anterior is to the left, NT is neural tube.

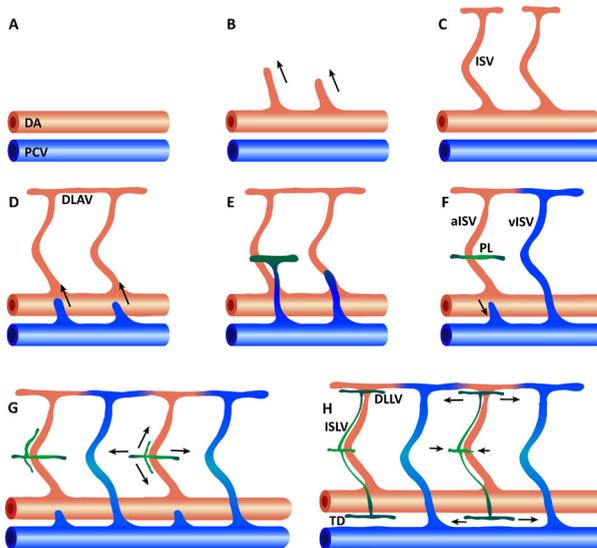


Fig. 3. Assembly of the zebrafish vascular tree.

The assembly of the vascular network in the zebrafish trunk proceeds in a highly coordinated fashion. Primary sprouts emerge bilaterally from the dorsal aorta (in red) at approximately 22hpf, which will migrate toward the dorsal side of the embryo (A,B). For clarity, sprouts from only one side of the embryo are displayed. At the dorsal side, the primary sprouts branch off in a “T-shaped” fashion, where they will meet neighboring endothelial cells (C). After connection of neighboring endothelial cells at the dorsal side of the embryo, the dorsal longitudinal anastomotic vessel is formed (28hpf) (D). Not long thereafter, secondary sprouts will arise from the posterior cardinal vein (blue) (D). Approximately 50% of the secondary sprouts will connect to the base of a primary sprout; ultimately these

intersegmental vessels (ISVs) become part of the venous ISVs, while the ones that are not remodeled serve as arterial ISVs (E). Precursors to the lymphatic vasculature (termed parachordal lymphangiogenic cells (PLs)) arise from secondary sprouts that do not connect with a primary sprout, but instead migrate to the parachordal region (green). At the parachordal region, these PLs show tangential migration, followed by ventral and dorsal migration along arterial ISVs along with the formation of intersegmental lymphatic vessels (ISLVs) (F,G). At the dorsal and ventral side of the developing zebrafish trunk, the dorsal longitudinal lymphatic vessel (DLLV) and the thoracic duct (TD) are both formed by longitudinal extension and fusion of lymphatic endothelial cells (LECs) (H).

(VEGFR-1/Flt1, VEGFR-2/Kdr/Flk1 and VEGFR-3/Flt4) (Shalaby et al., 1997; Yamashita et al., 2000) can be discriminated, all having different binding affinities for the different VEGF ligands. This allows tight regulation of the cellular responses to VEGF. VEGF-A for instance binds to VEGFR-2 and stimulates endothelial cell proliferation and differentiation. VEGFR-1, which has a higher binding affinity to VEGF-A, but a weaker tyrosine-kinase function, in turn antagonizes VEGFR-2 function. VEGF-C and VEGF-D, on the other hand, mainly bind to VEGFR-3 and play important roles during lymphatic development. In addition to the receptor tyrosine kinases (RTKs), VEGF interacts with a family of coreceptors, the neuropilins (Neufeld et al., 1999). The neuropilins have short intercellular domains and are therefore unlikely to fulfill a signaling role independent of the RTKs. Targeted disruption of neuropilin-1 however, leads to cardiovascular defects during early development, whereas VEGF stimulation of cells transfected with neuropilin-1 has no effect (Soker et al., 1998; Kitsukawa et al., 1997). It has been proposed that the neuropilins function as coreceptors for VEGF (Lee et al., 2002; Martyn and Schulte-Merker, 2004), enhancing the binding properties of VEGF to Flk-1. The interaction of the various VEGF forms and their receptors are summarized in Fig. 4.

Besides the VEGF-receptors, other RTKs are found on endothelial cells that play important roles in endothelial cell survival and vascular maturation, as illustrated by the Tie2-Angiopoetin signaling system. The Angiopoetin (Ang) ligand family consists of 4 different members, Ang-1 through Ang-4, while only two members of the Tie-receptor family are known, Tie1 and Tie2. Ang-1 is a specific ligand for Tie2, which upon activation stimulates

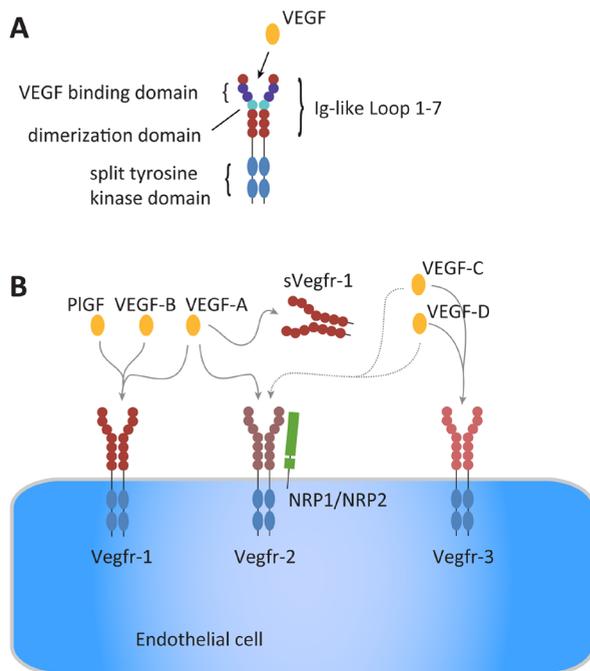


Fig. 4. Interaction of the various VEGF forms with their receptors. The VEGF-receptors contain seven immunoglobulin (Ig)-like loops in their extracellular part and a split tyrosine-kinase domain in their intracellular part. Two VEGF-receptor molecules form homodimers, facilitated through binding of the fourth Ig-like loop. The second and third Ig-like loops allow for binding of VEGF to its receptors, while the intracellular part is required for downstream signaling. VEGF-A binds to both VEGFR-1 and VEGFR-2, whereas VEGF-B and PIGF only bind to VEGFR-1. VEGF-C and VEGF-D can bind to VEGFR-2, but mainly function through VEGFR-3, which is present on lymphatic endothelial cells. The accessory proteins neuropilin-1 and neuropilin-2 also bind VEGF, but do not fulfill any signaling function; in turn they act as coreceptors for VEGF, enhancing the signaling properties of VEGFR-2. Although VEGFR-2 is the main regulator of angiogenic growth, the binding affinity of VEGF-A to VEGFR-1 is much higher. The presence of soluble VEGFR-1 together with the lower

tyrosine kinase function of VEGFR-1 and the absence of a phenotype in kinase-deficient knock out mice (Hiratsuka et al., 1998) has led to the conclusion that VEGFR-1 acts as a decoy receptor to control the availability of VEGF to other receptors.

vessel assembly and maturation. In contrast, binding of Ang-2 to Tie2 has an antagonistic effect on Ang-1 mediated Tie2 activation (Thomas and Augustin, 2009).

Functional studies in mice and fish have also shown the involvement of Notch signaling in the angiogenic growth of blood vessels and the arteriovenous differentiation of endothelial cells. The Notch signaling pathway is an evolutionarily highly conserved mechanism that plays an essential role in cell fate specification, tissue patterning, and morphogenesis. Notch receptors are transmembrane proteins with large extracellular domains that contain multiple epidermal growth factor (EGF)-like repeats. The Notch receptors interact with the Delta, Serrate and LAG-2 (DSL) cell-surface ligands Delta-like 1, Delta-like 3, Delta-like 4 (Dll4), Jagged1 and Jagged2. Upon binding of the DSL cell-surface ligands to the transmembrane Notch receptors, the Notch intracellular domain (NICD) is ultimately released (Weinmaster et al., 2000; Selkoe and Kopan 2003; Schweisguth et al., 2004). The NICD is then translocated to the nucleus where it causes the release of the RBP-J corepressor proteins to allow for downstream transcriptional activation of Notch target genes such as Hes and Hey (Fig. 5).

Given the common origin of blood and endothelial cells, it is not surprising that several of the factors required for the early development of endothelial cells are also important for hematopoietic development. For example the basic helix-loop-helix transcription factor *Tal1* (*Scf*) is indispensable for both blood and endothelial cell development. *Tal1* is expressed in both endothelial and hematopoietic precursor cells during early embryogenesis and its disruption leads to severe defects in the development of both the hematopoietic and vascular lineages in both mice and zebrafish (Visvader et al., 1998; Gering et al., 1998; Patterson et al., 2005; Bussmann et al., 2007).

The large ETS family of transcription factors plays a central role in controlling the transcriptional programs in hematopoietic and endothelial cell development. Characterization of endothelial enhancers and promoters revealed the presence of multiple ETS binding sites, while many Ets factors are expressed in endothelial cells (Hollenhorst et al., 2004; Liu and Patient, 2008). The large number of Ets factors present in the endothelial cells exhibit a substantial functional redundancy; knockout of the majority of single Ets genes in either mouse or zebrafish results in little to no vascular phenotype (Pham et al., 2007). The recently discovered *Etv2* (*Etsrp*) represents a single exception to this functional redundancy. Removal of *Etv2* protein function in mice or knockdown of the zebrafish orthologue *Etsrp* results in a severe impairment of vasculogenesis and it has been suggested that *Etv2*/*Etsrp* plays a central role in angioblast differentiation (Ferdous et al., 2009; Lee et al., 2008; Sumanas et al., 2008).

Many other genes have been found to fulfill important roles during vascular development, including members of the GATA family of transcription factors (Lee et al., 1991), members of the Forkhead (Fox) transcription factors (Pananicalaou et al., 2008) and members of the Krüppel-like factor (Klf) transcription factor family (Atkins and Jain, 2007), all fulfilling different functions to control the transcriptional pattern of vascular development.

ARTERIOVENOUS DIFFERENTIATION

Shortly after the differentiation of the angioblast, arteries and veins are formed in a process

known as arteriovenous differentiation (Jain, 2003; Swift and Weinstein, 2009). Before the initiation of circulation, but after the aggregation of the angioblasts into a cord-like structure, arteriovenous identity is determined by a variety of genetic factors. The two components of the vascular system have distinct functional and structural differences (Lawson and Weinstein, 2002). To meet the haemodynamic requirements of the vascular network, arteries are covered with vascular smooth-muscle cells (vSMCs), extracellular matrix, and elastic fibers that allow them to resist pressure and shear stress. The venous portion of the network facilitates low-pressure flow, and is thus covered with fewer vSMCs and contains valves that prevent backflow. Deregulation of arteriovenous differentiation or failure to segregate arterial and venous endothelial cells causes potentially lethal clinical conditions including hereditary hemorrhagic telangiectasia and cerebral cavernous malformations (Carmeliet, 2005; Irrthum et al., 2003; Sorensen et al., 2003; Urness et al., 2000).

Several signaling molecules are known to be involved in the specification of arteriovenous cell fate, including Hedgehog (Hh), VEGF, Notch, and chicken ovalbumin upstream-transcription factor II (COUP-TFII) (Lawson et al., 2003; Liang et al., 2001; Lawson et al., 2001; Lin et al., 2007). Other transcription factors that function downstream of these signaling cascades involve *hey2/Gridlock* (Kokubo et al., 2005; Zhong et al., 2000), a member of the hairy and enhancer of split related family bHLH transcription factor, the *Foxc1* and *Foxc2* transcription factors (Seo et al., 2006; Kume et al., 2006), and two members of the Sox-F family, *Sox7* and *Sox18* (Herpers et al., 2008; Cermenati et al., 2008; Pendeville et al., 2008) (Fig. 6). The complex hierarchal arrangement of interacting signaling pathways can either promote arterial cell fate at the expense of venous cell fate, or vice versa. The requirement of VEGF–Notch signaling for arterial cell specification in the zebrafish originally resulted in the belief that the venous state is derived from a default pathway, whereas arterial identity is conferred by the presence of additional signaling (Thurston and Yancopoulos, 2001). Recently however, COUP-TFII was identified to be an upstream genetic factor that acts as a positive mediator of venous specification. Disruption of COUP-TFII leads to the acquisition of arterial characteristics in veins, whereas ectopic expression results in the fusion of arteries and veins (You et al., 2005). It has been suggested that COUP-TFII establishes the venous identity by downregulation of Notch signaling via the release of factors such as EphB4 and Flt4 from Notch-mediated repression (You et al., 2005).

ANGIOGENIC SPROUT FORMATION

During angiogenic growth, growth factors and chemokines stimulate the endothelial cells to sprout and form new vessels from the walls of pre-existing ones to meet the oxygen demands of local tissues (Fraisl et al., 2009). After stimulation of endothelial cells towards angiogenic sprouting by environmental growth factor signals, formation of leading endothelial tip cells occurs. Stimulation of endothelial cells with VEGFA leads to the formation of long, dynamic filopodia that probe the environment for directional cues. The endothelial cells that directly follow the tip cells, termed the stalk cells, produce significantly fewer filopodia and proliferate upon stimulation with VEGFA (Gerhardt et al., 2003). The ability of endothelial cells within the vascular bed to respond differently to similar environmental factors is largely

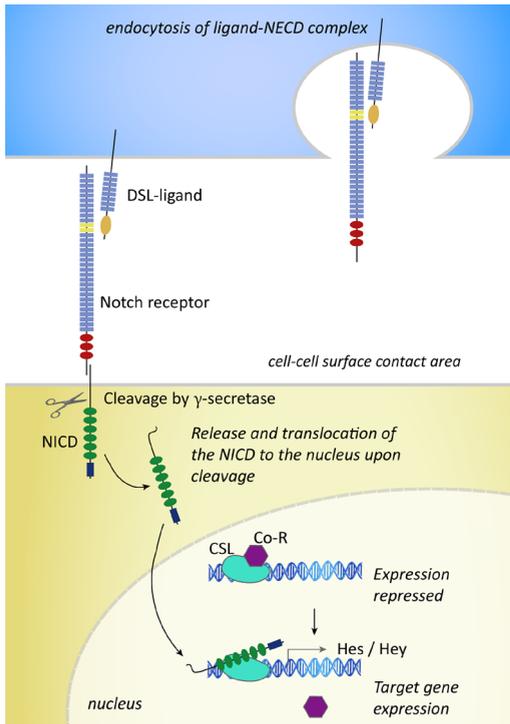


Fig. 5. Notch signaling. Simplified model of the Notch signaling pathway based on (Roca et al., 2007). The Delta-Notch pathway uses a distinct molecular mechanism to transduce a signal from the cell surface to the nucleus; after Delta, Serrate and LAG-2 (DSL) ligand binding, Notch is cleaved by γ -secretase and the Notch intracellular domain (NICD) is released. The Notch extracellular domain (NECD) is extracted from the plasma membrane by *trans*-endocytosis into the DSL cell-surface ligand-presenting cell. Release and nuclear translocation of the NICD and its interaction with the CBF1, Su(H) and LAG1 (CSL) family of transcription factors results in the release of the transcriptional co-repressor (Co-R) complex, which in turn triggers the expression of target genes such as Hey and Hes. The domains schematically highlighted in Notch are EGF-like repeats (light blue), some of which are involved in DSL binding (yellow), Notch/LIN-12 repeats (red), a single transmembrane (TM) region, intracellular ankyrin repeats (green), and the C-terminal PEST sequence (dark blue). Ligands contain an N-terminal DSL domain (orange), EGF repeats (light blue), a transmembrane region, and a cytoplasmic area with a C-terminal PDZ-binding motif.

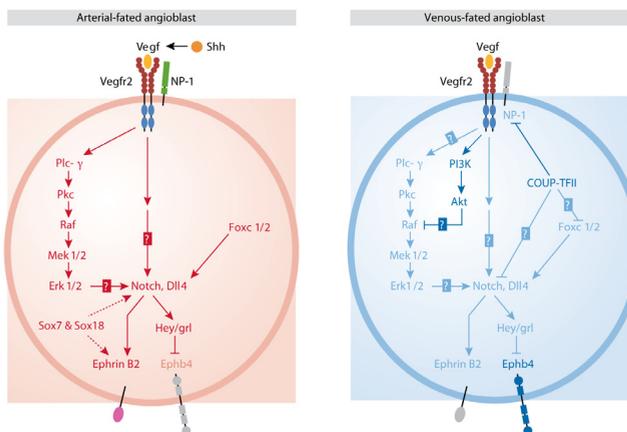


Fig. 6. Genetic model of arteriovenous specification in the developing embryo. Sonic hedgehog (Shh) secreted by the notochord and plate induces vascular endothelial growth factor (Vegf) levels in the somites, which in turn activate angioblasts arising from the lateral plate mesoderm. Within an arterial-fated angioblast, Vegf interacts with the Vegf receptor 2 (Vegfr2)–neuropilin 1 (NP-1) complex to activate downstream phospholipase Cy-1 (Plc- γ), extracellular signal-regulated kinase (Erk) and Notch signalling pathways, thereby inducing arterial marker expression, such as ephrin B2

(*efnb2*). Forkhead box c 1 (Foxc1)/Foxc2 proteins activate the Notch pathway by inducing the expression of Delta-like 4 (Dll4), thereby leading to an arterial fate. Conversely, chicken ovalbumin upstream promoter transcription factor II (COUP-TFII) and phosphatidylinositol-3 kinase (PI3K)–Akt signalling promote venous fate by suppression of the Notch pathway and Erk signalling, respectively, thereby repressing arterial fate. COUP-TFII not only suppresses the Notch pathway, but also inhibits NP-1 expression, therefore attenuating Vegf and downstream Notch activation. Unconfirmed interactions are indicated by question marks. Ephb4, B4 ephrin receptor; grl, gridlock; Hey, hairy-and-enhancer-of-split related; Mek, mitogen-activated protein kinase kinase; Pkc, protein kinase c. Adapted from Lamont and Childs, 2006; Lin et al., 2007.

accomplished by Delta-like-4 (Dll4)-Notch signaling. Expression of Dll4 is induced in the tip cell upon stimulation with VEGFA, and subsequent Notch signaling through lateral inhibition in adjacent endothelial cells is believed to impair sprouting of these cells (Suchting et al., 2007; Hellstrom et al., 2007). Reduced levels of Dll4 or abolishment of Notch signaling enhances the formation of tip cells, leading to increased sprouting (Hellstrom et al., 2007; Leslie et al., 2007; Siekmann and Lawson, 2007). These results show that, rather than following a static patterning of tip and stalk cells, cells continuously compete with each other for the tip cell position; the cell that produces more Dll4 than its neighboring cells will acquire and maintain the tip position of the extending sprout by suppressing its neighbors' response through activation of Notch signaling.

The exact mechanism whereby Notch signaling regulates endothelial cell motility during angiogenic sprouting is unclear. Downregulation of VEGFR2 and VEGFR3 upon Notch signaling (Sainson et al., 2005) could potentially reduce the migratory properties of endothelial cells by making them less responsive to VEGFA. Phosphorylation of distinct VEGFR2 tyrosine residues (Olsson et al., 2006) also leads to the activation of several signaling pathways, including PI3K, which are known to stimulate endothelial cell migration, which might explain how Notch signaling contributes to endothelial cell migration.

LYMPHATIC DEVELOPMENT

The lymphatic vasculature consists of blunt-ended vessels that form a unidirectional network of collecting vessels, capillaries and lymph nodes, the function of which is to retrieve protein-rich fluids from the interstitium and lipids from the intestine. The lymphatic network is also involved in immune responses; lymphocytes migrate towards the lymphoid organs, in which the immune responses are initiated, via the lymphatic vessels.

Lymphatic endothelial cells (LECs) are derived from blood vessel endothelial cells (BECs), and share many of their characteristics. However, in contrast to BECs, the LECs are not covered by a layer of vSMCs and exhibit weaker intercellular contacts. Anchoring filaments that bind the LECs to the extracellular matrix (ECM) allow the opening of intercellular gaps in the lymphatic vessels upon fluid accumulation in the interstitium, which facilitates the uptake of fluids by the lymphatics. The functional and architectural differences between LECs and BECs are genetically controlled. In mouse embryos, patched expression of the transcription factor prospero-related homeobox-1 (Prox1) can be detected in endothelial cells of the dorsal aspect of the jugular vein. Prox1 expressing cells upregulate several lymph-specific genes and eventually adopt the lymphatic fate (Wigle et al., 2002). Recently, another transcription factor, Sox18, was shown to directly induce the local expression of Prox1 (Francois et al., 2008).

In zebrafish, the thoracic duct (TD), which is located between the DA and PCV, is the first lumenized lymphatic vessel to arise (Küchler et al., 2006; Yaniv et al., 2006). During secondary angiogenic sprouting from the vein (Fig. 3), approximately half of the endothelial sprouts that emerge transdifferentiate to lymphatic endothelial cells (LECs) and bud off from the vein towards the parachordal region. These LECs first undergo tangential, then either ventral or dorsal migration along arterial ISVs, along with the formation of intersegmental lymphatic

vessels (ISLVs). At the dorsal and ventral side of the developing zebrafish trunk respectively the dorsal longitudinal lymphatic vessel (DLLV) and TD are formed by longitudinal extension and fusion of LECs (Fig. 3) (Hogan et al., 2009).

VASCULAR DEVELOPMENT AND PATHOLOGY

The adult vasculature acquires a quiescent, non-angiogenic state, while retaining its growth potential upon stimulation by certain environmental factors. Unfortunately, in several human diseases, angiogenesis is related to a pathological setting, during which blood vessels are stimulated by VEGF to grow and facilitate tumor growth and metastasis (Holash et al., 1999). Controlling the angiogenic growth potential of the vascular tree would constitute an attractive strategy of preventing tumor growth and tumor metastasis (Folkman, 1992; Ferrara, 2004). Additionally, controlled stimulation of angiogenic growth could be of great value in alleviating ischemic conditions by improving local tissue perfusion. As VEGF-mediated angiogenesis is relatively rare in adults, except during wound healing and female reproductive cycling, targeting of VEGF should have only little effect on physiological processes. In recent years, the possibility to reduce tumor growth by blocking angiogenesis has been intensively studied, resulting in several therapeutic benefits. As VEGF acts directly on endothelial cells and circulates via the blood it has proven a suitable target to limit angiogenic growth potential (Ferrara, 2005). Monoclonal antibodies targeted against VEGF have already successfully been used to that end (Ferrara, 2004); the newly formed vessels that invade tumor tissue upon VEGF secretion by the tumor cells are disorganized and blind-ended. These highly permeable vessels poorly perfuse the tumor and cause high tumor interstitial pressure. Therefore, the effectiveness of chemotherapy might be elevated by vessel normalization and reduction of interstitial tumor pressure by inhibition of VEGF. In recent years, targeting of the Notch ligand Dll4 has arisen as an important treatment option in anti-angiogenic therapies. Unlike VEGF, compromised Dll4 function leads to excessive, but paradoxically unproductive angiogenesis, which in turn leads to decreased tumor growth (Thurston et al., 2007). The vessels that form in the absence of Dll4 are highly branched and often lack a vessel lumen or are too disorganized to support perfusion. With the combined targeting of both VEGF and Dll4, even more potent effects on tumor growth have been achieved, stressing the effectiveness of combinatorial anti-angiogenesis strategies to improve anti-tumor therapies.

The major causes of lethality in westernized societies next to cancer are heart disease and stroke, which mainly arise as a result of atherosclerosis. Atherosclerosis is characterized by a progressive accumulation of lipids and fibrous elements in large arteries. The lesions that arise during atherosclerosis can cause an acute occlusion of the large arteries by the formation of a thrombus or blood clot after rupture of the lesion, ultimately leading to myocardial infarction and stroke. Studies that investigated the mechanisms underlying atherosclerosis have revealed several environmental and genetic factors to be causative of the progression of this pathological setting (Ross, 1993). Besides the lowering of cholesterol levels and high blood pressure as effective strategies of decreasing the mortality from atherosclerosis, a number of new, genetic targets are successfully being explored to improve

the stability of existing plaques (Schonbeck et al., 2000).

Other, potentially lethal vascular diseases are attributable to mutations in single genes. For example, cerebral cavernous malformations (CCMs) are vascular malformations characterized by enlarged thin-walled capillary clusters in the brain. CCM is inherited as an autosomal dominant trait and loss of function mutations in three genes, *CCM1*, *CCM2* or *CCM3*, have been demonstrated to cause CCM (Labauge et al., 2007; Hogan et al., 2008). The arteriovenous malformations in hereditary hemorrhagic telangiectasia and hypotrichosis–lymphedema–telangiectasia have also been associated with mutations in single genes, namely endoglin/activin-like receptor kinase-1 and SOX18 respectively (Irrthum et al., 2003; Sorenson et al., 2003; Urness et al., 2000). A greater understanding of vascular pathogenesis as well as an understanding of how vascular biology is intertwined with tumor development and metastasis will be of great help to improve current treatment strategies for a wide range of diseases.

CONCLUDING REMARKS

Recent studies have greatly improved our understanding of the various aspects of endothelial cell biology and our knowledge of hemangiogenic and lymphangiogenic development. Great progress in our ability to study vascular development has also been made by the use of increasingly sophisticated model systems, such as tissue specific knock-out mice, a wide variety of cell-culture systems, and *in vivo* imaging in transgenic reporter-fish. A well-based understanding of the fundamental mechanisms that underlie *de novo* formation and growth of the vascular system has proven invaluable in targeting pathological conditions that arise as a result of vascular dysfunction. Our knowledge of angiogenic growth of blood and lymphatic vessels is already being used in cancer therapies, where inhibition of vessel growth may prevent tumor growth and metastasis. With the clinical development of a variety of angiogenesis inhibitors, pathological angiogenesis in numerous tumor models can be inhibited. Likewise, pro-angiogenic treatments of ischemic conditions may benefit from improved growth of blood and lymphatic vessels.

The central question of this thesis is to gain insight into the molecular players during the initial stages of vascular assembly and growth. Although this chapter provides a summary of our current knowledge of the major aspects of vascular development and introduces zebrafish as a model organism for vascular studies, it is certainly not a complete overview of the many facets that drive the growth of the vascular tree. Rather, it is intended to support the following chapters described within this thesis.



Cross-species identification and characterization of novel vascular-specific genes

Robert Herpers^{1,2}, Esther van de Kamp¹, Stefan Schulte-Merker²,
Henricus J Duckers¹.

2

1. *Experimental Cardiology, Thoraxcenter, Erasmus University Medical Center, 's-Gravendijkwal 230, 3015 CE Rotterdam, The Netherlands.*

2. *Hubrecht Institute-KNAW & University Medical Centre, Utrecht, Uppsalalaan 8, 3584 CT Utrecht, The Netherlands.*



ABSTRACT

Knowledge of the genetic pathways controlling the emergence of the angioblast is essential to our understanding of both vascular and stem cell biology. To define the genetic pathways involved in angiogenesis we utilize fluorescent activated cell sorting of *Flk1*-positive cells at early stages during mouse embryonic development (E10.5, E11.5 and E16.0) and perform microarray analysis. Distinct differences were found in the comparison of the expression profiles of *Flk1*-positive and *Flk1*-negative cell populations at the timepoints analyzed. Subsequent *in situ* expression analysis using zebrafish embryos identified 61 genes with blood- or (cardio)vascular specific expression, of which 11 were novel. We next performed an *in vivo* functional screen in zebrafish using morpholino antisense oligomers to assess gene function. Our results represent a robust, high-throughput screen for the identification and characterization of novel genes involved in the molecular mechanisms of vascular development.

INTRODUCTION

Vascular development is a complex and tightly regulated process that involves the *de novo* assembly of blood vessels from mesodermally derived precursor cells, also referred to as vasculogenesis (Risau et al., 1997; Flamme et al., 1997). Vascular endothelial cells are derived from a common precursor, called the hemangioblast, which has been shown to contribute to both endothelial cells (angioblasts) and blood cells (hematopoietic stem cells) (Choi et al., 1998; Vogeli et al., 2006). After differentiation from the hemangioblast, the establishment of the vascular endothelial lineage involves several key processes including the migration and assembly of the angioblasts to form cord-like structures, which will lumenize and form the major vascular network. As early as embryonic day E6.5 extraembryonic angioblasts, marked by expression of *Flk1* (Fetal liver kinase 1), can be detected in regions where blood vessels form (Drake et al., 2000). Intraembryonic vasculogenesis of bilateral primordia, also referred to as the dorsal aortae, which later fuse to give rise to the dorsal aorta, can already be detected at E7.6. Only after the *de novo* formation of major vessels during vasculogenesis, will growth and remodeling of the vascular network occur through sprouting angiogenesis. At E9.0 an increase of markers associated with more mature vessels like PECAM and Tie2 (Suri et al., 1996; Drake et al., 2000) can be observed in the vasculature and rapid remodeling and expansion of the vascular system takes place, while dispersed angioblasts contributing to the developing aortae can still be detected. In addition to vessel maturation the vascular system progressively becomes more specialized as different structures like arteries, veins and lymphatics develop (Carmeliet, 2000; Adams and Alitalo, 2007).

Vascular endothelial growth factor (VEGF) is a highly specific mitogen for vascular endothelial cells (Ferrara, 2003) and has been shown to induce angiogenesis and plays a central role during vasculogenesis. Five different VEGF-A isoforms are generated as a result of alternative splicing of a single VEGF-A gene, which is part of a large family of angiogenic regulators like PLGF, VEGF-B, VEGF-C and VEGF-D. Three signaling tyrosine kinase receptors

belonging to the VEGF-receptor family (VEGFR-1/Flt1, VEGFR-2/Kdr /Flk1 and VEGFR-3/Flt4) can be distinguished, all exhibiting different binding affinities for the different VEGF ligands, allowing tight regulation of the cellular responses to VEGF. VEGF-A for instance binds to VEGFR-2 and stimulates endothelial cell proliferation and differentiation. In contrast, VEGFR-1, which has a higher binding affinity for VEGF-A, but a weaker tyrosine kinase function, antagonizes VEGFR-2 function (Fong et al., 1999). VEGF-C and VEGF-D mainly bind to VEGFR-3 and play important roles during lymphatic development (Karkkainen et al., 2004). Several studies have shown the association of Flk1 with vascular progenitors and vasculogenesis (Shalaby et al., 1997; Yamashita et al., 2000) and its importance during later stages of angiogenesis (Jain, 2003). Although significant progress has been made in the identification of the molecular mechanisms that control vasculogenesis and angiogenesis, there are still many unknowns.

In this study, we have combined zebrafish genetics with mouse genomics in an effort to identify genes governing vascular development. Zebrafish have recently become an attractive model organism for the study of vertebrate organogenesis (Roman and Weinstein, 2000; Baldessari and Mione, 2008). The transparency of the zebrafish embryo combined with the availability of various reporter lines allows for real-time non-invasive *in vivo* analysis of organogenesis. Its small size and fecundity greatly facilitate large scale forward genetic screens in which numerous mutants have been described. With the availability of morpholino antisense oligomers that either block translation or splicing of a gene transcript (Nasevicius et al., 2000), reverse genetic approaches for the characterization of candidate genes have also become possible. Several studies have used microarray analysis combined with whole mount *in situ* hybridisation analysis in order to analyze gene expression profiles during hematopoietic and vascular development (Weber et al., 2005; Sumanas et al., 2005; Eckfeldt et al., 2005; Covassin et al., 2006; Wong et al., 2009). Although these screens have been successful in the identification of novel genes involved in hematopoietic and vascular development, they generally relied on whole embryos as a source for RNA for microarray profiling. However, the cell types involved in the development of the hematopoietic and vascular cell lineages might only represent a small fraction of the total number of cells within the embryo. In an effort to tackle this problem one study made use of FACS enriched cell populations from transgenic zebrafish embryos expressing eGFP under the control of a *fli1* promoter (Covassin et al., 2006). However, expression of *fli1* is not restricted to the endothelial lineage, but is also found in cartilagenous tissues. In addition, eGFP expression in a transgenic background might not completely recapitulate endogenous *fli1* expression. Lastly, folding times for eGFP induce a time lag between transcriptional activation and actual protein detection, which could potentially obscure the dynamic temporal expression profiles in developing embryos. An even more sophisticated means of screening for novel molecular regulators of blood vessel development is thus desirable.

In this study, we describe the global analysis of gene expression in the developing mouse vasculature. We utilize fluorescent activated cell sorting to acquire a population of cells enriched for Flk1 expression at early stages of mouse development (E10.5, E11.5 and E16.0). Expression of Flk1 is already found within the early hemangioblast and continues

to be expressed on mature endothelial cells, making it a suitable marker for the sorting of both angioblasts and differentiated endothelial cells. Subsequently, we used microarray analysis at various timepoints for both the *Flk1*-positive and *Flk1*-negative cell populations and described the dynamic changes of expression profiles found. Gene transcripts showing elevated differential expression profiles in *Flk1*⁺ cells at the early timepoints (E10.5 and E11.5) were translated to their zebrafish orthologues. Next, whole mount *in situ* hybridization was used to assess the temporal and spatial expression pattern of the upregulated gene transcripts in zebrafish embryos. Finally, the gene function of transcripts that showed an expression pattern closely associated with vascular development was assessed by an *in vivo* functional screen using morpholino antisense oligomers in transgenic zebrafish embryos (summarized in Fig. 1). Using this strategy, not only have we identified a number of genes that potentially represent novel regulators of vascular development, but we also present functional data that links these genes to developmentally relevant processes.

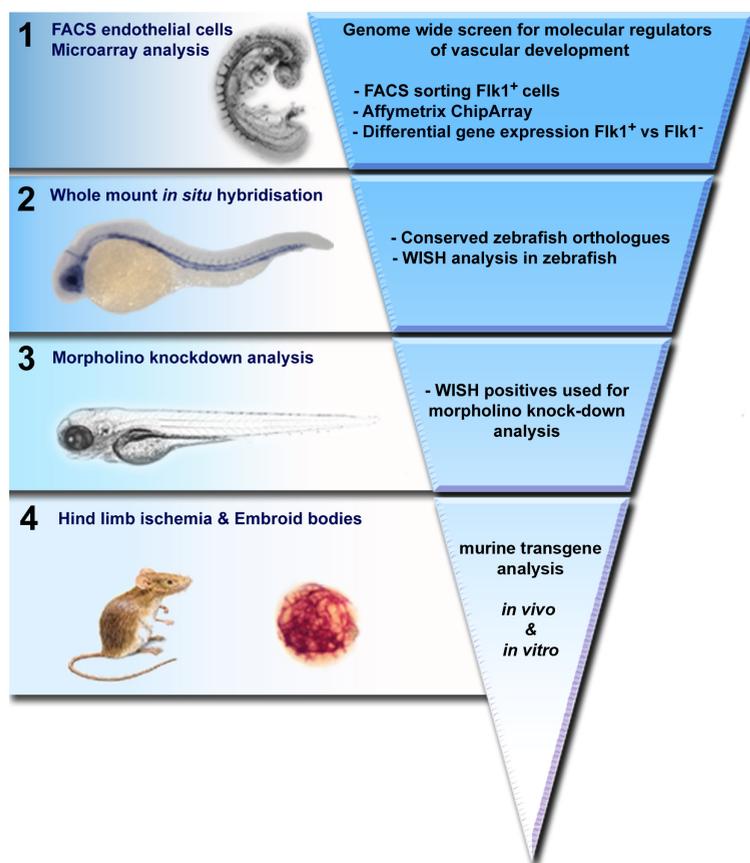


Fig. 1. Genome wide screen for molecular regulators of vascular development. General overview of the setup of the genome wide screen for molecular regulators of vascular development. Firstly, an enriched population of *Flk1*⁺ cells was harvested from mouse embryos at E10.5, E11.5 and E16.0 by using fluorescent activated cell sorting (FACS). Total RNA from both *Flk1*⁺ and *Flk1*⁻ cells was isolated for the various timepoints and used for subsequent microarray analysis (1). Secondly we translated all transcripts differentially upregulated in the *Flk1*⁺ population at early timepoints to their zebrafish orthologues and used these for wholemount *in situ* hybridisation to look for specific expression in the vascular bed (2).

Next we performed a functional analysis of the genes with an expression pattern closely linked to the vascular system by morpholino knockdown to assess gene function (3). Lastly, future research using *in vitro* assays and murine analysis will be performed to assess conserved gene function (4).

MATERIALS AND METHODS

ANIMAL HUSBANDRY

Zebrafish were kept under standard husbandry conditions at the Hubrecht Institute. Transgenic lines used were Tg(*kdr*:eGFP)^{S843} (Jin et al., 2005) and Tg(*fli1*:eGFP)⁷ (Lawson and Weinstein, 2002). Plugged FVB/N mice were ordered at Harlan, and embryos collected at the embryonic days indicated. Animal experiments were in accordance with the Animal Experimentation Committee of the Royal Netherlands Academy of Arts and Sciences (DEC) and performed according to their guidelines.

ISOLATION OF FLK1⁺ AND FLK1⁻ CELLS FROM MOUSE EMBRYOS

At the selected timepoints, embryos were collected from plugged FVB/N female mice and homogenized by incubation for 45 minutes at 37°C in DM (PBS (no Ca, no Mg) and 10% FCS) with 0.12 % Collagenase type I (Sigma C-0130). Single cells were stained at a concentration of 6x10⁷ cells/ml in a 1/50 PE anti mouse Flk1 antibody dilution (BD, 555308). Hoechst was used as a marker to select for dead cells. Two populations (Flk1⁺/Hoechst⁻ cells and Flk1⁻/Hoechst⁺ cells) were sorted on a FACS Diva using two consecutive rounds of sorting to improve purity. High quality mRNA was isolated using the Qiagen, RNeasy mini kit.

PROCESSING OF RNA SAMPLES AND MICROARRAY ANALYSIS

Microarray analysis was performed at the Rotterdam Erasmus University Medical Center. 5µg of mRNA was used to make double stranded cDNA using the Invitrogen choice system. Using the ENZO BioArray High Yield RNA Transcript, biotin labeled RNA was generated. After clean-up and fragmentation approximately 20 µg of labeled cRNA was hybridized to the GeneChip[®] Mouse Genome 430A & 430B 2.0 Arrays. Rosetta resolver was used to import calls and intensities, followed by quantile normalization. Raw data were merged into OmniViz and a threshold minimum for intensities was set at 30. Fold differences were calculated from log averages determined for the different experimental conditions. Correlating mouse gene transcripts with zebrafish orthologues was done by using BioMart and the Ensembl database <http://www.ensembl.org>, release 38, April 2006.

IN SITU PROBES GENERATION AND WHOLE MOUNT IN SITU HYBRIDISATION

Template DNA for *in situ* probe generation was obtained by direct amplification of target genes from genomic DNA. Primers for probe generation were designed to span exons of at least 250 basepairs in size to ensure probe specificity. Reverse primers were tagged with a T3 RNA polymerase promoter tail to allow direct *in vitro* transcription and generation of antisense probes after PCR purification. Primer sequences are listed in supplemental table 1. *In situ* probes were DIG labeled using the Roche DIG labeling mix. Bacterial clones for the generation of *in situ* probes of selected genes were obtained from Open Biosystems <http://www.openbiosystems.com>. Whole-mount *in situ* hybridization was performed as previously described (Thisse and Thisse, 2008). Coarse *in situ* transcript detection was automated using the Intavis AG *in situ* robot <http://www.intavis.com> followed by manual *in situ* transcript detection to increase the signal to noise ratio.

MORPHOLINO ANTISENSE OLIGOMER INJECTIONS

Morpholinos (MOs) were obtained from Gene Tools <http://www.gene-tools.com> and diluted in water containing 0.2% phenol red. One cell stage embryos were injected with 1 to 9ng of MO with a maximum volume of 3nl as described previously (Nasevicius, 2000). Morpholino sequences are displayed in supplemental table 2. Morpholino knockdown efficiency was tested for splice-site targeting morpholinos by RNA isolation from morpholino-injected fish. Subsequently cDNA was synthesized using the SuperScript II RT Kit (Invitrogen). Primers used for reverse transcriptase PCR are listed in supplemental table 3.

IMAGING PROCEDURES

Zebrafish embryos were mounted in 1% low melting point agarose in a culture dish with a cover slip replacing the bottom. Imaging was performed with a Leica Microsystems SP2, SPE or SP5 confocal microscope using a 10x, 20x or 40x objective with digital zoom. Angiography was performed as previously described (Weinstein et al., 1995). Images were processed by using Photoshop CS2 and Illustrator CS2 (Adobe).

RESULTS***ISOLATION OF ENRICHED FLK1⁺ CELL POPULATIONS FROM MICE***

Vascular development involves the proliferation, migration and differentiation of endothelial cells. However, these cells only represent a small fraction of the total number of cells within the developing embryo. As a result, genes expressed in endothelial cells might be poorly represented in cDNA libraries derived from whole embryo material. Moreover, subtle but important changes in temporal expression profiles within the endothelial cells might not be apparent as a result. Therefore, we took advantage of the possibility to sort enriched populations of endothelial cell types by fluorescent activated cell sorting (FACS) for subsequent expression analysis.

Developing mouse embryos were collected at E10.5, E11.5 and E16.0, timepoints at which intensive vascular development is seen (Drake et al., 2000). After proteolytic dissociation of the embryos, the Flk1⁺ cells were labeled with PE-labeled antibodies, to allow for FACS (Figure 2). Flk1 is an early marker for the hemangioblast, but is also expressed in endothelial cells during vasculogenesis and angiogenesis, making it an excellent marker for both early and late stage vascular development. Hoechst was used as a marker to sort for living versus dead cells. Diagnostic fluorescent activated cell sorting showed that approximately 1.5% of the cells were found to be Flk1-positive and we were able to sort Flk1-positive cells by FACS to a purity greater than 97%.

MICROARRAY ANALYSIS OF FLK1⁺ CELLS

We hypothesized that genes differentially expressed between Flk1⁺ and Flk1⁻ cell populations across E10.5 and E11.5 would represent genes that are involved in the molecular regulation of early vascular development. Exclusion of genes that were also differentially upregulated in Flk1⁺ cells at E16.0 was used to selectively filter for early regulators of vascular development. Total RNA from both Flk1⁺ and Flk1⁻ cell populations, collected by FACS, was isolated for all three timepoints (summarized in Fig. 2). We next acquired and compared the expression profiles for both Flk1⁺ and Flk1⁻ cell populations at the three different timepoints (E10.5, E11.5 and E16.0). Gene expression analysis for both Flk1⁺ and Flk1⁻ cells from E10.5, E11.5 and E16.0 mouse embryos showed a clear separation of the Flk1⁺ and Flk1⁻ cell populations as shown by the correlation plot (Fig. 2b), indicating that the sorted Flk1⁺ and Flk1⁻ cell populations show clear differences in their respective expression patterns. We also found a marked clustering within the duplicate experiments of the different timepoints analyzed, as well as a distinctive correlation for the expression profiles of Flk1⁺ cells at E10.5 and E11.5. The high values seen for the correlation of the earlier timepoints (e.g. compare E10.5 and E11.5) would gradually diminish by temporal changes in expression levels (e.g. compare E10.5 and E16.0), showing the dynamics of the expression profiles over time.

Differential gene expression among Flk1⁺ and Flk1⁻ cells was determined by the commonly used fold change cut-off calculated by using log transformed expression values. We found 2,161 transcripts that were differentially upregulated (fold-change >2.0) in Flk1⁺ at both E10.5 and E11.5, and only 784 after exclusion of genes that were also differentially upregulated in

Flk1⁺ cells at E16.0 (see supplemental table 4 and 5). The differential gene expression profiles for the early timepoints (E10.5 and E11.5) showed a high level of similarity, but appeared markedly different from the expression profile for E16.0 as illustrated by the heatmap (Fig. 2c). We anticipated finding such temporal differences in gene expression levels within Flk1⁺ cells as most intensive levels of vascular growth are found from E7.5 to E12.5 (Drake, 2000). Among the genes that are differentially upregulated in Flk1⁺ cells during early development, many are associated with vascular development, including Flt1, a member of the VEGF-receptor family (Ferrara et al., 2003). Several transcription factors implicated in either hematopoiesis (Lmo2) (Landry et al., 2003) or angiogenesis (Ets-family members) (De Val and Black, 2009) were also identified. Cell fate specification is mainly regulated through the action of transcription factors; therefore it is not surprising to find a number of transcription factors in the enriched gene list. Tie1, a member of the tyrosine kinase receptor family and

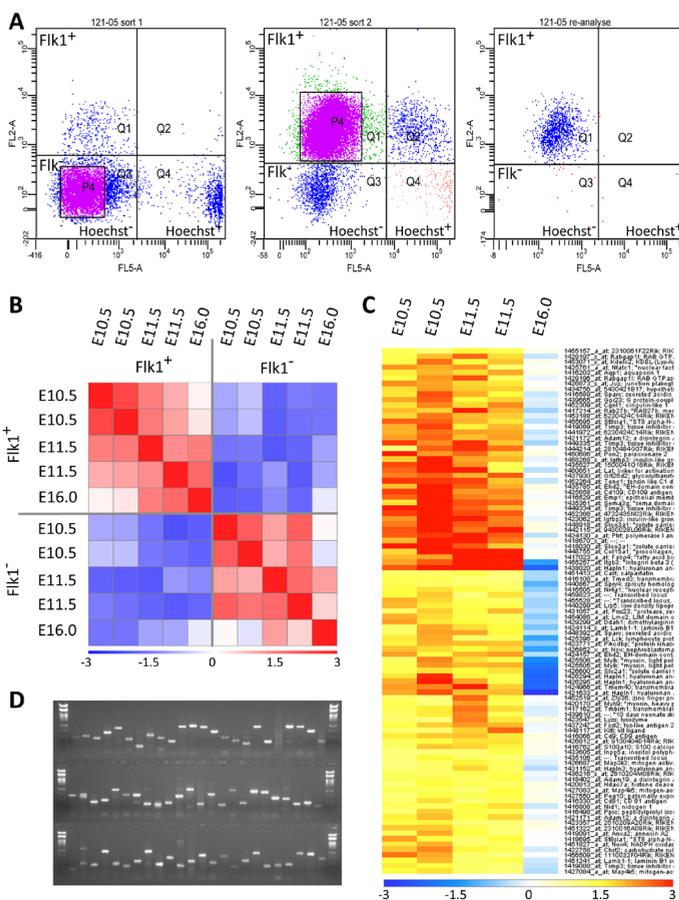


Fig. 2. Fluorescent activated cell sorting and gene expression analysis. (A) Mouse embryos were collected at E10.5, E11.5 and E16.0, followed by labeling of Flk1-positive cells by PE-labeled antibodies after proteolytic dissociation of the embryos. Both Flk1⁺/Hoechst and Flk1⁻/Hoechst cells were sorted for all of the selected timepoints (n=2 for E10.5 and E11.5) by means of fluorescent activated cell sorting, followed by total RNA isolation for all samples collected. Next, the isolated total RNA was directly labeled without any additional linear amplification steps and used for hybridization to the Affymetrix GeneChip[®] Mouse Genome 430A & 430B 2.0 Array for expression analysis. Gene expression analysis for both Flk1⁺ and Flk1⁻ cells from E10.5, E11.5 and E16.0 mouse embryos showed a clear separation of the Flk1⁺ and Flk1⁻ cell populations and clustering within the different timepoints analyzed as shown by the correlation plot (B). Whereas the differential gene expression profiles for the early timepoints (E10.5 and E11.5) showed a high level of

similarity, the differential gene expression profile for E16.0 appeared to be clearly distinctive from E10.5 and E11.5 as illustrated by the heatmap (C). Transcripts that showed a clear differential up-regulation at E10.5 and E11.5, but not E16.0 were translated into their corresponding zebrafish orthologues. Exons exceeding 250 basepairs in size of the corresponding genes were subsequently amplified from genomic DNA and used as a template for *in situ* probe generation (D).

its ligand Angiopoietin2 (Thurstson, 2003) were also found to be differentially upregulated in Flk1⁺ cells during early vascular development. Furthermore, we identified both Neuropilin1 and Neuropilin2 (Gerhardt et al., 2004) as well as several members of the Notch signaling pathway (Phng and Gerhardt, 2009) in the Flk1⁺ enriched gene list.

Remarkably, a number of genes that have been implied in vascular development are absent from the enriched gene list, including Flt4 and Flk1. These genes do show a significant differential expression in Flk1⁺ cells at E10.5 and E11.5, but are also differentially upregulated in Flk1⁺ cells at E16.0. As these genes continue to be expressed at high levels at later stages of development, they failed to meet our criteria of early expression and are excluded from further analysis.

EXPRESSION ANALYSIS SCREEN IN ZEBRAFISH

To further evaluate our gene expression data from microarray profiling, we set out to correlate the *in silico* data with *in situ* expression analysis. Our initial goal was to perform an unbiased, genome wide, screen to look for novel molecular regulators of vascular biology. However, the expression analysis of 784 individual murine genes would be a cumbersome and time-consuming task. We therefore reverted to the zebrafish model organism, which allows for high-throughput whole mount *in situ* hybridization analysis because of its small size, transparency and fecundity. Organogenesis has largely been evolutionarily conserved from zebrafish to mice and a lot of common genetic pathways are shared (Thisse and Zon, 2003). We used Biomart <http://www.ensembl.org> to look for evolutionarily conserved genes and found 419 corresponding zebrafish orthologues for the 784 transcripts present in the Flk1⁺ enriched mouse gene list. Comparison of our enriched gene list with expression data publicly available through ZFIN <http://www.zfin.org> shows that multiple genes are indeed expressed in vascular tissues. For a large number of genes however there was no corresponding expression pattern available. Therefore, we performed an expression analysis screen: we designed primers to specifically amplify exons from the translated orthologues, which then served as a template for probe generation. Using this strategy we successfully generated 363 unique zebrafish *in situ* probes (Fig. 2d and Supplemental table 6).

At approximately 10hpf mesoderm-derived angioblasts first arise in the zebrafish embryo, which will migrate towards the midline to coalesce and form a cord-like structure (Vogeli et al., 2006). This structure is then remodeled through tubulogenesis and as a result the dorsal aorta (DA) and posterior cardinal vein (PCV) are formed at 20hpf (Fouquet et al., 1997). At about 22hpf sprouting angiogenesis from the DA is initiated and the intersegmental vessels (ISVs) are formed (Isogai et al., 2003). Three different timepoints (12hpf, 18hpf and 24hpf) that span the early stages of vascular development within the zebrafish embryo were used, with a minimal number of 10 embryos per selected gene for each timepoint. Coarse whole mount *in situ* hybridisation expression analysis of the enriched gene list was achieved by using the Intavis AG *in situ* robot. *In situs* that showed a gene expression pattern closely linked to the vascular system were manually repeated to minimize the risk of probe carryover and to improve the signal to noise ratio. Expression patterns for genes that had not been described at the time this expression screen was performed are shown in Fig. 3. Angiotensin receptor-

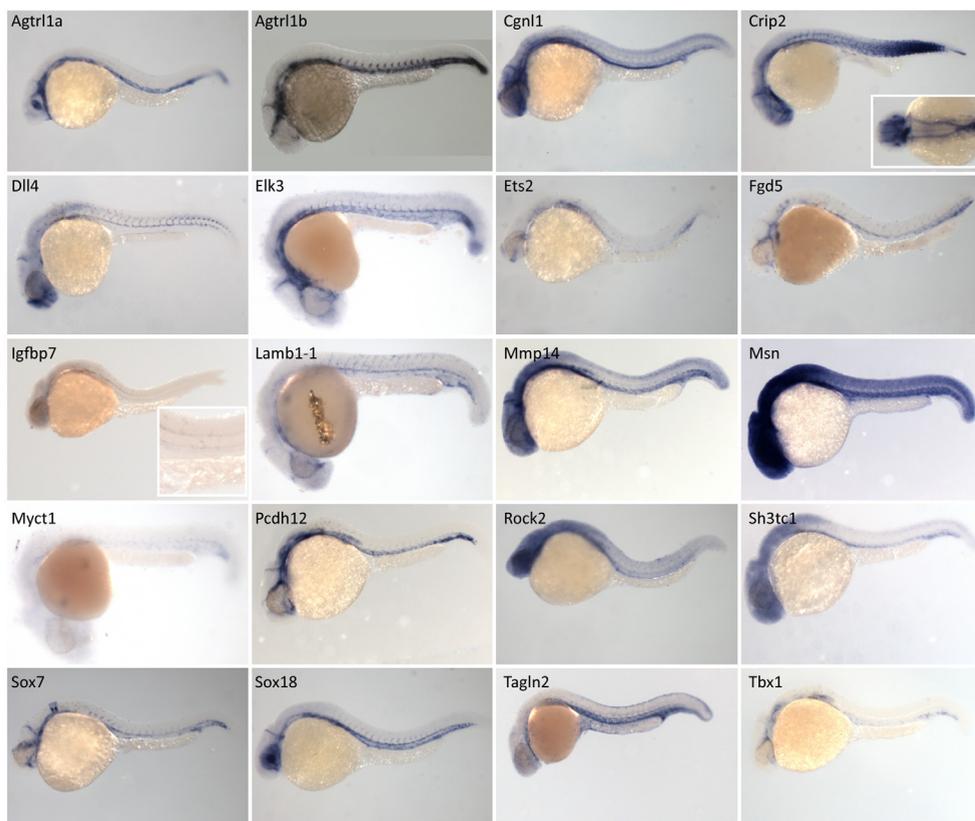


Fig. 3. Whole mount in situ hybridization analysis of vascular markers. Global whole mount expression profiles for *agtrl1a*, *agtrl1b*, *cgn1*, *crip2*, *dll4*, *elk3*, *ets2*, *fgd5*, *igfbp7*, *lamb1-1*, *mmp14*, *msn*, *myct1*, *pcdh12*, *rock2*, *sh3tc1*, *sox7*, *sox18*, *tagln2* and *tbx1* showed apparent vascular expression patterns at 24-28 hours post fertilization. Embryos are imaged from a lateral view (inset for *crip2* in dorsal view), anterior is to the left.

like 1, a gene duplicated in the zebrafish genome, shows strong expression in vascular tissues for both gene duplicates. Whereas *agtrl1a* is mainly expressed in the PCV, *agtrl1b* is expressed in the DA, PCV, midhindbrain channel (MHBC) and intersegmental vessels (ISVs) at 24hpf. Two members of the Ets-family of genes, *elk3* and *ets2*, were also identified as having marked vascular expression. *Ets2* is expressed in the angioblasts at 12hpf and in the DA, PCV and caudal vein (CV) at 24hpf. *elk3* is highly expressed in the angioblasts at both 12 and 16hpf and maintains a high level of expression at 24hpf within the DA, PCV, MHBC and ISVs. FYVE, RhoGEF and PH domain-containing protein 5 (*fgd5*), shows a very similar expression profile; early expression in the angioblast is marked, as well as continued expression within the DA, PCV, MHBC and ISVs at 24hpf. The recently characterized member of the family of cadherins, *cdh5*, as well as the uncharacterized protocadherin 12 (*pcdh12*), part of a subfamily of the superfamily of cadherins, were also identified as having vascular restricted expression at the timepoints analyzed. Other genes with expression patterns closely linked to vascular development were the laminin B1 subunit 1 (*lamb1-1*), the myc target 1 (*myct1*),

the matrix metalloproteinase 14 (*mmp14*), a family member of the metalloproteinases that are involved in the breakdown of extracellular matrix, moesin (*msn*), T-box transcription factor Tbx1 (*tbx1*) and transgelin2 (*tagln2*). Two members of the Sox-F family of transcription factors, *sox7* and *sox18* were found to be highly expressed during early stages of vascular development and with continued high levels of expression in the vascular bed at later stages. Several genes (*flt1*, *flt4*, *notch1* and *ephb2a*) show an expression pattern which is restricted to either the arterial or venous compartment of the vascular system. We found that the Notch-ligand *dll4* is exclusively expressed in arterial tissues, whereas the SH3 domain and tetratricopeptide repeats-containing protein 1 (*sh3tc1*) is restricted to venous structures.

The expression of another group of genes was not only restricted to the vascular system, but was also found in the developing zebrafish heart. For example, the cysteine-rich protein 2 (*crip2*), rho-associated, coiled-coil containing protein kinase 2 (*rock2*) and cingulin-like 1 (*cgnl1*) show strong expression in the myocardium as well as in vascular tissues (Supplemental Figure 2). Other genes, including *nfatc1*, *podxl*, *anxa6*, *rhoc* and *slco3a1* were also found to be expressed in the heart. Expression patterns closely associated with hematopoietic development were found for several genes, including *adora2a*, *lrcc13*, *spnb2* and *stk10* (Supplemental Figure 2). In total we found 61 genes with an expression pattern closely linked to cardiovascular or hematopoietic development, of which 11 had previously not been characterized (Supplemental table 6).

IN VIVO FUNCTIONAL SCREEN IN ZEBRAFISH

As expression data alone does not answer questions of functional relevance, we followed our initial findings up with an *in vivo* screen for vascular development in zebrafish. The common precursor for hematopoietic and angiogenic development, also referred to as the hemangioblast, was recently shown to be evolutionarily conserved in both zebrafish and mice (Vogeli et al, 2006). The signals (*gata1*, *tal1*, *lmo2*, *flk1*) required for the specification events in the establishment of both lineages to arise from the angioblast are also evolutionary conserved (Thisse and Zon, 2002). The evolutionarily conserved nature of these processes makes them an ideal subject for cross-species analysis and thus for rapid functional screening in zebrafish. We used morpholino knockdown (Nascevicus et al., 2002) as a reverse genetic approach to assess gene function in the developing zebrafish embryo. We designed 2 independent morpholinos for each of the 19 different genes targeted, including three gene duplicates. We further confirmed the specificity of the morpholino targeting of the genes of interest by using RT-PCR, the results of which are summarized in supplementary table 3 and supplemental figure 1. We injected the morpholinos into one- to two-cell stage embryos in a *kdrl:eGFP* transgenic background (the zebrafish orthologue of Flk1 (Bussmann et al., 2008)) and screened for effects in vascular development (table 1). Our initial findings classified 8/19 morpholinos as inducing an effect on vascular development, ranging from defective cardiac development and functionality to failure of vascular growth. Some of the injected morpholinos affected cardiovascular development, but the effects seen could partially be ascribed to secondary effects as a result of the abnormal development of the zebrafish embryo. For example, injection of morpholinos targeting both duplicates

Mouse gene	Penetrance	Phenotype
<i>Adora2a</i>	30-70%	General morphology affected; curved body axis, straight somites, reduced eye size, reduced pigmentation. ISV outgrowth affected.
<i>Agtrl1</i>	60-70%	Reduced or absence of heart. Defective sprouting/growth ISVs
<i>Cgnl1</i>	80-100%	Normal vascular development. Cardiac defects at 6dpf, loss of circulation.
<i>Crip2</i>	40%-70%	General morphology affected; curved body axis, necrosis, kidney-cyst, no heart jogging.
<i>Dll4</i>	70-80%	Initial normal development of vasculature. Excessive ISV sprouting >48hpf
<i>Elk3</i>	30-40%	Retention circulation initiation. Expansion of caudal vein.
<i>Ets2</i>	-	-
<i>Fgd5</i>	-	-
<i>Lamb1</i>	-	-
<i>Mmp14b</i>	-	-
<i>Pcdh12</i>	-	-
<i>Rin3</i>	-	-
<i>Rock2</i>	10-20%	Normal development, bleedings in head region.
<i>Sox7</i>	90-100%	Loss of circulation and loss of <i>kdr1:eGFP</i> expression when combined with <i>sox18</i> .
<i>Sox18</i>	90-100%	Loss of circulation and loss of <i>kdr1:eGFP</i> expression when combined with <i>sox7</i> .
<i>Tagln2</i>	<10%	Initial normal vascular development, hyperplasticity ISVs at 5dpf.

Table 1. Genes differentially expressed between mice *Flk1** and *Flk1⁻* cell populations subjected to the *in vivo* functional assay in zebrafish and the gross phenotypes observed upon knockdown.

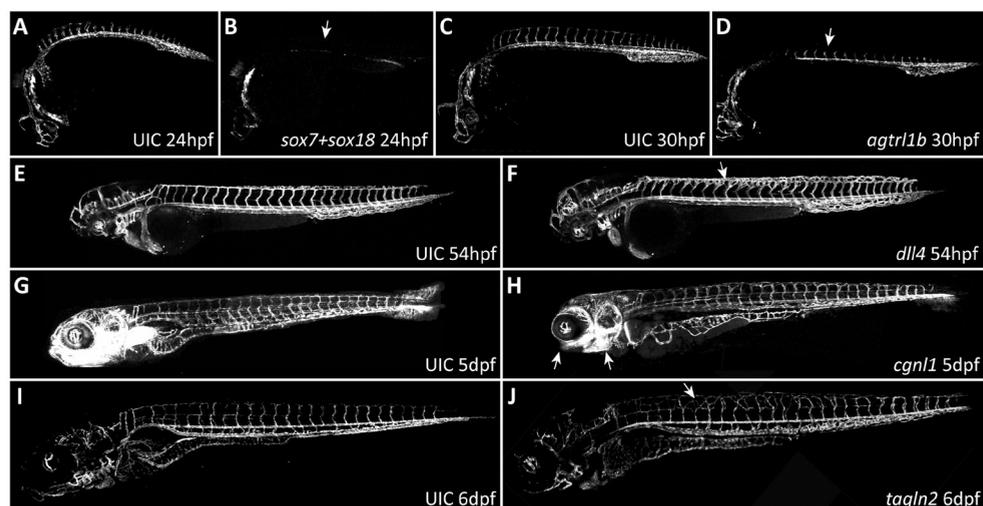


Fig. 4. Morpholino knockdown analysis of vascular genes. Global results of the *in vivo* functional screen revealed a specific requirement for normal vascular development for some of the genes found to be expressed in the vascular bed. Simultaneous injection of morpholinos targeting *sox7* and *sox18* led to a vast reduction of *kdr1:eGFP* expression in the endothelial cells at 24 hours post fertilization (hpf) (A and B, arrow). Loss of *Agtrl1b* function is characterized by defective outgrowth of the intersegmental vessels (ISVs) toward the dorsal side of the embryos and a concurrent loss of the dorsal longitudinal anastomotic vessel at 28 hpf (C and D). Morpholino targeting of *dll4* results in excessive angiogenic sprouting of the ISVs at the dorsal side of the embryo at 54hpf (E and F). Morpholino targeting of *cgnl1* results in a progressive loss of cardiac function at >5dpf, together with a failure of the formation of the gill vasculature (G and H, see also Fig. 5). Injection of morpholinos targeting *tagln2* resulted in the ectopic sprouting of ISVs at 6 dpf (I and J). Embryos are imaged in a lateral view, anterior is to the left. All embryos are in a *kdr1:eGFP* transgenic background, except for G and H, which are in a *Flt1:eGFP* transgenic background. High power images of the morpholino phenotypes are displayed in Fig. 5.

of *adora2a* affected the development of the intersegmental vessels, but also led to more general developmental defects including reduced eye size, necrosis, reduced pigmentation, defective yolk extension and abnormal somite formation. As the intersegmental vessels develop in close proximity to the somites, which are a local source of *vegfa*, it is most likely that the defects seen on the development of the intersegmental vessel are secondary in nature. To limit the possibility of taking along cardiovascular defects that are merely a secondary effect of general developmental abnormalities we excluded embryos that displayed an overall defective morphology from our screen. Examples of the effects seen on (cardio)vascular development are summarized in Fig. 4 and 5.

Two of our identified candidates, *sox7* and *sox18*, and the endodermally expressed *sox17* together form the Sox-F (Sry-related HMG box) family of DNA-binding proteins (Bowles et al., 2000). Members of the Sox-F family play crucial roles during the formation of definitive endoderm, and during hematopoietic stem cell, cardiovascular and lymphatic development (Kanai-Azuma, 2002; Kim et al., 2007; Pennisi et al., 2000; Francois et al., 2008). Morpholino targeting of either *sox7* or *sox18* showed no clear defect on vascular development. However, simultaneous targeting of both genes led to loss of *kdrl:eGFP* expression in almost all vascular tissues (Fig. 4 A,B). We found *sox7* and *sox18* to be essential for the arteriovenous differentiation of the angioblasts during the establishment of the vascular lineages as shown by molecular characterization of these morphant fish. Combinatorial knockdown of Sox7 and Sox18 function caused a loss of circulation in the posterior part of the developing embryo as a result of a failure of segregation of arteries and veins and the concurrent formation of shunts. A detailed characterization of the effects of the loss of combined Sox7 and Sox18 function is given in **chapter 3** of this thesis.

Recent studies in zebrafish showed an indispensable role for *agtrl1b* in the specification of myocardial cells during gastrulation (Scott et al., 2006; Zeng et al., 2006), while reporting no vascular abnormalities. Confirming this finding, morpholino knockdown of both *agtrl1a*

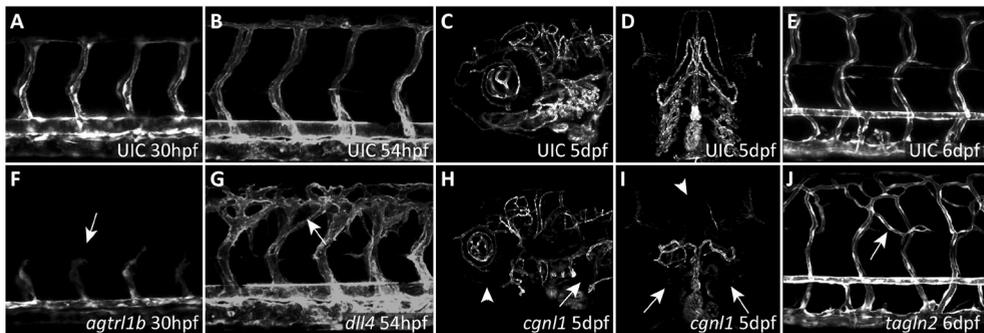


Fig. 5. Morpholino knockdown analysis of vascular genes. High power images of the results of the *in vivo* functional screen for *agtrl1b* clearly show a failure of the ISVs to extend towards the dorsal side of the embryo (A and F). Morpholino targeting of *dll4* leads to excessive angiogenic sprouting of the ISVs at the dorsal side of the embryo at 54hpf (B and G). Morpholino targeting of *cgn1* results in a progressive loss of cardiac function at >5dpf, concurrent with a failure of the formation of the gill vasculature (aortic arches, arrows) and the hypobranchial artery (arrowheads) (C,D and H,I). Injection of morpholinos targeting *tagln2* resulted in the ectopic sprouting of ISVs at 6 dpf (E and J). All embryos are in a *kdrl:eGFP* transgenic background, imaged in a lateral view, anterior is to the left. Embryos in D and I are imaged from in a ventral view, anterior to the top.

and *agtr1b* gave rise to a reduced heart size, and even a near complete loss of the heart in some embryos. However, by generation of a stable mutant knockout line for *agtr1b* we found a specific requirement for *agtr1b* in the extension of the ISVs towards the dorsal side of the embryo (Fig. 4 C,D) and the cellular architecture of the tip-cell during angiogenesis, independently of the reduced heart and the loss of circulation. The role of *agtr1b* during angiogenic migration of ISVs and tip-cell behavior is described in further detail in **chapter 4** of this thesis.

Cgn1 encodes a plaque protein localized in the apical junctional complex and has been reported to be specifically expressed in the endocardium of the embryonic heart (Narumiya et al., 2007). Cellular adhesion molecules are known to play important roles during the patterning of the embryonic heart (Simard et al., 2006). Knockdown of *cgn1* showed no obvious early defects of vascular development. However, at 5dpf, slight edema near the eyes was observed, as well as complete loss of circulation and death after 6dpf. Closer analysis of the embryos at earlier timepoints showed normal development of the heart and valves as well as normal expression of marker genes of cardiac specification (supplemental Figure 3). Analysis of the gill vasculature in contrast, showed a vast reduction in the number of vessels that contribute to the respiratory system, coincident with a substantial reduction of the cartilagenous tissues that support the craniofacial structures (supplemental Figure 3). Whether the loss of the gill vasculature is a direct result of the loss of *cgn1* protein function, or a secondary effect to the craniofacial defects remains to be seen.

In vertebrates, the maturation of the cardiovascular system is accompanied by the recruitment of smooth muscle cells, referred to as vascular myogenesis (Carmeliet et al., 2000; Jain et al., 2003). These smooth muscle cells are marked by *tagln2* (*sma22a*) expression and can be found perivascularly (Santoro et al., 2009; Yang et al., 2003). Knockdown of *tagln2* did not result in obvious defects in vascular development during the first 4 days after fertilization. In contrast, at 6dpf reduced vascularization of the gills and clear hyperplasticity of the ISVs (Fig. 4 G,H) was observed in a small proportion of the embryos, reminiscent of the effects caused by knockdown of *dll4*.

Dll4/Notch signaling has long been associated with cell fate specification and differentiation and plays a pivotal role in cardiovascular development (Phng and Gerhardt, 2009). Recent studies have shown an essential role for *dll4* in limiting the angiogenic properties of the ISVs (Siekman et al., 2007; Leslie et al., 2007). Embryos injected with morpholinos targeting *dll4* initially develop a normal DA, PCV, ISVs and dorsal longitudinal anastomotic vessels (DLAVs). After 2dpf however, marked ectopic sprouting of the ISVs at the dorsal side of the embryo is observed (Fig. 4 E,F). We found that one of the functions of Dll4 is to repress the angiogenic response of developing intersegmental vessels to Vegfc/Flt4 signaling, as discussed in **chapter 5** of this thesis. We also found a specific requirement for Dll4/Notch signaling in normal lymphatic development. The loss of lymphatic structures upon *dll4* knockdown and the molecular mechanism responsible are further described in **chapter 6** of this thesis.

DISCUSSION

In this study we describe an improved method for the identification of molecular regulators involved in early vascular development. By FACS sorting Flk1-positive cells from early mouse embryos that contribute to the vascular lineage we were able to compile a global expression profile of endothelial cells. Comparison and analysis of the temporal expression changes in both Flk1⁺ and Flk1⁻ cells yielded an enriched expression list of genes which was verified by whole mount *in situ* hybridization in zebrafish embryos. Novel genes found to be restrictively expressed in the vascular lineage were subjected to an *in vivo* functional screen in zebrafish to assess their function, which led to the identification of several factors essential for the assembly of the vascular bed.

Multiple genes with an essential role in vascular development were found to be significantly upregulated in our enriched gene list, validating our method. In addition, several genes with a previously uncharacterized role in vascular development were also found to have an expression pattern linked to vascular development in the whole mount *in situ* hybridization screen, proving the reliability of the approach taken in finding cell type specific genes. However, several genes known to be expressed in Flk1⁺ tissues are absent from the enriched gene list. One explanation for this could be that these genes are also abundantly expressed in other, non Flk1⁺ tissues, rendering the detection of a significant differential up-regulation virtually impossible. For example, in zebrafish, *notch3* is strongly expressed in the DA, but is also found at high levels in the neural tube (Lawson et al., 2001). Some genes known to be exclusively expressed in the vascular bed are not present in the enriched gene list either. This is a result of the strict selective criteria we set to look for early regulators of vascular development. *Flt4* for example, is expressed at high levels in Flk1⁺ tissues at early stages of development. Unsurprisingly, loss of *Flt4* function leads to several angiogenic and vasculogenic defects (Ober et al., 2004; Dumont et al., 1998; Hogan et al., 2009). At later timepoints, we find continued high levels of expression for *flt4* in Flk1⁺ tissues. Similarly, other studies have reported increasingly restricted expression of *flt4* to the lymphatic vasculature perinatally and shown a selective contribution of *flt4* to lymphangiogenesis (Karpanen et al., 2006; Hogan et al., 2009). As a result of its role in both early and late stages of vascular development, *flt4* fails to meet our criteria of early modulators of blood vessel formation and is excluded from the enriched gene list. A final explanation for the absence of some genes from our candidate gene list can be found in small but significant phenotypic changes of the cells that occur after proteolytic dissociation and during cell sorting. As a result changes in gene expression profiles might occur with a concurrent loss of expression of specific genes. Although we cannot rule out any of these scenarios, the expression profile of the endothelial cell type appears well represented in our enriched gene list.

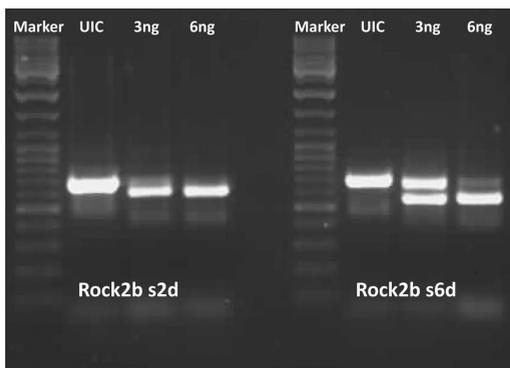
As a general rule, most genes expressed during vascular development were highly upregulated in Flk1⁺ cells, meaning that they clustered at the top of the enriched gene list. We also found that a number of the genes present in the enriched gene list were expressed in multiple cell types whereas others were expressed ubiquitously in the embryo. Yet according

to our microarray analysis these genes were upregulated in Flk1⁺ cells. These results suggest that combined sorting of specific cell types and microarray profiling may in some cases be more sensitive than *in situ* hybridisation profiling of cell type specific expression patterns. Novel genes with an expression pattern closely linked to vascular development, or with an uncharacterized role in vascular development at the time this screen was performed, served as candidate genes in our *in vivo* functional assay. By using morpholino oligomers we transiently knocked down the function of 19 different genes (including three gene duplicates) in zebrafish embryos, of some of which displayed some remarkable phenotypes. A detailed description of the phenotypes observed in this screen is provided in **chapter 3 - chapter 6** of this thesis.

In summary, we identified a set of genes that is specifically expressed in Flk1⁺ cells, which will generate the endothelial lineages, during early mouse development. This led to the identification of multiple genes that show an expression pattern restricted to the vascular lineage during early zebrafish development. Not only do we provide a robust and rapid means of screening for novel genes involved in cell type specific development, we also provide functional data linking these genes to essential processes during normal vascular development. The signaling pathways that act during early vascular development are evolutionarily highly conserved across species. In an ongoing effort to study the conserved nature of the molecular background of vascular development, the genes identified in this study have been subjected to analyses in other model organisms (Fig. 1). Linking functional data from several model organisms, supplemented with *in vitro* assays provides a solid basis for our understanding of the conserved nature of vascular development. The data presented here will help to provide insight in the molecular hierarchy of genetic control of angioblast specification events. A better understanding of the transcriptional networks and signaling pathways involved in the emergence of the angioblast lineage and subsequent vessel formation can ultimately contribute to therapeutic benefits such as new molecular targets for augmenting or inhibiting vessel growth.

SUPPLEMENTAL MATERIAL

Supplemental material, including 6 data tables and 3 supplemental figures can be found in the data supplement.

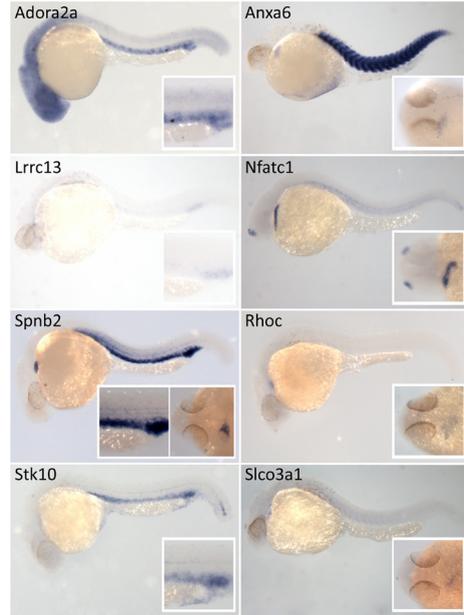


Supplemental figure 1

Representative example of the RT-PCR controls of morpholino knockdown efficiency; RNA from morpholino injected embryos was isolated and cDNA was generated. Following PCR reactions showed a shift in size for the morphant samples compared to the wild type controls, indicating improper splicing of the transcripts upon injection of splice-site targeting morpholinos.

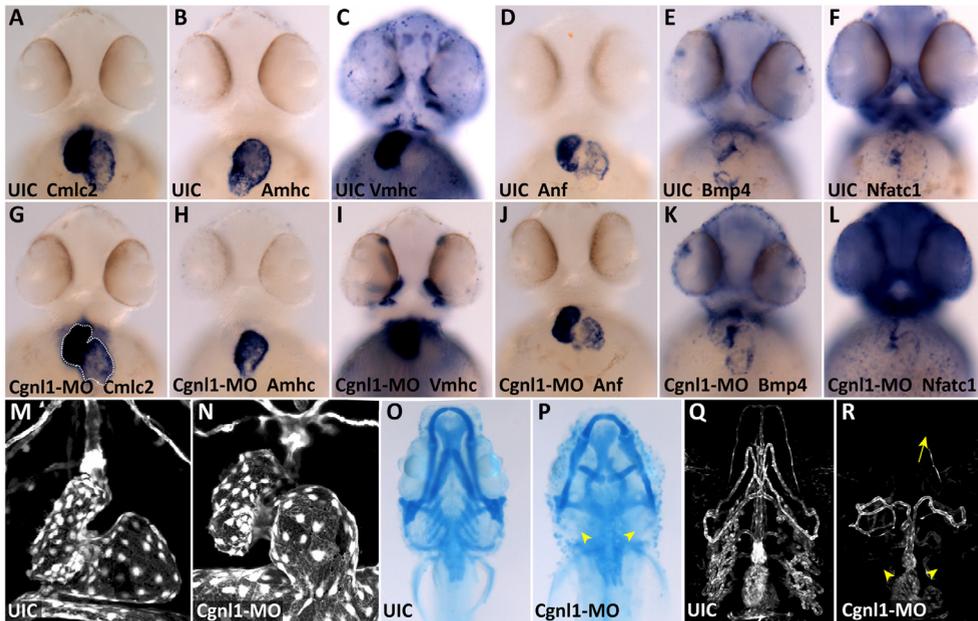
Supplemental figure 2

Global whole mount expression profiles of *adora2a*, *lrrc13*, *spnb2* and *stk10* at 24-28 hours post fertilization (hpf) are highly reminiscent of the expression of markers of the development of the blood lineage. Global whole mount expression profiles of *spnb2*, *anxa6*, *nfatc1*, *rhoc* and *slco3a1* at 24-28hpf are highly reminiscent of markers of cardiac development. Embryos are imaged from a lateral view (insets for *spnb2*, *anxa6*, *nfatc1* *rhoc* and *slco3a1* in dorsal view), anterior is to the left.



Supplemental figure 3

Cardiac development in *cgnl1* morphants was assessed by expression analysis of several cardiac markers at stages (56hpf) prior to the onset of the cardiac failure (5dpf) observed in *cgnl1* morphants. No changes were found in the expression of myocardial markers *cmlc2* (which labels all myocardial cells), *amhc* (which labels the myocardial cells of the atrium) and *vmhc* (which labels the myocardial cells of the ventricle) (compare A-C with G-I). Expression analysis of the markers *anf*, *bmp4* and *nfatc1* showed no apparent changes (compare D-F with J-L), indicating wildtype development of the cardiac valves. Confocal imaging of *cgnl1* morphants in a *kdr1:eGFP* background (which labels all endocardial cells) at 78hpf showed no morphologic defects when compared to wildtype siblings (M and N). Cartilage staining (alcian blue staining) of 5dpf old *cgnl1* morphants however, revealed gross abnormalities in cranio-facial development of these embryos compared to wildtype siblings (O and P). The gill-arches are completely lacking (yellow arrowhead in P), with a concurrent mis-patterning of the anterior part of the head. Similarly, confocal imaging of *cgnl1* morphants in a *kdr1:eGFP* background at 5dpf showed a loss the gill vasculature (aortic arches, yellow arrow) and absence of the hypobranchial artery (yellow arrowhead) (compare Q and R). All embryos are imaged from a ventral view, at the position of the head/heart region, anterior is to the top.



Reprinted with permission from:

(*Circ Res.* 2008;102:12-15.)

© 2008 American Heart Association, Inc.

***Circulation Research* is available at <http://circres.ahajournals.org>**

DOI: 10.1161/CIRCRESAHA.107.166066 12 Report

Redundant Roles for *Sox7* and *Sox18* in Arteriovenous Specification in Zebrafish

Robert Herpers, Esther van de Kamp, Henricus J. Duckers,*
Stefan Schulte-Merker*

3

From the Hubrecht Institute (R.H., S.S.-M.), Utrecht; and Molecular Cardiology Laboratory (R.H., E.v.d.K., H.J.D.), Experimental Cardiology, Thoraxcenter, Erasmus University Medical Center, Rotterdam, The Netherlands.

**Both authors contributed equally to this work.*



ABSTRACT

The specification of arteries and veins is an essential process in establishing and maintaining a functional blood vessel system. Incorrect arteriovenous specification disrupts embryonic development but has also been diagnosed in human syndromes such as hypotrichosis-lymphedema-telangiectasia, characterized by defects in blood and lymphatic vessels and associated with mutations in *SOX18*. Here we characterize the role of *sox7* and *sox18* during zebrafish vasculogenesis. *Sox7* and *sox18* are specifically expressed in the developing vasculature, and simultaneous loss of their function results in a severe loss of the arterial identity of the presumptive aorta which instead expresses venous markers, followed by dramatic arteriovenous shunt formations. Our study identifies members of the Sox family as key factors in specifying arteriovenous identity and will help to better understand hypotrichosis-lymphedema-telangiectasia and other diseases.

INTRODUCTION

Arteriovenous (AV) specification and differentiation are two critical events required for the progression of vascular development and function, as evidenced by diseases such as hypotrichosis-lymphedema-telangiectasia and hereditary hemorrhagic telangiectasia, which have been associated with mutations in *SOX18* and endoglin/activin-like receptor kinase-1, respectively (Irrthum et al., 2003; Sorensen et al., 2003; Urness et al., 2000). To study the process of AV specification, zebrafish embryos have proven particularly useful. Following the specification of arterial and venous cell types (Lawson et al., 2002), endothelial cells coalesce into cord-like midline structures and subsequently reshape into tubes (Jin et al., 2005). However, although several signaling molecules and transcription factors (Lawson et al., 2002; Liang et al., 2001; Fouquet et al., 1997; Sumanas et al., 2006) have been implicated in these processes, we are still only beginning to understand their regulation. In an attempt to identify new factors involved in the regulation of AV specification and vasculogenesis, we analyzed the function of *sox7* and *sox18*, which, together with the endodermally expressed *sox17*, form the Sox-F (Sry-related HMG box) family of DNA-binding proteins (Bowles et al., 2000). Members of the Sox-F family play crucial roles during the formation of definitive endoderm (Kanai-Azuma et al., 2002), hematopoietic stem cell regulation (Kim et al., 2007), and cardiovascular development (Pennisi et al., 2000). Here we show temporal and spatial overlap of *sox7* and *sox18* expression and identify functionally redundant roles for these genes during vascular development in zebrafish embryos. Our results demonstrate a novel role for *sox7* and *sox18* in specifying the molecular identity of endothelial cells in their commitment to arterial tissues during vasculogenesis.

MATERIALS AND METHODS**ZEBRAFISH HUSBANDRY**

Zebrafish (*Danio rerio*) were raised as described (Bussmann et al., 2007). Transgenic lines used were *Tg(vegfr4:gfp)*

s843 (Busmann et al., 2007), originally referred to as *Tg(flk1:EGFP)s843* (Jin et al., 2005), and *Tg(fli1a:gfp)y1* (Lawson and Weinstein, 2002).

HISTOLOGICAL PROCEDURES

In situ hybridization and immuno-histochemistry were performed as described (Jin et al., 2005; Busmann et al., 2007). The riboprobes used are specified in the online data supplement, available at <http://circres.ahajournals.org>.

MORPHOLINO INJECTIONS AND MICROANGIOGRAPHS

Procedures are specified in the online data supplement.

RESULTS AND DISCUSSION

EXPRESSION ANALYSIS FOR SOX7 AND SOX18

We first examined embryonic expression of *sox7* and *sox18*. RT-PCR expression analysis (Figure I in the online data supplement) revealed that *sox7* and *sox18* are provided maternally. In situ hybridization showed that *sox7* and *sox18* transcripts localized to the lateral mesoderm at 12 hours post fertilization (supplemental Figure I). Reminiscent of migrating angioblasts, these presumptive precursor cells localized to the midline during somitogenesis (supplemental Figure I) and finally homed to the endothelium of the axial, head, and intersegmental vessels at 26 hpf (Figure 1A and 1B). Cells expressing *sox7* and *sox18* are likely endothelial based on the expression pattern of these genes at later stages and the absence of mesodermal *sox7* and *sox18* expression in *cloche* mutants and *etsrp* morphants (Sumanas et al., 2006), both of which lack the endothelial lineage (supplemental Figure II). In addition, *sox7*-expressing cells were found in rhombomeres at 26 hpf (Figure 1A, arrowhead), whereas *sox18* expression was observed in the eye and retina (Figure 1B, arrowhead). The expression patterns of zebrafish *sox7* and *sox18* closely resemble the expression pattern of *Sox18* in mice (Pennisi et al., 2000).

MORPHOLINO KNOCKDOWN ANALYSIS OF SOX7 AND SOX18

Embryos injected with morpholinos (MOs) targeting *sox7* or *sox18* individually (two independent MOs for each gene; see supplemental Figure III for specificity tests) did not show any apparent morphological defects, or loss of endothelial cells (supplemental Figure I), or loss of circulation (supplementary Movies 2 to 3). Strikingly, on simultaneous injection of low amounts of both *sox7*- and *sox18*-MO, virtually all double knockdowns (dKDs) exhibited a loss of circulation in the posterior part of the embryo, whereas cardiac contractile function was normal (Figure 1E; supplementary Movie 1). Later, blood accumulated in a short circulatory loop near the heart leading to pericardial edema (>2 days post fertilization; not shown). Endothelial cells were specified in *sox7/sox18*-dKDs as demonstrated by *fli1a:gfp* expression, but we noticed poor segregation of artery and vein (compare supplemental Figure Ij and Im, insets). In addition, in microangiographs, the major axial vessels in the posterior part of *sox7/sox18*-dKDs were not filled with dye at 2 days postfertilization (Figure 1C and 1D). Dye injected into the sinus venosus drained from the heart into the posterior cardinal vein (PCV) rather than the dorsal aorta (DA) (Figure 1D, arrow). We conclude that combined loss of *sox7* and *sox18* function results in a severe disturbance of circulation.

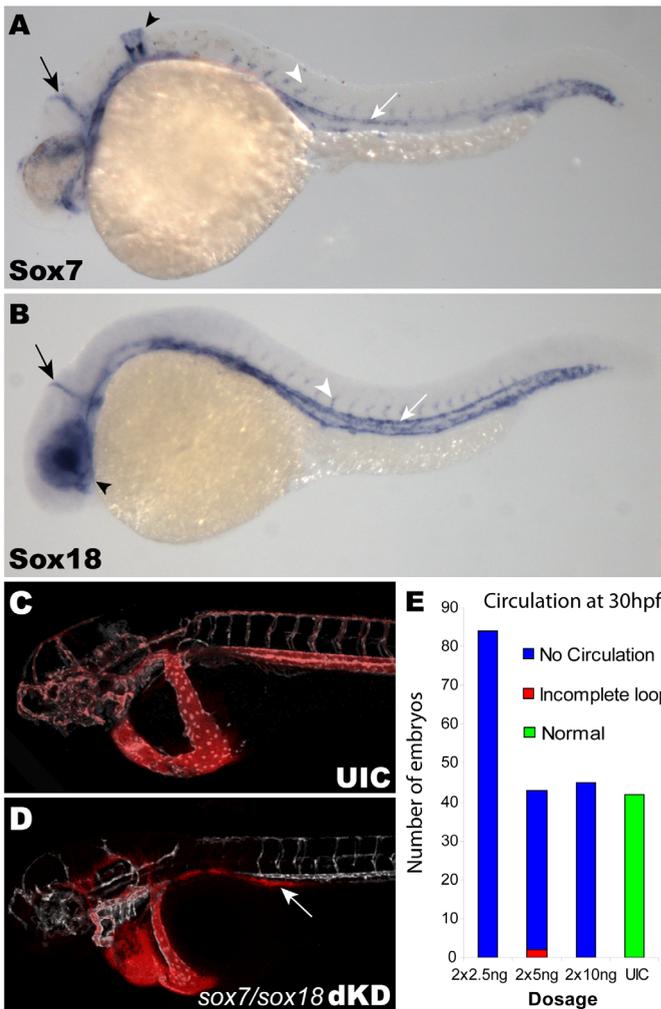


Figure 1. *Sox7* and *sox18* expression profiles and lack of trunk circulation in *sox7/sox18*-KDs. A and B, Twenty-six hours post fertilization, lateral view; anterior is to the left. A, *Sox7* expression is restricted to the endothelial cells of the main axial (white arrow), head (black arrow), and intersegmental (white arrowhead) vessels, as well as to 2 rhombomeres (black arrowhead). B, *Sox18* expression is restricted to endothelial cells of the main axial (white arrow), head (black arrow), and intersegmental (white arrowhead) vessels, as well as to the eye (black arrowhead). C and D, Confocal images of microangiographs at 2.5 days postfertilization of an uninjected *vegfr4:gfp* embryo (C) and a *vegfr4:gfp sox7/sox18*-dKD embryo (D). Dye injected into the sinus venosus drained from the heart into the posterior cardinal vein rather than the dorsal aorta (arrow) in *sox7/sox18*-dKDs. E, Near-complete loss of circulation in the posterior part of the embryo is consistently observed in *sox7/sox18*-dKDs, as evidenced by different injection regimes using varying concentrations of the respective morpholinos. dKD, double knockdown.

ARTERIOVENOUS SPECIFICATION AND VASCULAR TUBE FORMATION IN *SOX7/SOX18*-DKDs

To further investigate this phenotype, we analyzed the expression of several molecular markers in *sox7/sox18*-dKDs compared with uninjected control embryos or silent heart morphants (Sehnert et al., 2002). No alteration was detectable in the primitive erythroid lineage marker *gata1* (supplemental Figure IV), *vegfr* receptors 2 and 4, or pan-endothelial markers like *tie2*, *cdh5*, and *fli1a* (not shown). However, we observed a dramatic decrease in the expression of arterial markers *notch3*, *ephrinB2a* (Figure 2A through 2D), and *dll4* (supplemental Figure IV) and a concurrent increase in the expression of venous markers *dab2* and *flt4* in arterial tissues, such as the DA and intersegmental vessels (supplemental Figure IV and Figure 2C and 2F, respectively). These results suggest a key role for *sox7* and *sox18* in specifying the arterial fate of endothelial cells. A possible shift in AV identity attributable to the lack of circulation was excluded by analyzing silent heart morphants,

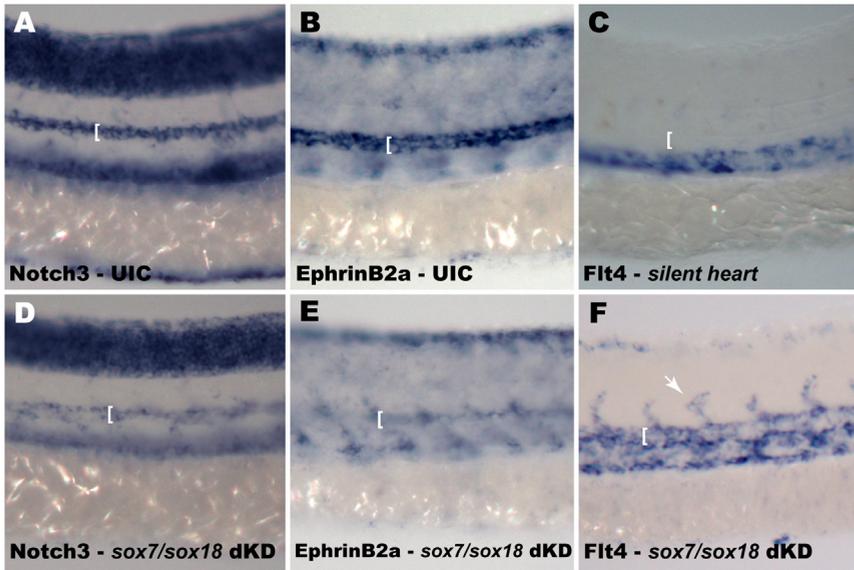


Figure 2. Arterial specification is perturbed in *sox7/sox18*-dKDs. A and B, Uninjected control embryos. C, Silent heart morphant. D through F, *sox7/sox18*-dKDs. All embryos were at 26 hpf; *notch3* (A and D), *ephrinB2a* (B and E), *flt4* (C and F). A, B, D, and E, Note the dramatic reduction in expression levels of arterial markers *notch3* and *ephrinB2a* in the dorsal aorta (brackets) in *sox7/sox18*-dKDs. C and F, Ectopic expression of the venous marker *flt4* in the dorsal aorta (brackets) and intersegmental vessels (white arrow) in *sox7/sox18*-dKDs.

D, and E, Note the dramatic reduction in expression levels of arterial markers *notch3* and *ephrinB2a* in the dorsal aorta (brackets) in *sox7/sox18*-dKDs. C and F, Ectopic expression of the venous marker *flt4* in the dorsal aorta (brackets) and intersegmental vessels (white arrow) in *sox7/sox18*-dKDs.

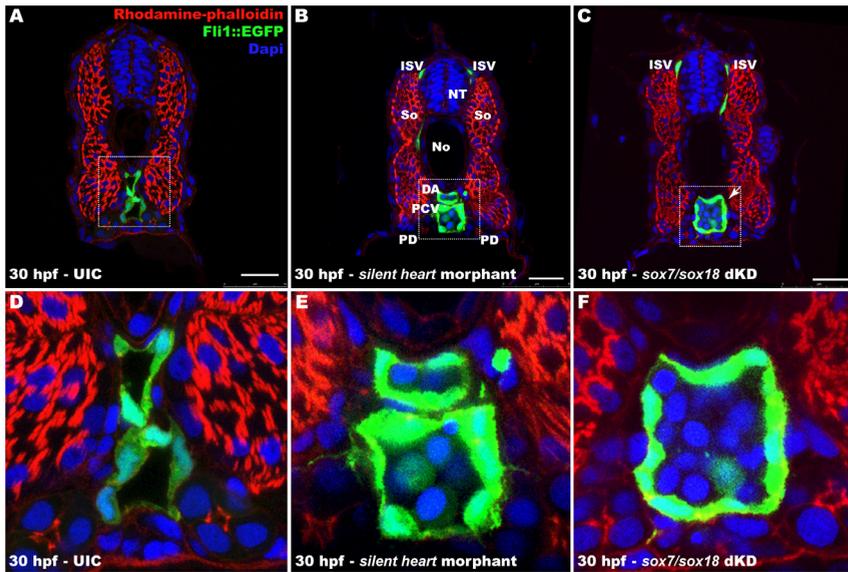


Figure 3. Vascular tube formation is perturbed in *sox7/sox18*-dKDs. Transverse sections of the trunk region of 30 hpf *fli1a:gfp* embryos, stained with phalloidin (red) and DAPI (blue). Two distinct, lumenized vessels (the DA and the PCV) can be observed in uninjected control embryos (A and D) and silent heart morphants (B and E). C and F, *Sox7/sox18*-dKDs show a fusion of the DA and PCV (white arrow). ISV indicates intersegmental vessel; No, notochord; NT, neural tube; PD, pronephric duct; So, somites. Scale bar in A through C, 25 μ m.

C and F, *Sox7/sox18*-dKDs show a fusion of the DA and PCV (white arrow). ISV indicates intersegmental vessel; No, notochord; NT, neural tube; PD, pronephric duct; So, somites. Scale bar in A through C, 25 μ m.

which showed no alteration in marker gene expression (Figure 2C and supplemental Figure VI). This demonstrates that *sox7* and *sox18* are essential regulators of AV identity. To better understand the lack of lumen formation observed in *sox7/sox18*-dKDs in microangiographs, we next examined transverse sections of *sox7/sox18*-dKDs, uninjected control embryos, and silent heart morphants. The nonvascular morphology in *sox7/sox18*-dKDs (Figure 3C) was completely normal, suggesting a vessel-specific phenotype. Uninjected controls and silent heart morphants exhibited normal segregation and lumenization of axial vessels (Figure 3A, 3B, 3D, and 3E). In all *sox7/sox18*-dKDs (n=16), we observed stretches of normal and physically separated axial vessels, alternating with regions where only a single PCV was present. At particular locations in *sox7/sox18*-dKDs, the DA apparently fused with the PCV (Figure 3C and 3F; see also supplemental Figure V). We conclude that the combined loss of Sox7 and Sox18 function disrupts AV specification and leads to severe shunt formation. Our study provides novel insights into the molecular roles of *sox7* and *sox18*, which are essential to the specification of the molecular identity of the dorsal aorta during embryogenesis and possibly during later stages of life. These findings, for the first time, offer direct insights into the molecular consequences of Sox function in endothelial cells at the *in vivo* level. Understanding the requirement for Sox7 and Sox18 in the process of arteriovenous specification might help to better understand syndromes such as hypotrichosis-lymphedema-telangiectasia and hereditary hemorrhagic telangiectasia.

ACKNOWLEDGMENTS

We thank G. Soete, B. Hogan, J. Bussmann, J. Korving, J. Peterson-Maduro and L. de Windt for help with the manuscript and the anonymous reviewers for helpful suggestions.

SOURCES OF FUNDING

This work was supported by a VIDI grant (H.J.D.) and the Royal Netherlands Academy of Arts and Sciences (S.S.-M.).

DISCLOSURES

None.

SUPPLEMENTAL MATERIAL

SUPPLEMENTAL MATERIAL

Supplementary information, including 6 figures and 3 movies can be found in the data supplement or online, at <http://circres.ahajournals.org>.

ZEBRAFISH HUSBANDRY

Zebrafish (*Danio rerio*) embryos were obtained from wild-type strains and raised at 28°C as previously described. The transgenic line *Tg(vegfr4:gfp)s843*, originally referred to as *Tg(flk1:EGFP)s843* was obtained from Didier Stainier (San Francisco, CA, USA). The transgenic line *Tg(fli1a:gfp)y1* was obtained from Brant Weinstein (Bethesda, ML, USA). Homozygous mutant *cloche* or *scl* (*tal1t21384*) embryos were obtained by incrossing these fish.

RT-PCR ANALYSIS

cDNA was synthesized from RNA isolated from 0, 1, 2.5, 6, 8, 10 and 24 hours post fertilization old embryos using the SuperScript II RT Kit (Invitrogen). Primers used for reverse transcriptase PCR were:

sox7-Fwd: 5'-ACCAGCTGCTCACTCAAAC-3'
sox7-Rev: 5'-GATCTCTGAAGACCTGACG-3'
sox18-Fwd: 5'-ACACTTCCGAGACCTCCAC-3'
sox18-Rev: 5'-GGTCAAACCAATCCTGTCC-3'

WHOLE-MOUNT IN SITU HYBRIDIZATION AND IMMUNO-HISTOCHEMISTRY

Whole-mount in situ hybridization was performed as previously described. Previously described riboprobes used in this manuscript were: *notch3*, *ephrinB2a*, *dll4*, *dab*, *flt4*, *vegf-receptors 2 and 4*, *gata1*, *tie2*, *cdh5*, *fli1a*. Bacterial clones for *sox7* and *sox18* were obtained from Open Biosystems (<http://www.openbiosystems.com>). Embryos were mounted in glycerol and documented with a Zeiss axioplan mounted with a Leica DFC 480 camera.

Immuno-histochemistry was performed as previously described. Briefly, embryos were fixed overnight with 2% paraformaldehyde and embedded in 4% low melting point agarose (Invitrogen). Embedded embryos were cut using a HM650V vibratome (Microm) into 250µm sections. Filamentous actin was visualized with rhodamine phalloidin (Fluka). Nuclei were visualized with 4,6-diamino-2-phenylindole (DAPI) (Sigma). Processed samples were mounted in Aquamount improved (BDH laboratory supplies) and imaged using a Leica TCS SPE confocal microscope.

MORPHOLINO INJECTIONS AND MICROANGIOGRAMS

Morpholinos (MOs) were obtained from Gene Tools (<http://www.gene-tools.com>) and diluted in water containing 0.2% phenol red. One cell stage embryos were injected (maximum volume of 2nl) as described. Live embryos were anaesthetized using MS222 and mounted in a glass-bottom dish containing 0.4% agarose. Images were taken with a LEICA CLSM SP2 AOBS confocal microscope. Confocal microangiography was performed as described. Embryos were injected with *silent heart*, *etsrp*, or *sox7* and *sox18* specific morpholinos. Morpholino (MO) sequences were:

MO*sox7*-ATG: 5'-CGCACTTATCAGAGCCGCCATGTGC-3'
MO*sox18*-ATG: 5'-ATATTCATTCCAGCAAGACCAACAC-3'
MO*sox7*-UTR: 5'-CTGTCAAACCTTAGGCTTCCTTTTG-3'
MO*sox18*-UTR: 5'-AGCAAGCTGTTGTCTTTGAGTAAAG-3'
MO*silent heart*: 5'-CATGTTTGCTCTGATCTGACACGCA-3'
MO*etsrp*: 5'-CACTGAGTCCTTATTTCACTATATC-3'

MOVIE LEGENDS

SUPPLEMENTARY MOVIE 1.

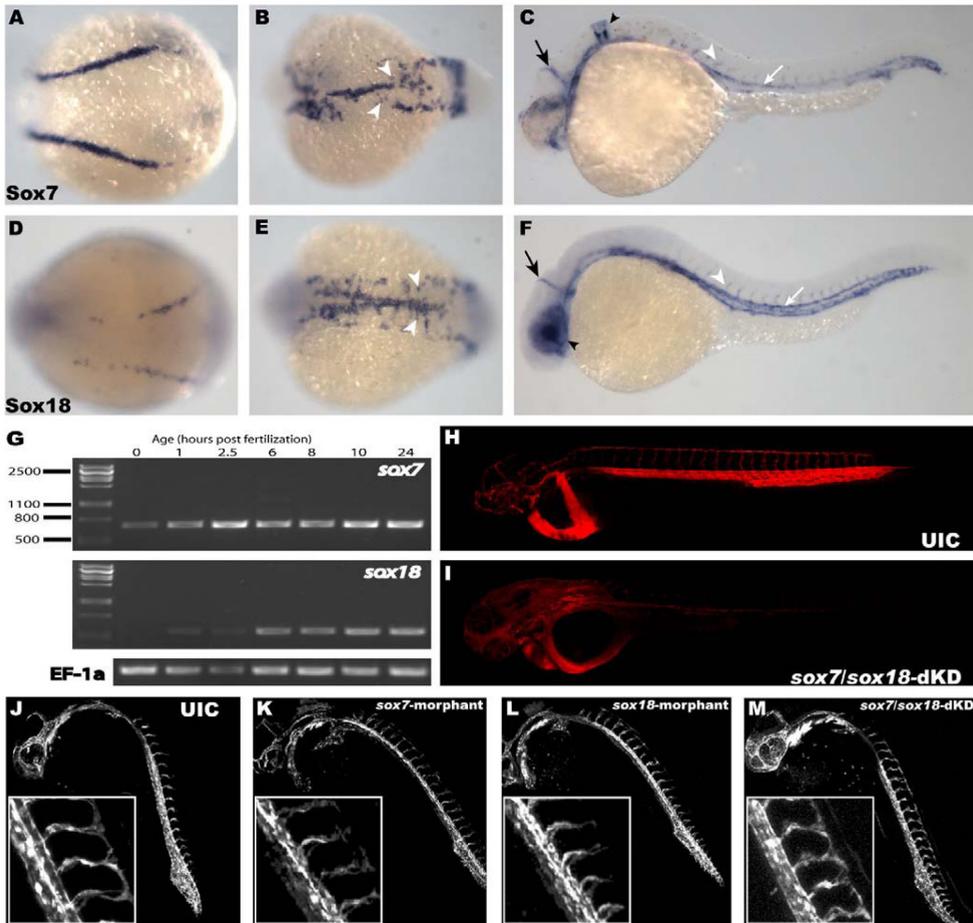
Phase-contrast movie showing circulation in trunk and tail of an uninjected control embryo at 2.5dpf (top, dorsal is up) and loss of circulation in trunk and tail of a *sox7/sox18*-dKD embryo at 3dpf (bottom, ventral is up). Anterior is to the right.

SUPPLEMENTARY MOVIE 2.

Phase-contrast movie showing circulation in trunk and tail of an uninjected control embryo at 2.5dpf (top, dorsal is up) and a *sox7*-morphant embryo at 2.5dpf (bottom, dorsal is up). Anterior is to the left.

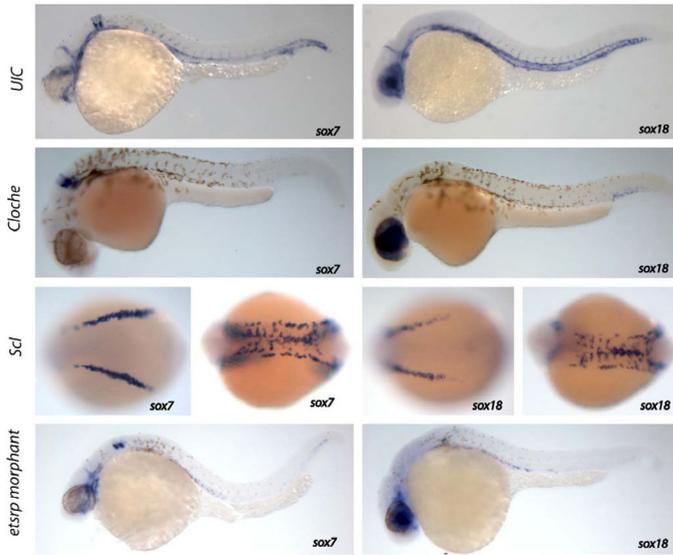
SUPPLEMENTARY MOVIE 3.

Phase-contrast movie showing circulation in trunk and tail of an uninjected control embryo at 2.5dpf (top, dorsal is up) and a *sox18*-morphant embryo at 2.5dpf (bottom, dorsal is up). Anterior is to the left.



SUPPLEMENTARY FIGURE 1: SOX7 AND SOX18 EXPRESSION AND LACK OF TRUNK CIRCULATION IN SOX7/SOX18-DKDs

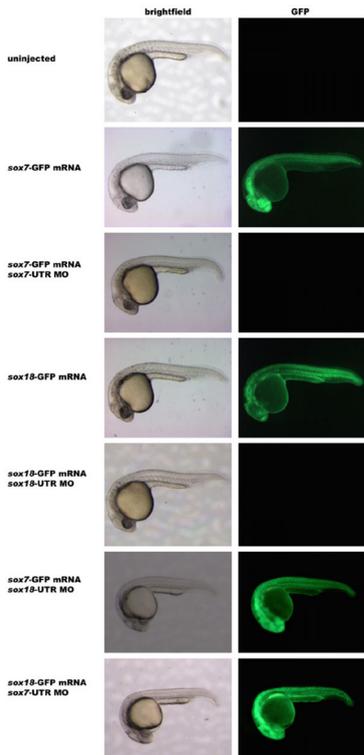
a-c. Expression profile of *sox7* (**a**) At 12hpf, *sox7* is expressed in the lateral mesoderm of the embryo. (**b**) At 18hpf, *sox7* expression is found in a cord-like structure (future DA and PCV) and in presumptive migrating angioblasts (arrowheads). (**c**) At 26 hpf (lateral view), *sox7* expression is restricted to the endothelial cells of the main axial (white arrow), head (black arrow) and intersegmental (white arrowhead) vessels, as well as to two rhombomeres (black arrowhead). **d-f.** Expression profile of *sox18* (**d**) At 12hpf, *sox18* is expressed within the lateral mesoderm of the embryo. (**e**) At 18hpf, *sox18* expression is found in a cord-like structure and in presumptive migrating angioblasts (arrowheads). (**f**) At 26 hpf (lateral view), *sox18* expression is restricted to endothelial cells of the main axial (white arrow), head (black arrow), and intersegmental (white arrowhead) vessels, as well as to the eye (black arrowhead). (**g**) RT-PCR expression analysis showed maternal expression of both *sox7* and *sox18*, expression levels for *sox18* however are lower at 0, 1 and 2.5 hours post fertilization compared to expression levels for *sox7*. *Sox7* and *sox18* mRNA expression shown for 0, 1, 2.5, 6, 8, 10 and 24 hours post fertilization old embryos. **h-i.** Microangiographies at 2.5 dpf. Major axial vessels in the posterior part of *sox7/sox18*-dKDs were not filled with dye. **j-m.** Confocal images (30hpf) of (**j**) an uninjected *fli1a:gfp* embryo, (**k**) a *vegfr4:gfp* embryo injected with 10ng of *sox7*-MO, (**l**) a *vegfr4:gfp* embryo injected with 10ng of *sox18*-MO and (**m**) a *fli1a:gfp* embryo injected with 5ng of both *sox7*-MO and *sox18*-MO. Insets show magnifications at the posterior level of the trunk. (**m, inset**) Note the partial fusion of the DA and PCV in *sox7/sox18*-dKDs. DA, dorsal aorta; dKD, double knock-down; MO, morpholino; PCV, posterior cardinal vein.



**SUPPLEMENTARY FIGURE 2:
SOX7 AND SOX18 EXPRESSION IN
CLOCHE MUTANTS, SCL MUTANTS
AND ETSRP MORPHANTS**

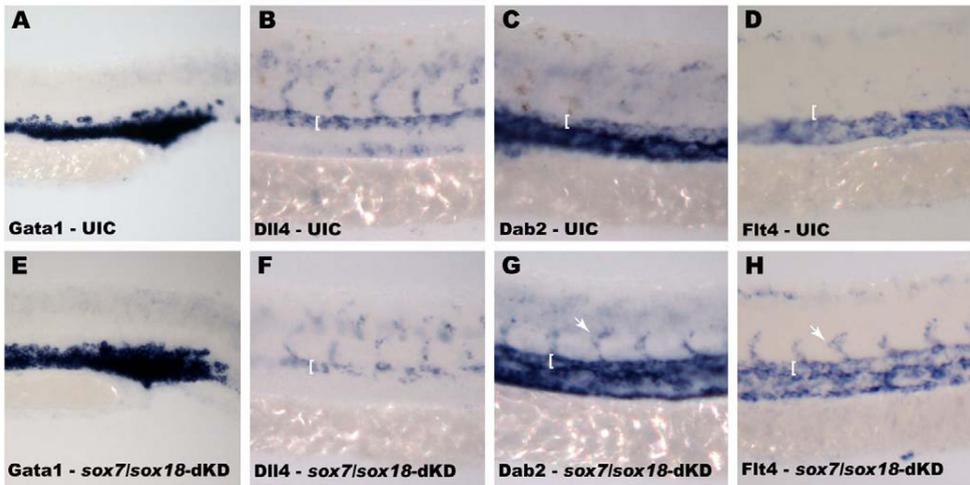
Whole mount in situ hybridization expression analysis for *sox7* and *sox18* in embryos defective in the blood lineage, the endothelial lineage or both. Mesodermal *sox7* and *sox18* expression was lost in *cloche* mutants, which lack nearly all blood and endothelial cells. Early *sox7* and *sox18* expression in *scl* mutants, defective in dorsal aorta as well as blood formation, appeared normal. Mesodermal *sox7* and *sox18* expression was vastly reduced in *etsrp* morphants, which lack the endothelial lineage only.

Based on these results and the expression pattern of these genes at later stages we conclude that *sox7* and *sox18* expression is restricted to the endothelial lineage and does not contribute to other cell lineages derived from the mesoderm.



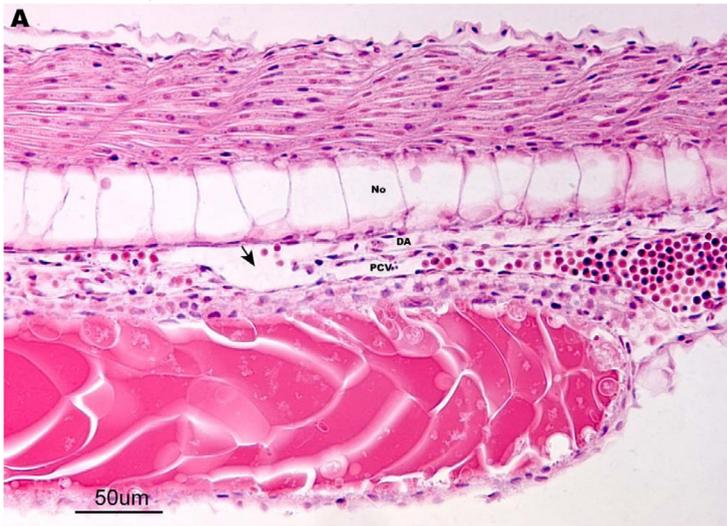
SUPPLEMENTARY FIGURE 3: MORPHOLINO SPECIFICITY CONTROLS

MO*sox7*-ATG-, MO*sox18*-ATG-, MO*sox7*-UTR- and MO*sox18*-UTR-binding sites were cloned into pCS2+, which contained a transcript encoding for GFP, upstream of the translation initiation site. Translation of capped mRNA was efficiently blocked by the respective MOs, demonstrating efficacy and specificity (*sox7*-MO does not block *sox18* translation) of the reagents used. Results shown for MO*sox7*-UTR- and MO*sox18*-UTR; similar results were obtained with MO*sox7*-ATG-, MO*sox18*-ATG. Given the efficacy and specificity of the MOs used, we did not perform rescue experiments by co-injection of *sox7*- or *sox18*-mRNA.



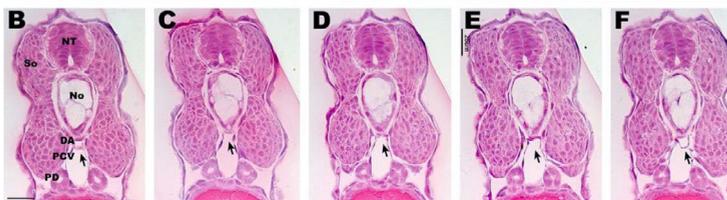
SUPPLEMENTARY FIGURE 4: ARTERIAL SPECIFICATION IS PERTURBED IN SOX7/SOX18-DKDs

a-d. Uninjected control embryos; e-h. *sox7/sox18*-dKDs. All embryos at 26hpf. (a,e) *gata1*, (b,f) *dll4*, (c,g) *dab2*, (d,h) *flt4*. (a,e) Levels of *gata1* appear normal in *sox7/sox18*-dKDs. (b,f) Note the dramatic reduction in expression levels of the arterial marker *dll4* in the dorsal aorta (brackets) in *sox7/sox18*-dKDs. (c,d; g,h) Ectopic expression of the venous markers *dab2* and *flt4* in the dorsal aorta (brackets) and intersegmental vessels (white arrow) in *sox7/sox18*-dKDs. dKD, double knock-down.

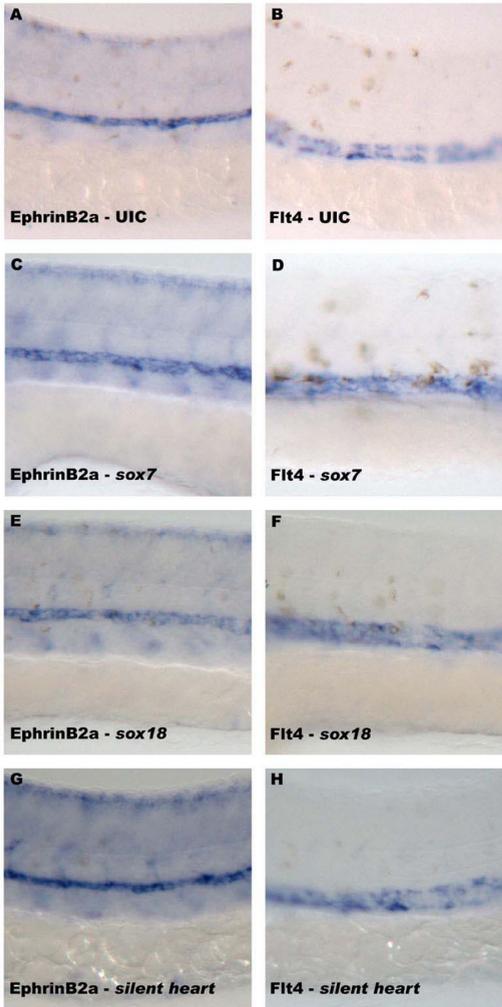


SUPPLEMENTARY FIGURE 5: VASCULAR TUBE FORMATION IS PERTURBED IN SOX7/SOX18-DKDs

The lack of lumen formation observed in *sox7/sox18*-double knock downs (dKDs) was examined in both sagittal and transverse 7µm thick sections of *sox7/sox18*-dKDs and uninjected control (UIC) embryos. a. Sagittal section of the tail section of a 30hpf *sox7/sox18*-dKD (n=10) showing shunt formation between DA and PCV, indicated by the arrow. No shunts were observed in a comparable number of UIC embryos (data not shown). b-f. Consecutive transverse sections of the midtrunk region of a 30hpf *sox7/sox18*-dKD, showing the loss and reappearance of the physical boundary between the DA and PCV, indicated by the arrows. This is a representative case from 10 examined *sox7/sox18*-dKDs. No shunts were observed in UIC embryos (n=10) (data not shown). Sections were stained with hematoxylin and eosin. Scale bar in b-f 25 µm.

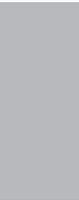


indicated by the arrows. This is a representative case from 10 examined *sox7/sox18*-dKDs. No shunts were observed in UIC embryos (n=10) (data not shown). Sections were stained with hematoxylin and eosin. Scale bar in b-f 25 µm. NT, neural tube; No, notochord; So, somites; DA, Dorsal Aorta; PCV, Posterior Cardinal Vein; PD, pronephric duct.



SUPPLEMENTARY FIGURE 6: ARTERIOVENOUS SPECIFICATION IS UNALTERED IN *SOX7*-, *SOX18*- AND SILENT HEART MORPHANTS

a,b. Uninjected control (UIC) embryos; **c-d.** *sox7*-morphants; **e-f.** *sox18*-morphants; **g-h.** *silent heart*-morphants. Expression analysis of 26 hpf old embryos using the markers (**a,c,e,g**) *ephrinB2a* or (**b,d,f,h**) *flt4* as a probe. *Sox7*- and *sox18*-morphants show normal levels of expression for *ephrinB2a* and *flt4* compared to *sox7/sox18*-double knock downs (**Figure 2 and Supplementary Figure 4**), confirming the observed redundancy amongst *sox7* and *sox18*. Expression levels of the markers tested appeared normal in *silent heart*-morphants, excluding the possibility of a shift in arteriovenous identity caused by a lack of circulation.



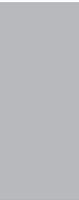
The G protein-coupled receptor Agtr1b controls early zebrafish angiogenesis

Robert Herpers^{1,2}, Joëlle Kartopawiro², Stefan Schulte-Merker²,
Henricus J Duckers¹

4

1. *Experimental Cardiology, Thoraxcenter, Erasmus University Medical Center, 's-Gravendijkwal 230, 3015 CE Rotterdam, The Netherlands.*

2. *Hubrecht Institute-KNAW & University Medical Centre, Utrecht, Uppsalalaan 8, 3584 CT Utrecht, The Netherlands.*



ABSTRACT

The G protein-coupled receptor Angiotensin receptor like 1b (Agtr1b, APJ, Msr) is expressed in the developing vasculature where it serves as a receptor for the small peptide Apelin. Recent studies showed an indispensable role for Agtr1b-Apelin signaling in controlling heart field formation. Here we report a novel role for Agtr1b in facilitating angiogenic sprout migration from the dorsal aorta in early zebrafish development independent of cardiac specification. We show that *agtr1b* mutant fish exhibit normal cell numbers in sprouting intersegmental vessels, but that the tip-cells of the intersegmental vessels display abnormal filopodic behavior and that the migration of the intersegmental vessels is defective.

INTRODUCTION

The vertebrate vascular system is critical for the uptake and exchange of gases, nutrients, delivery of hormones, and for facilitating immune responses. The development of a functional vasculature involves the specification of arteries, veins and lymphatic vessels in a timely and spatially highly coordinated fashion. A strong hierarchical control of genetic factors enables the coordinated sprouting, proliferation and migration of endothelial cells in a process called angiogenesis. Factors including the *vegf-receptors* (Ferrara et al., 1997), *scl* (Patterson et al., 2005) and *plcy* (Lawson et al., 2003) have been shown to be indispensable for early angiogenic sprouting from the dorsal aorta (DA) of the developing zebrafish embryo. Other factors like *semaphorins* and *plexins* (Torrez-Vasques et al., 2004) in turn guide the patterning of the developing vasculature. Although several factors have been described in early angiogenesis, this process is yet not fully understood.

Recently, two independent studies in zebrafish showed a critical role for Agtr1b in myocardial specification, but reported no Agtr1b function in vascular development despite its restricted expression in the vasculature (Scott et al, 2007; Zeng et al, 2007). Two similar studies in *Xenopus* reported differing findings; whereas one study showed perturbed intersegmental vessel branching (Cox et al, 2006), another study showed a more pronounced effect on cardiovascular development (Inui et al, 2006). The nature of these discrepancies is largely unclear, but is in part ascribed to differences in the experimental setup (Kälin et al., 2007). Knockout studies in mice showed a hypotensive effect for APJ but reported no vascular abnormalities (Ishida et al., 2004), whereas Apelin deficient mice showed a retardation of retinal vascular development (Kasai et al., 2008). Apelin signaling has also been associated with regenerative and tumour (neo)angiogenesis (Eyries et al., 2008; Sorli et al., 2007; Kälin et al., 2007) and has recently become a promising target for drug development (Masri et al., 2005; Sorli et al., 2006).

In this study we used reverse genetics to generate an Agtr1b knockout zebrafish. As reported previously the embryos display a loss of cardiomyocytes in only a limited subset of the mutant embryos (Scott et al, 2007). Strikingly, all mutant embryos failed to form fully grown ISVs and had no dorsal longitudinal anastomotic vessel (DLAV). We show that

defective ISV outgrowth in *agtrl1b* mutant embryos is independent of blood flow and is not caused by a lower number of cells per ISV, but rather by defective migration of the ISVs and concurrent abnormal filopodic behavior of the tip-cells of the ISVs.

MATERIALS AND METHODS

ZEBRAFISH

Zebrafish were kept under standard husbandry conditions at the Hubrecht Institute. Transgenic lines used were Tg(*kdr-l:GFP*)^{s843} (Jin et al., 2005) and Tg(*fli1:neGFP*)⁷ (Roman et al., 2002).

TILLING OF *AGTRL1B*

A library of randomly ENU mutagenized F₁-zebrafish was screened for mutations in the *agtrl1b* gene by DNA resequencing (Wienholds, 2002). After filtering for SNPs, 26 ENU-induced mutations were detected of which one led to a premature stop just after the first transmembrane domain (W54Stop). The identified F₁ carrier fish (*agtrl1b*^{W4145}) was crossed into the desired transgenic backgrounds and bred for several generations (up to F₃) to remove the majority of background mutations. Primers used for TILLING were:

Ag1-1A-1-5'-GACCTGAGCACATGACAAAC-3',

Ag1-1A-2-5'-TGATAAACGACGGCCAGTTGGACAACATGACTGCTGAC-3',

Ag1-1A-3-5'-AGGAAACAGCTATGACCATCAGATGGCTGTGAGAGAGG-3' and

Ag1-1A-4-5'-ATACACTGTGTGCGGAAG-3'.

MORPHOLINO INJECTIONS

Morpholinos (MOs) against silent heart (SIH) (5'-CATGTTGCTCTGATCTGACAGCA-3') (Sehnert et al., 2002) were obtained from Gene Tools <http://www.gene-tools.com> and diluted in water containing 0.2% phenol red. One cell stage embryos were injected with 1ng of MO with a maximum volume of 1nl.

HISTOLOGICAL AND IMAGING PROCEDURES

Whole-mount *in situ* hybridization was performed as previously described (Zeng et al., 2007). Bacterial clones for *apln* and *agtrl1b* were obtained from Open Biosystems <http://www.openbiosystems.com>. Immunohistochemistry (rabbit α GFP 1:200) was performed as described previously (Jin et al., 2005) following *in situ* hybridization immediately after the staining was completed.

Embryos were mounted in 1% low melting point agarose in a culture dish with a cover slip replacing the bottom. Imaging was performed with a Leica Microsystems SP2, SPE or SP5 confocal microscope using a 10x, 20x or 40x objective with digital zoom. Timelapse movies were assembled using ImageJ. Cellcounts were performed using Velocity software (PerkinElmer). Angiography was performed as previously described (Weinstein et al., 1995). Images were processed by using Photoshop CS2 and Illustrator CS2 (Adobe).

STATISTICAL ANALYSES

Calculations for mean, standard deviation, the probability associated with the Student's t-test were carried out in Microsoft Excel.

RESULTS

EXPRESSION ANALYSIS FOR *APLN* AND *AGTRL1B*

We examined the expression of *agtrl1b* and its ligand *apln* at 24 hours post fertilization (hpf) and found *agtrl1b* to be expressed in the vascular system (Fig. 1A), whereas *apln* was found at the dorsal side of the trunk where the future DLAV will form (Fig. B) as reported previously (Zeng et al., 2007). Immunohistochemistry using α GFP in Tg(*kdr-l:GFP*)^{s843} fish immediately following *in situ* hybridisation showed a colocalization of *agtrl1b* in all cells of the ISV (Fig. 1C).

GENERATION OF AN AGTRL1B MUTANT

After screening of a library of randomly ENU mutagenized F_1 -zebrafish a premature stop (Fig. 1D) just after the first transmembrane domain (W54Stop) (Fig. 1E) was identified for *agtrl1b*. The identified mutant carrier was crossed into the desired transgenic backgrounds.

ANALYSIS OF AGTRL1B^{-/-} MUTANT FISH REVEALS AN ANGIOGENESIS DEFECT

Agtrl1b mutant analysis showed a loss or reduction of the heart field in only a limited number of embryos (13.8%, n=58) similar to what was reported previously (Scott et al., 2007), whereas defective ISV sprouting surprisingly was found at a Mendelian ratio (24.1%, n=58). Major vessels like the DA and the Posterior Cardinal Vein (PCV) formed normally, and showed normal expression of markers like *ephB2a*, *flt4*, *kdr-1* and *cdh5* (data not shown). Circulation was initiated normally in a subset of mutant embryos (10.3%, n=58), but to our surprise the ISVs that sprout from the DA failed to complete migration to the dorsal side of the trunk and no DLAV was ever formed (Fig. 1F,G).

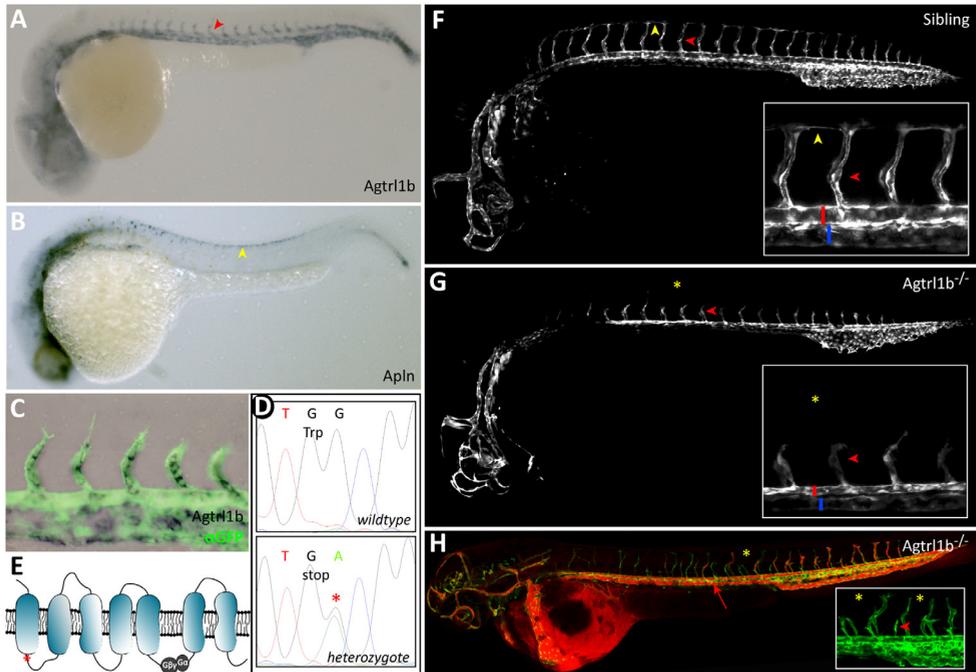


Fig. 1. Zebrafish *agtrl1b* mutants display defects of the intersegmental vessels. (A-C) Expression patterns for *agtrl1b* and *apl*n at 24 hours post fertilization (hpf). *Agtrl1b* is expressed in the dorsal aorta (DA), posterior cardinal vein (PCV) and intersegmental vessel (ISV) (A, red arrowhead) and colocalizes with the pan-endothelial marker *kdr-1* (C). *Apl*n is expressed at the dorsal side of the trunk at the location of the future dorsal longitudinal anastomotic vessel (DLAV) (B, yellow arrowhead). **(D and E)** Screening of a library of ENU mutagenized F_1 -zebrafish for mutations in the *agtrl1b* gene by DNA resequencing identified a G>A mutating (see chromatogram in D), changing a Tryptophan residue to a premature stop (W54Stop) just after the first transmembrane domain (E). **(F-H)** Confocal analysis of *agtrl1b* mutants in a Tg(*kdr1*:GFP)^{S843} background at 28hpf showed normal development of the DA (red bar), PCV (blue bar), ISVs (red arrowhead) and DLAV (yellow arrowhead) in wildtype siblings (F, inset). *Agtrl1b^{-/-}* mutant embryos displayed normal development of the DA (red bar) and PCV (blue bar), but had abnormal ISVs (red arrowhead) and completely lacked a DLAV (yellow asterisk) (G, inset). Angiographies at 50 hpf in *agtrl1b^{-/-}* embryos demonstrated flow in major vessels like the DA and PCV (H).

Closer analysis of the observed phenotype by confocal timelapse analysis revealed normal timing of the initial sprouting of ISVs from the DA in *agtrl1b* mutants. After initial sprouting the ISVs migrated towards the dorsal side of the embryo at a lower pace relative to wildtype siblings, only to stall halfway the dorso-ventral axis of the trunk (Supplementary movies 1 and 2; supplementary figure 1).

DEFECTIVE ARTERIAL SPROUTING IN *AGTRL1B*^{-/-} MUTANT FISH IS INDEPENDENT OF FLOW

To rule out the possibility that perturbed angiogenic sprouting in *agtrl1b* mutants is caused by a reduction or lack of blood flow (Lawson and Weinstein, 2002), we performed angiographies at 50 hpf which demonstrated flow in major vessels like the DA and PCV (Fig. 1H). At this stage, after which secondary sprouting from the PCV has taken place (Isogai et al., 2003), some ISV had lumenized and migrated to the dorsal side of the trunk and these blunt-ended vessels would readily take up dye. Formation of a DLAV however was never observed. To further investigate the importance of flow on angiogenic sprouting from the DA we injected *silent heart* (SIH) morpholinos, which have been shown to effectively block cardiac contractility and thus blood flow (Sehnert et al., 2002) and assessed ISV sprouting in these morphants by confocal timelapse analysis. Normal sprouting of ISVs and formation of a DLAV in these morphants was observed (supplementary figure 1), indicating that ISV sprouting, DLAV formation and migration from the DA towards the dorsal side of the trunk is independent of flow.

***AGTRL1B*^{-/-} ISVS HAVE NORMAL NUMBERS OF CELLS BUT ALTERED FILOPODIC BEHAVIOR**

As *Apln* has been suggested as a mitogenic factor (Cox et al., 2006), we investigated the number of cells in ISVs in *agtrl1b* mutants at 28 hpf, when most wildtype siblings had started to form a DLAV, using *fli:neGFP* embryos, which express nuclear localized eGFP in all endothelial cells (ECs). Surprisingly, we found the number of nuclei per ISV in *agtrl1b* mutants (2.76 ± 0.93 , $n=330$ in 55 embryos) to be almost identical to that of wildtype counterparts (2.73 ± 0.97 , $n=348$ in 58 embryos) (Fig. 2A-C). Although they proliferated normally, the ECs of *agtrl1b* mutant ISVs failed to both elongate and to migrate towards the dorsal side of the trunk, but rather stayed compacted in close proximity to their origin of sprouting from the DA (compare Fig. 2A and Fig. 2B).

Typically, two different cell populations are distinguished within a sprouting vessel; the leading tip-cell and the stalk-cells, which are both specialized in a distinct manner (Gerhardt et al., 2003; Phng and Gerhardt, 2009). The tip-cell is characterized by guided migration, has numerous actin rich filopodic protrusions and hardly ever proliferates. The stalk-cells on the other hand are capable of proliferation and form the vascular lumen. As we found no alteration in typical stalk-cell behavior, we determined whether more features of the tip-cell besides migration were affected in *agtrl1b* mutants. We analyzed individual ISVs in both wildtype and mutant embryos and categorized them for having normal (I), moderate (II) or weak (III) filopodic behavior (Fig. 2D-F). Whereas most wildtype ISV could be placed in categories (I) & (II), the mutant genotype was almost completely absent from category (I), but was enriched in the category of weak sprouting (III) (Fig. 2G). These data show that

defective ISV outgrowth in *agtrl1b* mutant embryos is not caused by a lower number of cells per ISV, but rather by abnormal filopodic behavior of the tip-cells of the ISVs which potentially causes the migratory defects observed.

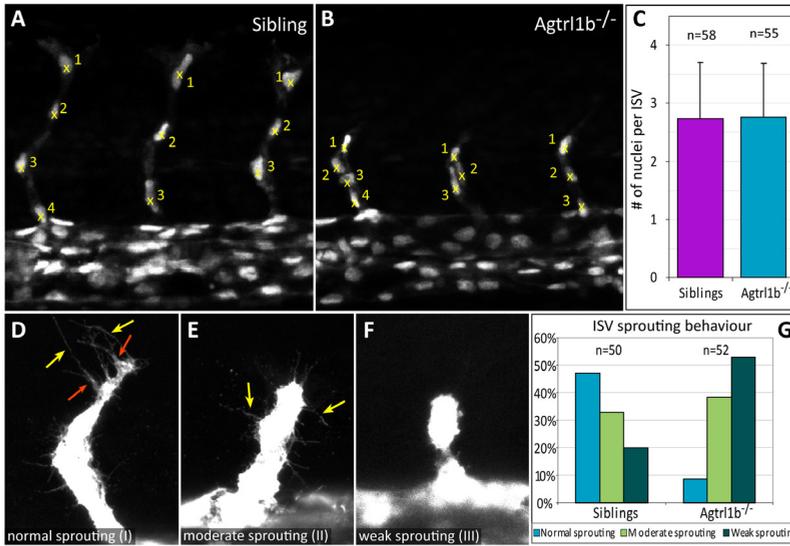


Fig. 2. *agtrl1b*^{-/-} ISVs have wildtype numbers of cells but display altered filopodic behavior. (A-C) The number of cells constituting an intersegmental vessel (ISV) at 28 hours post fertilization (hpf) was assessed in both wildtype (A) and *agtrl1b*^{-/-} mutant (B) embryos in a Tg(*flil1*:neGFP)^{v7} background. No significant difference ($p=0.67$) in the number of nuclei per ISV in wildtype (2.73 ± 0.97, n=348 in 58 embryos) compared to *agtrl1b*^{-/-} mutant embryos (2.76 ± 0.93, n=330 in 55 embryos) was found (C). (D-G) ISVs at 26 hpf were categorized into three different groups for having either (I) normal sprouting behavior (showing distinct protrusions (red arrows) and extending filopodia (yellow arrow)) (D), (II) moderate sprouting behavior (showing no protrusions but normal extending filopodia (yellow arrow)) (E) or (III) weak sprouting behavior (no protrusions and few to no filopodia) (F). Subsequent genotyping showed a vast reduction of the mutant genotype in category (I) compared to wildtype genotype (8.7% vs 50%) and a concurrent enrichment of the mutant genotype in category (III) compared to wildtype genotype (52.9% vs 20%) (G).

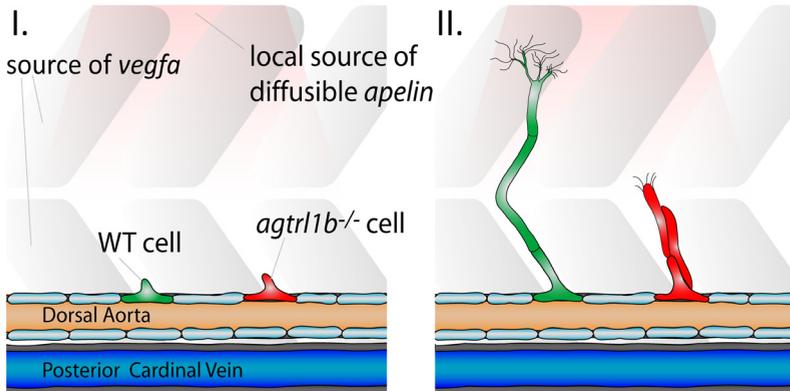


Fig. 3. *Agtrl1b* is required for the filopodic behavior of the angiogenic sprout. (I and II) Schematic overview of the developing vasculature of the zebrafish trunk. *Agtrl1b* is expressed in the dorsal aorta (DA), posterior cardinal vein (PCV) and the intersegmental vessels (ISVs). *Apln*

is expressed at the dorsal side of the zebrafish trunk and induces an *Apln* gradient along the dorso-ventral axis. ISVs sprout from the DA in response to *Vegfa*, locally produced in the neighboring somites (I). In wildtype embryos, the endothelial cells (ECs) in the sprouting ISV proliferate and migrate towards the *Apln* source, guided by intensive filopodic behavior of the tip-cell. In *agtrl1b* mutants however, proliferation of the ECs is unaltered, but fewer and shorter filopodia are present and migration stalls at the midline (II).

DISCUSSION

Here we describe a novel zebrafish mutant for the G-protein coupled receptor *agtrl1b* which encodes a premature stop just after the first transmembrane domain. Using this *in vivo* model we uncovered a specific requirement for *agtrl1b* in the early development of the zebrafish arterial vasculature formed by angiogenesis. The major blood vessels like the dorsal aorta (DA) and posterior cardinal vein (PCV), develop normally in zebrafish *agtrl1b* mutants, but the intersegmental vessels (ISVs) fail to extend to the dorsal side of the trunk. Consequently no dorsal longitudinal anastomotic vessels (DLAVs) are formed. This phenotype is not due to a proliferative defect as the ISVs in *agtrl1b* mutants had normal numbers of cells. In contrast, the filopodic behavior of the ISVs in *agtrl1b* mutants is severely affected.

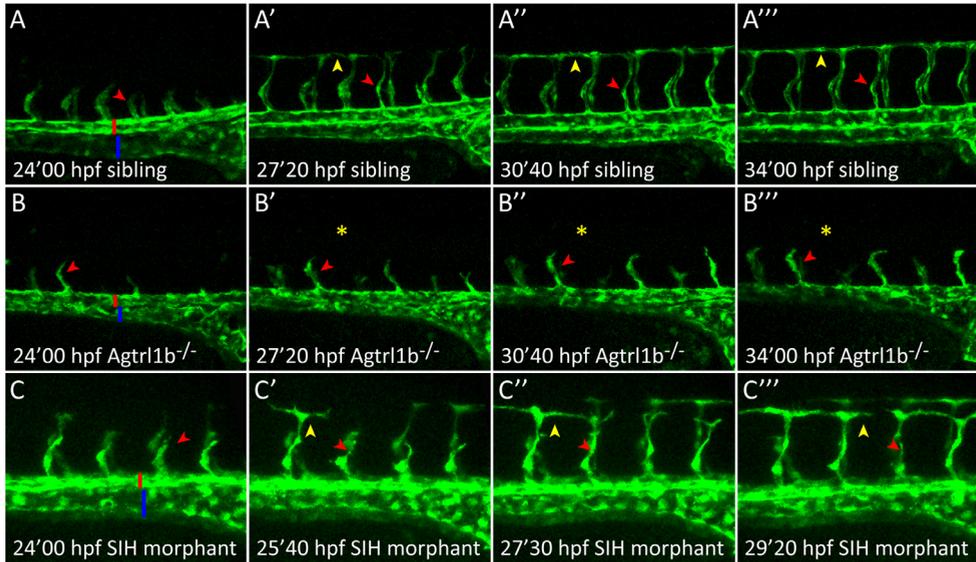
Previous studies have shown a temporal delay in the early stages of vascular development of retinal vascularization in *apelin* null mice (Kasai, 2008). In addition, a chemotactic role for Apln, the ligand for Agtr1b, has been reported (Cox et al., 2006; Kälin et al, 2007). In mice and tadpoles, *apln* is expressed in the tip-cells of the angiogenic sprout preceding ISV angiogenesis and Agtr1b/APJ expression (Sorli et al., 2006; Kälin et al, 2007). Mammalian signaling of Agtr1 via binding of Apelin, results in the activation of the PI3K/Akt pathway (Masri et al., 2005; Kojima and Quertermous, 2008). PI3K and Akt have previously been implicated in the control of directional cell migration and the sensing of chemoattractant gradients by the cell (reviewed by Shiojima and Walsh, 2002; Sasaki and Firtel, 2006); Akt transiently localizes to the leading edge membrane of migratory cells in a PI3K dependent manner (Meili et al., 1999; Servant et al., 2000). In order for a cell to generate contractile forces to migrate towards a chemotactic source, the establishment of a leading edge and the reorganization of the actin cytoskeleton are essential. The Rho family of small G proteins have been identified as major regulators of actin reorganisation, and its member Cdc42 induces the formation of filopodia and is involved in chemotactic sensing (van Nieuw Amerongen and Hinsbergh, 2001). Constitutively active Akt in turn has been shown to be able to activate Cdc42 (Higuchi et al., 2001).

In zebrafish, we find expression of the receptor *agtrl1b* in the DA, PCV and all cells of the ISVs, while *apln* is expressed at the dorsal side of the trunk at the location of the future DLAV. Our data suggests a requirement for *agtrl1b* during angiogenesis in which the sprouting ISVs are guided along a gradient of Apln across the dorso-ventral axis of the embryo trunk by signaling through Agtr1b. During this migration process, tip-cells send out numerous filopodia, enabling guided migration towards a chemotactic source, while at the same time stalk-cells proliferate and form the vascular lumen. In *agtrl1b* mutant fish we find normal characteristics of stalk-cells as endothelial cell proliferation within the ISVs is normal and lumenization of the ISVs is observed (summarized in Fig. 3). Initially, we hypothesized that the ISVs would have increased numbers of filopodia and/or show multi-directionality when chemotaxis through Apln-Agtr1b signaling could not be established. However, the impaired migration of ISVs in *agtrl1b* zebrafish mutants was coincident with reduced filopodic behavior. This finding is in concert with the notion that Agtr1b not only mediates chemotaxis, but also influences architectural aspects of tip-cells through downstream

signaling via the PI3K/Akt pathway. In summary, this study shows that *Agtr1b* is essential for the wildtype behavior of tip-cells and subsequent migration of endothelial cells during the development of angiogenic intersegmental sprouts.

SUPPLEMENTAL MATERIAL

Two supplemental movies can be found in the data supplement.



Supplementary figure 1.

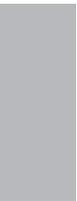
Still pictures from confocal timelapse movies showing the migration of the intersegmental vessels (ISVs) (red arrowhead) from the dorsal aorta (DA) (red bar) towards the dorsal side of the embryo to form the dorsal longitudinal anastomotic vessel (DLAV) (yellow arrowhead) in a wildtype *Tg(kdr-l:GFP)^{s843}* embryo (a-a’’’). *Agtr1b^{-/-}* fish develop a lumenized DA (red bar) and posterior cardinal vein (PCV) (blue bar) and have sprouting ISVs (red arrowhead) from the DA that fail to extend to the dorsal side of the embryo (b-b’’’). Whereas wildtype ISVs would have reached the dorsal side of the embryo and started to extend laterally at ~26hpf (a’), *agtr1b^{-/-}* mutant ISVs would stall at the midline and never form a DLAV (yellow asterisk) even at later stages (b’-b’’’). Silent heart (SIH) injected *Tg(kdr-l:GFP)^{s843}* embryos show normal migration of intersegmental vessels (ISVs) (red arrowhead) from the dorsal aorta (DA) towards the dorsal side of the embryo and formation of the dorsal longitudinal anastomotic vessel (DLAV) (yellow arrowhead) compared to wildtype embryos (compare a-a’’’ and c-c’’’).

Supplementary movie 1.

Representative example of a confocal timelapse movie of the development of the intersegmental vessels (ISV) and the dorsal longitudinal anastomotic vessel (DLAV) just after sprouting from the dorsal aorta (DA) (24 - 34 hours post fertilization) in a wildtype *Tg(kdr-l:GFP)^{s843}* embryo. Note the typical filopodic behavior of the ISVs while migrating towards the dorsal side of the trunk (~24-26 hpf) after which they extend laterally (~26-28 hpf) and connect with neighboring ISVs to form the DLAV (>28hpf).

Supplementary movie 2.

Representative example of a confocal timelapse movie of the development of the intersegmental vessels (ISVs) just after sprouting from the dorsal aorta (DA) (24 - 34 hours post fertilization) in an *agtr1b^{-/-}* *Tg(kdr-l:GFP)^{s843}* mutant embryo. Initial sprouting of ISVs from the DA is timed normally, however the ISVs fail to extend to the dorsal side of the trunk and no dorsal longitudinal anastomotic vessel is formed, but instead remain stalled halfway the dorsal-ventral axis of the trunk.



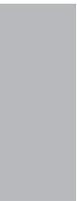
Role of Dll4 / Notch in the formation and wiring of the lymphatic network in zebrafish

Robert Herpers^{1,2*}, Ilse Geudens^{3,4*}, Karlien Hermans^{3,4*}, Inmaculada Segura⁴, Carmen Ruiz de Almodovar^{3,4}, Jeroen Bussmann¹, Frederik De Smet^{1,2}, Wouter Vandavelde^{3,4}, Ben Hogan¹, Arndt Siekmann⁵, Filip Claes^{3,4}, John Moore⁵, Anna Silvia Pistocchi⁶, Sonja Loges^{3,4}, Massimiliano Mazzone^{3,4}, Giovanni Mariggi⁸, Françoise Bruyère⁹, Franco Cotelli⁶, Donscho Kerjaschki⁷, Agnes Noël⁹, Jean-Michel Foidart⁹, Holger Gerhardt⁸, Annelii Ny^{3,4}, Tobias Langenberg^{3,4}, Nathan Lawson⁵, Henricus J Duckers², Stefan Schulte-Merker^{1*}, Peter Carmeliet^{3,4*} and Mieke Dewerchin^{3,4*}

5

¹HubrechtInstitute, Utrecht, the Netherlands; ²Experimental Cardiology, Thoraxcenter, Erasmus University Medical Center, Rotterdam, the Netherlands; ³Vesalius Research Center, VIB, Leuven, Belgium; ⁴Vesalius Research Center, K.U. Leuven, Leuven, Belgium; ⁵Program in Gene Function & Expression, University of Massachusetts Medical School, Worcester MA, USA; ⁶Department of Biology, University of Milan, Milan, Italy; ⁷Clinical Institute of Pathology, Medical University Vienna, Vienna, Austria; ⁸Vascular Biology Laboratory, London Research Institute - Cancer Research, London, UK; ⁹Laboratory of Tumor and Developmental Biology, University of Liège, Sart Tilman, B-4000 Liège, Belgium

* These authors contributed equally to this work



SUMMARY

In zebrafish embryos, sprouts from the axial vein have lymphangiogenic potential, as they give rise to the first lymphatics. Here, we studied whether Notch signaling, which regulates cell fate decisions and blood vessel morphogenesis, controls lymphatic development. Knockdown of Dll4 or its receptors Notch-1b or Notch-6 in zebrafish embryos impaired lymphangiogenesis at two levels. First, Dll4/Notch silencing reduced the number of lymphangiogenic sprouts from their venous precursor; instead, angiogenic sprouts were formed. Also, activation of Notch in venous endothelial cells upregulated lymphatic markers *in vitro*. Second, silencing of Notch signaling impaired navigation of lymphatic intersomitic vessels along their arterial templates. These studies imply critical roles for Notch signaling in the formation and wiring of the early lymphatic network.

INTRODUCTION

The lymphatic vasculature regulates interstitial fluid homeostasis, fat resorption, immune defense, inflammation and metastasis (Alitalo et al., 2005). In mammalian embryos, venous blood vascular endothelial cells (BECs) differentiate to lymphatic endothelial cells (LECs) (Ny et al., 2005; Oliver and Srinivasan, 2008). Previous studies documented that, in response to Sox18, Prox-1 induces lymphatic transdifferentiation of venous BECs (Francois et al., 2008; Johnson et al., 2008; Oliver and Srinivasan, 2008). Additional cues regulate lymphatic development, but their molecular nature remains unknown. Another outstanding question is how lymph vessels, particularly the larger ones, become wired into a stereotyped network. Circumstantial evidence indicates that deep lymphatics regularly fasciculate with other vessels and, in particular, track along arteries (Alitalo et al., 2005; Gale et al., 2002; Jensen et al., 2009). Similar to blood vessels (De Smet et al., 2009; Larrivee et al., 2009), lymphatic sprouts have tip cells at their front, with filopodia to probe guidance cues (Tammela et al., 2005). Though molecules, such as VEGFR-3, VEGF-C, Neuropilin-2, Ccbe1 and others regulate lymphatic migration (Alitalo et al., 2005; Hogan et al., 2009a), navigation of lymph vessels remains poorly understood. Which mechanisms and molecules underlie the development and wiring of the lymphatic network therefore remains largely unknown.

Intriguingly, despite the venous origin of lymph vessels, several molecular players that are involved in arterial BEC regulation, also regulate lymphangiogenesis. For instance, EphrinB2, an initial marker of arterial BECs (Herbert et al., 2009; Lawson et al., 2001), regulates lymphatics later in development (Makinen et al., 2005). Also, forkhead transcription factors are required for arterial specification, but later regulate sprouting of LECs from veins (Seo et al., 2006). This relationship between “arterial” factors and lymphangiogenesis, as well as the anatomical congruence between arteries and lymphatics prompted us to investigate whether Notch, known to induce arterial endothelial fate (Emuss et al., 2009; Herbert et al., 2009; Hofmann and Iruela-Arispe, 2007; Shawber and Kitajewski, 2008; Swift and Weinstein, 2009), also regulates lymphatic development. Notch and its ligand Dll4 seemed intriguing candidates, given their role in vessel branching (Phng and Gerhardt, 2009; Roca and Adams,

2007; Sainson and Harris, 2007).

In zebrafish embryos, the thoracic duct (TD) develops between the dorsal aorta (DA) and posterior cardinal vein (PCV); it is considered to be the first perfused lymphatic, as it expresses Prox-1, contains anchoring filaments and drains interstitial dyes (Jensen et al., 2009; Kuchler et al., 2006; Yaniv et al., 2006). For reasons of clarity, formation of this early lymphatic network is schematically illustrated in Figure S1. Around 30 hpf, half of the secondary sprouts from the PCV, on average one per two unilateral somite segments, migrate radially in the ventral-dorsal direction to the horizontal myoseptum; these sprouts exist transiently (Hogan et al., 2009a; Isogai et al., 2003). At the horizontal myoseptum, cells of these sprouts then migrate tangentially in the anterior-posterior direction to form a string of parachordal lymphangioblasts (PL), which act as progenitors of the future LECs in the TD (36 to 60 hpf); the PL string also exists only transiently. Since the secondary sprouts, which give rise to the PL, participate in the process that leads to the formation of the TD, they have been termed “lymphangiogenic secondary sprouts” (Hogan et al., 2009a). The other secondary sprouts connect to the primary intersomitic vessels (ISVs), which thereby become intersomitic veins (vISV), and have therefore been termed “angiogenic secondary sprouts” (Hogan et al., 2009a; Isogai et al., 2003).

From 60 hpf onwards, the PL cells switch to radial migration again, and navigate both ventrally and dorsally alongside arterial intersomitic vessels (aISVs), whereby they form structures, that later persist as lymphatic intersomitic vessels (IISVs) (Hogan et al., 2009a). These radially migrating cells are termed IISV-PLs to distinguish them from the cells in the PL string. Once ventrally migrating IISV-PLs reach their final location in between the DA and PCV, they switch again to tangential migration, grow towards each other and fuse to establish the TD (3 to 6 dpf) (Hogan et al., 2009a; Isogai et al., 2003). While lymphangiogenic secondary sprouts migrate at a distance from and independently of aISVs (Hogan et al., 2009a), IISVs always navigate alongside aISVs, almost “creeping” over them in their initial dorsal and ventral trajectory, but never track alongside vISVs. This close association of IISVs with aISVs raised the question whether aISVs act as guidance templates for navigating IISVs-PLs.

Using this lymphatic model, we thus explored a possible role of Notch signaling in lymphatic development by gene silencing methods in zebrafish. Our findings reveal novel roles for Dll4/Notch signaling at multiple steps during early lymphangiogenesis.

Experimental procedures

ZEBRAFISH HUSBANDRY

Transgenic zebrafish lines used were *Fli1:eGFP^{v1}* (Lawson and Weinstein, 2002), *Flt1:YFP*, *kdr-l:mCherry*, *Stab1:YFP* (Hogan et al., 2009a), *Fli1:DsRed*, *Tp1bglob:eGFP* (Parsons et al., 2009) and intercrosses. Embryos and fish were grown and maintained as described (Lu et al., 2004). All animal experimentation was approved by the local institutional ethical committee.

MORPHOLINO INJECTION OF ZEBRAFISH EMBRYOS

Gene-specific antisense morpholino oligos were purchased from Gene Tools (LLC, Corvallis). Sequences are listed in Supplementary Table S1. For reasons of consistency, we used the zebrafish nomenclature: zebrafish Notch-5 and -6 are mammalian homologues of Notch-3 and -2, respectively, while zebrafish Notch-1a and -1b are duplicated

mammalian orthologues of Notch-1 (Theodosiou et al., 2009). As a negative control we made use of a standard control morpholino (Gene tools, LLC) (Table S1). For the previously unpublished morpholinos, silencing efficiencies of morpholinos directed against the ATG region were determined as previously described (Ny et al., 2005) using a luciferase reporter assay (Figure S8). Morpholino injection at the indicated doses was performed as described (Hogan et al., 2009a; Lu et al., 2004) Phenotyping data are pooled data from at least 3 independent experiments, with analysis of between 33 and 185 injected embryos per injected dose.

WHOLE-MOUNT *IN SITU* HYBRIDIZATION STAINING OF ZEBRAFISH EMBRYOS

For whole-mount *in situ* hybridization, dechorionated embryos were fixed overnight in 4% paraformaldehyde at 4°C. *In situ* hybridization using antisense probes for *EphrinB2a* (Chan et al., 2001), *Vegfr3* (Thompson et al., 1998), *Notch-1b*, *Notch-6*, *Dll4*, *Tie2*, *Dab2* (Herpers et al., 2008; Hogan et al., 2009a), *Tbx20* (Szeto et al., 2002), *Cmlc2* or *MyoD* was performed as described (Chittenden et al., 2006). Stained embryos were paraffin- or plastic-embedded, sectioned and counterstained with nuclear fast red.

ZEBRAFISH COMPOUND INHIBITOR TREATMENT

A 10 mM stock solution of DAPT (γ -secretase inhibitor IX; Calbiochem) in DMSO was diluted in embryo water to the indicated treatment concentrations. Embryos were dechorionated by trypsinization (Sigma, 1.5 mg/ml in PBS) at 24 hpf and incubated in 6.25 to 25 mM DAPT in embryo water. DMSO was added to the lower concentrations to equalize total DMSO to 0.25% in all conditions. Control embryos were incubated in 0.25% DMSO in embryo water.

SCORING OF TD AND PL STRING FORMATION IN ZEBRAFISH

Live screening and quantification of thoracic duct formation was performed on anaesthetized *Fli1:eGFP^{fl}* embryos (a few drops of 4 mg/ml Tricaine (Sigma) stock solution in 5 ml embryo water) at 4 or 6 dpf. For DAPT treated fish, screening at 6 dpf became impossible because fish became opaque due to loss of trunk circulation and edema and many fish died between 4 and 6 dpf. For screening, images were acquired using Zeiss AxioVision 4.6 software on a Leica DM RBE fluorescence stereomicroscope equipped with a Zeiss AxioCam Mrc5 digital camera (Carl Zeiss, Munich, Germany; Leica Microsystems, Wetzlar, Germany). The percentage of thoracic duct formation was quantified by scoring its percentile presence in 10 consecutive somite segments in the trunk after the junction of DA and PCV (i.e. somites 5-15, see Figure S3E). For screening of thoracic duct formation only embryos with normal overall morphology and normal trunk circulation were included. All data are based on scorings of 33-185 embryos per condition, generated in at least 3 independent experiments. All analyses were performed by investigators blinded for the experimental treatment. Screening of PL string formation in the 10-somite segment of the trunk was performed in a similar manner at 52 hpf. Confocal imaging of *Fli1:eGFP^{fl}* embryos was performed using a Zeiss laser scanning microscope LSM510 or Leica SP2, SPE and SP5 confocal microscopes. Embryos were anaesthetized and positioned on a coverslip in a drop of 0.5% low melting point agarose. Fluorescence signal of *Stab1:YFP* images was transformed to a gray-scale image for better contrast.

TIME LAPSE IMAGING

Embryos were mounted in 0.5% low melting point agarose in a culture dish with a cover slip replacing the bottom. Imaging was performed with a Leica SP2 or SP5 confocal microscope using a 10x, 20x or 40x objective with digital zoom. Timelapse analysis was compiled using ImageJ software (<http://rsb.info.nih.gov/ij/>). Time points were recorded every 10 minutes for the stated time period. A heated stage maintained the embryos at approximately 28.3 °C.

FUNCTIONAL ASSESSMENT OF THE THORACIC DUCT

For functional studies, anesthetized larvae were subcutaneously injected with 1 nl fluorescent dextran (2.5 mg/ml) into the muscle mass of the posterior trunk by using glass capillaries and a conventional microinjection setup (Kuchler et al., 2006).

CELL CULTURE EXPERIMENTS

Proliferation, migration and expression analyses of LEC or HUVEC cells in conditions of activation or inhibition of Notch signaling are detailed in Supplemental Information.

STATISTICAL ANALYSES

Each gene-specific morpholino (or compound dose) was always compared to the control morpholino or vehicle

in every single experiment. To determine the penetrance of the phenotype, we counted the number of zebrafish embryos, exhibiting the different severities of morphant phenotype. Chi-square analysis was used to determine whether the severity distribution differed between treatment groups. Absolute values were used to calculate means and SEMs. Pairwise comparisons between different conditions were performed by two-sided t-test unless otherwise specified. The asterisks on the figures represent the treatment difference at a significance level of $P < 0.05$.

RESULTS

SILENCING STRATEGIES TO STUDY THE ROLE OF NOTCH IN LYMPH VESSEL FORMATION

To explore a role for Notch signaling in lymphatic development, we silenced every known zebrafish orthologue of the Notch ligands (DeltaA-D, Dll4, Jagged-1a/b, Jagged-2) and receptors (Notch-1a/b, -5, -6) as well as of Notch activators and effectors (presenilins, Su(H)) in *Fli1:eGFP^{fl}* zebrafish embryos, in which lymphatic, arterial and venous ECs are labeled (Kuchler et al., 2006; Lawson and Weinstein, 2002; Yaniv et al., 2006). As Notch-family members have been implicated in angiogenesis (Hofmann and Iruela-Arispe, 2007; Roca and Adams, 2007; Sainson and Harris, 2007), we used submaximal doses of all morpholinos to minimize secondary effects of vascular malformations on lymphatic development (referred to as “incomplete silencing” and “Notch hypomorphants”; Figure S2A-H). Only morphant embryos with a normal size, trunk circulation and blood flow, and without developmental delay, tissue malformations, general edema or toxic defects were included (Figure S3A-D). As a read-out of lymphatic development, we quantified the formation of the TD by measuring the length over which it formed by 6 dpf, when this vessel was completely developed in control embryos. For reasons of standardization and to correct for slight differences in embryo size, the length of the TD was expressed as % of the 10-somite fragment analyzed (Figure S3E). Because the penetrance of the lymphatic phenotype was variable (Note S1), we also determined the fraction of embryos with severe, intermediate or subtle lymphatic defects for each morpholino dose. Phenotypic defects were dose-dependent, but for reasons of brevity, only the highest dose is shown. A standard control and two independent target-specific morpholinos were used routinely.

KNOCKDOWN OF DLL4 IMPAIRS DEVELOPMENT OF THE THORACIC DUCT

Dll4 knockdown (Dll4^{KD}) inhibited the formation of the TD. Upon injection of a morpholino affecting Dll4 mRNA splicing (Dll4^{SPL}; 10 ng), the TD failed to form at all by 6 dpf in up to 52% of the morphant embryos, indicating that lymphatic development was completely aborted (“severe defects”; Figure 1A-C). In another 27% of Dll4^{SPL} embryos, the TD formed over only 10 to 30% of its normal length (“intermediate defects”), while in another 15% of morphant embryos, the TD formed over 30 to 90% (“subtle defects”) (Figure 1C). As explained above, initiation of TD formation occurs via sprouting of lymphangiogenic secondary sprouts at discrete locations alongside the PCV, i.e. on average one per two unilateral somite segments. Thus, if the TD formed over only 20% of its entire length, then TD development was in fact completely aborted in eight out of ten somites analyzed. Follow-up studies at later stages (up to 12 dpf) revealed that, in embryos with intermediate defects, the few LECs that did arise and formed parts of the TD, were unable to reconstitute the entire TD and could

not compensate for the lymphatic failure in nearby somites (not shown). DII4^{KD} embryos without TD at 6 dpf also failed to form a TD, even not partially, at later stages (Figure S2G,H), indicating that lymphatic development was not simply delayed, but aborted.

Lymphangiography in 7-dpf *kdr-l:mCherryRed* DII4^{KD} embryos (in which blood vessels express mCherryRed while lymph vessels are not labeled) revealed no drainage of green fluorescent dye in the region where the TD normally forms, confirming that the lack of a GFP⁺ TD in *Fli1:eGFP^{y1}* DII4^{KD} embryos was not due to reduced expression of this marker, but to actual absence of the vessel itself (Figure 1D,E). The lymphatic defects in DII4^{KD} embryos were specific, as no overt changes in the formation and differentiation of the DA and PCV were noticeable (Figure S4A-H). Consistent with previous reports (Hogan et al., 2009b; Leslie et al., 2007), some hyperbranching of the primary ISVs was detected in DII4^{KD} hypomorphant embryos, but to a variable degree and in only 20% of DII4^{KD} embryos (red arrowheads in Figure 1B; Movie S2); hence, TD defects were detected in the majority of DII4^{KD} embryos that did not exhibit any signs of ISV hyperbranching. Also, no abnormalities in heart or somite development were observed (Figure S2I-L). Similar TD defects were obtained with another morpholino, targeting the ATG of DII4 (DII4^{ATG}) (Figure S5A), but silencing of the Notch ligands DeltaA-D, Jagged-1a/b or Jagged-2 did not induce lymphatic defects (not shown).

NOTCH-1B (AND NOTCH-6) REGULATE FORMATION OF THE THORACIC DUCT

Incomplete silencing of Notch-1b and, to a lesser extent, of Notch-6, similarly impaired TD formation (Figure 1F,G). Of note, the mammalian orthologues of these genes, Notch-1 and Notch-2, respectively, are expressed in LECs (Ota et al., 2007; Petrova et al., 2002; Wick et al., 2007). Complete loss of TD formation was observed in 30% of the embryos at the highest dose of the Notch-1b^{SPL} morpholino (15 ng; Figure 1G). In another 31% of Notch-1b^{SPL} embryos, the TD formed in only one to three of the ten somites analyzed. Similar lymphatic defects were obtained with a morpholino directed against the start site (Notch-1b^{ATG}) (Figure S5B). The TD also failed to form in 14% of Notch-6^{SPL} embryos (15 ng; Figure 1G). Combined silencing of Notch-1b and Notch-6 yielded more severe lymphatic defects, suggesting cooperation of both receptors (not shown). Since Notch-1b down-regulation results in more penetrant defects in lymphatic development, only data for Notch-1b^{KD} will be shown from hereon. Silencing of Notch-1a or Notch-5, the zebrafish orthologues of mammalian Notch-1 and Notch-3, failed to cause any lymphatic defects (not shown). Incomplete knockdown of the Notch receptors also did not affect, or only minimally influenced the formation, differentiation and morphogenesis of blood vessels (Figure S4I-N; not shown)

SILENCING OF γ -SECRETASE IMPEDES LYMPH VESSEL FORMATION

Presenilin-1 (PS-1) is the catalytic subunit of the γ -secretase complex that activates Notch through proteolytic cleavage (Wolfe et al., 1999). Consistent with the results above, silencing of PS-1 by morpholino knockdown also impaired TD formation (Figure 1H; Figure S5C), without deregulation of blood vessel differentiation (Figure S4O,P). The role of PS-1 was specific, as silencing of PS-2 did not cause lymphatic defects, neither did combined double knockdown of PS-1 and PS-2 exacerbate the PS-1^{KD} phenotype (not shown). These

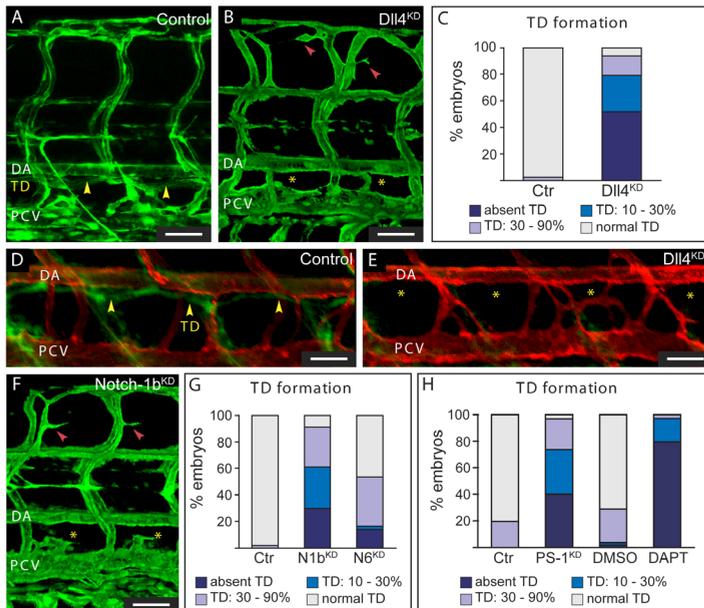


Fig. 1. Role of Notch in TD formation. In panels A,B,D-F, the head of the embryo faces left. DA, dorsal aorta; PCV, posterior cardinal vein; TD, thoracic duct. **A,B,** Confocal images of GFP+ vessels in the trunk of 6 dpf *Fli1:eGFP⁺* zebrafish embryos.

The control embryo has a normal lymphatic TD (yellow arrowheads in A), while the TD is entirely absent in the *Dll4^{KD}* embryo (B). The yellow asterisks in panel B denote the location where the TD should have developed, while the red arrowheads indicate minimal hyperbranching of the upper part of the ISVs. **C,** Bar graphs, representing the percentage of embryos at 6 dpf, which develop a normal TD (grey), a

TD over 30-90% (lilac) or over 10-30% (blue) of its normal length, or completely lack any TD (dark blue) in the indicated fraction of control embryos ($N=122$) or *Dll4^{KD}* embryos ($N=80$; 10 ng *Dll4^{SPL}*; $P<0.001$ versus controls by Chi-Square test). **D,E,** Lymphangiography, performed by injecting a green fluorescent dye in the trunk of 7-dpf *kdrl:mCherryRed* embryos, in which blood vessels are red, revealed normal uptake and drainage of the green dye by the TD in the control embryo (yellow arrowheads in D), but not in the *Dll4^{KD}* embryo (yellow asterisks in E). At 7 dpf, side-branches of the TD are formed, which also drain lymph. **F,** Abnormal TD formation in 6 dpf *Notch-1b^{KD}* embryos. Absence of the TD is marked with yellow asterisks; minor signs of ISV hyperbranching are indicated by red arrowheads. **G,H,** Bar graphs, representing the percentage of embryos at 6 dpf, which develop a normal TD (grey), a TD over 30-90% (lilac) or over 10-30% (blue) of its normal length, or completely lack any TD (dark blue) in the indicated fraction of control embryos ($N=185$ in G; 87 in panel H), *Notch-1b^{KD}* (*N1b^{KD}*) embryos ($N=84$; 15 ng *Notch-1b^{SPL}*; $P<0.001$ versus controls; panel G), *Notch-6^{KD}* (*Ng^{KD}*) embryos ($N=63$; 15 ng *Notch-6^{SPL}*; $P<0.001$ versus controls; panel G), *PS-1^{KD}* embryos ($N=65$; 2.5 ng *PS-1^{ATG1}*; $P<0.001$ versus controls; panel H), or of embryos treated with control vehicle ($N=171$; DMSO; panel H) or DAPT ($N=34$; 25 μ M; $P<0.001$ versus controls; panel H). Scale bars represent 50 μ m.

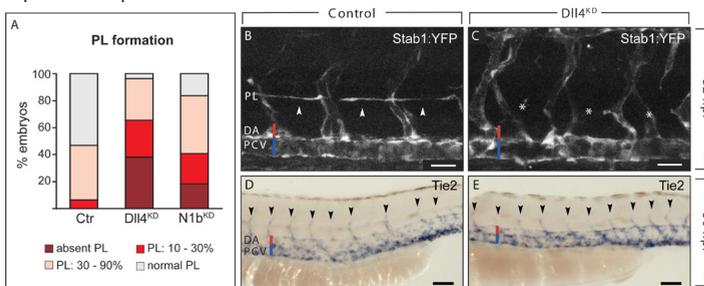


Fig. 2. Incomplete silencing of Notch blocks PL string formation. In panels B-E, the head of the embryo faces left; the red vertical bar denotes the dorsal aorta (DA); the blue vertical bar the posterior cardinal vein (PCV). PL: parachordal lymphangioblast string. **A,** Bar graphs, representing the percentage of embryos at 52 hpf, which

develop a normal PL (grey), a PL over 30-90% (pink) or over 10-30% (red) of its normal length, or completely lack any PL (dark red) in the indicated fraction of control embryos ($N=73$), *Dll4^{KD}* embryos ($N=55$; 10 ng *Dll4^{SPL}*; $P<0.001$ versus controls) or *Notch-1b^{KD}* (*N1b^{KD}*) embryos ($N=49$; 20 ng *Notch-1b^{ATG}*; $P<0.001$ versus controls). **B,C,** Confocal images of embryos of the venous / lymphatic reporter line *Stab1:YFP* at 52 hpf, showing normal PL formation in the control embryo (arrowheads in B), but complete absence in the *Dll4^{KD}* embryo (asterisks in C). **D,E,** Whole-mount *in situ* staining for *Tie2* at 50 hpf, revealing a normal number of secondary sprouts (arrowheads) in the control (D) and *Dll4^{KD}* (E) embryo. Scale bars are 50 μ m in panels B,C; 100 μ m in panels D,E.

genetic findings were confirmed by pharmacological inhibition of the γ -secretase activity by exposing zebrafish embryos to *N*-[*N*-(3,5-difluorophenacetyl)-*L*-alanyl]-*S*-phenylglycine *t*-butyl ester (DAPT), a well known γ -secretase inhibitor, that has been previously used to block Notch signaling in zebrafish embryos (Geling et al., 2002) (Figure 1H; Figure S4Q,R). Silencing of *Su(H)*, a transcription factor involved in Notch signaling, yielded too severe embryonic malformations, precluding trustworthy analysis of the lymphatic vasculature (not shown).

NOTCH SIGNALING IS REQUIRED FOR PL STRING FORMATION

To characterize the role of Notch signaling in lymphatic development in more detail, we analyzed whether silencing of Notch would impair development of PL cells, as they directly contribute to TD formation. Since PL cells develop initially from lymphangiogenic secondary sprouts in a segmented pattern, we used a similar quantification method as employed for analysis of the TD. At 52 hpf, formation of the string of PL cells was still proceeding in control embryos (already completely formed in 53% and largely completed in another 40% of the embryos; Figure 2A). By contrast, in *Dll4*^{SPL} embryos, the PL string was completely absent in 38% and formed only in a few segments in another 27% of embryos (Figure 2A). Notably, largely comparable fractions of *Dll4*^{SPL} embryos exhibited similar types of severe, intermediate or subtle PL string and TD lymphatic defects (compare Figure 1C with Figure 2A), suggesting that the TD defects were, at least in part, attributable to defects in the initial formation of the PL string. Imaging of lymphangiogenic structures in *Dll4*^{SPL} embryos using a novel transgenic reporter line, the *Stab1:YFP* line (Hogan et al., 2009a), which primarily visualizes venous and lymphatic ECs, confirmed these findings (Figure 2B,C). A similar absence of the PL string was observed when using the *Dll4*^{ATG} morpholino (not shown), or upon knockdown of Notch-1b (Figure 2A) or Notch-6 (not shown). Since the string of PL cells forms as a result of lymphangiogenic secondary sprouting from the PCV, these findings suggest that Notch signaling acts in part at very early steps prior to formation of the perfused lymphatics.

DLL4 SILENCING REDUCES THE FRACTION OF LYMPHANGIOGENIC SECONDARY SPROUTS

Since the lymphangiogenic secondary sprouts are anatomically transiently connected with the PL cells, we also studied whether inhibition of Notch signaling might even act at an earlier stage, i.e., during branching of these lymphangiogenic secondary sprouts. Whole-mount staining for *Tie2*, which marks all secondary sprouts (Hogan et al., 2009b), showed a normal number of secondary sprouts in all *Dll4*^{KD} embryos analyzed ($N=20$; 50 hpf; Figure 2D,E). However, high resolution imaging of the trunk vasculature in 4 dpf *Fli1:eGFP^{v1}* embryos revealed alterations in the proportion of primary ISVs that adopted a venous phenotype (vISVs), based on the criterion that they were connected to the PCV. As expected, in control embryos, approximately half of the ISVs were connected to the PCV (vISVs, % of total ISVs: $54 \pm 1.3\%$; $N=33$). In contrast, in *Dll4*^{SPL} embryos, a larger fraction of ISVs was connected to the PCV and therefore venous (vISVs, % of total ISVs in all *Dll4*^{SPL} embryos analyzed: $82 \pm 1.8\%$; $N=55$, $P<0.05$ versus control). Similar findings were obtained in Notch-1b^{SPL} embryos (vISVs, % of total: $69 \pm 2.7\%$; $N=27$, $P<0.05$ versus control). Even though this arterial-venous

ISV shift was most prominent in hypomorphant embryos with the most severe lymphatic defects, not all aISVs underwent a venous shift (maximally ~90%), possibly reflecting an incomplete knockdown or, perhaps, a fundamental physiological need to establish at least some residual trunk circulation from aISVs to vISVs. These findings, and the observation that silencing of *Dll4*, *Notch-1b* or *Notch-6* aborted PL string formation in a substantial fraction of morphant embryos, indicate that a fraction of secondary sprouts, that would normally have been lymphangiogenic, were angiogenic, thereby impairing TD formation (see scheme in Figure 6A,B).

To provide additional experimental support for the aforementioned model, we also used high resolution video-imaging of a double transgenic reporter line, the *kdr-l:mCherryRed* line which labels arterial and venous ECs, combined with the *Flt1:YFP* line which exclusively labels arterial ECs (Hogan et al., 2009a). Hence, in the *Flt1:YFPxkdr-l:mCherryRed* line, venous cells are red (CherryRed⁺) and arterial cells are yellow (YFP⁺CherryRed⁺) in merged images. We expected that, once a primary aISV adopts a venous identity when being “co-opted” by a secondary venous angiogenic sprout, this vessel would gradually change its pattern of marker expression from yellow (arteries) to red (veins) only. In control embryos, those primary aISVs that became connected with a venous secondary sprout and thus adopted a venous identity, indeed progressively lost their “arterial” yellow color and acquired a “venous” red color (blue arrows in Figure 3A”), while the other half of the aISVs remained connected with the DA and retained their yellow color (white arrows in Figure 3A”). Closer inspection revealed that, upon establishing a connection with a venous secondary sprout, the arterial ECs of the aISV became gradually replaced by venous ECs from the secondary sprout in a ventral-to-dorsal direction. In contrast, in *Dll4*^{KD} embryos with severe lymphatic defects, nearly all yellow aISV connections with the DA disappeared (see the single white arrow in Figure 3B”), and were gradually replaced by red vISV connections with the PCV (blue arrows in Figure 3B”). The kinetics of these changes are shown in Movies S1,2. Thus, a supernumerary fraction of angiogenic secondary sprouts is formed in *Dll4*^{KD} embryos at the expense of lymphangiogenic sprouts, that would otherwise go on to form the PL string, suggesting that Notch participates in the acquisition of lymphatic potential.

ACTIVATION OF NOTCH BY DLL4 PROMOTES LYMPHATIC CHARACTERISTICS IN VITRO

To evaluate whether activation of Notch in venous ECs would induce lymphatic properties, we cultured human umbilical venous ECs (HUVECs, which express Notch receptors including NOTCH-1, but negligible levels of PROX-1; not shown) on a feeder layer of COS cells, expressing DLL4 (COS^{Dll4}) or a control vector (COS^{CTR}), and analyzed by RT-PCR with human gene-specific primers the expression of lymphatic markers. As shown in Figure 4, several downstream Notch target genes (HEY1, HEY2, HES1, NRARP) were upregulated in HUVECs, when cultured on COS^{Dll4} feeder cells as compared to control COS^{CTR} feeder cells, indicating that Notch signaling was activated. Furthermore, COS^{Dll4}-activated HUVECs expressed elevated levels of the lymphatic markers PROX-1, VEGFR3, LYVE-1 and Sox18 (Figure 4; Note S2). Notably, expression of *EPHRINB2* which has been implicated in both arterial and lymphatic processes (Lawson et al., 2001; Makinen et al., 2005), and *COUP-TFII* which is expressed in both venous

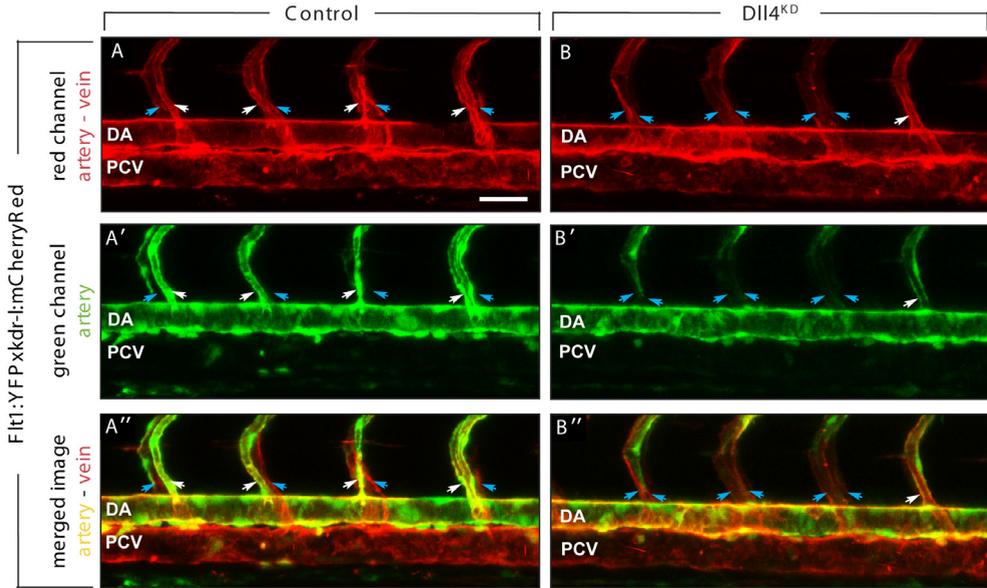


Fig. 3. Notch silencing reduces the fraction of lymphangiogenic sprouts. In all panels, the head of the embryo faces left. DA, dorsal aorta; PCV, posterior cardinal vein. **A,B** Confocal images of the trunk vasculature in *Flt1:YFPxkdr-l:mCherryRed* embryos, where *kdr-l:mCherryRed* marks both venous and arterial vessels in red (A,B), *Flt1:YFP* labels arterial vessels in green (A',B'), and the merged images show arterial vessels in yellow (green-red) and venous vessels in red (A'',B''). Lateral view images of the entire embryo were taken, such that the ISVs at both the left and right side of the embryo are shown, partially superimposed onto each other. Embryos were imaged at 54 hpf, when secondary sprouts had already connected to the primary ISVs, and the latter were in the process of changing their arterial to venous identity in a ventral-to-dorsal pattern. In control embryos (A-A''), on average half of the aISVs became connected to the PCV and thus acquired a venous identity, thereby progressively losing their green arterial signal (blue arrows in A') and thus becoming marked in red only (blue arrows in A'',A''), while the other half of the aISVs remained connected to the DA and labeled in green (white arrows in A') and thus in yellow on the merged images (white arrows in A''). By contrast, in the *Dll4*^{KD} embryo shown (B-B''), most ISVs lost their green arterial marker in a ventral-to-dorsal direction (blue arrows in B',B''); note the single white arrow, and became marked in red only, while losing their yellow label (blue arrows in B''). White arrow in B-B'' denotes a residual aISV retaining its green (B') or yellow (B'') label. Scale bar in B, representative for all panels, is 50 μ m.

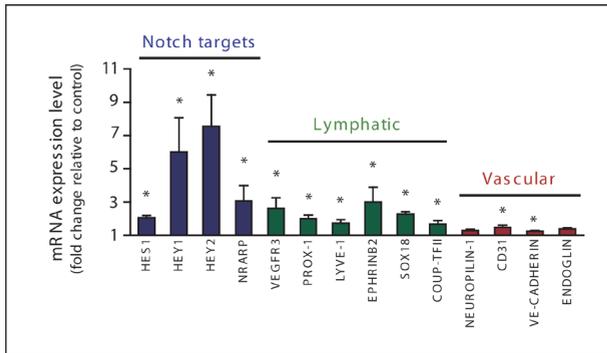


Fig. 4. Activation of Notch by Dll4 promotes lymphatic characteristics in vitro. RT-PCR analysis of HUVECs, co-cultured with COS cells stably expressing hDll4 (*COS*^{Dll4}) or a control vector (GFP; *COS*^{CTR}), revealing upregulation of Notch target genes (HES1, HEY1, HEY2, NRARP; blue bars) and lymphatic marker genes (VEGFR3, PROX-1, LYVE-1, EPHRINB2, Sox18; green bars), while vascular genes such as NEUROFILIN-1, CD31, VE-CADHERIN or ENDOGLIN (red bars) were only minimally affected. COUP-TFII, which is expressed in venous and lymphatic ECs, was also

upregulated. Results are represented as fold change in HUVEC/*COS*^{Dll4} co-culture versus HUVEC/*COS*^{CTR}. Mean \pm SEM; N= 3-11; *, p < 0.05.

and lymphatic ECs (Yamazaki et al., 2009), were also upregulated, but levels of other blood vessel markers (NEUROFILIN-1, ENDOGLIN, VE-CADHERIN, CD31) were not or only minimally affected (Figure 4). This upregulation of lymphatic markers was abolished by treatment of the cells with DAPT (30 μ M; not shown). These *in vitro* experiments are consistent with a model, whereby venous endothelial activation of Notch by Dll4 promotes lymphatic reprogramming.

SILENCING OF DLL4 IMPAIRS PL CELL MIGRATION ALONG AISVS

We also explored whether Notch signaling might regulate the development of the TD by controlling LISV formation, as the TD failed to form in a substantial fraction of Dll4^{SPL} embryos (25%), even despite the fact that its precursor, the PL string, developed partially in these embryos. Several types of LISV abnormalities were observed in Dll4^{KD} embryos, the most frequent being absence of LISVs. In control embryos, LISV-PLs only migrated along aISVs but never along vISVs, suggesting that vISVs are not permissive (Figure 5A,B). Since there were more vISVs and fewer aISVs in Dll4^{KD} embryos, migrating LISV-PLs were deprived from their usual arterial template and could therefore not contribute to the formation of the TD (Figure 5C; Figure 7C). Intriguingly, however, we also noticed that, even when residual aISVs formed in Dll4^{SPL} embryos, LISV-PLs bypassed the aISV post, and failed to turn and migrate along aISVs (Figure 5D). Indeed, when analyzing the fraction of aISVs that was accompanied by LISV-PLs in Dll4^{SPL} embryos with a nearly complete PL string (over >90% of its length), as much as $49 \pm 6\%$ of these aISVs were not accompanied by LISV-PLs in Dll4^{SPL} embryos ($N=61$), while only a few aISVs lacked accompanying LISV-PLs in control embryos ($15 \pm 4\%$; $N=29$; $P<0.05$).

Other, much less frequent, LISV defects were observed in this subgroup of Dll4^{SPL} embryos. For instance, some LISV-PLs that accomplished to turn ventrally alongside the aISV, stalled (Figure 5E; Figure 7C''). Occasionally, LISV-PLs erroneously navigated away from their aISV template, with their tip at the forefront of the sprout projecting erroneously in the surroundings (Figure 5E). In a few cases, LISV-PLs became even misrouted and migrated along vISVs (Figure 5F; Figure 7C'''). Additional *in vitro* studies revealed that inhibition of Notch signaling did not affect the cellular migratory/motility capacity nor proliferation of primary LECs in various assays (Figure S6A-D), nor did it inhibit lymphatic capillary tube formation or sprouting *in vitro* (not shown).

EXPRESSION OF DLL4 AND NOTCH

To examine the expression of Dll4 and Notch, we used whole-mount *in situ* hybridization in control embryos during the developmental processes that were affected in Notch hypomorphants. At 30 hpf, when secondary sprout formation starts, Dll4 was strongly expressed in the DA but undetectable in the PCV (Figure 6A,B), consistent with previous findings (Hogan et al., 2009b; Leslie et al., 2007; Siekmann and Lawson, 2007). Robust expression of Notch-1b was detected in the DA (Figure 6C,D), while a weaker signal was detectable in the PCV, that appeared to localize more to the dorsal part of the PCV (Figure S7). Expression of Notch-6 was at or below the threshold of detection of the *in situ*

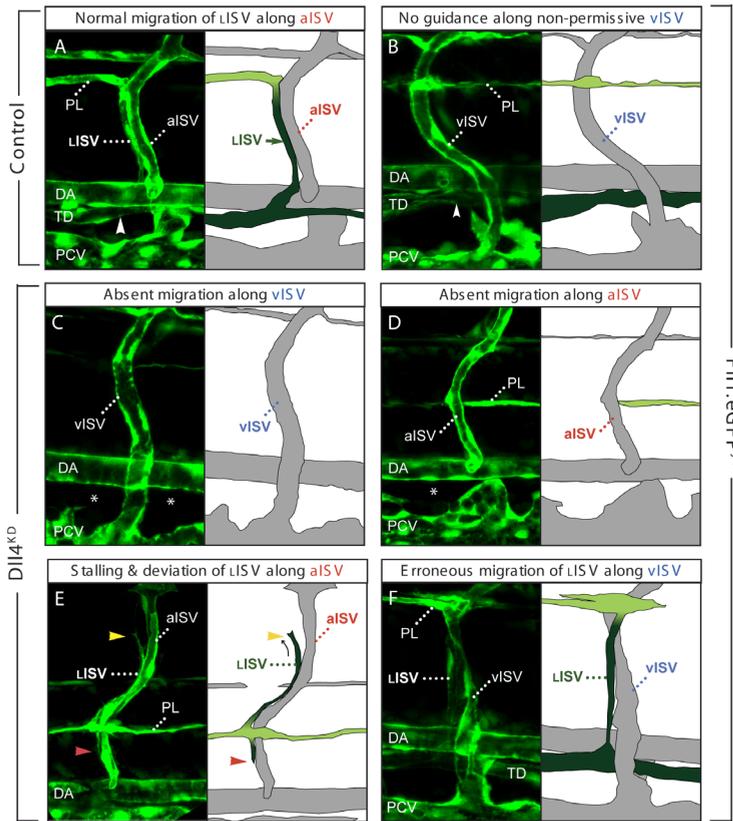


Fig. 5. Incomplete silencing of Notch perturbs lymphatic navigation. In all panels, the head of the embryo faces left. DA, dorsal aorta; ISV, intersomitic vessel; aISV, arterial ISV; LISV, lymphatic ISV; vISV, venous ISV; PCV, posterior cardinal vein; PL, parachordal lymphangioblast string; LISV-PLs, migrating PL cells during LISV formation; TD, thoracic duct. Panels A-F are confocal images with accompanying schematic redrawing of the navigation routes of LISVs along aISVs or vISVs in control (A,B) and *Dll4*^{KD} (C-F) *Fli1:eGFP*⁺ embryos at 4 dpf. Permanent lymphatic structures (LISV, TD) are labeled dark green, and the transient lymphangiogenic structures (PL) are consistently labeled light green to denote

their participation in the process of lymphangiogenesis. **A**, In control embryos, LISV-PLs navigate alongside aISVs and establish a continuous TD (arrowhead). Note how the LISV “creeps” over the aISV, and slides down along this guidance template. The curved arrow indicates the point where LISV-PLs have to make a ventral turn and switch from tangential to radial migration along aISVs. **B**, LISV-PLs never navigate along vISVs in control embryos. Arrowhead indicates the TD. **C-F**, Different types of navigation defects in *Dll4*^{KD} embryos. **C**, In a fraction of morphant somites, LISV-PLs lacked migration templates because fewer aISVs developed. As LISV-PLs do not normally migrate along vISVs, no TD was formed in these somites (asterisks). **D**, In other morphant somites, LISV-PLs bypassed the point of turning at the aISVs, and failed to switch to radial migration. Therefore, no TD could be formed (asterisks). **E**, In a small fraction of somites in *Dll4*^{KD} embryos, LISV-PLs accomplished to make the turn and switched to radial migration, but then stalled shortly thereafter (red arrowhead denotes the arrested tip of a ventrally navigating LISV) or became misrouted away from their guidance aISV template (yellow arrowhead denotes LISV-PL tip cell from a dorsally navigating LISV, that detached from its aISV scaffold). This picture was taken from a more oblique angle to visualize both the ventrally and dorsally navigating LISVs. **F**, In most *Dll4*^{KD} embryos, vISVs were not permissive to guide LISV-PLs, but, occasionally, LISV-PLs erroneously navigated alongside a vISV.

hybridization technique; when expression was detectable, a weak signal was observed in the axial vasculature consistent with its previously reported expression pattern (Thisse et al., 2001). Thus, ligand and receptor appear to be expressed in the near vicinity of the emerging lymphangiogenic secondary sprouts. The limited resolution of *in situ* hybridization (whole-mount or sections) did not allow us to evaluate possible expression in the thin lymphangiogenic secondary sprouts or the PL string.

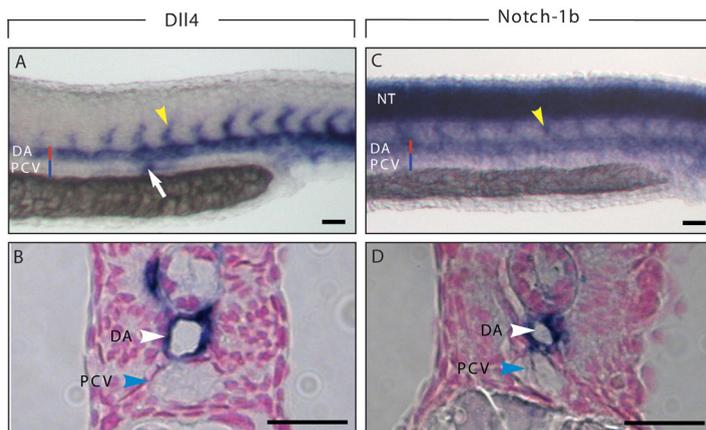
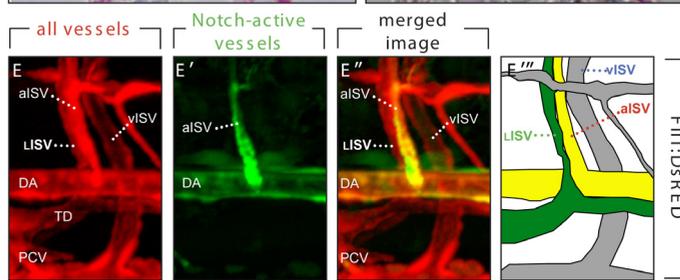


Fig. 6. Expression of Dll4 / Notch-1b. In all panels the head of the embryo faces left. DA, dorsal aorta; ISV, intersomitic vessel; aISV, arterial ISV; lISV, lymphatic ISV; vISV, venous ISV; PCV, posterior cardinal vein; TD, thoracic duct. **A-D**, Whole-mount embryos at 30 hpf, when lymphangiogenic sprouting occurs, were stained for Dll4 (A,B) or Notch-1b (C,D); expression was analyzed by imaging of whole-mount embryos (A,C) or cross-sections of the same embryos (B,D). The DA is indicated by a red vertical bar (A,C) or white arrowhead (B,D), while the PCV is denoted by a blue vertical bar (A,C) or arrowhead (B,D); primary ISVs are indicated by yellow arrowheads (A,C). Scale bars are 50 μ m. **A,B**, Dll4 expression was detected in the DA and primary aISVs, besides its known expression in the pronephric duct (white arrow



in A). **C,D**, Notch-1b is strongly expressed in the neural tube (NT), and in the DA and primary aISVs. **E**, Confocal images of the trunk vasculature in untreated *Tp1bglob:eGFPFli1:DsRed* embryos, in which *Fli1:DsRed* marks all vessels (both blood and lymph vessels) in red (E) and *Tp1bglob:eGFP* labels cells with activated canonical Notch activity in green (E'). The merged image shows arterial vessels (DA; aISV) with active Notch in yellow (green-red), while the lISV are only red (E''). In the schematic representation (right panel), the lymphatic structures are indicated in green, Notch-activated vessels in yellow, and other vessels in grey (E'''). Representative images of the arterial activation of Notch in a 6-dpf embryo are shown (for technical reasons), but similar data were obtained at 60 hpf.

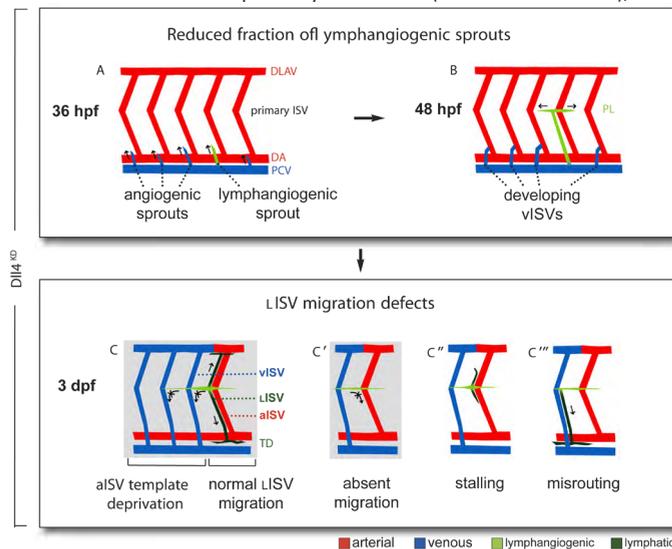


Fig. 7. Schematic model of Notch in lymphatic development. Scheme, illustrating the different types of lymphatic defects in *Dll4^{KO}* embryos (for normal lymphatic development in control embryos, see Figure S1). Permanent lymphatic structures (lISV, TD) are labeled dark green; transient lymphangiogenic structures (lymphangiogenic secondary sprouts; parachordal lymphangioblasts) are labeled light green. **A,B**, UPPER PANELS: LYMPHANGIOGENIC SECONDARY SPROUTING DEFECTS: The reduction of the fraction of lymphangiogenic secondary sprouts results in (continued on next page)

Dll4 and Notch-1b were also detected in primary ISVs by *in situ* hybridization at 30 hpf (Figure 6A-C), consistent with previous findings (Leslie et al., 2007; Siekmann and Lawson, 2007). To analyze expression in ISVs at later stages, when LISV-PLs migrate along aISVs (from 2.5 dpf onwards), we used the *Tp1bglob:eGFPxFlil1:DsRed* line, in which all endothelial cells are red, and cells with canonical Notch activity are green (GFP expression is driven by a promotor containing 12 Su(H) DNA binding sequences (Parsons et al., 2009)). Imaging of this line at the time when PL cells make the turn and switch from tangential to radial ventral migration revealed that the DA and aISVs are yellow in the merged image, indicating that canonical Notch signaling was active in arterial vessels, but not in LISVs or vISVs (Figure 6E).

DISCUSSION

The cardinal finding of this study is that incomplete silencing or pharmacological inhibition of Notch signaling impaired lymphatic development in zebrafish. Mechanistic analysis indicates that Notch signaling regulates the formation of lymphangiogenic sprouts and their descendent PL cells, which give rise to the TD (Figure 7A,B). At a later stage, Notch signaling is required for guided migration of LISV-PLs along aISVs (Figure 7C-C’’’).

ROLE OF NOTCH IN LYMPHANGIOGENIC SECONDARY SPROUT FORMATION

Given that Notch has been implicated in the morphogenesis of blood vessels (Hofmann and Iruela-Arispe, 2007; Li and Harris, 2009; Roca and Adams, 2007), a reasonable assumption was that Notch might regulate lymphatic morphogenesis as well. This hypothesis was indeed confirmed by our genetic and imaging experiments. Up to half of the Notch hypomorphant embryos failed to form a TD without later rescue, indicating that lymphatic development in the trunk was aborted and not simply delayed. The earliest identifiable defect in Notch-silenced embryos occurred at the time of secondary sprout formation, when fewer lymphangiogenic and more angiogenic sprouts emanated from the PCV (Figure 7A,B). That this phenotypic change may underlie the defective formation of the TD in morphant embryos is suggested by various findings. First, anatomically, lymphangiogenic secondary sprouts give rise to the string of PL cells, which in their turn form the LECs of the TD. Genetic studies underscore the participation of these lymphangiogenic secondary sprouts in lymphangiogenesis, as loss of *Vegf-c*, *Ccbe1*, or *synectin* impairs the formation of lymphangiogenic secondary sprouts and, in association, also of the TD ((Hogan et al., 2009a), unpublished). Second, there is a close

Fig. 7. (continued) underdevelopment of the PL string (or even complete absence of PL cells), with accompanying overrepresentation of angiogenic secondary sprouts. **C-C’’’**, LOWER PANELS: LISV MIGRATION DEFECTS: **C**, As a result of the overrepresentation of vISVs, LISV-PLs are deprived of their normal aISV guidance template. **C’-C’’’**, LISV formation is further impaired by additional navigation defects, most frequently because LISV-PLs cells bypass their turning point and never initiate ventral radial migration (**C’**), or occasionally make the turn but then stall (**C’’**). Still more rarely, navigating LISV-PLs deviate from their path (**C’’’**), or become misrouted along vISVs (**C’’’’**). The most frequent defects are boxed in grey. DA, dorsal aorta; DLAV, dorsal longitudinal anastomosing vessel; DLLV, dorsal longitudinal lymph vessel; ISV, intersomitic vessel; aISV, arterial ISV; LISV, lymphatic ISV; vISV, venous ISV; PCV, posterior cardinal vein; PL, parachordal lymphangioblast string; LISV-PLs: migrating PL cells during LISV formation; TD, thoracic duct.

correlation between the impaired formation of the lymphangiogenic secondary sprouts, of the string of PL cells and of the TD.

The secondary sprouts that emerge from the PCV and give rise to the PL string, as well as the PL string itself, were termed “lymphangiogenic” to denote their participation in the process of lymphangiogenesis. It is unknown whether ECs of these sprouts have the potential to become a LEC (“competence”), or are already programmed to become a LEC, albeit reversibly (“specification”) (Donner et al., 2006). In mammals, Prox-1 has been implicated in lymphatic specification (Oliver and Srinivasan, 2008); other candidates, such as Podoplanin, Neuropilin-2, Foxc2 and others have been implicated as markers or regulators of later stages of lymphatic development (Baluk and McDonald, 2008; Oliver and Srinivasan, 2008). Although currently available techniques are not sufficiently sensitive to define these precise stages of lymphatic development in zebrafish embryos (and, hence, to define the precise role of Notch in these processes), a number of findings suggests that these lymphangiogenic structures belong to the lymphatic lineage. Indeed, the lymphangiogenic sprouts and PL cells contribute only to lymphangiogenesis but not to angiogenesis, are not labeled in the *kdr-l:mCherryRed* line which marks only arterial and venous ECs (Hogan et al., 2009a), and fail to form upon silencing of genes that regulate lymphangiogenesis in mice and humans, e.g., *Ccbe1*, *Vegf-c*, *Synectin* and *Prox-1* (Alders M et al.; Hogan et al., 2009a) and unpublished). Although our *in vitro* findings that activation of Notch in venous ECs upregulated LEC-specific markers could suggest a role for Notch in the acquisition of lymphatic properties, other mechanisms cannot be excluded. For instance, Notch silencing might impair budding of lymphangiogenic cells, as occurs in VEGF-C knockout mice (Karkkainen et al., 2004). The latter mechanism is, however, more difficult to reconcile with the observation that the total number of secondary sprouts was normal in Notch hypomorphants.

Notch expression was detected at two sites along the trajectory of lymphangiogenic cells from the PCV to the TD. First, Notch was detectable in the DA. Since the DA and PCV lie in close juxtaposition to each other at the time of lymphangiogenic sprouting, Notch activation in arterial ECs by Dll4, expressed by the same or adjacent arterial cells, might induce expression of intermediate cues, that indirectly instruct venous ECs of the nearby PCV to acquire lymphangiogenic potential. Notch is known to elevate the expression of lymphatic signals such as EphrinB2 and VEGF-D (Makinen et al., 2005; O’Neill et al., 2007). A similar indirect model has been recently proposed to explain how BECs in the DA differentiate to venous BECs in the PCV (Herbert et al., 2009). Another non-exclusive model might rely on our observations of a weak Notch signal in ECs on the dorsal side of the PCV. In this case, intercellular communication between arterial Dll4 and venous Notch *in trans* could occur, whereby Notch activation in venous BECs might promote lymphatic development. Second, Notch activity was also detectable in aISVs at a time, when PL cells make the turn and switch from tangential to radial ventral migration to form the LISVs and TD. Since LISVs and aISVs lie very closely together, Notch signaling in the latter could indirectly signal to the former and thereby regulate lymphatic development.

The lymphatic phenotype in the Notch hypomorphants is unlikely to be secondary to a primary change in the formation or differentiation of the PCV. Indeed, no differences in

the initial formation and expression of venous markers were detected in the PCV a few hours prior to or after secondary sprout formation in Notch hypomorphants, consistent with previous reports (Leslie et al., 2007; Siekmann and Lawson, 2007). Similarly, no obvious abnormalities were observed in the formation, differentiation and marker expression of the primary ISVs. Nonetheless, we cannot formally exclude the possibility that subtle alterations in their arterial characteristics upon silencing of Notch might have favoured or facilitated supernumerary connections with secondary sprouts, thereby “entrapping” sprouts that would otherwise have remained lymphangiogenic. Regardless of these possibilities, our findings document a novel role of Notch in lymphangiogenic secondary sprouting and PL string formation, the initial steps of lymphatic development in zebrafish.

ROLE OF NOTCH IN LYMPHATIC MIGRATION FROM THE PL

Notch signaling also regulated lymphangiogenesis by controlling the formation of LISVs, which arise from the PL cells and form the TD. Most frequently, the LISV was absent, but in other rarer cases, migrating LISV-PLs stalled or became misrouted. The available evidence suggests that lymphangiogenic EC migration *per se* (motility) was normal. Indeed, in embryos that formed a partial TD, cells of the lymphangiogenic secondary sprouts migrated dorsally without stalling and thereafter tangentially to establish the string of PL cells. Also, for PL cells that finished their ventral migration to the TD, Notch signaling was dispensable for their subsequent tangential outgrowth (not shown). Furthermore, *in vitro* migration or proliferation of LECs was also not affected by Notch signaling. Also, we did not detect signs of lymphatic regression or retraction (not shown). Together, this analysis suggests that defects in the intrinsic motoric, mitogenic or survival machinery of lymphangiogenic ECs unlikely explain the LISVs defects in Notch hypomorphant embryos.

It is therefore tempting to speculate that the LISV defects in Notch-silenced embryos may relate to an abnormality in lymphangiogenic cell pathfinding, though future studies will be required to characterize this process and its molecular basis in more detail. Our imaging analysis shows that LISV-PLs navigated in very close association along aISV templates when migrating away from the horizontal myoseptum and forming the TD. This remarkable interaction between LISVs and aISVs raises the question whether aISVs act as guidance templates for LISV-PLs, reminiscent of how *follower* axons navigate along a *pioneer* axon's pathway in the nervous system or how autonomic nerves use arterial tracks to reach their target (Bak and Fraser, 2003; Glebova and Ginty, 2005; Honma et al., 2002; Makita et al., 2008; Mukouyama et al., 2002). Hence, it is tempting to speculate that, when fewer aISVs are present in Notch hypomorphants because of lymphangiogenic sprouting defects, PL cells are deprived of navigation templates and therefore cannot form LISVs normally (Figure 7C). Other observations that LISV-PLs failed to turn and switch from tangential to radial migration or, more rarely, stalled, explored new routes, and erroneously selected incorrect paths are reminiscent of classic neuronal guidance defects (Figure 7C'-C'''). That arteries may act as navigation templates is evidenced by reports that autonomic nerves stall or become misrouted, when these arteries do not produce appropriate guidance cues (Honma et al., 2002; Makita et al., 2008). Whether this may suggest that Notch regulates the production

of guidance cues for LISV-PL cells by aISVs or nearby (somatic) cells to induce turning and radial migration at this guidance post or to guide them along aISV templates, to name only a few possible explanations, remains to be further determined. Phenotypic analysis of other morphant zebrafish lines also suggests that LISV development requires arterial-lymphatic congruence (SSM et al, unpublished findings).

CONCLUSIONS

This study provides novel insight for a role of Notch in lymphatic development, in part by regulating the initial steps of lymphangiogenic secondary sprouting and PL formation. Our data are in accordance with an involvement of Notch in the acquisition of lymphatic potential. In addition, the navigation defects of LISV-PL cells along aISVs, in which Notch signaling is activated, suggest that Notch also regulates lymph vessel pathfinding along arteries, though the exact molecular mechanisms need to be further explored in the future.

ACKNOWLEDGEMENTS

IG, FD, KH and WV are sponsored by a Ph.D. grant of the Institute for the promotion of Innovation through Science and Technology in Flanders (IWT-Vlaanderen), Belgium; IS is a postdoctoral fellow of the European Union Seventh framework program (Marie Curie Intra European fellowship); CRA is a postdoctoral fellow of the Federation of European Biochemistry Societies (FEBS); SL is a postdoctoral fellow of Deutsche Krebshilfe; JB; was supported by the Vrienden van het Hubrecht Stichting; BH by a CJ Martin fellowship. This work is supported in part by an unrestricted Bristol-Myers-Squibb grant to PC, by grant #LSHG-CT-2004-503573 of the EU FP6, and by Methusalem Grant. HJD acknowledges support from a VIDI grant. FC acknowledges support from CARIPLO N.O.B.E.L. The authors thank AL Harris (Oxford, UK) for his gift of the LZRSpBMN-WT and LZRSpBMN-DLL4 constructs, H Pendeuille (Liege, Belgium) for the zebrafish Tbx20 probe, and J den Hertog (Utrecht, the Netherlands) for the zebrafish Dab2 probe. The authors thank K Brepoels, A Carton, A Cobut, M De Mol, F Hendrickx, E Janssens, S Louwette, A Manderveld, M Peeters, J Souffreau, B Tembuysen, A Van den Eynde, A Van Nuffelen, B Vanwetswinkel, S Verstraeten and S Vinckier for technical assistance.

CONFLICT-OF-INTEREST DISCLOSURE: The authors declare no competing financial interests.

SUPPLEMENTAL MATERIAL

Supplemental material, including 8 supplemental figure and 2 supplemental movies can be found in the data supplement.

Note S1: Variable penetrance of lymphatic phenotypes in Notch hypomorphants

We speculate that the variably penetrant lymphatic phenotypes and spectrum of defects in the Notch hypomorphants is due to a combination of reasons, including the use of a submaximal dose of morpholino (incomplete silencing), technical limitations of injecting an identical dose of morpholino, genetic differences of the morphant embryos analyzed (outbred background), uneven dispersion of morpholinos upon daughter cell division, and variable timing of angiogenic/lymphangiogenic secondary sprout formation along the PCV (occurring within a time window of 30 to 50 hpf (Hogan et al., 2009)). As a result, achieving the necessary degree of silencing below the critical biological threshold at the distinct sprouting locations along the PCV becomes stochastic in such experimental conditions.

Note S2: Lymphatic reprogramming

In the *in vitro* experiments, expression of *VEGFR3* was upregulated by activation of Notch, consistent with some, though not all previous reports (likely reflecting the context-dependent regulation of this receptor which has different roles in vascular versus lymphatic development) (Shawber et al., 2007; Tammela et al., 2008). In our silencing conditions, no difference in *Vefgr3* expression was detectable by *in situ* hybridization (Figure S4), but the semi-quantitative and insensitive nature of this technique, may have precluded detection of such subtle differences.

Cell culture experiments

HUVEC cells (Lonza, Invitrogen, Merelbeke, Belgium) and HUVEC/COS co-cultures were grown in EGM2-MV medium (Lonza, Invitrogen) at 37°C. COS cells were grown in standard DMEM medium (Lonza, Invitrogen) supplemented with 10% FBS, 2 mM glutamin, 100 U/ml penicillin, and 0.1 mg/ml streptomycin (Lonza).

CO-CULTURE ASSAY: COS cells stably expressing full length human DII4 (COS^{DII4}) or expressing GFP (COS^{GFP}) were prepared using the retroviral constructs LZRSpBMN-DLL4 and LZRSpBMN-WT, respectively (Williams et al., 2006). HUVECs were co-seeded with COS^{DII4} or COS^{GFP} cells in 6-wells at a density of 200,000 cells each, grown for 24 hours and harvested for RNA analysis by quantitative RT-PCR using human gene-specific primers (Table S2). **PROLIFERATION ASSAY:** Primary LEC (HMVEC-DLy or HMVEC-LLy; Lonza, Invitrogen) were starved overnight in EGM2 medium (Lonza, Invitrogen) containing 0.1% serum and no growth factors (starvation medium). The starved cells were seeded at 2,000 cells per well in 96-well microtiter plates, after which proliferation was induced with fully supplemented EGM2-MV medium with or without increasing concentrations of DAPT (20-60 µM). Proliferation was measured as the number of viable cells after further culturing for 48 hours, expressed in % of DMSO control. Viable cells were quantified using the Rapid Cell Proliferation assay (Calbiochem, San Diego, CA). **SCRATCH WOUND MIGRATION ASSAY:** Confluent monolayers of LECs growing in 0.1% gelatin-coated wells of a 24-well plate were starved overnight, pretreated in starvation medium containing 30 µM DAPT or 0.3% DMSO (control), scratch wounded and photographed (T0). The cells were further incubated for 24 hrs and photographed again (T24). Migration distance (gap width at T0 minus gap width at T24; 10 measurements per wound at regular intervals along the wound) was determined by image analysis using KS300 morphometry software, and is expressed relative to the control (DMSO). **TRANSWELL MIGRATION ASSAY IN CONDITIONS OF NOTCH INHIBITION:** LECs were pretreated with DAPT (60µ) or vehicle (DMSO) in starvation medium overnight, seeded at 30,000 cells per transwell on 0.1% gelatin-coated transwells in starvation medium with DAPT or DMSO, and cultured for 2 hours until adherence. Migration was induced by transferring the transwell insets into wells (bottom well) containing fully supplemented EGM2-MV medium with 100 ng recombinant human VEGF-C (Reliatech, TecoMedical NL, Nijkerk, the Netherlands), and DAPT or DMSO. Background migration was determined by including transwells with starvation medium in both the top and bottom well (baseline). After culturing for 16 hours, the non-migrated cells on the top side of the transwell filters were wiped off using PBS-soaked cotton swabs, and the transwells were fixed with 1% p-formaldehyde. The transwell filters were cut out and mounted upside-down on microscope slides with DAPI containing mounting medium. The filters were photographed under DAPI fluorescence at 20x magnification, and the nuclei were counted as a measure of migrated cells. Five transwells were prepared per condition and five optical fields were counted and averaged per transwell filter. **TRANSWELL MIGRATION ASSAY IN CONDITIONS OF NOTCH ACTIVATION:** LECs were starved overnight and seeded at 30,000 cells per transwell on transwell filters coated with BSA or with the extracellular domain of DII4 (DII4-ECD; R&D Systems Europe Ltd., Abingdon, UK) to activate the Notch pathway as described (Harrington et al., 2008). Further manipulation was as described above, using starvation medium in all top wells and fully supplemented medium containing VEGF-C in all bottom wells except for the baseline conditions. The filters were photographed under DAPI fluorescence at 10x magnification, Five transwells were prepared per condition and 1 central optical field was counted per transwell filter.

Movie S1: Normal formation of arterial and venous ISVs in control embryos

Confocal time-lapse video-imaging analysis of a control *Flt1:YFPxkdr-l:mCherryRed* reporter embryo from 32 to 72 hpf (representative movie of >100 embryos analyzed), in which venous cells are red (CherryRed⁺) and arterial cells yellow (YFP⁺CherryRed⁻). Imaging revealed normal progressive ventral-to-dorsal loss of the arterial YFP colour in approximately half of the ISVs, once connected by angiogenic secondary sprouts of the PCV. For instance, the second and third primary ISV (numbering according to the location at the start of the movie) retain their connection with the DA as well as their yellow arterial colour, and are thus arterial. In contrast, the fourth and fifth ISV loose their connection with the DA as well as their yellow arterial colour, progressively become red after establishing a connection with the PCV, and thus become venous ISVs.

Note: This *Flt1:YFPxkdr-l:mCherryRed* reporter does not label lymph vessels. However, since lymphangiogenic

secondary sprouts emanate from the PCV (CherryRed⁺) and the CherryRed protein is only degraded after some time, the presence of these lymphangiogenic secondary sprouts and of the PL cells is also transiently visible. For instance, around 40 hpf, red lymphangiogenic secondary sprouts can be seen adjacent to the second and third ISV. These secondary sprouts do, however, not connect to the primary ISVs, but migrate dorsally to the horizontal myoseptum, where they then migrate tangentially and form the PL string. The lymphangiogenic nature of the PL string is illustrated by the gradual loss of its residual mCherryRed colour beyond 52 hpf; this is not due to regression of the PL cells, since this string disappears only around 4 dpf, i.e. after giving rise to the LISVs (not visible in this reporter line) that descend ventrally to the level between the DA and PCV to form the TD. DA, dorsal aorta; PCV, posterior cardinal vein; PL, parachordal lymphangioblast string; TD, thoracic duct.

Movie S2: Arterial-to-venous shift of ISVs in Dll4KD embryos

Confocal time-lapse video-imaging analysis of a *Dll4^{KD} Flt1:YFPxkdr-l:mCherryRed* embryo from 32-72 hpf (representative movie of >100 embryos analyzed), in which venous cells are red (CherryRed⁺) and arterial cells yellow (YFP⁺CherryRed⁺). Imaging revealed progressive ventral-to-dorsal loss of the arterial YFP colour in all primary ISVs, when they became connected by an angiogenic secondary sprout and therefore adopted a venous fate. In this embryo, there was a shift of lymphangiogenic to angiogenic secondary sprouting in all somites imaged.

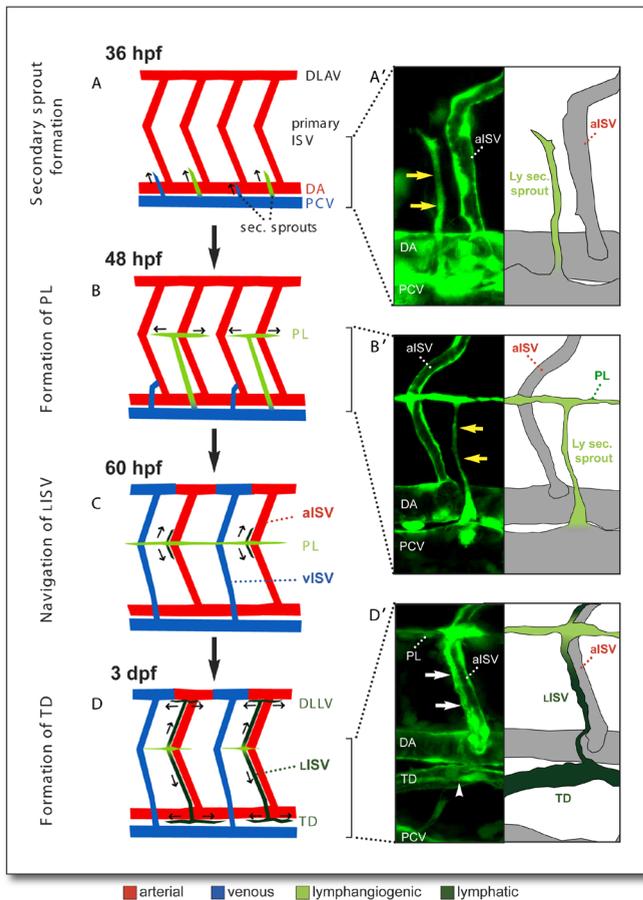


Figure S1: Model of lymphatic development in zebrafish embryos

In all panels, a schematic figure is shown on the left, and for panel A,B,D a high-magnification image of the blood and lymphatic vasculature at different stages of development in *Flt1:eGFP^{+/+}* zebrafish on the right. For clarity, the confocal images are flanked by redrawings of the vessel contours. DA, dorsal aorta; DLAV, dorsal longitudinal anastomosing vessel; DLLV, dorsal longitudinal lymph vessel; ISV, intersomitic vessel; aISV, arterial ISV; LISV, lymphatic ISV; vISV, venous ISV; PCV, posterior cardinal vein; PL, parachordal lymphangioblast string; TD, thoracic duct. Permanent lymphatic structures (LISV, TD) are labeled dark green; transient lymphangiogenic structures (lymphangiogenic secondary sprouts; PL cells) are labeled light green. **A,A'**, From around 30 hpf onwards, secondary sprouts arise from the PCV. About half of them will give rise to lymphatic structures and are therefore named lymphangiogenic secondary sprout (Ly sec. sprout; yellow arrows in A'). The other half of the secondary sprouts remain venous in nature (angiogenic secondary sprouts) (blue in A). **B,B'**, By 48 hpf, the lymphangiogenic sprouts (yellow

arrows in B') radially migrate dorsally to the level of the horizontal myoseptum, where they migrate tangentially to give rise to a transiently existing string of PL cells. The angiogenic sprouts connect to the aISV (red), which thereby

Figure S1 (continued): will acquire a venous identity. **C**, Around 60 hpf, PL cells turn and switch from tangential to radial migration closely along aISVs, thereby forming lymphatic intersomitic vessels (lISVs); note the close association of lISVs with aISVs. lISVs that ascend form the dorsal longitudinal lymph vessel (DLLV), while those that descend form the TD. ISVs that connected to the angiogenic secondary sprouts progressively loose their arterial identity and acquire a venous fate. **D,D'**, From 3 days onwards, the first TD fragments appear at distinct locations along the trunk and, via tangential migration, extend rostrally and caudally to merge into a complete TD. The lISV and TD are indicated by white arrows and arrowhead, respectively, in D'.

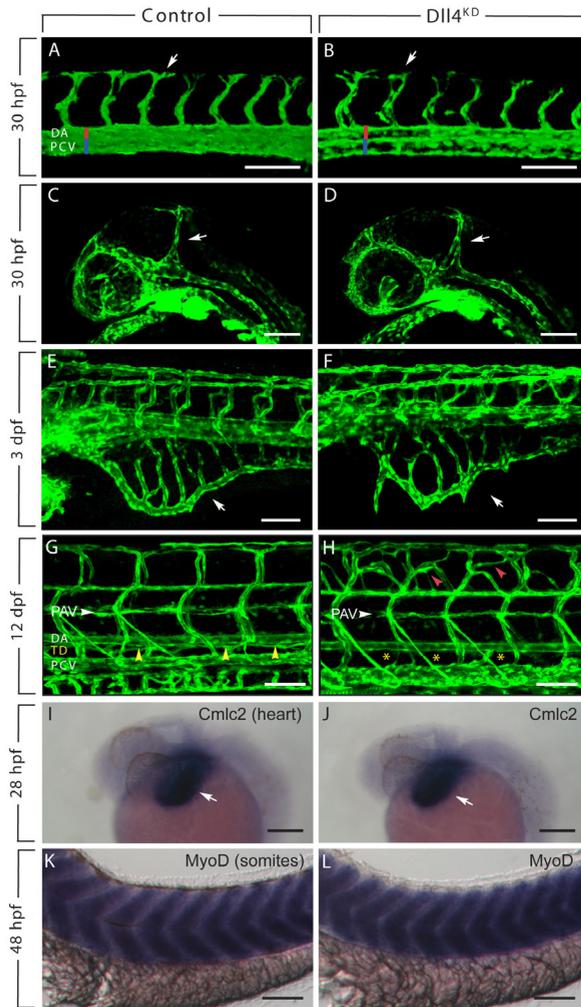


Figure S2: Development of embryos upon incomplete inhibition of Dll4

Complete silencing of Dll4/Notch signaling causes pronounced angiogenic defects (Hofmann and Iruela-Arispe, 2007; Roca and Adams, 2007; Phng and Gerhardt, 2009; Swift and Weinstein, 2009). We therefore performed a detailed analysis, using high-resolution imaging, of the vasculature of control (A,C,E,G) and Dll4^{KD} hypomorphant *Fli1:eGFP^{v1}* embryos (10 ng Dll4^{SPL}; B,D,F,H). In all panels, the head of the embryo faces left. Scale bars are 100 μ m. DA, dorsal aorta; PAV, parachordal vessel; PCV, posterior cardinal vein; TD, thoracic duct. **A,B**, The early vasculogenic stages proceeded normally in morphant embryos, resulting in the formation of properly sized and shaped axial vessels at timely developmental stages. Knockdown of Dll4 did not affect the timing or pathfinding of primary ISVs, or the subsequent formation of the DLAV (arrows) in embryos at 30 hpf. The DA is indicated by a red vertical bar, while the PCV is denoted by a blue vertical bar. **C,D**, Close-up images of the head vasculature at 30 hpf, showing similar appearance in control and Dll4^{KD} embryos. The arrow denotes the mid-cerebral vein. **E,F**, The subintestinal vessels (arrows) in 3-dpf Dll4^{KD} embryos displayed a largely comparable network morphogenesis with only minimal signs of hyperbranching. **G,H**, Image of a 12-dpf embryo, revealing that knockdown of Dll4 did not prevent the formation of the PAV, which develops only after the TD is established. Note the absence of the TD in the morphant embryo (asterisks in panel H), indicating that the TD defect persisted and was not rescued over time. The yellow arrowheads in G denote the course

of the TD in the control embryo. The red arrowheads in H denote mild hyperbranching of the ISVs in the Dll4^{KD} embryo. **I-L**, Whole-mount *in situ* stainings for *Cmlc2* (I,J; 30 hpf) and *MyoD* (K,L; 48 hpf), showing that size and positioning of the heart (arrow) and somite development are normal in Dll4^{KD} embryos. Overall, at the morpholino concentrations used in our analyses, no overt angiogenic malformations were detected in Dll4^{KD} embryos prior to or during lymphangiogenesis. Further, imaging of the *Fli1:YFP* reporter line, in which only arterial ECs are labeled, confirmed that primary aISVs expressed the YFP transgene in Dll4^{KD} embryos, indicating that their initial arterial specification occurred normally (see Movie S2).

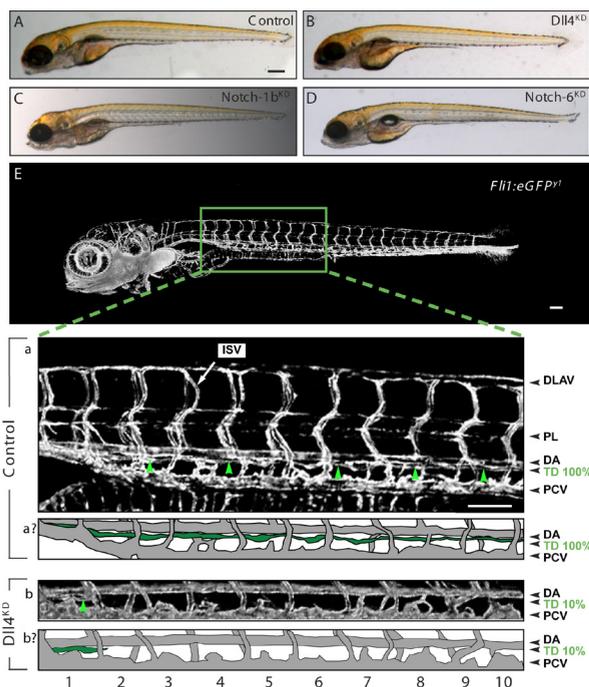


Figure S3: General morphology and analysis of TD formation

A-D, Bright field images of 6-dpf control (A), Dll4^{KD} (10 ng Dll4^{SPL}; B), Notch-1b^{KD} (15 ng Notch-1b^{SPL}; C) and Notch-6^{KD} (15 ng Notch-6^{SPL}; D) embryos, showing normal overall morphological development. Only morphant embryos with a normal trunk circulation and body size, without developmental delay, tissue malformations, general edema or toxic defects were included in TD screening assays. **E**, TD quantification. In all panels the head of the embryos faces left. DA, dorsal aorta; DLAV, dorsal longitudinal anastomosing vessels; ISV, intersomitic vessel; PCV, posterial cardinal vein; PL, parachordal lymphangioblast string; TD, thoracic duct. TD formation was quantified by measuring the length over which it formed in 10 consecutive somite segments (i.e. somites 5-15; demarcated by the green rectangle). Confocal images of control and morphant *Fli1:eGFP^{fl}* embryos are depicted in the insets. Inset a: in the control embryo, a continuous TD formed over all 10 somite segments (100% TD formation; green arrowheads). Inset b: severely morphant embryo, in which the TD formed over only 10% (green arrowhead). Inset a' and b': schematic redrawing of the DA, TD and PCV in the embryo shown in inset a and b, respectively, with the TD or TD segment marked in green. Scale bars are 200 mm in A-D, 100 mm in E and insets of E.

arrowheads). Inset b: severely morphant embryo, in which the TD formed over only 10% (green arrowhead). Inset a' and b': schematic redrawing of the DA, TD and PCV in the embryo shown in inset a and b, respectively, with the TD or TD segment marked in green. Scale bars are 200 mm in A-D, 100 mm in E and insets of E.

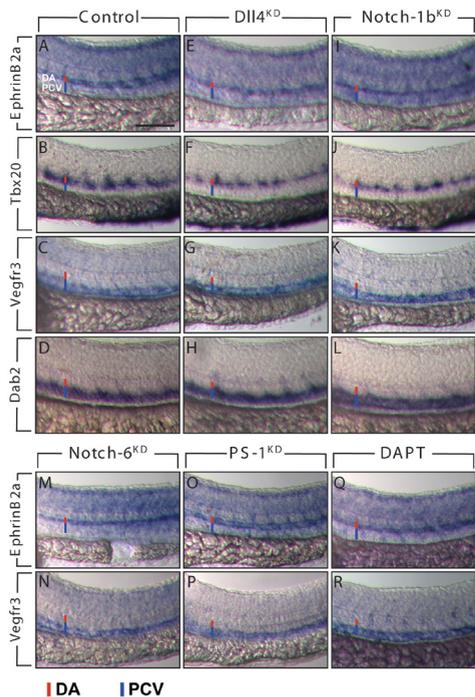


Figure S4: Normal arterial-venous differentiation after inhibition of Notch

A-R, Arterial-venous differentiation of the large axial vessels was evaluated upon incomplete silencing of the components of the Dll4/Notch signaling pathway that were shown in this study to affect lymphatic development. Therefore, whole-mount embryos were *in situ* stained for arterial (*EphrinB2a*; *Tbx20* (Szeto et al., 2002; Pendeville et al., 2008)) and venous (*Vegfr3*; *Dab2* (Song et al., 2004; Herpers et al., 2008)) markers in control embryos (A-D) and in Dll4^{KD} (10 ng Dll4^{SPL}; E-H), Notch-1b^{KD} (15 ng Notch-1b^{SPL}; I-L), Notch-6 (15 ng Notch-6^{SPL}; M,N), PS-1 (15 ng PS-1^{ATG1}; O,P) or DAPT-treated (25 μM; Q,R) hypomorphant embryos. Staining was performed at 28 hpf (few hours prior to secondary sprout formation) for *EphrinB2a*, *Vegfr3* and *Tbx20*, and at 48 hpf for *Dab2*, when arterial and venous differentiation of the DA and PCV were completed. Overall, expression of arterial markers in the DA and of venous markers in the PCV was comparable in control and morphant embryos. Also, note that there is no ectopic expression of these markers. In all panels, the head of the embryo faces left. The DA is indicated by a red vertical bar, while the PCV is denoted by a blue vertical bar. DA, dorsal aorta; PCV, posterior cardinal vein. Scale bar, representative for all panels, is 100 μm.

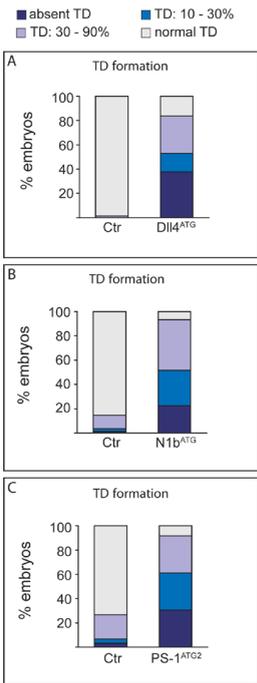


Figure S5: Impaired TD formation upon silencing of Notch

Specificity of the TD defects observed upon knockdown of Dll4, Notch-1b and PS-1 (Figure 1), was confirmed by second independent morpholinos targeting each of these genes. **A-C**, Bar graphs, representing the percentage of embryos at 6 dpf, that develop a normal TD (grey), a TD over 30-90% (lilac) or over 10-30% (blue) of its normal length, or completely lack any TD (dark blue) in the indicated fraction of control embryos ($N=144$ in panel A; 61 in panel B; 90 in panel C) and Dll4^{KD} ($N=172$; 2.5 ng Dll4^{ATG}; $P<0.001$ versus controls by Chi-Square test; panel A), Notch-1b^{KD} ($N=89$; 20 ng Notch-1b^{ATG}; $P<0.001$ versus controls; panel B) and PS-1^{KD} embryos ($N=36$; 15 ng PS-1^{ATG2}; $P<0.001$ versus controls; panel C).

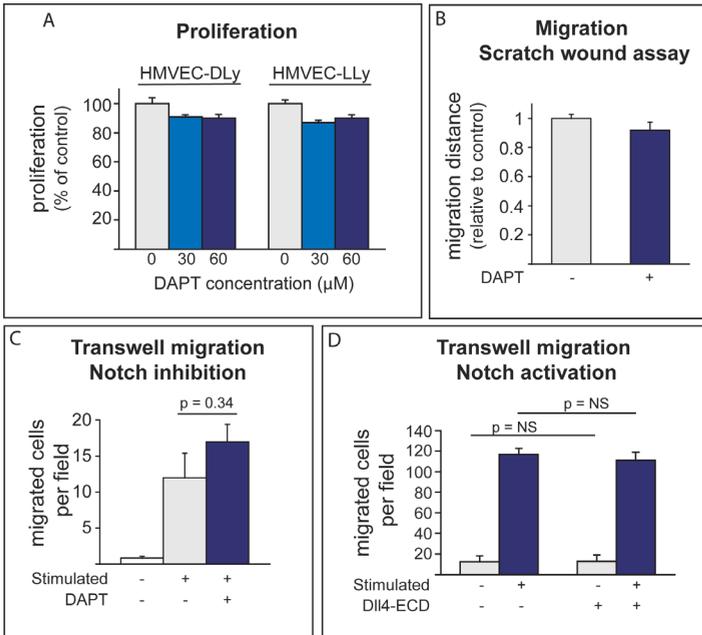


Figure S6: Inhibition of Notch does not affect in vitro proliferation and migration

A, Primary LECs of dermal (HMVEC-DLy) and lung (HMVEC-LLy) origin were starved overnight, after which proliferation was induced with full growth medium with or without increasing concentrations of DAPT (30-60 μM). Proliferation was measured as the number of viable cells after further culturing for 48 hours, expressed in % of control. **B**, Migration of LECs, analyzed using a scratch wound healing assay, was not inhibited by DAPT (30 μM). **C**, Transwell migration of LECs in response to culture medium containing 10% FBS and 100 ng/ml VEGF-C in the lower

compartment ("stimulated") was not affected by DAPT (60 μM). **D**, Transwell migration of LECs in response to culture medium containing 10% FBS and 100 ng/ml VEGF-C in the lower compartment was comparable, when cells were seeded on transwell filters coated with BSA (control) or the extracellular domain of Dll4 (Dll4-ECD), previously shown to activate Notch signaling (Harrington et al., 2008). Error bars represent SEM; $N=5-11$.

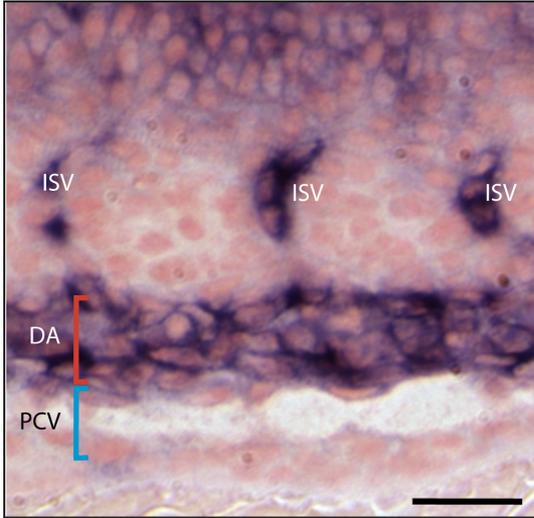


Figure S7: Expression of Notch-1B

Sagittal section of an embryo at 30 hpf, when lymphangiogenic sprouting occurs, whole-mount stained for Notch-1b. Head of the embryo faces left. DA, dorsal aorta; ISV, intersomitic vessel; PCV, posterior cardinal vein. Scale bar is 50 μ m. Notch-1b is strongly expressed in the DA and ISVs. A weak signal can be observed in the dorsal part of the PCV.

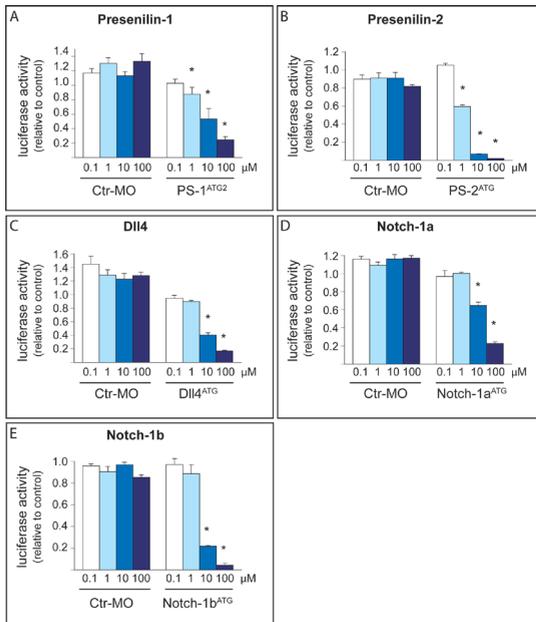


Figure S8: Morpholino efficacy assays

To knock down Notch family members, we injected one-cell stage embryos with morpholinos that block initiation of translation, either by targeting the ATG or nearby 5'UTR sequence (termed DII4^{ATG}, in the case of DII4) or splicing (DII4^{SPL}); each gene was silenced by these complementary approaches for confirmation; a control morpholino was consistently included in each experiment. **A-E**, The silencing efficiency of the newly described ATG targeting morpholinos was tested *in vitro*. To demonstrate the efficacy of the morpholinos PS-1^{ATG2} (A), PS-2^{ATG} (B), DII4^{ATG} (C), Notch-1a^{ATG} (D) and Notch-1b^{ATG} (E), we performed a luciferase reporter assay, as previously developed (Ny et al., 2005). We therefore cloned 25 nucleotides of the 5'UTR and 40 nucleotides of the coding sequence of the different genes (containing the ATG) upstream of and in frame with an open reading frame of the luciferase cDNA (lacking the initiator ATG codon) in an expression vector. Expression of this chimeric reporter protein in the erythrocyte lysate assay was monitored via luminometry (Ny et al., 2005). Values are represented as luciferase

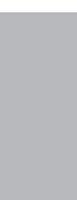
activity relative to control treatment (no addition of morpholino). Unlike the standard control morpholino (Ctrl-MO), supplementation of the gene-specific morpholinos dose-dependently blocked the expression of this chimeric reporter. Error bars represent SEM ($N=3$). *, $P<0.05$ versus the no morpholino treatment.

TABLE S1: MORPHOLINO OLIGONUCLEOTIDE SEQUENCES

MO	MO sequence	Target	Ref
DeltaA ^{ATG}	5'-CGCCGACTGATTCATTGGTGGAGAC-3'	Start site	
DeltaB ^{ATG}	5'-CGCCATCTCGCTCACTTTATCCTAA-3'	Start site	
DeltaC ^{ATG}	5'-GCACGTTAATAAAAACAGGCCATC-3'	Start site	
DeltaD ^{ATG}	5'-AACAGCTATCATTAGTCGTCATG-3'	Start site	
Dll4 ^{ATG}	5'-GAGAAAGGTGAGCCAAGCTGCG-3'	Start site	
Dll4 ^{SPL}	5'-TAGGGTTTAGTCTTACCTTGGTCAC-3' 5'-TGATCTCTGATTGCTTACGTTCTTC-3'	Exon6/intron6 Exon4/intron4	(Leslie et al., 2007)
Jag1a ^{ATG}	5'-GTCTGTCTGTGTCTGTGCTGTG-3'	5' UTR	
Jag1b ^{ATG}	5'-CTGAACTCCGTCGAGAATCATGCC-3'	Start site	
Jag2 ^{ATG}	5'-TCCTGATACAATTCCACATGCCGCC-3'	Start site	
Notch-1a ^{ATG}	5'-TTCACCAAGAAACGGTTCATAACTC-3'	Start site	
Notch-1b ^{ATG}	5'-ATGCATTCCTTCTTATGGATAGTCC-3'	Start site	
Notch-1b ^{SPL}	5'-AATCTCAAACCTGACCTCAAACCGAC-3'	intron28/exon29	(Milan et al., 2006; Leslie et al., 2007)
Notch-5 ^{ATG}	5'-ATATCCAAAGGCTGTAATCCCCAT-3'	Start site	(Lorent et al., 2004; Leslie et al., 2007)
Notch-6 ^{SPL}	5'-AGGTGAACACTTACTTCATGCCAAA-3'	exon7/intron7	(Lorent et al., 2004; Leslie et al., 2007)
PS-1 ^{ATG1}	5'-CCGGGATCATAGAAACAGCGGGAAC-3'	5' UTR	
PS-1 ^{ATG2}	5'-CATTCTGCACTAAATCAGCCATCGG-3'	Start site	
PS-2 ^{ATG}	5'-CTCTTCACTGTCTGAGGTATTCATG-3'	Start site	
control MO	5'-CCTTTACCTCAGTTACAATTATA-3'	Standard control MO (Gene Tools)	

TABLE S2: qRT-PCR PRIMER AND PROBE SEQUENCES

Human genes		
Hes1	Hs00232622_m1 (Premade Taqman Gene expression assays, Applied Biosystems)	
HEY1	Hs00232618_m1 (Premade Taqman Gene expression assays, Applied Biosystems)	
HEY2	Hs00232622_m1 (Premade Taqman Gene expression assays, Applied Biosystems)	
NRARP	Hs01104102_s1 (Premade Taqman Gene expression assays, Applied Biosystems)	
VEGFR3	For Rev Probe	5'-TTC CTG GCT TCC CGA AAG T-3' 5'-AGG CCA AAG TCA CAG ATC TTC AC-3' 5'-FAM-ACC TGG CTG CTC GGA ACA TTC TGC-TAMRA-3'
PROX-1	For Rev Probe	5'-GTG CTT TGG CGA CGT CAT C-3' 5'-TCA GTG GAA CTG GCC ATC TG-3' 5'-FAM-TTC CGA ACC CCC TGG ACA CCT TTG-TAMRA-3'
LYVE-1	For Rev Probe	5'-CAA AGA TCC CAT ATT CAA CAC TCA A-3' 5'-GGG ATG CCA CCG AGT AGG TA-3' 5'-FAM-CTG CAA CAC AAA CAA CAG AAT TTA TTG TCA GTG ACA-TAMRA-3'
EPHRINB2	Hs00970627_m1 (Premade Taqman Gene expression assays, Applied Biosystems)	
Sox18	For Rev	5'-AGA ACC CGG ACC TGC ACA-3' (Sybr Green qRT-PCR) 5'-CAG CTC CTT CCA CGC TTT G-3'
COUP-TFII	Hs00819630_m1 (Premade Taqman Gene expression assays, Applied Biosystems)	
NEUROFILIN1	For Rev Probe	5'-TGT GAA GTG GAA GCC CCT ACA-3' 5'-GGC CTG -GTC GTC ATC ACA TT-3' 5'-FAM-CCG ACC ACT CCC AAC GGG AAC TTG-TAMRA-3'
CD31	For Rev	5'-TCT GCA CTG CAG GTA TTG ACA A-3' (Sybr Green qRT-PCR) 5'-CTG ATC GAT TCG CAA CGG A-3'
VE-CADHERIN	Hs00174344_m1 (Premade Taqman Gene expression assays, Applied Biosystems)	
ENDOGLIN	Hs00164438_m1 (Premade Taqman Gene expression assays, Applied Biosystems)	
B-ACTIN	Hs99999903_m1 (Premade Taqman Gene expression assays, Applied Biosystems)	
B-ACTIN	For Rev	5'-TGG CAC CAC ACC TTC TAC AAT G-3' (Sybr Green qRT-PCR) 5'-TAG CAA CGT ACA TGG CTG GG-3'



Reprinted with permission from:
Development 136, 4001-4009 (2009) doi:10.1242/dev.039990

Vegfc/Flt4 signalling is suppressed by Dll4 in developing zebrafish intersegmental arteries

Robert Herpers^{1,2,*}, Benjamin M. Hogan^{1,*}, Merlijn Witte¹,
Hanna Heloterä³, Kari Alitalo³, Henricus J. Duckers², and Stefan
Schulte-Merker¹

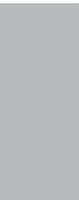
6

1. Hubrecht Institute-KNAW & University Medical Centre, Utrecht, and Centre for Biomedical Genetics Uppsalalaan 8, 3584 CT Utrecht, The Netherlands

2. Experimental Cardiology, Thoraxcenter, Erasmus University Medical Centre, s-Gravendijkwal 230, 3015 CE Rotterdam, The Netherlands.

3. Molecular Cancer Biology Laboratory, Department of Pathology, Haartman Institute, Biomedicum Helsinki, University of Helsinki, Haartmaninkatu 8, P.O.B. 63, 00014 Helsinki, Finland.

* These authors contributed equally.



ABSTRACT

The development of arteries, veins and lymphatics from pre-existing vessels are intimately linked processes controlled by a number of well studied, reiteratively acting signalling pathways. To delineate the mechanisms governing vessel formation *in vivo*, we performed a forward genetic screen in zebrafish and isolated the mutant *expando*. Molecular characterization revealed a loss-of-function mutation in the highly conserved kinase insert region of *flt4*. Consistent with previous reports, *flt4* mutants were deficient in lymphatic vascular development. Recent studies have demonstrated a role for Flt4 in blood vessels and showed that Dll4 limits angiogenic potential by limiting Flt4 function in developing blood vessels. We found that arterial angiogenesis proceeded normally, yet the *dll4* loss-of-function arterial hyper-branching phenotype was rescued, in *flt4* signalling mutants. Furthermore, we found that the Flt4 ligand Vegfc drives arterial hyper-branching in the absence of *dll4*. Upon knockdown of *dll4*, intersegmental arteries were sensitised to increased *vegfc* levels and the overexpression of *dll4* inhibited Vegfc/Flt4 dependent angiogenesis events. Taken together, these data demonstrate that *dll4* functions to suppress the ability of developing intersegmental arteries to respond to Vegfc driven Flt4 signalling in zebrafish. We propose that this mechanism contributes to the differential response of developing arteries and veins to a constant source of Vegfc present in the embryo during angiogenesis.

INTRODUCTION

During developmental angiogenesis, arteries, veins and lymphatics arise from pre-existing vessels by carefully regulated processes of sprouting, migration, proliferation and patterning of endothelial cells, collectively termed haemangiogenesis (for arteries and veins) or lymphangiogenesis (for lymphatic vessels). In the zebrafish embryonic trunk, developmental angiogenesis takes place in two distinct stages: primary sprouts form from the dorsal aorta to give rise to intersegmental vessels from ~22 hours post-fertilisation (hpf), and then secondary sprouts form from the posterior cardinal vein (PCV) to give rise to intersegmental veins and lymphatic vascular precursors from ~32 hpf (Isogai et al., 2003; Yaniv et al., 2006). Although primary sprouts will contribute to both functional arteries and veins after the later remodelling of the trunk vasculature (Isogai et al., 2003), primary sprouting is considered an arterial angiogenic process as sprouts derive exclusively from the dorsal aorta and express arterial markers (Siekman and Lawson, 2007), whilst secondary sprouting from the PCV is a venous angiogenic process. These processes are regulated by vascular endothelial growth factors and their receptors. The primary sprouting of intersegmental arteries (ISAs) is dependent on Vegfa, Kdr and Kdr-I (Bahary et al., 2007; Covassin et al., 2009; Covassin et al., 2006; Habeck et al., 2002) and the growth of ISAs has been reported to stall transiently upon morpholino (MO) knockdown of Flt4 or Vegfc (Covassin et al., 2006). *flt4* and *vegfc* are essential for lymphangiogenesis in the zebrafish trunk (Kuchler et al., 2006; Yaniv et al., 2006) and *vegfc* is required at the level of venous angiogenic sprouting (Hogan et al., 2009).

Mouse mutants or transgenic mice deficient for the ligand *Vegfc*, or for signalling by its receptor *Flt4*, lack lymphatic vessels and consequently display lymphedema (Karkkainen et al., 2004; Makinen et al., 2001; Veikkola et al., 2001). *Vegfc* deficient mice lack lymphatic vessels, due to a block in lymphangiogenesis that occurs at the level of budding of lymphangioblasts from venous endothelium, the earliest event in lymphatic vascular differentiation (Karkkainen et al., 2004). Consistent with the established functions of these factors during development, *Vegfc* and *Flt4* drive tumour lymphangiogenesis (Karpanen et al., 2001), their antagonists inhibit tumour metastasis (He et al., 2002) and *FLT4* mutations lead to primary (inherited) lymphedema in humans (Karkkainen et al., 2000).

A recent study has demonstrated a role for *Flt4* in haemangiogenesis (Tammela et al., 2008). The inhibition of *Flt4* reduced angiogenic sprouting of blood vessels during retinal or tumour associated angiogenesis (Tammela et al., 2008). Consistent with this role, *Flt4* is expressed in intersegmental vessels in the trunk of the developing mouse embryo and in the vasculature of the retina during angiogenesis, with enhanced expression in sprouting tip cells (Tammela et al., 2008). Notch signalling generally acts to robustly repress angiogenic potential of endothelial cells during development and disease (Hellstrom et al., 2007; Noguera-Troise et al., 2006; Siekmann and Lawson, 2007; Suchting et al., 2007). Consistent with this model, *Dll4* inhibition leads to dramatically increased angiogenesis that produces morphologically abnormal and non-functional blood vessels (Leslie et al., 2007; Noguera-Troise et al., 2006; Siekmann and Lawson, 2007). During retinal angiogenesis, *Dll4* induced signalling suppresses *Flt4* expression in endothelial tip cells but when *Dll4* or Notch signalling is inhibited, up-regulated *Flt4* activity drives ectopic sprouting and increased angiogenesis (Tammela et al., 2008).

During arterial angiogenesis in zebrafish, increased vessel sprouting induced by the loss of the Notch target transcription factor *Rbpsuh* (*Rbpja* – Zebrafish Information Network) can be suppressed, at least in part, by the depletion of *Flt4* using MOs, indicating that there is likely to be a conserved relationship between Notch signalling and *Flt4* function in zebrafish arteries (Siekmann and Lawson, 2007). During both arterial and venous angiogenesis, there is a constant source of *vegfc* in the zebrafish trunk, expressed first in the hypochord and then in the dorsal aorta (Covassin et al., 2006). Zebrafish *flt4* expression is found at high levels in venous endothelial cells during both arterial and venous angiogenesis but has also recently been identified in arterial cells (Covassin et al., 2009; Siekmann and Lawson, 2007). The presence of a constant source of ligand in the developing embryo, as well as receptor expression in sprouting endothelial cells during both arterial and venous angiogenesis, raises the question of how developing arteries and veins are programmed to differentially respond to *Vegfc/Flt4* signalling and what role Notch signalling may play.

Here we report the identification of a *Flt4* signalling deficient zebrafish mutant and investigate the relationship between *Dll4* function in arteries and *Vegfc/Flt4* signalling in the developing vasculature. As with *vegfc*, *flt4* is required for all venous derived angiogenesis in the zebrafish trunk, both in lymphangiogenesis and for the formation of intersegmental venous sprouts. Surprisingly, arterial angiogenesis is normal in zebrafish *flt4* signalling deficient mutants and we show that *dll4* suppresses *Vegfc/Flt4* signalling in zebrafish

arteries in order to allow for normal ISA development. Analysis of the expression of *vegfc* and *flt4* in *dll4* deficient arteries indicates that this suppression is not due to any observable changes in ligand or receptor transcription. We propose that this role of *dll4* contributes to the differential response of arteries and veins to a constant source of Vegfc in the trunk of the embryo during developmental angiogenesis.

MATERIALS AND METHODS

ZEBRAFISH

All zebrafish strains were maintained in the Hubrecht Institute using standard husbandry conditions. Animal experiments were performed in accordance with the rules of the Animal Experimentation Committee of the Royal Netherlands Academy of Arts and Sciences (DEC). The published transgenic lines used were *TG(fli1a:gfp)^{v1}* (Lawson and Weinstein, 2002), *TG(flt1:YFP)^{hu4624}* (Hogan et al., 2009) and *TG(kdr-l:Cherry)⁵⁹¹⁶* (Hogan et al., 2009). Embryos genotyped in Fig. 4 were of the *TG(fli1a:gfp)^{v1}* strain.

ENU mutagenesis was performed as previously described (Wienholds et al., 2002). The F1 progeny of mutagenised males were crossed to the *TG(fli1a:gfp)* strain to produce transgenic F2 families. Subsequent in-crossing of F2 progeny generated F3 embryos that were screened for the presence or absence of the thoracic duct.

POSITIONAL CLONING OF EXPANDO

The *flt4^{hu4602}* mutation was mapped using standard meiotic mapping with simple sequence length polymorphisms (SSLPs). The primers used for SSLP markers depicted in Fig. 2 were: z43267 – 5'-CAAAGGGTGCAAAGTCATT-3' and 5'-AGCAAAGTGCTGGTGATCA-3'; z26376 – 5'-CTGCTAACCTGCGTTCTTC-3' and 5'-CGTTAGCATATGCGCACTCT-3'; and z11725 – 5'-GCTCCAGAAGTGGAGCAAC-3' and 5'-TGATTTTGATTGGGGACCAT-3'. Subsequent genotyping and SNP analyses were performed by sequencing using the primer pair: 5'-AGCTCTTGATTGGCTTAG-3' and 5'-GGAAAGTATCCTTGCTCTGC-3'. Bioinformatic construction of the genomic region was performed using the Ensembl database <http://www.ensembl.org>, release 44, April 2007.

FLT4 KINASE ASSAY

Full-length human wild-type FLT4 and I1034S mutant FLT4 constructs were cloned into the pMXs vector (generous gift from Dr Toshio Kitamura, University of Tokyo, Japan) and transfected to HEK 293T cells (American Type Culture Collection) grown in DMEM supplemented with 10% foetal bovine serum (FBS) (PromoCell), glutamine and antibiotics. For immunoprecipitation and immunoblotting analysis, confluent plates of the cells were serum-starved for 2 hours, stimulated with VEGF-C (100ng/ml) and lysed in lysis buffer (50 mM HEPES, pH 7.5, 1% Triton X-100, 5% glycerol, 1 mM EGTA, 150 mM NaCl, 1.5 mM MgCl₂, 100 mM NaF, 1 mM each Na₃VO₄, PMSF, Aprotinin and leupeptin) (Saharinen et al., 1997). Equal amounts of protein in the lysates were used for immunoprecipitation using mouse monoclonal anti-human FLT4 antibodies (9D9) (Petrova et al., 2008). The immunocomplexes were captured using protein-G sepharose (GE Healthcare Bio-Sciences, Uppsala, Sweden), separated by 7.5% SDS-PAGE, transferred to a nitrocellulose membrane and detected using monoclonal mouse anti-phosphotyrosine (4G10; Upstate Biotechnology, Lake Placid, NY) or rabbit anti-human FLT4 antibodies, biotinylated secondary antibodies (Dako Denmark A/S, Glostrup, Denmark) and streptavidin-biotinylated horseradish peroxidase complex (GE Healthcare, Little Chalfont, UK) followed by enhanced chemiluminescence detection with the SuperSignal West Femto Maximum Sensitivity Substrate (Pierce, Rockford, IL). For re-probing, the membranes were stripped for 15 min at room temperature using Re-Blot Plus Strong Solution (Chemicon).

MRNA AND MORPHOLINO INJECTIONS

MOs targeting the *vegfc* and *flt4* start codons were as follows: *flt4* ATG MO – 5'-CTCTTCATTCCAGGTTTCAAGTCC-3' (Open Biosystems) and *vegfc* ATG MO 5'-GAAAATCCAAATAAGTGCATTTAG-3' (Genetools LLC), both injected at a concentration of 5 ng/embryo. The *dll4* MO targeted the exon 4/intron 4 splice donor site (5'-TGATCTCTGATTGCTTACGTTCTTC-3') and was injected at concentrations of 3ng or 6ng/embryo as indicated.

The *sFLT4*, *vegfc* and *vegfd* cDNA clones used have been previously described (Hogan et al., 2009; Ober et al., 2004). The full length *dll4* cDNA was sub-cloned into the pCS2+ vector by first amplifying from a full length template cDNA clone (accession number BC117624; Open Biosystems) using the PCR primers: 5'-GCGGGATCCACCATGGCAGCTTGGCTCACCTTTC-3' and 5'-GCGCTCTAGATTACTCTAGTTGCTATGAC-3' followed

by sub-cloning with *Bam*HI and *Xba*I. mRNA was transcribed from a *Kpn*I-linearised template using the SP6 RNA polymerase and the mMessage mMachine kit (Ambion) and injected at a concentration of 200 pg/embryo. The full-length human wild-type FLT4 and I1034S mutant constructs were cloned into the pCS2+ vector using the primers 5'-GCGCGGATCCACCATGCGACGGGGCGCCGCT-3' and 5'-GCGCTCTAGACTACCTGAAGCCGCTTCTT-3' to amplify the cDNA from the templates described above and the restriction enzymes *Bam*HI and *Xba*I digestion for cloning. mRNA for the wildtype and mutant forms of human *FLT4*, *sFLT4* and zebrafish *vegfc* and *vegfd* was transcribed from *Not*I digested template using the SP6 RNA polymerase and the mMessage mMachine kit (Ambion) and injected at the concentrations indicated.

TRANSGENESIS

The stable, germline transmitted *TG(flt4:YFP)^{hu4881}* transgenic line was generated by recombining a citrine-neomycin cassette using Red/ET Recombination Technology (Gene Bridges) into the BAC (bacterial artificial chromosome) clone DKEY-58G10 using the homology arm tagged PCR primers: aacgcgaggtttgctagaatatctaaaacccccggaggactggaacacctgACCATGGTGAGCAAGGGCGAGGAG-3' and 5'-aagaaggggaatcccaatccaaatccgacagaaaaacgtaaatctctctTCAGAAGAACTCGTCAAGAAGGCG-3' (homology arms are shown in lowercase). We found that BAC transgenesis produced germline founders but that embryos expressing YFP were highly dismorphic and died at stages prior to 24 hpf (data not shown). Hence, 6.6kb of the 5'UTR of *flt4* as well as the YFP coding sequence was PCR amplified using Phusion high fidelity PCR (Finnzymes) followed by cloning into the miniTol2 transgenesis vector (Kawakami, 2005). Amplification primers were: 5'-GCGCGAATCTAAGCAAAGTCAGACCTTACTGTCC-3' and 5'-CACGTACGGTGTGGTAACG-3'. One cell-stage embryos were co-injected with construct DNA (25ng/ μ L) and transposase mRNA (25ng/ μ L) and the progeny was screened for germline transmission. Low level-expressing germline stable lines were generated but expression was found to wane after 48 hpf suggesting that the construct may not contain all necessary regulatory elements for late expression.

IMAGING AND EXPRESSION ANALYSIS

In situ hybridisation was performed as previously described (Bussmann et al., 2007). The *tie2* (Lyons et al., 1998), *flt4* (Thompson et al., 1998), *vegfc* (Hogan et al., 2009), *vegfd* (Hogan et al., 2009), *dll4* (Herpers et al., 2008) and *hey2* (Zhong et al., 2000) probes were prepared as previously described. Embryos were mounted in 1% low melting point agarose in a culture dish with a cover slip replacing the bottom. Imaging was performed with Leica SPE or SP5 confocal microscopes (Leica Microsystems) using a 10x or 40x objective with digital zoom. Angiography was performed as previously described (Kuchler et al., 2006).

RESULTS

EXPANDO IS A FLT4 SIGNALLING DEFICIENT MUTANT

In a screen for developmental mutants that fail to form lymphatic vessels, we identified the mutant *expando^{hu4602}* that lacked the thoracic duct at 5 days post fertilisation (dpf) whilst retaining blood circulation (Fig. 1A-D). To determine the stage at which lymphangiogenesis was first impaired in *expando* mutants, we examined the phenotype in double transgenic *TG(fli1:GFP, kdr-l:Cherry)* embryos in which trunk blood vessels express both GFP and Cherry but lymphatic vessels express only GFP (Hogan et al., 2009). We found that all trunk lymphatic vessels, including the intersegmental lymphatic vessels (islv) and dorsal longitudinal lymphatic vessel (dllv) vessels, were absent in *expando* mutants at 5 dpf and that parachordal lymphangioblasts (PLs) had failed to bud from the PCV and were absent at 54 (hpf) (Fig. 1E-H). We examined *tie2* expression at 48 hpf as a marker for venous derived intersegmental vessels and found that venous sprouts were absent in *expando* mutants (Fig. 1I,J), a phenotype identical to that of *vegfc* MO-injected embryos which lack all venous angiogenic sprouting (Hogan et al., 2009).

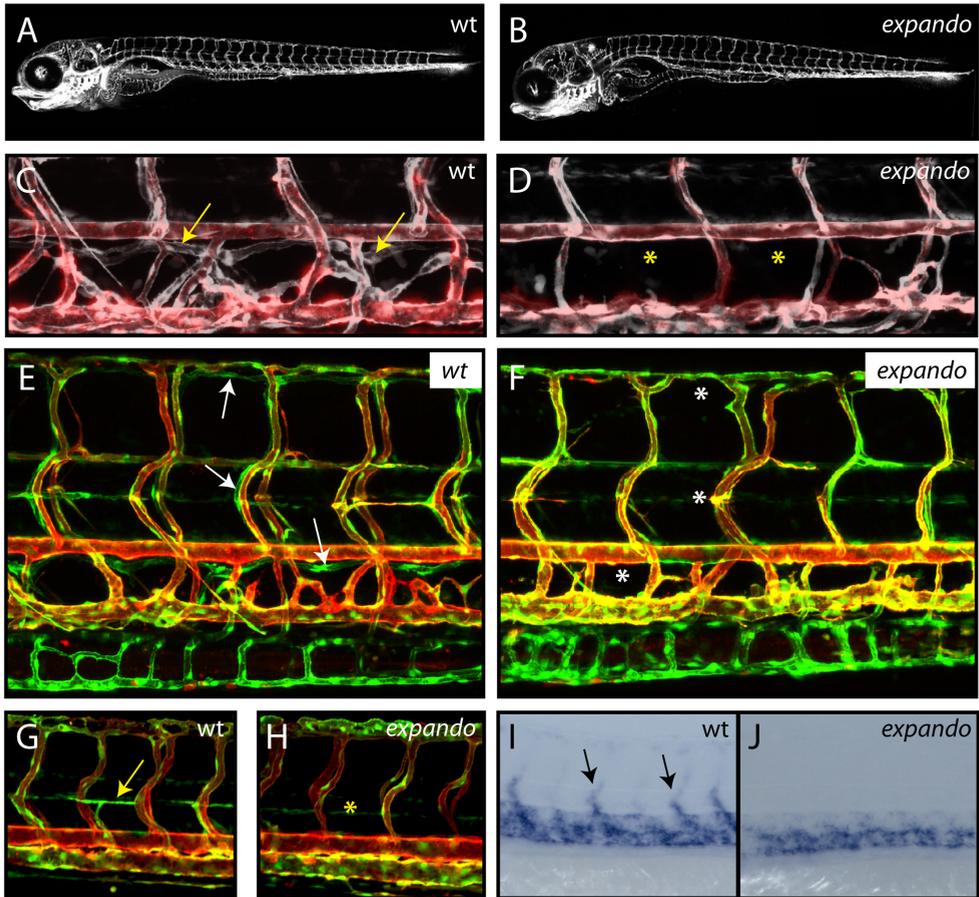


Fig. 1. Zebrafish *expando* mutants lack lymphatic vessels and venous sprouting. (A,B) Lateral views of *TG(fli1:GFP)* expression in wild-type (wt; A) and *expando* mutant (B) larvae at 5 dpf demonstrate that overall vascular patterning is not perturbed in *expando* mutants. (C,D) Overlay image of angiogram (red) and *TG(fli1:GFP)* (white) indicating the presence of blood flow in wildtype (C) and mutant (D) embryos. The thoracic duct (arrows) is present in wildtype but absent (asterisks) in mutant larvae. (E,F) Lateral views of wildtype (E) and *expando* mutants (F) in a double transgenic *TG(fli1:GFP)*, *TG(kdr-I:Cherry)* background. All lymphatic vessels are absent in mutants at 5dpf. Arrows indicate the thoracic duct (td), intersegmental lymphatic vessels (islv) and dorsal longitudinal lymphatic vessels (dllv) in wildtype embryos. Asterisks indicate their absence in *expando* mutants. (G,H) Parachordal lymphangioblasts (PLs) are absent from the horizontal myoseptum in *expando* mutants (asterisk in H) compared with wildtype siblings (arrow in G indicates PL) in the double transgenic *TG(fli1:GFP)*, *TG(kdr-I:Cherry)* background at 54 hpf. (I,J). *tie2* expression in venous sprouts (arrows in I) is absent in *expando* mutants (J) (n=6/29 embryos scored and confirmed by genotyping).

To identify the causative mutation for the *expando* phenotype, we used a traditional positional cloning approach and found the *expando* locus to be linked to a region of chromosome 14 containing the *flt4* gene (Fig. 2A). Sequencing of *flt4* revealed a point mutation predicted to change a conserved isoleucine residue into a serine at position 1042 in the split kinase domain (Fig. 2 B,C). To examine the functional consequence of this mutation we introduced the equivalent mutation (I1034S) into human FLT4 and compared the ability

of VEGFC to stimulate kinase domain activity of the wildtype and mutant forms of the receptor. We found that the I1034S mutation led to a loss of kinase domain function in this *in vitro* assay (Fig. 2D). Consistent with a *flt4* mutation leading to the *expando* phenotype, we found that the injection of either a *flt4* targeting morpholino oligomer (MO) or an mRNA encoding the soluble Ig domain of human FLT4 (*sFLT4*) that acts as a dominant inhibitor of Flt4 signalling in zebrafish (Ober et al., 2004), phenocopied the loss of lymphatic vessels (Fig. 3G; data not shown) as previously described (Kuchler et al., 2006; Yaniv et al., 2006). We hereafter refer to the *expando* (Flt4 I1042S) mutant as *flt4^{hu4602}*.

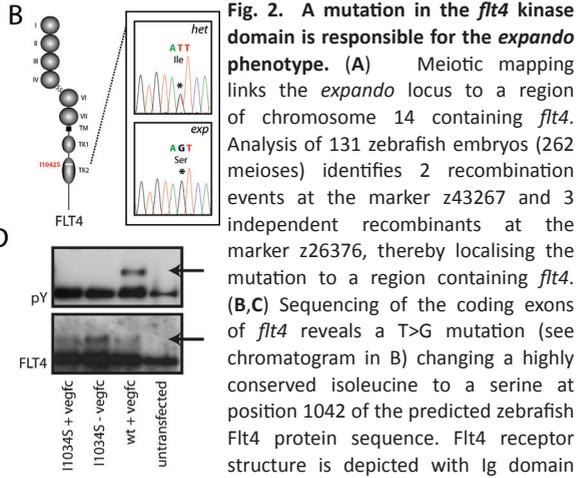
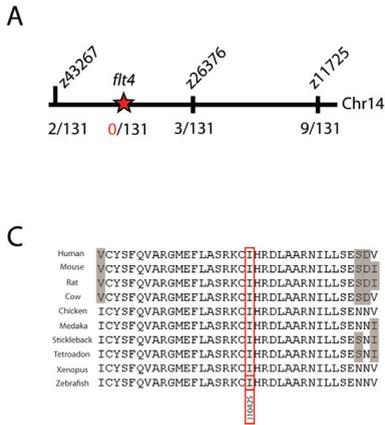
ANGIOGENESIS DEFECTS OF THE PRIMORDIAL HIND-BRAIN CHANNEL ARE OBSERVED IN FLT4 MORPHANTS, VEGFC MORPHANTS AND SFLT4 mRNA INJECTED EMBRYOS BUT NOT IN FLT4^{HU4602} MUTANTS

Previous studies have described angiogenesis defects after inhibition of *flt4* translation by MO injection (Covassin et al., 2006; Siekmann and Lawson, 2007). We injected *sFLT4* mRNA and also MOs targeting the start codons of *flt4* and *vegfc*. We found that these injections consistently induced angiogenesis defects during the formation of the Primordial Hind-Brain Channel (PHBC) (Fig. 3 C-E) in 20-40% of injected embryos. When all injected embryos from the same clutch were grown to 5 dpf they completely lacked lymphatic vessels, phenocopying the *flt4^{hu4602}* phenotype with 100% penetrance (Fig. 3 F,G). The dependency of PHBC formation upon Vegfc and Flt4 in zebrafish has been previously reported (Covassin et al., 2006). Surprisingly, in contrast to the injected embryo phenotypes, detailed examination of *flt4^{hu4602}* mutant embryos failed to reveal PHBC defects (Fig. 3B).

Taken together, these observations suggest two distinct possibilities: (1) that different thresholds of Flt4 signalling are required for distinct angiogenesis events in the zebrafish embryo such that normal signalling is necessary for lymphangiogenesis and venous angiogenesis, whereas very low level, residual signalling in the presence of the I1042S mutation is sufficient for PHBC development; or (2) that a non-signalling function of Flt4 regulates PHBC angiogenesis whereas signalling is indispensable for PCV sprouting and lymphangiogenesis.

To evaluate the possibility of performing experiments to rescue the morphant PHBC defect with mutant or truncated forms of Flt4, we injected full length mRNA encoding the human wildtype and I1034S mutant forms of FLT4 (300pg/embryo). We found that upon forced expression, both of these mRNAs were capable of inhibiting thoracic duct formation (wildtype *FLT4* mRNA 47% thoracic duct deficient, n=42; I1034S *FLT4* mRNA 26% thoracic duct deficient, n=31 (data not shown)) indicating that FLT4 has mild dominant negative activity upon overexpression by mRNA injection in zebrafish, therefore precluding an attempt to rescue PHBC defects.

Fig. 3 (continued): *vegfc* MO (5ng/embryo) inhibits PHBC development in 22% of injected embryos (n=41) and TD development in 97% of embryos in the same injection (n=37) and *sFLT4* mRNA (200pg/embryo) inhibits PHBC development in 42% of injected embryos and TD development in 100% of embryos in the same injection (n=120). Uninjected control embryos showed normal PHBC and thoracic duct (TD) development in 100% of cases (n=20) at 28 hpf and 4 dpf (F and G).



(I-VII), transmembrane domain (TM) and split tyrosine kinase domain (TK1 and TK2). An alignment of conserved residues (C) demonstrates that I1042 is a conserved residue, with grey shading indicating non-conserved residues. (D) Tyrosine phosphorylation (pY; upper panel, phosphotyrosine blot) was seen upon *in vitro* stimulation with VEGFC of wildtype human FLT4, but not of I1034S mutant FLT4. Lower panel (Flt4 protein blot) indicates the presence of the FLT4 protein post transfection in the assayed samples.

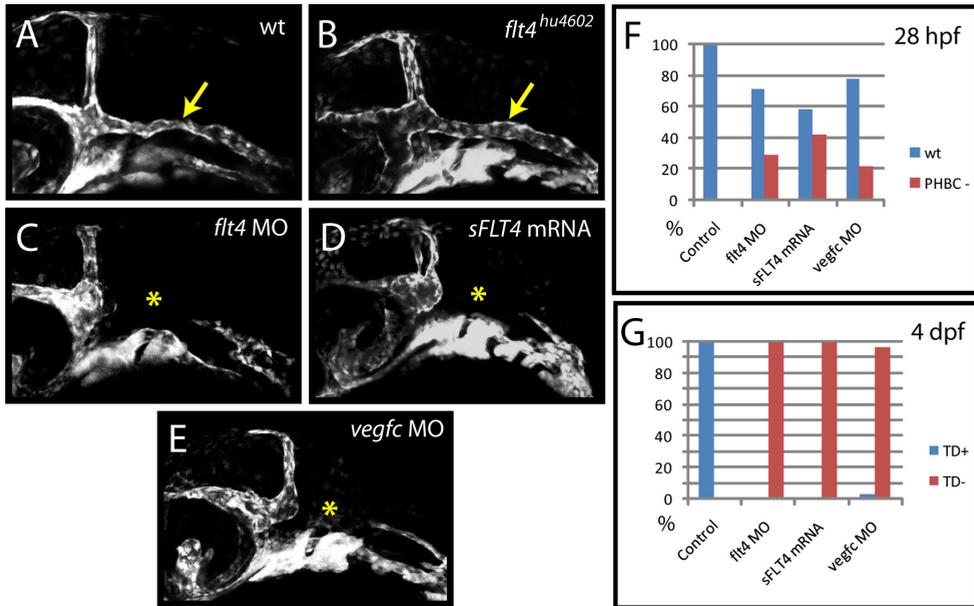


Fig. 3: Zebrafish *flt4*^{hu4602} mutants lack PHBC defects observed upon *flt4* morpholino, *vegfc* morpholino or *sFLT4* mRNA injection. (A-E) Angiogenesis of the primordial hind-brain channel (PHBC) fails to occur in *flt4* MO injected (5ng) (C), *sFLT4* mRNA injected (200pg/embryo) (D) and *vegfc* MO injected (E) embryos (yellow asterisk) compared with wildtype controls (A), but is unaffected (yellow arrow) in individually genotyped *flt4*^{hu4602} mutants (B) at 28 hpf. (F,G) Angiogenesis of the PHBC and lymphangiogenesis respond differently to injection of *flt4* MO, *vegfc* MO and *sFLT4* mRNA. Injection of *flt4* MO (5ng/embryo) inhibits PHBC development in 29% of injected embryos at 28 hpf but inhibits lymphangiogenesis (thoracic duct (TD) scored as readout) with 100% efficiency at 4dpf in the same injection (n=55 embryos scored). (continued on previous page)

EXCESSIVE ARTERIAL ANGIOGENESIS CAUSED BY THE DEPLETION OF DLL4 IS RESCUED IN FLT4^{hu4602} MUTANTS

We next examined arterial development in *flt4*^{hu4602} mutants by taking advantage of the *TG(flt1:YFP)*^{hu4624} transgenic line, in which the arteries of the embryonic trunk are labelled by YFP (Hogan et al., 2009). We examined the presence of the venous derived ISV components: these sprouts form during secondary sprouting from the vein, connect to ISAs in order to establish intersegmental venous vessels (Isogai et al., 2003) and are identifiable by the absence of *flt1* expression in the ventral component of functional intersegmental vessels at 3 dpf (Hogan et al., 2009). We found that like *vegfc* MO injected embryos (Hogan et al., 2009), *flt4*^{hu4602} mutants failed to form intersegmental venous derived vessels and in the absence of these venous sprouts, an increased number of ISA connections to the dorsal aorta were formed (Fig. 4A,B). Apart from the increased ISA connections to the dorsal aorta, the ISAs appeared otherwise normal in *flt4*^{hu4602} mutants.

Given the known relationship between *Dll4* and *Flt4* in angiogenesis (Siekmann and Lawson, 2007; Tammela et al., 2008), we injected a *dll4* MO that recapitulated the previously described *dll4* loss-of-function arterial hyper-branching phenotype (Leslie et al., 2007) into embryos derived from *flt4*^{hu4602} heterozygous crosses (*flt4*^{hu4602 +/-} x *flt4*^{hu4602 +/-}). We found the hyper-branching phenotype to be variable and sorted embryos displaying severe arterial hyper-branching (e.g. Fig. 4C) from those not displaying hyper-branching phenotypes (e.g. Fig. 4D) into separate groups for genotyping. We found that the mutant genotype was almost completely absent from the severe phenotypic category (present in 1/29 genotyped hyper-branching embryos) and was enriched in the non hyper-branching category (present in 21/55 genotyped embryos) indicating a rescue of the arterial hyper-branching phenotype associated with the mutant allele (Fig. 4E).

EXCESSIVE ARTERIAL ANGIOGENESIS CAUSED BY THE DEPLETION OF DLL4 IS DEPENDENT ON VEGFC

To test whether the *flt4* dependent *dll4* hyperbranching phenotype is driven by *Vegfc*, we injected embryos with *dll4* MO alone, *dll4* MO with *vegfc* MO or *dll4* MO with *sFLT4* mRNA. For all treatments, the *dll4* MO induced arterial hyper-branching phenotype was scored as either severe, mild or wildtype (no hyper-branching) (for examples, see Fig. S1 in the supplementary material). We found that the injection of either *vegfc* MO or *sFLT4* mRNA rescued the *dll4* excessive angiogenesis phenotype at 72 hpf (Fig. 4F). We observed no ISA defects upon injection of either *vegfc* MO or *sFLT4* mRNA at concentrations that completely inhibited lymphangiogenesis and also rescued the *dll4* phenotype.

FLT4 AND VEGFC ARE EXPRESSED IN ARTERIAL ENDOTHELIAL CELLS DURING ANGIOGENESIS AND THEIR EXPRESSION IS UNALTERED UPON LOSS OF DLL4

To determine if the phenotype could be explained by changes in gene expression during arterial angiogenesis, we analysed the expression of *flt4*, *vegfc*, *vegfd* (*figf* – Zebrafish Information Network) and *hey2* in *dll4* morphants at 24 hpf. We found *flt4* expression to be present in all ISAs and in the dorsal aorta at 24 hpf, but rapidly down-regulated thereafter, with expression vastly reduced in arteries as compared with the PCV by 26 hpf (Fig. 5A,C).

We carefully staged *dll4* MO injected and uninjected control embryos at 24 hpf (based on head angle and tail extension) and detected no appreciable change in *flt4* expression in the ISAs at 24 hpf (Fig. 5 A,B) or later during down-regulation of *flt4* expression (25, 27, 29 and 31 hpf; see Fig. S2 in the supplementary material) although we cannot exclude the possibility of mild changes for which *in situ* hybridisation is insufficiently sensitive to detect. We next generated a *flt4* promoter driven transgenic line utilising a 6.6 kb fragment of the *flt4* 5'UTR. We found that this promoter fragment drove expression of YFP in ISAs, the dorsal aorta and the PCV in both wildtype and *dll4* MO injected embryos with no apparent change in expression levels in stage matched embryos (Fig. 5 D,E). In *dll4* morphants at 24hpf, *vegfc* expression in the dorsal aorta (Fig. 5F,G) and *vegfd* expression in the tailbud (Fig. 5 H,I) were unchanged. In addition, we observed no change in the expression of *hey2*, indicating that developmental gene expression programs in arterial endothelial cells were largely normal in *dll4* MO injected embryos (Fig. 5 J,K).

DLL4 MORPHANT ARTERIES ARE SENSITISED TO INCREASED VEGFC DURING PRIMARY SPROUTING OF INTERSEGMENTAL ARTERIES

The arterial phenotype induced by the loss of *dll4* is not observed before 28-32 hpf, after which time the ISAs progressively display excessive angiogenesis and hyperbranching defects. Given that this phenotype is dependent on Vegfc/Flt4 signalling we hypothesised that the introduction of excessive *vegfc* may increase the severity or alter the onset of the phenotype. We introduced mRNA encoding full length zebrafish *vegfc* into wildtype and *dll4* MO injected embryos in the *TG(flt1:YFP)^{hu4624}* transgenic background and examined the ISAs at 28 hpf, a timepoint preceding secondary sprouting of vessels from the PCV and the arterial phenotype induced by the knockdown of *dll4*. We found that *vegfc* mRNA injection in combination with *dll4* MO synergistically induced aberrant sprouting of ISAs, which turned bilaterally at approximately the level of the base of the neural tube in a distinctive manner (Fig. 5 L-N,P). This phenotype was robustly reproducible, was not present in embryos injected with *dll4* MO only, and occurred only rarely upon injection of *vegfc* mRNA only (Fig. 5M,N,R). Interestingly, we also observed this phenotype upon injection of full length zebrafish *vegfd* mRNA, but found no difference when *vegfd* mRNA was injected in combination with *dll4* MO (Fig. 5O,Q,R). Taken together, these data indicate that in the absence of *dll4*, arterial cells are more responsive to exogenously introduced *vegfc* at stages prior to venous sprouting, confirming an early capability, as well as an ongoing, suppressive role for *dll4* during Vegfc/Flt4 signalling in arterial angiogenesis.

OVEREXPRESSION OF DLL4 REDUCES SPROUTING FROM VENOUS ENDOTHELIUM

Taken together, the above data suggest that *dll4*, which is restricted in expression to the early arteries in developing embryos (Leslie et al., 2007; Siekmann and Lawson, 2007), functions to suppress the response of arteries to Vegfc mediated Flt4 signalling. This would predict that ectopic *dll4* in embryonic veins may inhibit or reduce Vegfc/Flt4 driven venous sprouting. To test whether this was the case, we injected mRNA encoding full-length *dll4* into *TG(flt1:YFP)^{hu4624}* embryos and examined the formation of venous sprouts at 52 hpf.

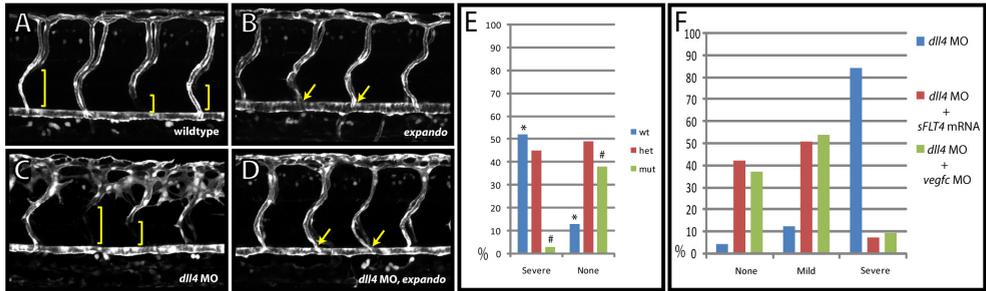
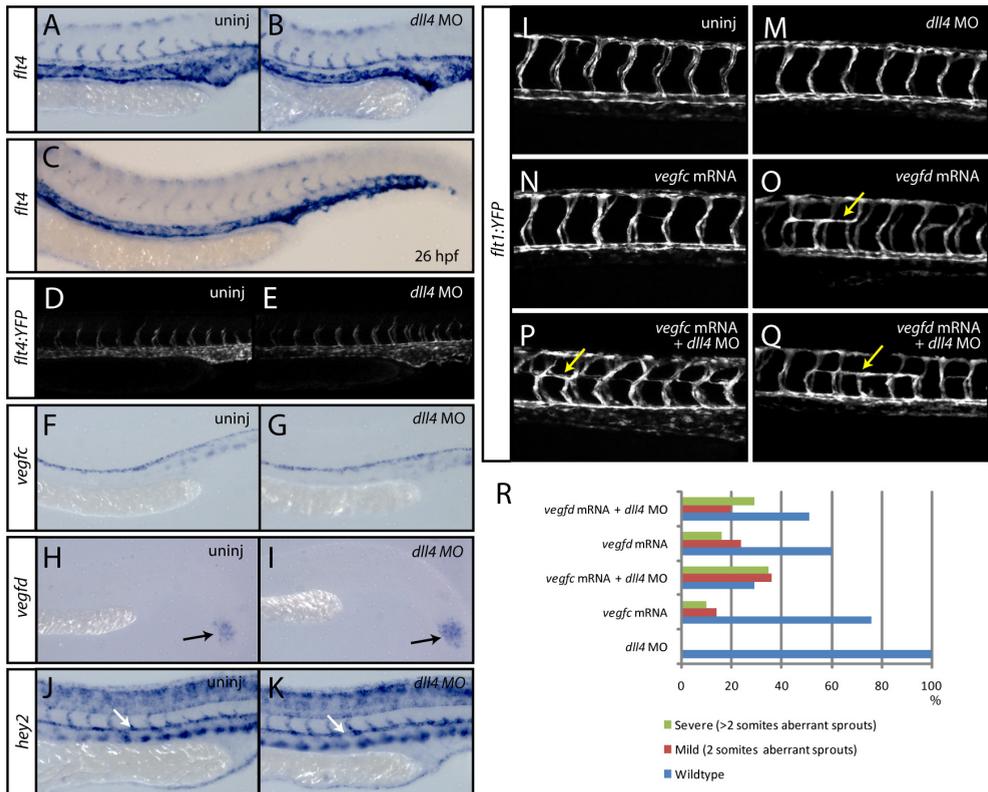


Fig. 4. The *dll4* morphant hyper-branching phenotype is rescued in *flt4*^{hu4602} mutants, *vegfc* morphants and *sFLT4* mRNA injected embryos. (A-D) Lateral views of uninjected control (A) and *flt4*^{hu4602} mutant (B) compared with wildtype (C) and *flt4*^{hu4602} mutant zebrafish embryos (D) injected with *dll4* morpholino. Images taken in the *TG(flt1:YFP)*^{hu4624} background labelling trunk arteries to reveal the failure to form intersegmental venous sprouts in *expando* mutants (B), indicated by the yellow arrows. The *dll4* morphant arterial hyper-branching phenotype (C) is rescued in *flt4*^{hu4602} mutants (D). Venous sprouts were identified by the absence of *flt1:YFP* expression in ISVs as indicated by the brackets. Embryos at 72 hpf. (E) Arterial hyper-branching phenotypes were scored post-injection of *dll4* MO and subsequently genotyped. The mutant genotype was almost completely absent from the severe category (e.g. C) (1/29 embryos, * $p < 0.01$ by Chi Square test) and was enriched in the category not displaying hyper-branching (e.g. D) (21/55 embryos, # $p < 0.01$ by Chi Square test). (F) In transgenic *TG(flt1:YFP)*^{hu4624} embryos, co-injection with *dll4* MO together with *vegfc* MO (green bars, n=57 embryos), or of *dll4* MO together with *sFLT4* mRNA (200pg/embryo) (red bars, n=67 embryos) led to a rescue of the arterial hyperbranching phenotype observed upon injection of *dll4* MO alone (blue bars, n=81 embryos). Arterial hyper-branching phenotypes were categorized as no hyperbranching (none), mild or severe (see Fig. S1 in the Supplementary material)



We identified venous sprouts by scoring the ventral segments of intersegmental vessels that did not express *TG(ftl1:YFP)^{hu4624}* at 52 hpf. We found that *dll4* overexpression led to cardiac defects and loss of circulation when injected at high doses but did not lead to the ectopic venous expression of *flt1* (data not shown). We selected embryos with normal blood circulation and omitted embryos severely affected by *dll4* overexpression. When the number of venous sprouts present across the first 12 intersegmental vessels anterior to the cloaca was scored, there was a significant reduction in the number of venous sprouts present in injected embryos compared with uninjected controls (Fig. 6).

DISCUSSION

FLT4 SIGNALLING IS REQUIRED FOR ZEBRAFISH LYMPHANGIOGENESIS AND VENOUS SPROUTING

Here we describe a new zebrafish *flt4* mutant phenotype that is caused by an amino acid substitution in the conserved split kinase domain of Flt4 (I1042S). Using this *in vivo* model, we have shown a strict requirement for normal Flt4 signalling for venous angiogenesis. We find that primary angiogenesis of ISAs can occur independently of normal Flt4 signalling in zebrafish. This finding is consistent with previous studies suggesting that ISA sprouting is chiefly regulated by Vegfa, Kdr and Kdr-I (Bahary et al., 2007; Covassin et al., 2006; Habeck et al., 2002; Lawson et al., 2003) but would suggest that previously described ISA morphant phenotypes for Vegfc and Flt4 do not reflect a requirement for wildtype kinase domain activity of the Flt4 receptor (Covassin et al., 2006). The defects in secondary sprouting from the veins observed in *flt4^{hu4602}* mutants are apparently identical to the previously described phenotypes of *full of fluid (ccbe1)* mutants and *vegfc* morphants (Hogan et al., 2009). *flt4* MO, *vegfc* MO or *sFLT4* mRNA injections led to the failure of PHBC development but the defects observed were far less penetrant than lymphangiogenesis failure seen within the same injection experiments and were not observed in *flt4^{hu4602}* mutants. These data suggest (1) that there is a differential dosage sensitivity for Flt4 signalling during different

Fig. 5. Sprouting intersegmental arteries express *flt4* and are sensitised to exogenously introduced Vegfc in the absence of *dll4*. (A-E) At 24 hpf (A and B) the expression of *flt4* is present in all arterial cells (A) and is unaltered upon loss of *dll4* (B) (n=40 uninjected control and n=40 *dll4* MO injected embryos scored). By 26 hpf (C), *flt4* is down-regulated in the dorsal aorta (n=20 embryos analysed). Analysis of a *flt4* promoter-driven transgenic line identifies YFP expression in all arterial cells at 24hpf (D). The expression of YFP is unaltered in *dll4* MO injected embryos (E). (F,G) At 24hpf the expression of *vegfc* is present in the dorsal aorta (F) and is unaltered in *dll4* MO injected embryos (G) (n=20 uninjected and n=20 MO injected embryos analysed). (H,I) The expression of *vegfd* in the tailbud is unaltered in *dll4* MO injected embryos (I) compared with uninjected control (H) embryos (n=20 uninjected and n=20 MO injected embryos analysed). (J,K) The expression of the arterial marker gene *hey2* is unaltered in *dll4* MO injected embryos (K) compared with uninjected control (J) embryos (n=20 uninjected and n=20 MO injected embryos analysed). (L-R) *dll4* morphants are sensitised to exogenously introduced *vegfc* mRNA during arterial angiogenesis. Forced expression by the injection of mRNA encoding full length zebrafish *vegfc* into *dll4* MO injected embryos (n=133) (P) led to aberrant ectopic bilateral turning of ISAs by 28 hpf (yellow arrows) which was never observed in either wildtype (L) or in those injected with *dll4* MO only (n=90) (M). ISAs rarely turn bilaterally upon injection of *vegfc* mRNA only (n=106) (N), whereas injection of full length zebrafish *vegfd* mRNA did robustly show this phenotype without (O) (n=211) or with *dll4* MO (Q) (n=227). For each of the conditions tested, the percentage of embryos showing wildtype, mild (aberrant ISAs spanning two somites) or severe (aberrant ISAs spanning more than two somites) ISA phenotypes is shown in (R).

angiogenesis events and/or (2) that some degree of *flt4* regulated angiogenesis may occur independently of kinase domain function. The scenario described here closely resembles that observed in the mouse, where mutants for *Vegfc*, double mutants for *Vegfd* and *Vegfc* together, or a hypomorphic *Flt4* allele all produce lymphatic vascular specific defects, whereas the complete loss of *Flt4* leads to defects in haemangiogenesis and early lethality (Dumont et al., 1998; Haiko et al., 2008).

DLL4 FUNCTION PROVIDES A MECHANISM BY WHICH ARTERIES, BUT NOT VEINS, SUPPRESS THE RESPONSE TO VEGFC DRIVEN FLT4 SIGNALLING DURING DEVELOPMENT

Despite the lack of a marked arterial phenotype in *flt4*^{hu4602} mutants, we find that *flt4* is actively transcribed in the ISAs and the dorsal aorta concurrent with sprouting arterial angiogenesis at 24 hpf. Furthermore, a source of *Vegfc* is present in the trunk derived from the dorsal aorta during this period. We find that the severe hyper-branching phenotypes observed in the absence of *dll4* are dependent on *Vegfc* and on *Flt4* kinase domain activity, indicating that one function of *dll4* is to suppress the arterial response to *Vegfc/Flt4* signalling in developing arteries of the trunk. Consistent with this, *Dll4* depleted arteries are sensitised to increased *Vegfc* levels supplied exogenously by mRNA injection and the overexpression of *dll4* reduces venous sprouting, which is dependent on *Vegfc/Flt4* signalling. Hence, the severe, progressive arterial hyperbranching phenotype that has been previously described upon loss of *dll4* in zebrafish is predominantly a consequence of failing to suppress the ability of developing arteries to respond to endogenous *Vegfc/Flt4* signalling. A working model summarising the contribution of *Dll4* in the context of arterial and venous angiogenesis and *Vegfc/Flt4* signalling is outlined in Fig. 7.

CHANGES IN VEGFC OR FLT4 EXPRESSION DO NOT EXPLAIN THE SUPPRESSION OF THE ARTERIAL RESPONSE TO VEGFC/FLT4 SIGNALLING

We find that *flt4* transcript levels are progressively down-regulated in developing arteries after 24 hpf, an event likely to contribute to lowering the responsiveness of arteries to endogenous *Vegfc*. However, the increased responsiveness of *dll4* morphants to *Vegfc/Flt4* signalling does not coincide with changes in *vegfc* or *flt4* transcription. In particular, there is no change in *vegfc* or *flt4* expression in *dll4* morphants during the formation of primary arterial sprouts (24-31 hpf) despite the fact that these sprouts are sensitised to increased levels of *vegfc* at early stages, prior to 28 hpf (Fig. 5). This indicates that *dll4* can regulate *Vegfc/Flt4* signalling at a level independent of *vegfc* or *flt4* gene transcription. In zebrafish, it has been previously demonstrated that *notch1b* knockdown or chemical treatment with a γ -secretase inhibitor (DAPT) that blocks the cleavage of the Notch intracellular domain (Geling et al., 2002) leads to the same increased exploratory behaviour of arterial endothelial cells that is observed upon *dll4* loss-of-function (Leslie et al., 2007). This correlation is suggestive of *dll4* acting through intracellular Notch signalling and would indicate that altered transcription should precede an altered response to *Vegfc/Flt4* signalling. In this context, the unchanged expression of the key molecular players (*flt4*, *vegfc*, *vegfd*) in *dll4* morphants implies that other, yet to be identified, molecular regulators are involved.

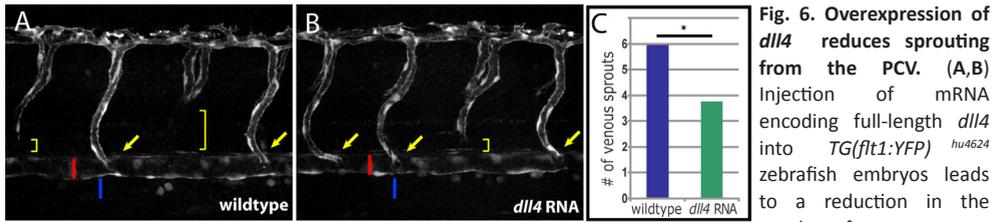


Fig. 6. Overexpression of *dll4* reduces sprouting from the PCV. (A,B) Injection of mRNA encoding full-length *dll4* into *TG(ftl1:YFP)^{hu4624}* zebrafish embryos leads to a reduction in the number of venous sprouts

in injected embryos (B), compared with uninjected control embryos (A) at 52hpf. ISAs that connect directly to the dorsal aorta (red bar) are indicated by yellow arrows. Venous spouts (yellow brackets) can be readily identified by the absence of *TG(ftl1:YFP)^{hu4624}* expression in the ventral component of an intersegmental vessel. Venous sprouts connect directly to the posterior cardinal vein (blue bar) from which they derive during secondary sprouting. (C) Quantification of the number of venous sprouts (Y-axis) on one side of the embryo across 12 segments anterior to the cloaca (n=23 embryos scored for both *dll4* MO injected and uninjected controls). *dll4* MO injected embryos showed a significant decrease in the number of intersegmental venous sprouts (P < 0.001, Mann-Whitney Rank Sum Test).

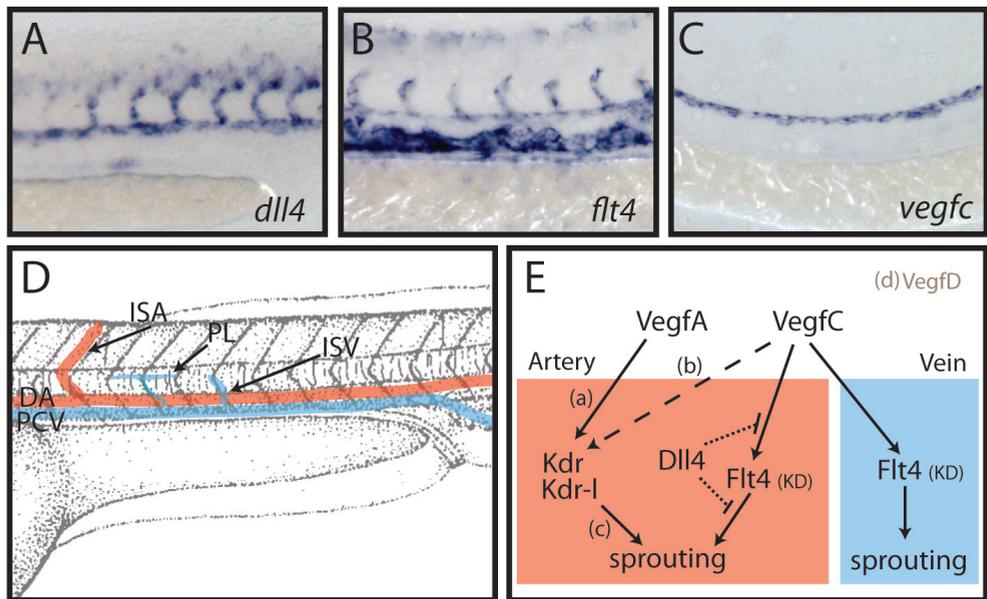


Fig. 7. Dll4 inhibits arterial Vegfc/Flt4 signalling in the developing zebrafish trunk (A-C) Expression analysis at 24hpf for *dll4* (A), *flt4* (B) and *vegfc* (C) indicates the arterial restricted expression of *dll4*, expression of *flt4* in all venous and arterial cells and expression of *vegfc* restricted to the dorsal aorta. (D) Schematic overview of the developing vasculature in the zebrafish trunk. DA indicates dorsal aorta; PCV, posterior cardinal vein; ISA, intersegmental artery; ISV, intersegmental vein; PL, parachordal lymphangioblast. (E) Working model of the interplay between Dll4 and Vegfc/Flt4 signalling. Previous studies have shown that *vegfa* (*vegfaa* and *vegfab* duplicates in zebrafish) is necessary for ISA development [a (Bahary et al., 2007; Nasevicus et al., 2000)], that *vegfc* influences ISA development [b (Covassin et al., 2006)], and that the receptors *kdr* and *kdr-l* mediate intracellular signalling to control ISA development [c (Bahary et al., 2007; Covassin et al., 2009; Covassin et al., 2006; Habeck et al., 2002; Lawson et al., 2003; Meng et al., 2008)]. We have previously shown that *vegfd* is unlikely to play a role in ISA development due to its restricted expression [d (Hogan et al., 2009)]. Here we demonstrate that signalling through the Flt4 kinase domain (KD) does not contribute to ISA development as it is suppressed by Dll4 (dotted lines indicate that the mechanism of suppression is unknown). In the absence of Dll4, endogenous Vegfc drives a Flt4 (KD) dependent ISA hyperbranching phenotype. In the vein (which does not express *dll4*), Vegfc/Flt4 signalling is indispensable for normal venous angiogenesis and lymphangiogenesis.

Interestingly, we find that *vegfd* mRNA injection alone can lead to the early ectopic turning of developing ISAs, but these defects were not enhanced upon knockdown of *dll4*. *Vegfd* has varying capabilities in mammals: for example it is a Flt4 specific ligand in mouse but, like VEGFC, can bind to both VEGFR2 (KDR) and FLT4 in humans (Baldwin et al., 2001). The capability of *Vegfd* to stimulate aberrant angiogenesis of ISAs likely explains why the embryonic expression of *vegfd* is highly restricted to the tailbud during zebrafish development (Fig. 5) (Hogan et al., 2009). This restriction of *vegfd* expression would be required for normal arterial angiogenesis to occur in the absence of Flt4 activation.

COMPARISON OF EXPRESSION PATTERNS AND PHENOTYPES FOR DIFFERENT NOTCH SIGNALLING COMPONENTS SUGGESTS COMBINATORIAL AND CONTEXT DEPENDENT ROLES DURING ANGIOGENESIS

In the developing mammalian retina, both *dll4* and *flt4* display restricted expression in tip cells during angiogenesis (Hellstrom et al., 2007; Tammela et al., 2008). In zebrafish, we did not see any restricted expression of *flt4* in tip cells at 24 hpf during ISA angiogenesis and *dll4* expression is found in all arterial cells at this stage (as discussed in (Leslie et al., 2007)). In the developing mouse trunk, Flt4 expression is also seen in all arterial cells of the intersegmental vasculature although it is enriched in tip-cells when assayed by immunohistochemistry (Tammela et al., 2008). These data suggest context dependent differences in the expression patterns of Flt4 and Dll4.

Previous studies in zebrafish have shown that *mindbomb* mutants (which cause a block in intracellular Notch signalling) have up-regulated *flt4* expression throughout the developing arterial system (Lawson et al., 2001) and *rbpsuh* morphants have up-regulated expression specifically in the tip cells of arterial sprouts (Siekmann and Lawson, 2007). However, we found no marked increase in *flt4* expression by *in situ* hybridisation in *dll4* morphants, suggesting significant differences between loss-of-function phenotypes for different Notch pathway components during angiogenesis. Furthermore, the phenotype seen upon MO knock-down of *rbpsuh* is observed earlier than that of *dll4* morphants or mutants. Dramatically increased arterial angiogenesis is seen in *rbpsuh* morphants during the initial stages of primary sprouting (Siekmann and Lawson, 2007) whilst *dll4* morphants or mutants (Leslie et al., 2007) do not display defects until hours later. Given that multiple Notch ligands are expressed and capable of acting during angiogenesis in vertebrates (Benedito et al., 2009; Lawson et al., 2001; Smithers et al., 2000), it is likely that the combinatorial use of ligands contributes to these differences in loss-of-function phenotypes. It seems plausible that differences in Notch ligand or receptor gene expression patterns and activities could be very widely utilised to allow for unique, context dependent and restricted Vegf signalling outputs in order to generate diverse spatial and temporal responses during angiogenesis in the embryo or the adult.

Taken together, the above findings indicate that one function of arterial Dll4 is to inhibit the responsiveness of arteries to Vegfc, whilst the development of the venous and lymphatic lineages (which do not express *dll4*) are completely dependent on Vegfc/Flt4 signalling in the developing zebrafish trunk. This mechanism contributes to the differential response

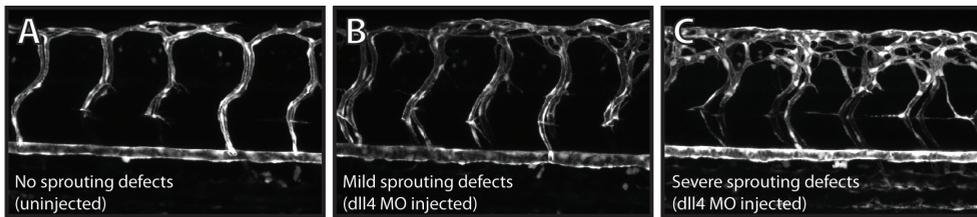
of arteries and veins to a constant source of Vegfc in the embryonic trunk and further characterises a specific role of the Notch ligand Dll4 in regulating the Vegfc/Flt4 signalling axis.

ACKNOWLEDGEMENTS

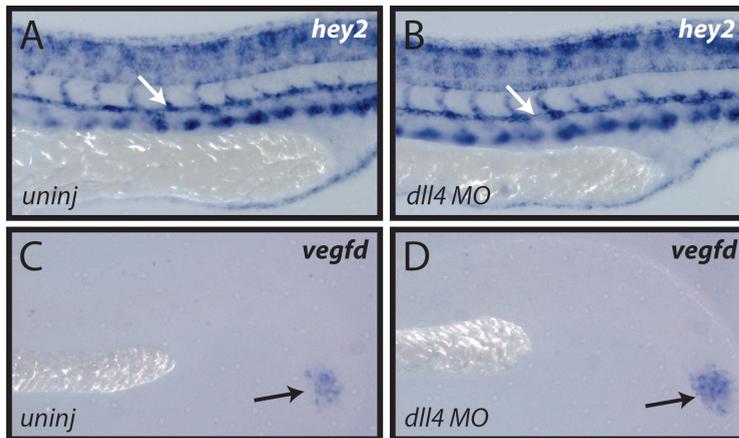
BMH was supported by an NHMRC CJ Martin Postdoctoral Training Fellowship. SSM was supported by the Koninklijke Nederlandse Akademie van Wetenschappen (KNAW). HJD received an NWO VIDI grant. We thank the Hubrecht Screen Team, Ville Pihlajaniemi and Tessa Lange for technical assistance.

SUPPLEMENTAL MATERIAL

Supplementary information, including 2 figures can be found in the data supplement or online, at <http://dev.biologists.org/cgi/content/full/136/23/4001/DC1>.

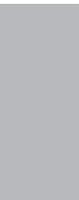


Supplementary Figure 1: Categories of hyperbranching scored in Figure 4. (A-C) Examples of embryos categorised as having no sprouting defects (wildtype) (A), Mild sprouting defects (B) or severe sprouting defects (C) at 72 hpf taken from experiment summarised in Figure 4F. Arrows in B and bracket in C indicate regions of hyperbranching.



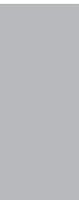
Supplementary Figure 2: No appreciable change in arterial *flt4* expression in *dll4* morphants between 25 and 31 hpf. (A-H) Expression of *flt4* in trunk arteries and veins in stage matched wildtype uninjected control and *dll4* MO injected (6ng/embryo) embryos. No difference was observed at 25 hpf (A and B) between control (n=15 embryos) compared with morphant (n=28) embryos. At 27 hpf (C and

D), no difference was seen between carefully stage matched control (n=18) and morphant (n=29) embryos. Some morphants that were clearly developmentally delayed (n=11) showed higher levels of *flt4* expression than controls, consistent with the dynamic down regulation of ISA *flt4* expression between 25 and 29 hpf, and demonstrating the need to stage match rather than age match embryos during this analysis. At 29 hpf, (E and F, n=16 control and n=34 morphant embryos analysed) and at 31 hpf (G and H, n=16 control and n=33 morphant embryos analysed), no difference was observed in the ISA expression of *flt4* between control and morphant embryos. Embryos from the same morpholino injection sessions were grown to 3dpf and the robust *dll4* MO induced hyperbranching phenotype observed, demonstrating that the embryos analysed were morphants



Summarizing Discussion

7



The subject of this thesis is the molecular and genetic regulation of the differentiation of angioblasts into a functional network of blood and lymphatic vessels, with a focus on the early stages of development of the vascular tree. The complex vertebrate body requires an effective means of transportation of liquids, gases, nutrients and circulating cells to tissues and organs for its normal functioning. This requirement is met by the blood and lymphatic vessels. Over the past few decades, it has become increasingly apparent that the malformation or malfunctioning of blood and lymphatic vessels contributes to an important part of the pathogenesis of diseases like cancer, atherosclerosis, myocardial infarction and others (Cueni and Detmar, 2006; Alitalo et al., 2005; Adams and Alitalo, 2007). It has been hypothesized that controlling the angiogenic growth potential of the vascular tree could be an effective strategy for preventing tumor growth and tumor metastasis (Folkman, 1992; Ferrara, 2004). Alternatively, controlled stimulation of angiogenic growth could be of great value in alleviating ischemic conditions by reconstituting local tissue perfusion. Recent research has greatly improved our understanding of the origin and growth of the vascular system concurrent with the identification of several genetic factors essential during this process. However, some fundamental questions, like what are the genetic factors required for the migration or differentiation of the angioblasts, remain unanswered. To contribute to the growing knowledge on endothelial cell biology we have designed a screening strategy to identify novel players in the genetic control of vessel development and growth. The findings of this study are briefly summarized here.

In chapter 2 we elaborate on the setup of the screen which was the starting point for this work. For this screen we made use of the respective strengths of two model organisms; mouse (*Mus musculus*), which is widely used within endothelial cell biology, and zebrafish (*Danio rerio*), a relatively new but increasingly widely used model organism. To determine the genetic pathways of angioblast emergence and subsequent angiogenesis we performed a global expression analysis of endothelial cells during early vascular development in mouse embryos by using a combination of FACS sorting and microarray gene-profiling. The genetic fingerprint conveyed by these analyses was further characterized by a whole mount *in situ* hybridization screen in zebrafish. The positive identification of a given candidate gene was followed by an assessment of its function using a morpholino based (Nasevicius and Ekker, 2000) gene knock-down strategy. Functional data for candidate genes that could be linked to the process of vascular development provided the basis for the in depth analyses described in chapters 3 to 6. Taken together, we analyzed nearly 400 transcripts of individual gene products in our *in situ* hybridization screen and found 61 genes with an expression pattern closely linked to the endothelial lineage. Eleven of these vascular restricted genes were not or only poorly characterized and thus included in our functional analyses (see chapter 3 to 6). In summary, we have developed a robust, high-throughput means of screening for and characterizing of novel genes involved in vascular development by the use of the combined strengths of both mice and zebrafish as model organisms.

SOX7 AND SOX18 ARE REDUNDANTLY REQUIRED FOR ARTERIOVENOUS DIFFERENTIATION

In chapter 3 we describe a novel role for *sox7* and *sox18* in the process of arteriovenous differentiation in zebrafish embryos. Both genes are part of the Sox-F family of transcription factors, are expressed in early angioblasts and continue to be expressed in the vascular bed at later stages of development of the zebrafish embryo (Herpers et al., 2008; Cermenati et al., 2008; Pendeville et al., 2008). Single knock-down of either *sox7* or *sox18* did not yield any obvious vascular malformations, whereas combinatorial repression of both gene functions led to arteriovenous shunting and fusion. Next to the arteriovenous fusions we observed based on immuno-histochemistry, we detected a marked change in both arterial and venous marker gene expression: the dorsal aorta (DA) showed a loss or reduction of several arterial markers and concurrent ectopic expression of venous markers. Similar examples of redundancy within the Sox-F family of transcription factors can be found in mice or tadpoles, where for example *Sox17* and *Sox18* or *sox7* and *sox18* respectively play redundant roles in cardiovascular development (Sakamoto et al., 2007; Zhang et al., 2005). Unsurprisingly, a similar role for members of the Sox-F family of transcription factors in arteriovenous differentiation can be observed in other species. In humans, mutations in *SOX18* cause vascular, lymphatic and hair follicle defects in subjects with dominant and recessive forms of hypotrichosis-lymphedema-telangiectasia (HLT) syndrome (Irrthum et al., 2003). Vascular dysfunction in HLT is characterized by cutaneous telangiectasias and other abnormal dilations of the superficial vasculature. HLT has been attributed to recessive missense mutations within the *SOX18* HMG-type DNA binding region and, in one case, to a dominant nonsense mutation that interrupts the *trans*-activation domain and removes the native C-terminus of the *SOX18* protein. *Sox18* mutations also underlie the *ragged* series of spontaneous mouse mutants, which all show phenotypes reminiscent of the syndromes typical for human HLT patients. The four alleles of *ragged* (*ragged* (*Ra*), *ragged-Jackson* (*RaJ*), *ragged-like* (*Ragl*) and *ragged-opossum* (*RaOp*)) carry single base deletions in *Sox18* associated with the *trans*-activation domain-encoding region, reflecting the dominant mutation observed in HLT. In contrast to the dominant-negative loss of function of *SOX18* as a result of these mutations (Downes and Koopman, 2001), *SOX18*-null mice did not reveal any vascular dysfunction (Pennisi et al., 2000). It has been hypothesized that the point mutations found in the *ragged* series of mouse mutants generate a *SOX18* protein that acts in a dominant-negative fashion to hamper wildtype *SOX18* function and of related proteins that underlie the phenotypes observed upon disruption. In *SOX18*-null mice this dominant-negative character is diminished by the compensatory action of other redundant *SOX* factors (James et al., 2003; Downes and Koopman, 2001), which is indeed reflected by our studies in zebrafish. As the interplay of the various *SOX* factors in the process of vascular development appears largely conserved across species, the zebrafish could be an attractive model organism to use to elucidate the downstream targets of these transcription factors. In a recent study, *Sox18* was shown to be directly upstream of *Prox-1*, placing itself at a central point of lymphatic development (Francois et al., 2008). Other putative downstream targets of the *SOX* transcription targets could be rapidly verified in the zebrafish using either *in situ* hybridization or a gene knock-down strategy.

AGTRL1B IS REQUIRED DURING ANGIOGENESIS

The G protein-coupled receptors Angiotensin receptor like 1b (Agtrl1b) and Agtrl1a, which have been duplicated in the zebrafish genome, are expressed in the developing vasculature where they serve as a receptor for the Apelin (Apln) peptide (Tucker et al., 2006; Scott et al., 2007; Zeng et al., 2007). This small, diffusible ligand is locally produced at the dorsal side of the embryo during primary angiogenesis and diffuses in a gradient across the dorsoventral axis. The Apln gradient is sensed by the intersegmental sprouts emerging from the DA, which facilitates the normal growth of the ISVs toward the dorsal side of the trunk and the subsequent formation of the dorsal longitudinal anastomitic vessels (DLAVs). We showed that the ISVs show abnormal migratory behavior upon loss of *agtrl1b* and a concurrent failure of formation of the DLAV. No differences were found in the number of endothelial cells within a single ISV in *agtrl1b* mutants compared to wildtype siblings, arguing against the possibility that Agtrl1b-Apln signaling exerts a mitogenic function on the endothelial cells of an ISV during angiogenesis. Analysis of the extending filopodia of the ISVs during angiogenic migration showed a clear reduction in both number and length of these filopodia in *agtrl1b* mutants compared to wildtype siblings. The function of the extending filopodia formed at the tip of migrating ISVs is to probe the environment for directional cues (Gerhardt et al., 2003). Thus, loss or reduction of the number of filopodia could very well explain the reduced migratory behavior of the ISVs in *agtrl1b* mutants. Previous studies showed that upon stimulation with Apln, Agtrl1b can activate Cdc42 through the activation of the PI3K/Akt pathway (Masri et al., 2005; Kojima and Quertermous, 2008), which in turn induces cytoskeletal rearrangements and the formation of filopodia (Shiojima and Walsh, 2002; Sasaki and Firtel, 2006). This would suggest that Apln not only sets out the directional cue for chemotactic migration, but also amplifies the response of migrating endothelial cells by inducing the formation of filopodia upon binding to its receptor. Both *apln* receptors (*agtrl1a* and *agtrl1b*) are expressed in the endothelial compartment, with *agtrl1b* being expressed in all endothelial cells and *agtrl1a* being restricted to the venous compartment. This differential expression pattern for both gene duplicates might prove insightful in unveiling the potential function of *agtrl1a* during angiogenesis. The recent acquirement of a zebrafish *agtrl1a* mutant will be instrumental in studying the role of *agtrl1a* during secondary sprouting from the PCV. If *agtrl1a-apln* signaling in secondary sprouts from the PCV has a similar function to that of *agtrl1b-apln* signaling in primary sprouts from the DA, it is to be expected that the secondary sprouts from the PCV would fail to migrate in a wildtype fashion in *agtrl1a* mutants. As a result of this, potentially fewer venous intersegmental vessels or PLs would be formed, resulting in defective lymphangiogenesis in these animals.

THE ROLE OF DLL4 DURING LYMPHANGIOGENESIS

In chapter 5 we put forward a novel role for Dll4-Notch signaling during lymphangiogenesis. Lymphangiogenesis is initiated by Sox18-induced localized expression of Prox-1 in the cardinal vein (Francois et al., 2008). Prox-1 positive endothelial cells within the cardinal vein will transdifferentiate to lymphatic endothelial cells and bud off from the cardinal vein to contribute to lymphangiogenesis (Wigle et al., 2002). In zebrafish, lymphatic precursor cells

(termed parachordal lymphangiogenic cells (PLs)) arise during secondary sprouting from the posterior cardinal vein (PCV). Approximately one half of the sprouts that emerge from the PCV during secondary sprouting have angiogenic potential and remodel the primary arterial sprouts to venous connections, whereas the other half of secondary sprouts have lymphangiogenic potential and ultimately contribute to lymphatic development (Hogan et al., 2009; Chapter 5 of this thesis). In our study we find that in zebrafish embryos with compromised Dll4-Notch signaling, the proportion of venous intersegmental vessels (vISVs) is increased as a result of a larger proportion of the secondary sprouts from the PCV that connect to and remodel the primary sprouts. As a consequence, fewer or no PLs as well as fewer arterial intersegmental vessels (aISVs) are present in zebrafish embryos with compromised Dll4-Notch signaling. During these studies we also found a close association of the PLs with the aISVs, which appeared to serve as guidance templates for PL migration during lymphangiogenesis. The few residual PLs that still formed upon loss of Dll4-Notch signaling would thus be deprived of these migratory templates, contributing to the failure of formation of lymphatic vasculature in zebrafish embryos with compromised Dll4-Notch signaling. The close association of lymphatic cells with intersegmental arteries and the localized expression of *dll4* in zebrafish arteries are suggestive of a potential role of the arteries contributing to the development of lymphatic vessels. The analogy with other model organisms would dictate that particular cells in the dorsal roof of the PCV become specified to differentiate to lymphatic endothelial cells in response to Sox18-Prox1 signals, eventually contributing to lymphangiogenesis. To date however, no specification marker of lymphatic commitment in zebrafish embryos has been identified. Although the DA and PCV develop in close association with each other, and even make physical contact during early development, it is an open question as to how *dll4* exerts its function on the endothelial cells of the PCV. *Notch1b*, a receptor for *dll4*, is highly expressed in the DA, but can also be detected at low levels at discrete locations of the dorsal roof of the PCV. In a scenario where there is physical contact between *dll4* expressing arterial endothelial cells and *notch1b* expressing venous endothelial cells, an instructive signal to lymphangiogenesis could be conveyed. Alternatively, the secondary sprouts that arise from the PCV could fulfill a rather passive role during lymphangiogenesis, whereas the already formed primary sprouts from the DA would then dictate the final specification (angiogenic vs. lymphangiogenic) of the secondary sprouts from the PCV. In this model, the reconnection of a secondary sprout from the PCV with a primary sprout from the DA (thus fulfilling an angiogenic role) is defined by *dll4-notch* signaling within the primary (DA-derived) sprout. Secondary sprouts from the PCV that are not recruited by the primary sprouts from the DA to remodel the intersegmental vessel to an intersegmental vein continue their dorsal migration and contribute to the lymphatic lineage. In this scenario the molecular nature of lymphatic commitment can arise either as a default state by the downregulation of vascular markers, as is seen by the downregulation of *kdr-l:mCherry* in the PLs (Chapter 5 of this thesis), or by another, as of yet unknown, mechanism. Either way, lineage differentiation of venous endothelial cells towards lymphatic endothelial cells would be controlled by the activity of Dll4-Notch signaling in the arterial derived intersegmental vessels. The reported role for *dll4* in limiting angiogenesis and the increased

number of angiogenic sprouts and connections being formed upon loss of *dll4* (Siekmann and Lawson, 2007, Leslie et al., 2007), provide a logical explanation for the supernumerary fraction of venous intersegmental vessels. During angiogenesis, the leading cells of the ISV sprouts (tip cells) and the cells that follow behind them (stalk cells) show intense filopodial activity and express similar levels of *dll4* (Leslie et al., 2007). When filopodial activity ceases upon formation of the DLAV, it ceases throughout the entire population of intersegmental endothelial cells. It has been suggested that the contact between the tip cells of the sprouts that meet triggers this event through the mutual activation of Notch, (Leslie et al., 2007). Timelapse confocal imaging of the primary sprouts showed an increased filopodic behavior of the endothelial cells at the ventral base of a primary sprout (Chapter 5 of this thesis), which suggests prolonged angiogenic potential of these cells even after formation of the DLAV. From this observation, it would follow that a greater number of secondary sprouts would be reconnected to the vascular system and few sprouts from the PCV would undergo lymphatic commitment. Future studies that utilize mutants defective in primary sprouting from the DA, but not secondary sprouting from the PCV, should yield insights into the exact role of the intersegmental arteries during lymphangiogenesis. According to this model, an increase in the number of PLs would be expected, since fewer primary arterial sprouts are present to remodel the secondary sprouts. Other studies, including transplantation of wildtype arterial endothelial cells into *dll4* morphant hosts or ablation of whole arteries should contribute to answering the question whether lymphangiogenic development in zebrafish embryos is primarily controlled by cellular and molecular processes in the PCV or intersegmental arteries.

DLL4 RESTRICTS VEGFC-FLT4 SIGNALING IN ARTERIES

In chapter 6 we elaborate on the role of Dll4 in restricting the response of developing zebrafish intersegmental arteries to Vegfc-Flt4 signaling. This work was initiated upon the isolation of the mutant *expando* from a forward genetic screen aimed at finding novel players in lymphatic development. Molecular characterization of *expando* mutants revealed a loss-of-function mutation in the highly conserved kinase insert region of *flt4*. Secondary sprouting, including both venous and lymphangiogenic sprouting, from the PCV in *flt4* signaling mutants was completely abolished, in agreement with previous reports on the loss of *vegfc* (Küchler et al., 2006; Hogan et al., 2009). Although *flt4* is consistently expressed in the PCV, but also DA and ISVs, primary, arterial angiogenesis proceeded normally in *expando* mutants. Previous studies have shown that Flt4 signaling is required for hemangiogenesis and that Dll4 limits angiogenic potential by limiting Flt4 function in developing vessels (Tammela et al., 2008). Strikingly, *dll4* loss-of-function induced an arterial hyper-branching phenotype (Siekmann and Lawson, 2007, Leslie et al., 2007), which was rescued when *dll4* morpholinos were injected in *flt4* signalling mutants. Furthermore, we found that ectopic expression of the Flt4 ligand *vegfc* is capable of driving arterial hyper-branching in the absence of *dll4*. Upon knockdown of *dll4*, intersegmental arteries were sensitised to increased *vegfc* levels, while ectopic expression of *dll4* reduced *vegfc*/Flt4 dependent sprouting from the PCV. In summary, these data demonstrate that *dll4* suppresses the ability of primary ISVs to

respond to Vegfc driven Flt4 signalling in zebrafish. This sophisticated mechanism of control contributes to the differential response of developing arteries and veins to a constant source of Vegfc present in the embryo during angiogenesis.

CLINICAL IMPLICATIONS

In the westernized world, the two major causes of lethality are cardiovascular diseases and cancer, both of which are linked to vascular dysfunction. Increasing evidence of hereditary genetic aberrations as a risk factor in vascular malformations has underlined the importance of research in the field of the genetic regulation of endothelial cell biology. Some of the genetic factors identified in this screen have already been linked to a human pathological condition, such as HHT and HLT for Sox18 (Irrthum et al., 2008). Given the role of the Sox-F factors in cardio-vascular and lymphatic development, these transcription factors have become attractive targets for therapies designed to control angiogenesis or lymphangiogenesis (Francois et al., 2009). It has already been shown that a dramatic reduction of tumor growth through the reduction of angiogenesis occurs in mice lacking Sox18 function (Young et al., 2006). With the utilization of zebrafish as a novel model organism for the function of Sox18, previously impossible studies on the molecular nature of HHT and HLT become feasible.

The evolutionarily conserved nature of the genetic control of vascular development also enables us to study the process of tumor growth and tumor metastasis. The ability of endothelial cells to grow and proliferate in response to secreted growth factors is hijacked by tumors to allow tumor vascularization and growth (Holash et al., 1999). Similarly, tumor metastasis chiefly occurs through the spread of tumor cells via the lymphatic system. Thus, both growth and spread of tumors is facilitated by the endothelial lineage, which would be a highly attractive target during cancer treatment. Some exciting clinical progress has been made in limiting tumor growth by the use of monoclonal antibodies targeted at VEGF (Ferrara, 2004; Hurwitz et al., 2004; Laskin and Sandler, 2005). Nonetheless, these strategies have also been shown to induce tumor hypoxia and resulting tumor resistance by a systemic feedback loop of VEGF production. Similarly, withdrawal of the anti-VEGF treatment leads to rapid re-growth of endothelial sprouts into empty sleeves of vascular basement membranes that function as a scaffold for revascularization. As not all tumors are sensitive to anti-VEGF therapies, and as initially susceptible tumors might become resistant, additional targets will be required to exploit the full advantages of anti-angiogenesis therapies. Currently, the inhibition of Dll4 function is being developed as a method to induce aberrant growth of tumor associated vasculature, leading to non-functional vasculature and reduced tumor growth (Noguera-Troise et al., 2006). Unlike VEGF, compromised Dll4 function leads to excessive, but non-productive, angiogenesis, which leads to decreased tumor growth (Thurston et al., 2007, Li Harris 2009). The vessels that form in the absence of Dll4 are highly branched and often lack a vessel lumen or are too disorganized to support perfusion of the tumor. Combinatorial blockage of both the DLL4-Notch and VEGF pathways inhibits tumor growth in preclinical models and may lead to exciting new therapies for clinical application. In this context, it is noteworthy that our studies on the role of Dll4 in suppressing Flt4/VEGFC-dependent angiogenesis suggest that Dll4 inhibitors might exhibit a higher therapeutic effect

in tumors expressing high levels of VEGFC by increasing non-productive tumor angiogenesis. Besides increased non-productive tumor angiogenesis upon Dll4 inhibition, a concurrent block in tumor lymphatic growth upon Dll4 blockage might also be induced as our studies show a specific requirement for Dll4 during lymphangiogenesis.

GENERAL DISCUSSION & FUTURE DIRECTIONS

The emergence of the hemangioblast is an essential step towards vascular development (Choi et al., 1998; Vogeli et al., 2006). These pluripotent cells form the precursors to the very first steps in both hematopoietic development and vascular development. The question of hemangioblast emergence and subsequent differentiation towards endothelial cell fate has been a central question in vascular and stem cell biology for a long time. The reverse genetic screen described within this thesis addressed the molecular mechanisms that underlie early vascular development. This resulted in the identification of several (novel) factors contributing to angiogenesis and lymphangiogenesis, as described within this thesis. In recent years a number of other studies have addressed a largely similar question, using a slightly different approach (Weber et al., 2005; Sumanas et al., 2005; Eckfeldt et al., 2005; Covassin et al., 2006; Wong et al., 2009). A quantitative comparison of the various screens conducted using zebrafish to identify novel regulators of vascular development showed that well known key players in vascular development were nearly all identified with a relatively large overlap between our and other studies. In all studies, the number of newly identified genes associated with vascular development represented only a fraction of the total number of genes involved in vascular development, suggestive of a degree of saturation of such screens. Nonetheless, new genes involved in more specialized requirements of vascular development are still being discovered, whereas only few key regulators of early vasculogenic events have been identified over the last few years (e.g. Sumanas and Lin, 2006). Although no direct comparison between the different screens can be made, a qualitative comparison of the various screens favored our screen over others in that it used a cross-species approach that combined functional analyses with expression data, rather than relying on expression data alone. Conserved gene expression across different species positively correlates with conserved gene function, i.e. a gene with vascular expression in both mouse and zebrafish is highly likely of fulfilling a similar role in the process of vascular development in both species. These implications, together with other advantages of cross-species screening, including relative ease and speed of screening could greatly benefit future studies aimed at the identification of regulators of tissue specific development. Moreover, with the recent availability of transgenic zebrafish that express fluorescent proteins in only a subset of the endothelial cell lineage, previously unattainable experiments become feasible. For instance, a purified population of either arterial, venous or lymphatic endothelial cells can be obtained by FACS sorting of the right combination of transgenic fish. Expression analysis of such populations has the potential of answering some of the fundamental questions outstanding.

The initial goal of identifying novel regulators of vascular development was met by the discovery and characterization of several genes, but to what extent can these discoveries

lead to a better understanding of vascular development? The *de novo* formation of the vasculature is defined by three distinct stages; during *vasculogenesis*, mesodermally derived angioblasts coalesce and give rise to the major axial vessels, followed by subsequent *angiogenesis* in which capillaries sprout from pre-existing vessels (Risau et al., 1995; Carmeliet, 2000). Finally, a transdifferentiation of a subset of venous endothelial cells will allow for *lymphangiogenesis* during which the lymphatic vasculature is formed (Adams and Alitalo, 2007). Although this screen was designed to uncover regulators of early vascular development, all three abovementioned stages are covered by the genetic factors identified in this work. The demarcation between these stages is clear; however it has become increasingly obvious during this study that no such demarcation is reflected in the genetic control of the three stages of vascular formation. For example, *sox7* and *sox18* control arteriovenous differentiation, which takes place during *vasculogenesis*. Later, during *lymphangiogenesis*, *Sox18* fulfils a second, different role in controlling the induction of Prox-1 expression in lymphangioblasts (Francois et al., 2008). Similarly, *dll4* limits the angiogenic potential of sprouting blood vessels (Siekmann and Lawson, 2007, Leslie et al., 2007), and at later stages contributes to lymphatic development (Chapter 5 of this thesis). Other examples such as the intimate relationship between the development of arteries and that of veins (Lawson and Weinstein, 2002; Herbert et al., 2009), as well as the close association of developing lymphatic vessels with arterial intersegmental vessels (Chapter 5 of this thesis) suggests that the three stages of vascular development mentioned are highly linked processes that share many common molecular and genetic regulators. Rather than having differing genetic factors for differing vascular developmental processes, precise temporal and spatial control of action of re-used genetic factors controls the development of the vertebrate embryo. Therefore, the study of individual genetic factors during vascular development should not be limited to only a single aspect of the endothelial lineage, but rather take into account the vasculature as a whole.

References

- Achen, M. G., Mann, G. B. and Stacker, S. A.** (2006). Targeting lymphangiogenesis to prevent tumour metastasis. *Br J Cancer* **94**, 1355-60.
- Adams, R. H. and Alitalo, K.** (2007). Molecular regulation of angiogenesis and lymphangiogenesis. *Nat Rev Mol Cell Biol* **8**, 464-78.
- Alders, M., Hogan, B. M., Gjini, E., Salehi, F., Al-Gazali, L., Hennekam, E. A., Holmberg, E. E., Mannens, M. M., Mulder, M. F., Offerhaus, G. J. et al.** (2009). Mutations in CCBE1 cause generalized lymph vessel dysplasia in humans. *Nat Genet*.
- Alitalo, K., Tammela, T. and Petrova, T. V.** (2005). Lymphangiogenesis in development and human disease. *Nature* **438**, 946-53.
- Armulik, A., Abramsson, A. and Betsholtz, C.** (2005). Endothelial/pericyte interactions. *Circ Res* **97**, 512-23.
- Atkins, G. B. and Jain, M. K.** (2007). Role of Kruppel-like transcription factors in endothelial biology. *Circ Res* **100**, 1686-95.
- Bahary, N., Goishi, K., Stuckenholtz, C., Weber, G., Leblanc, J., Schafer, C. A., Berman, S. S., Klagsbrun, M. and Zon, L. I.** (2007). Duplicate VegfA genes and orthologues of the KDR receptor tyrosine kinase family mediate vascular development in the zebrafish. *Blood* **110**, 3627-36.
- Bak, M. and Fraser, S. E.** (2003). Axon fasciculation and differences in midline kinetics between pioneer and follower axons within commissural fascicles. *Development* **130**, 4999.
- Baldessari, D. and Mione, M.** (2008). How to create the vascular tree? (Latest) help from the zebrafish. *Pharmacol Ther* **118**, 206-30.
- Baldwin, M. E., Catimel, B., Nice, E. C., Roufail, S., Hall, N. E., Stenvers, K. L., Karkkainen, M. J., Alitalo, K., Stacker, S. A. and Achen, M. G.** (2001). The specificity of receptor binding by vascular endothelial growth factor-d is different in mouse and man. *J Biol Chem* **276**, 19166-71.
- Baluk, P. and McDonald, D. M.** (2008). Markers for microscopic imaging of lymphangiogenesis and angiogenesis. *Ann N Y Acad Sci* **1131**, 1.
- Benedito, R., Roca, C., Sorensen, I., Adams, S., Gossler, A., Fruttiger, M. and Adams, R. H.** (2009). The notch ligands Dll4 and Jagged1 have opposing effects on angiogenesis. *Cell* **137**, 1124-35.
- Bergers, G. and Song, S.** (2005). The role of pericytes in blood-vessel formation and maintenance. *Neuro Oncol* **7**, 452-64.
- Blum, Y., Belting, H. G., Ellertsdottir, E., Herwig, L., Luders, F. and Affolter, M.** (2008). Complex cell rearrangements during intersegmental vessel sprouting and vessel fusion in the zebrafish embryo. *Dev Biol* **316**, 312-22.
- Bowles, J., Schepers, G. and Koopman, P.** (2000). Phylogeny of the SOX family of developmental transcription factors based on sequence and structural indicators. *Dev Biol* **227**, 239-55.
- Bussmann, J., Bakkers, J. and Schulte-Merker, S.** (2007). Early endocardial morphogenesis requires Scf/Tal1. *PLoS Genet* **3**, e140.
- Bussmann, J., Lawson, N., Zon, L. and Schulte-Merker, S.** (2008). Zebrafish VEGF receptors: a guideline to nomenclature. *PLoS Genet* **4**, e1000064.
- Carmeliet, P.** (2000). Mechanisms of angiogenesis and arteriogenesis. *Nat Med* **6**, 389-95.
- Carmeliet, P.** (2005a). Angiogenesis in life, disease and medicine. *Nature* **438**, 932-6.
- Carmeliet, P.** (2005b). VEGF as a key mediator of angiogenesis in cancer. *Oncology* **69 Suppl 3**, 4-10.
- Cermenati, S., Moleri, S., Cimbri, S., Corti, P., Del Giacco, L., Amodeo, R., Dejana, E., Koopman, P., Cotelli, F. and Beltrame, M.** (2008). Sox18 and Sox7 play redundant roles in vascular development. *Blood* **111**, 2657-66.
- Chan, J., Mably, J. D., Serluca, F. C., Chen, J. N., Goldstein, N. B., Thomas, M. C., Cleary, J. A., Brennan, C., Fishman, M. C. and Roberts, T. M.** (2001). Morphogenesis of prechordal plate and notochord requires intact Eph/ephrin B signaling. *Dev Biol* **234**, 470.
- Childs, S., Chen, J. N., Garrity, D. M. and Fishman, M. C.** (2002). Patterning of angiogenesis in the zebrafish embryo. *Development* **129**, 973-82.
- Chittenden, T. W., Claes, F., Lanahan, A. A., Autiero, M., Palac, R. T., Tkachenko, E. V., Elfenbein, A., Ruiz de Almodovar, C., Dedkov, E., Tomanek, R. et al.** (2006). Selective regulation of arterial branching morphogenesis by syndectin. *Dev Cell* **10**, 783.
- Choi, K., Kennedy, M., Kazarov, A., Papadimitriou, J. C. and Keller, G.** (1998). A common precursor for hematopoietic and endothelial cells. *Development* **125**, 725-32.

- Covassin, L., Amigo, J. D., Suzuki, K., Teplyuk, V., Straubhaar, J. and Lawson, N. D. (2006a). Global analysis of hematopoietic and vascular endothelial gene expression by tissue specific microarray profiling in zebrafish. *Dev Biol* **299**, 551-62.
- Covassin, L. D., Siekmann, A. F., Kacergis, M. C., Laver, E., Moore, J. C., Villefranc, J. A., Weinstein, B. M. and Lawson, N. D. (2009). A genetic screen for vascular mutants in zebrafish reveals dynamic roles for Vegf/Plcg1 signaling during artery development. *Dev Biol* **329**, 212-26.
- Covassin, L. D., Villefranc, J. A., Kacergis, M. C., Weinstein, B. M. and Lawson, N. D. (2006b). Distinct genetic interactions between multiple Vegf receptors are required for development of different blood vessel types in zebrafish. *Proc Natl Acad Sci U S A* **103**, 6554-9.
- Cox, C. M., D'Agostino, S. L., Miller, M. K., Heimark, R. L. and Krieg, P. A. (2006). Apelin, the ligand for the endothelial G-protein-coupled receptor, APJ, is a potent angiogenic factor required for normal vascular development of the frog embryo. *Dev Biol* **296**, 177-89.
- Cueni, L. N. and Detmar, M. (2006). New insights into the molecular control of the lymphatic vascular system and its role in disease. *J Invest Dermatol* **126**, 2167-77.
- Dahl Ejby Jensen, L., Cao, R., Hedlund, E. M., Soll, I., Lundberg, J. O., Hauptmann, G., Steffensen, J. F. and Cao, Y. (2009). Nitric oxide permits hypoxia-induced lymphatic perfusion by controlling arterial-lymphatic conduits in zebrafish and glass catfish. *Proc Natl Acad Sci U S A* **106**, 18408-13.
- De Smet, F., Segura, I., De Bock, K., Hohensinner, P. J. and Carmeliet, P. (2009). Mechanisms of vessel branching: filopodia on endothelial tip cells lead the way. *Arterioscler Thromb Vasc Biol* **29**, 639.
- De Val, S. and Black, B. L. (2009). Transcriptional control of endothelial cell development. *Dev Cell* **16**, 180-95.
- Detrich, H. W., 3rd, Kieran, M. W., Chan, F. Y., Barone, L. M., Yee, K., Rundstadler, J. A., Pratt, S., Ransom, D. and Zon, L. I. (1995). Intraembryonic hematopoietic cell migration during vertebrate development. *Proc Natl Acad Sci U S A* **92**, 10713-7.
- Donner, A. L., Lachke, S. A. and Maas, R. L. (2006). Lens induction in vertebrates: variations on a conserved theme of signaling events. *Semin Cell Dev Biol* **17**, 676.
- Downes, M. and Koopman, P. (2001). SOX18 and the transcriptional regulation of blood vessel development. *Trends Cardiovasc Med* **11**, 318-24.
- Drake, C. J. and Fleming, P. A. (2000). Vasculogenesis in the day 6.5 to 9.5 mouse embryo. *Blood* **95**, 1671-9.
- Dumont, D. J., Jussila, L., Taipale, J., Lymboussaki, A., Mustonen, T., Pajusola, K., Breitman, M. and Alitalo, K. (1998). Cardiovascular failure in mouse embryos deficient in VEGF receptor-3. *Science* **282**, 946-9.
- Eckfeldt, C. E., Mendenhall, E. M., Flynn, C. M., Wang, T. F., Pickart, M. A., Grindle, S. M., Ekker, S. C. and Verfaillie, C. M. (2005). Functional analysis of human hematopoietic stem cell gene expression using zebrafish. *PLoS Biol* **3**, e254.
- Emuss, V., Lagos, D., Pizzey, A., Gratrix, F., Henderson, S. R. and Boshoff, C. (2009). KSHV manipulates Notch signaling by DLL4 and JAG1 to alter cell cycle genes in lymphatic endothelia. *PLoS Pathog* **5**.
- Eyries, M., Siegfried, G., Ciumas, M., Montagne, K., Agrapart, M., Lebrin, F. and Soubrier, F. (2008). Hypoxia-induced apelin expression regulates endothelial cell proliferation and regenerative angiogenesis. *Circ Res* **103**, 432-40.
- Ferdous, A., Caprioli, A., Iacovino, M., Martin, C. M., Morris, J., Richardson, J. A., Latif, S., Hammer, R. E., Harvey, R. P., Olson, E. N. et al. (2009). Nkx2-5 transactivates the Ets-related protein 71 gene and specifies an endothelial/endocardial fate in the developing embryo. *Proc Natl Acad Sci U S A* **106**, 814-9.
- Ferrara, N. (2004). Vascular endothelial growth factor as a target for anticancer therapy. *Oncologist* **9 Suppl 1**, 2-10.
- Ferrara, N. (2005). VEGF as a therapeutic target in cancer. *Oncology* **69 Suppl 3**, 11-6.
- Ferrara, N. and Alitalo, K. (1999). Clinical applications of angiogenic growth factors and their inhibitors. *Nat Med* **5**, 1359-64.
- Ferrara, N. and Davis-Smyth, T. (1997). The biology of vascular endothelial growth factor. *Endocr Rev* **18**, 4-25.
- Ferrara, N., Gerber, H. P. and LeCouter, J. (2003). The biology of VEGF and its receptors. *Nat Med* **9**, 669-76.
- Flamme, I., Frolich, T. and Risau, W. (1997). Molecular mechanisms of vasculogenesis and embryonic angiogenesis. *J Cell Physiol* **173**, 206-10.
- Folkman, J. (1992). The role of angiogenesis in tumor growth. *Semin Cancer Biol* **3**, 65-71.
- Folkman, J. and D'Amore, P. A. (1996). Blood vessel formation: what is its molecular basis? *Cell* **87**, 1153-5.
- Fong, G. H., Zhang, L., Bryce, D. M. and Peng, J. (1999). Increased hemangioblast commitment, not vascular disorganization, is the primary defect in flt-1 knock-out

- mice. *Development* **126**, 3015-25.
- Fouquet, B., Weinstein, B. M., Serluca, F. C. and Fishman, M. C.** (1997). Vessel patterning in the embryo of the zebrafish: guidance by notochord. *Dev Biol* **183**, 37-48.
- Fraisil, P., Mazzone, M., Schmidt, T. and Carmeliet, P.** (2009). Regulation of angiogenesis by oxygen and metabolism. *Dev Cell* **16**, 167-79.
- Francois, M., Caprini, A., Hosking, B., Orsenigo, F., Wilhelm, D., Browne, C., Paavonen, K., Karnezis, T., Shayan, R., Downes, M. et al.** (2008a). Sox18 induces development of the lymphatic vasculature in mice. *Nature* **456**, 643-7.
- Francois, M., Caprini, A., Hosking, B., Orsenigo, F., Wilhelm, D., Browne, C., Paavonen, K., Karnezis, T., Shayan, R., Downes, M. et al.** (2008b). Sox18 induces development of the lymphatic vasculature in mice. *Nature* **456**, 643.
- Francois, M., Koopman, P. and Beltrame, M.** (2009). SoxF genes: Key players in the development of the cardio-vascular system. *Int J Biochem Cell Biol*.
- Gale, N. W., Thurston, G., Hackett, S. F., Renard, R., Wang, Q., McClain, J., Martin, C., Witte, C., Witte, M. H., Jackson, D. et al.** (2002). Angiopoietin-2 is required for postnatal angiogenesis and lymphatic patterning, and only the latter role is rescued by Angiopoietin-1. *Dev Cell* **3**, 411.
- Geling, A., Steiner, H., Willem, M., Bally-Cuif, L. and Haass, C.** (2002). A gamma-secretase inhibitor blocks Notch signaling in vivo and causes a severe neurogenic phenotype in zebrafish. *EMBO Rep* **3**, 688.
- Gerhardt, H., Golding, M., Fruttiger, M., Ruhrberg, C., Lundkvist, A., Abramsson, A., Jeltsch, M., Mitchell, C., Alitalo, K., Shima, D. et al.** (2003). VEGF guides angiogenic sprouting utilizing endothelial tip cell filopodia. *J Cell Biol* **161**, 1163-77.
- Gerhardt, H., Ruhrberg, C., Abramsson, A., Fujisawa, H., Shima, D. and Betsholtz, C.** (2004). Neuropilin-1 is required for endothelial tip cell guidance in the developing central nervous system. *Dev Dyn* **231**, 503-9.
- Gering, M., Rodaway, A. R., Gottgens, B., Patient, R. K. and Green, A. R.** (1998). The SCL gene specifies haemangioblast development from early mesoderm. *Embo J* **17**, 4029-45.
- Glebova, N. O. and Ginty, D. D.** (2005). Growth and survival signals controlling sympathetic nervous system development. *Annu Rev Neurosci* **28**, 191.
- Habeck, H., Odenthal, J., Walderich, B., Maischein, H. and Schulte-Merker, S.** (2002). Analysis of a zebrafish VEGF receptor mutant reveals specific disruption of angiogenesis. *Curr Biol* **12**, 1405-12.
- Haiko, P., Makinen, T., Keskkitalo, S., Taipale, J., Karkkainen, M. J., Baldwin, M. E., Stacker, S. A., Achen, M. G. and Alitalo, K.** (2008). Deletion of vascular endothelial growth factor C (VEGF-C) and VEGF-D is not equivalent to VEGF receptor 3 deletion in mouse embryos. *Mol Cell Biol* **28**, 4843-50.
- Harrington, L. S., Sainson, R. C. A., Williams, C. K., Taylor, J. M., Shi, W., Li, J.-L. and Harris, A. L.** (2008). Regulation of multiple angiogenic pathways by Dll4 and Notch in human umbilical vein endothelial cells. *Microvasc Res* **75**, 144.
- He, Y., Kozaki, K., Karpanen, T., Koshikawa, K., Yla-Herttuala, S., Takahashi, T. and Alitalo, K.** (2002). Suppression of tumor lymphangiogenesis and lymph node metastasis by blocking vascular endothelial growth factor receptor 3 signaling. *J Natl Cancer Inst* **94**, 819-25.
- Hellstrom, M., Phng, L. K., Hofmann, J. J., Wallgard, E., Coultas, L., Lindblom, P., Alva, J., Nilsson, A. K., Karlsson, L., Gaiano, N. et al.** (2007). Dll4 signalling through Notch1 regulates formation of tip cells during angiogenesis. *Nature* **445**, 776-80.
- Herbert, S. P., Huisken, J., Kim, T. N., Feldman, M. E., Houseman, B. T., Wang, R. A., Shokat, K. M. and Stainier, D. Y.** (2009a). Arterial-venous segregation by selective cell sprouting: an alternative mode of blood vessel formation. *Science* **326**, 294-8.
- Herbert, S. P., Huisken, J., Kim, T. N., Feldman, M. E., Houseman, B. T., Wang, R. A., Shokat, K. M. and Stainier, D. Y. R.** (2009b). Arterial-venous segregation by selective cell sprouting: an alternative mode of blood vessel formation. *Science* **326**, 294.
- Herpers, R., van de Kamp, E., Duckers, H. J. and Schulte-Merker, S.** (2008). Redundant roles for sox7 and sox18 in arteriovenous specification in zebrafish. *Circ Res* **102**, 12-5.
- Higuchi, M., Masuyama, N., Fukui, Y., Suzuki, A. and Gotoh, Y.** (2001). Akt mediates Rac/Cdc42-regulated cell motility in growth factor-stimulated cells and in invasive PTEN knockout cells. *Curr Biol* **11**, 1958-62.
- Hiratsuka, S., Minowa, O., Kuno, J., Noda, T. and Shibuya, M.** (1998). Flt-1 lacking the tyrosine kinase domain is sufficient for normal development and angiogenesis in mice. *Proc Natl Acad Sci U S A* **95**, 9349-54.

- Hofmann, J. J. and Iruela-Arispe, M. L. (2007). Notch signaling in blood vessels: who is talking to whom about what? *Circ Res* **100**, 1556.
- Hogan, B. M., Bos, F. L., Bussmann, J., Witte, M., Chi, N. C., Duckers, H. J. and Schulte-Merker, S. (2009a). Ccbe1 is required for embryonic lymphangiogenesis and venous sprouting. *Nat Genet* **41**, 396-8.
- Hogan, B. M., Bussmann, J., Wolburg, H. and Schulte-Merker, S. (2008). ccm1 cell autonomously regulates endothelial cellular morphogenesis and vascular tubulogenesis in zebrafish. *Hum Mol Genet* **17**, 2424-32.
- Hogan, B. M., Herpers, R., Witte, M., Helotera, H., Alitalo, K., Duckers, H. J. and Schulte-Merker, S. (2009b). Vegfc/Flt4 signalling is suppressed by Dll4 in developing zebrafish intersegmental arteries. *Development* **136**, 4001.
- Holash, J., Maisonpierre, P. C., Compton, D., Boland, P., Alexander, C. R., Zagzag, D., Yancopoulos, G. D. and Wiegand, S. J. (1999). Vessel cooption, regression, and growth in tumors mediated by angiopoietins and VEGF. *Science* **284**, 1994-8.
- Hollenhorst, P. C., Jones, D. A. and Graves, B. J. (2004). Expression profiles frame the promoter specificity dilemma of the ETS family of transcription factors. *Nucleic Acids Res* **32**, 5693-702.
- Honma, Y., Araki, T., Gianino, S., Bruce, A., Heuckeroth, R., Johnson, E. and Milbrandt, J. (2002). Artemin is a vascular-derived neurotropic factor for developing sympathetic neurons. *Neuron* **35**, 267.
- Hurwitz, H., Fehrenbacher, L., Novotny, W., Cartwright, T., Hainsworth, J., Heim, W., Berlin, J., Baron, A., Griffing, S., Holmgren, E. et al. (2004). Bevacizumab plus irinotecan, fluorouracil, and leucovorin for metastatic colorectal cancer. *N Engl J Med* **350**, 2335-42.
- Inui, M., Fukui, A., Ito, Y. and Asashima, M. (2006). Xapelin and Xmsr are required for cardiovascular development in *Xenopus laevis*. *Dev Biol* **298**, 188-200.
- Irrthum, A., Devriendt, K., Chitayat, D., Matthijs, G., Glade, C., Steijlen, P. M., Fryns, J. P., Van Steensel, M. A. and Vikkula, M. (2003). Mutations in the transcription factor gene SOX18 underlie recessive and dominant forms of hypotrichosis-lymphedema-telangiectasia. *Am J Hum Genet* **72**, 1470-8.
- Ishida, J., Hashimoto, T., Hashimoto, Y., Nishiwaki, S., Iguchi, T., Harada, S., Sugaya, T., Matsuzaki, H., Yamamoto, R., Shiota, N. et al. (2004). Regulatory roles for APJ, a seven-transmembrane receptor related to angiotensin-type 1 receptor in blood pressure in vivo. *J Biol Chem* **279**, 26274-9.
- Isogai, S., Horiguchi, M. and Weinstein, B. M. (2001). The vascular anatomy of the developing zebrafish: an atlas of embryonic and early larval development. *Dev Biol* **230**, 278-301.
- Isogai, S., Lawson, N. D., Torrealday, S., Horiguchi, M. and Weinstein, B. M. (2003). Angiogenic network formation in the developing vertebrate trunk. *Development* **130**, 5281-90.
- Jain, R. K. (2003). Molecular regulation of vessel maturation. *Nat Med* **9**, 685-93.
- James, K., Hosking, B., Gardner, J., Muscat, G. E. and Koopman, P. (2003). Sox18 mutations in the ragged mouse alleles ragged-like and opossum. *Genesis* **36**, 1-6.
- Jin, S. W., Beis, D., Mitchell, T., Chen, J. N. and Stainier, D. Y. (2005). Cellular and molecular analyses of vascular tube and lumen formation in zebrafish. *Development* **132**, 5199-209.
- Kalin, R. E., Kretz, M. P., Meyer, A. M., Kispert, A., Heppner, F. L. and Brandli, A. W. (2007). Paracrine and autocrine mechanisms of apelin signaling govern embryonic and tumor angiogenesis. *Dev Biol* **305**, 599-614.
- Kamei, M., Saunders, W. B., Bayless, K. J., Dye, L., Davis, G. E. and Weinstein, B. M. (2006). Endothelial tubes assemble from intracellular vacuoles in vivo. *Nature* **442**, 453-6.
- Kanai-Azuma, M., Kanai, Y., Gad, J. M., Tajima, Y., Taya, C., Kurohmaru, M., Sanai, Y., Yonekawa, H., Yazaki, K., Tam, P. P. et al. (2002). Depletion of definitive gut endoderm in Sox17-null mutant mice. *Development* **129**, 2367-79.
- Karkkainen, M. J., Ferrell, R. E., Lawrence, E. C., Kimak, M. A., Levinson, K. L., McTigue, M. A., Alitalo, K. and Finegold, D. N. (2000). Missense mutations interfere with VEGFR-3 signalling in primary lymphoedema. *Nat Genet* **25**, 153-9.
- Karkkainen, M. J., Haiko, P., Sainio, K., Partanen, J., Taipale, J., Petrova, T. V., Jeltsch, M., Jackson, D. G., Talikka, M., Rauvala, H. et al. (2004). Vascular endothelial growth factor C is required for sprouting of the first lymphatic vessels from embryonic veins. *Nat Immunol* **5**, 74-80.
- Karpanen, T., Egeblad, M., Karkkainen, M. J., Kubo, H., Yla-Herttuala, S., Jaattela, M. and Alitalo, K. (2001). Vascular endothelial growth factor C promotes tumor lymphangiogenesis and intralymphatic tumor growth.

Cancer Res **61**, 1786-90.

Karpanen, T., Wirzenius, M., Makinen, T., Veikkola, T., Haisma, H. J., Achen, M. G., Stacker, S. A., Pytowski, B., Yla-Herttuala, S. and Alitalo, K. (2006). Lymphangiogenic growth factor responsiveness is modulated by postnatal lymphatic vessel maturation. *Am J Pathol* **169**, 708-18.

Kasai, A., Shintani, N., Kato, H., Matsuda, S., Gomi, F., Haba, R., Hashimoto, H., Kakuda, M., Tano, Y. and Baba, A. (2008). Retardation of retinal vascular development in apelin-deficient mice. *Arterioscler Thromb Vasc Biol* **28**, 1717-22.

Kasai, A., Shintani, N., Oda, M., Kakuda, M., Hashimoto, H., Matsuda, T., Hinuma, S. and Baba, A. (2004). Apelin is a novel angiogenic factor in retinal endothelial cells. *Biochem Biophys Res Commun* **325**, 395-400.

Kawakami, K. (2005). Transposon tools and methods in zebrafish. *Dev Dyn* **234**, 244-54.

Kim, I., Saunders, T. L. and Morrison, S. J. (2007). Sox17 dependence distinguishes the transcriptional regulation of fetal from adult hematopoietic stem cells. *Cell* **130**, 470-83.

Kitsukawa, T., Shimizu, M., Sanbo, M., Hirata, T., Taniguchi, M., Bekku, Y., Yagi, T. and Fujisawa, H. (1997). Neuropilin-semaphorin III/D-mediated chemorepulsive signals play a crucial role in peripheral nerve projection in mice. *Neuron* **19**, 995-1005.

Kojima, Y. and Quertermous, T. (2008). Apelin-APJ signaling in retinal angiogenesis. *Arterioscler Thromb Vasc Biol* **28**, 1687-8.

Kokubo, H., Miyagawa-Tomita, S., Nakazawa, M., Saga, Y. and Johnson, R. L. (2005). Mouse hesr1 and hesr2 genes are redundantly required to mediate Notch signaling in the developing cardiovascular system. *Dev Biol* **278**, 301-9.

Kuchler, A. M., Gjini, E., Peterson-Maduro, J., Cancilla, B., Wolburg, H. and Schulte-Merker, S. (2006). Development of the zebrafish lymphatic system requires VEGFC signaling. *Curr Biol* **16**, 1244-8.

Kume, T., Jiang, H., Topczewska, J. M. and Hogan, B. L. (2001). The murine winged helix transcription factors, Foxc1 and Foxc2, are both required for cardiovascular development and somitogenesis. *Genes Dev* **15**, 2470-82.

Labauge, P., Denier, C., Bergametti, F. and Tournier-Lasserre, E. (2007). Genetics of cavernous angiomas. *Lancet Neurol* **6**, 237-44.

Ladomery, M. R., Harper, S. J. and Bates, D. O. (2007). Alternative splicing in angiogenesis: the vascular endothelial growth factor paradigm. *Cancer Lett* **249**, 133-42.

Lamont, R. E. and Childs, S. (2006). MAPping out arteries and veins. *Sci STKE* **2006**, pe39.

Landry, J. R., Kinston, S., Knezevic, K., Donaldson, I. J., Green, A. R. and Gottgens, B. (2005). Fli1, Elf1, and Ets1 regulate the proximal promoter of the LMO2 gene in endothelial cells. *Blood* **106**, 2680-7.

Larrivee, B., Freitas, C., Suchting, S., Brunet, I. and Eichmann, A. (2009). Guidance of vascular development: lessons from the nervous system. *Circ Res* **104**, 428.

Larson, J. D., Wadman, S. A., Chen, E., Kerley, L., Clark, K. J., Eide, M., Lippert, S., Nasevicius, A., Ekker, S. C., Hackett, P. B. et al. (2004). Expression of VE-cadherin in zebrafish embryos: a new tool to evaluate vascular development. *Dev Dyn* **231**, 204-13.

Laskin, J. J. and Sandler, A. B. (2005). First-line treatment for advanced non-small-cell lung cancer. *Oncology (Williston Park)* **19**, 1671-6; discussion 1678-80.

Lawson, N. D., Mugford, J. W., Diamond, B. A. and Weinstein, B. M. (2003). phospholipase C gamma-1 is required downstream of vascular endothelial growth factor during arterial development. *Genes Dev* **17**, 1346-51.

Lawson, N. D., Scheer, N., Pham, V. N., Kim, C. H., Chitnis, A. B., Campos-Ortega, J. A. and Weinstein, B. M. (2001). Notch signaling is required for arterial-venous differentiation during embryonic vascular development. *Development* **128**, 3675-83.

Lawson, N. D., Vogel, A. M. and Weinstein, B. M. (2002). sonic hedgehog and vascular endothelial growth factor act upstream of the Notch pathway during arterial endothelial differentiation. *Dev Cell* **3**, 127-36.

Lawson, N. D. and Weinstein, B. M. (2002a). Arteries and veins: making a difference with zebrafish. *Nat Rev Genet* **3**, 674-82.

Lawson, N. D. and Weinstein, B. M. (2002b). In vivo imaging of embryonic vascular development using transgenic zebrafish. *Dev Biol* **248**, 307-18.

Lee, D., Park, C., Lee, H., Lugus, J. J., Kim, S. H., Arentson, E., Chung, Y. S., Gomez, G., Kyba, M., Lin, S. et al. (2008). ER71 acts downstream of BMP, Notch, and Wnt signaling in blood and vessel progenitor specification. *Cell Stem Cell* **2**, 497-507.

- Lee, M. E., Temizer, D. H., Clifford, J. A. and Quertermous, T. (1991). Cloning of the GATA-binding protein that regulates endothelin-1 gene expression in endothelial cells. *J Biol Chem* **266**, 16188-92.
- Lee, P., Goishi, K., Davidson, A. J., Mannix, R., Zon, L. and Klagsbrun, M. (2002). Neuropilin-1 is required for vascular development and is a mediator of VEGF-dependent angiogenesis in zebrafish. *Proc Natl Acad Sci U S A* **99**, 10470-5.
- Leslie, J. D., Ariza-McNaughton, L., Bermange, A. L., McAdow, R., Johnson, S. L. and Lewis, J. (2007). Endothelial signalling by the Notch ligand Delta-like 4 restricts angiogenesis. *Development* **134**, 839-44.
- Li, J. L. and Harris, A. L. (2009). Crosstalk of VEGF and Notch pathways in tumour angiogenesis: therapeutic implications. *Front Biosci* **14**, 3094-110.
- Li, W., Camargo, P. H. C., Au, L., Zhang, Q., Rycenga, M. and Xia, Y. (2009). Etching and Dimerization: A Simple and Versatile Route to Dimers of Silver Nanospheres with a Range of Sizes. *Angew Chem Int Ed Engl*.
- Liang, D., Chang, J. R., Chin, A. J., Smith, A., Kelly, C., Weinberg, E. S. and Ge, R. (2001). The role of vascular endothelial growth factor (VEGF) in vasculogenesis, angiogenesis, and hematopoiesis in zebrafish development. *Mech Dev* **108**, 29-43.
- Lin, F. J., Tsai, M. J. and Tsai, S. Y. (2007). Artery and vein formation: a tug of war between different forces. *EMBO Rep* **8**, 920-4.
- Liu, F. and Patient, R. (2008). Genome-wide analysis of the zebrafish ETS family identifies three genes required for hemangioblast differentiation or angiogenesis. *Circ Res* **103**, 1147-54.
- Lorent, K., Yeo, S.-Y., Oda, T., Chandrasekharappa, S., Chitnis, A., Matthews, R. P. and Pack, M. (2004). Inhibition of Jagged-mediated Notch signaling disrupts zebrafish biliary development and generates multi-organ defects compatible with an Alagille syndrome phenocopy. *Development* **131**, 5753.
- Lu, X., Le Noble, F., Yuan, L., Jiang, Q., De Lafarge, B., Sugiyama, D., Breant, C., Claes, F., De Smet, F., Thomas, J.-L. et al. (2004). The netrin receptor UNC5B mediates guidance events controlling morphogenesis of the vascular system. *Nature* **432**, 179.
- Lusis, A. J. (2000). Atherosclerosis. *Nature* **407**, 233-41.
- Lyons, M. S., Bell, B., Stainier, D. and Peters, K. G. (1998). Isolation of the zebrafish homologues for the tie-1 and tie-2 endothelium-specific receptor tyrosine kinases. *Dev Dyn* **212**, 133-40.
- Makinen, T., Adams, R. H., Bailey, J., Lu, Q., Ziemiecki, A., Alitalo, K., Klein, R. and Wilkinson, G. A. (2005). PDZ interaction site in ephrinB2 is required for the remodeling of lymphatic vasculature. *Genes Dev* **19**, 397.
- Makinen, T., Jussila, L., Veikkola, T., Karpanen, T., Kettunen, M. I., Pulkkanen, K. J., Kauppinen, R., Jackson, D. G., Kubo, H., Nishikawa, S. et al. (2001). Inhibition of lymphangiogenesis with resulting lymphedema in transgenic mice expressing soluble VEGF receptor-3. *Nat Med* **7**, 199-205.
- Makita, T., Suvoc, H. M., Garipey, C. E., Yanagisawa, M. and Ginty, D. D. (2008). Endothelins are vascular-derived axonal guidance cues for developing sympathetic neurons. *Nature* **452**, 759.
- Martyn, U. and Schulte-Merker, S. (2004). Zebrafish neuropilins are differentially expressed and interact with vascular endothelial growth factor during embryonic vascular development. *Dev Dyn* **231**, 33-42.
- Masri, B., Knibiehler, B. and Audigier, Y. (2005). Apelin signalling: a promising pathway from cloning to pharmacology. *Cell Signal* **17**, 415-26.
- Meili, R., Ellsworth, C., Lee, S., Reddy, T. B., Ma, H. and Firtel, R. A. (1999). Chemoattractant-mediated transient activation and membrane localization of Akt/PKB is required for efficient chemotaxis to cAMP in Dictyostelium. *Embo J* **18**, 2092-105.
- Meng, X., Noyes, M. B., Zhu, L. J., Lawson, N. D. and Wolfe, S. A. (2008). Targeted gene inactivation in zebrafish using engineered zinc-finger nucleases. *Nat Biotechnol* **26**, 695-701.
- Milan, D. J., Giokas, A. C., Serluca, F. C., Peterson, R. T. and MacRae, C. A. (2006). Notch1b and neuregulin are required for specification of central cardiac conduction tissue. *Development* **133**, 1125.
- Mukoyama, Y.-s., Shin, D., Britsch, S., Taniguchi, M. and Anderson, D. J. (2002). Sensory nerves determine the pattern of arterial differentiation and blood vessel branching in the skin. *Cell* **109**, 693.
- Narumiya, H., Hidaka, K., Shirai, M., Terami, H., Aburatani, H. and Morisaki, T. (2007). Endocardiogenesis in embryoid bodies: novel markers identified by gene expression profiling. *Biochem Biophys Res Commun* **357**, 896-902.
- Nasevicius, A. and Ekker, S. C. (2000). Effective targeted gene 'knockdown' in zebrafish. *Nat Genet* **26**, 216-20.
- Nasevicius, A., Larson, J. and Ekker, S. C. (2000). Distinct requirements for zebrafish angiogenesis revealed by a VEGF-A morphant. *Yeast* **17**, 294-301.

- Neufeld, G., Cohen, T., Gengrinovitch, S. and Poltorak, Z.** (1999). Vascular endothelial growth factor (VEGF) and its receptors. *Faseb J* **13**, 9-22.
- Noguera-Troise, I., Daly, C., Papadopoulos, N. J., Coetzee, S., Boland, P., Gale, N. W., Lin, H. C., Yancopoulos, G. D. and Thurston, G.** (2006). Blockade of Dll4 inhibits tumour growth by promoting non-productive angiogenesis. *Nature* **444**, 1032-7.
- Ny, A., Koch, M., Schneider, M., Neven, E., Tong, R. T., Maity, S., Fischer, C., Plaisance, S., Lambrechts, D., Heligon, C. et al.** (2005). A genetic *Xenopus laevis* tadpole model to study lymphangiogenesis. *Nat Med* **11**, 998.
- O'Neill, C. F., Urs, S., Cinelli, C., Lincoln, A., Nadeau, R. J., Leon, R., Toher, J., Mouta-Bellum, C., Friesel, R. E. and Liaw, L.** (2007). Notch2 signaling induces apoptosis and inhibits human MDA-MB-231 xenograft growth. *Am J Pathol* **171**, 1023-36.
- Ober, E. A., Olofsson, B., Makinen, T., Jin, S. W., Shoji, W., Koh, G. Y., Alitalo, K. and Stainier, D. Y.** (2004). Vegfc is required for vascular development and endoderm morphogenesis in zebrafish. *EMBO Rep* **5**, 78-84.
- Oliver, G. and Srinivasan, R. S.** (2008). Lymphatic vasculature development: current concepts. *Ann N Y Acad Sci* **1131**, 75-81.
- Olsson, A. K., Dimberg, A., Kreuger, J. and Claesson-Welsh, L.** (2006). VEGF receptor signalling - in control of vascular function. *Nat Rev Mol Cell Biol* **7**, 359-71.
- Ota, H., Katsube, K., Ogawa, J. and Yanagishita, M.** (2007). Hypoxia/Notch signaling in primary culture of rat lymphatic endothelial cells. *FEBS Lett* **581**, 5220-6.
- Papanicolaou, K. N., Izumiya, Y. and Walsh, K.** (2008). Forkhead transcription factors and cardiovascular biology. *Circ Res* **102**, 16-31.
- Parsons, M. J., Pisharath, H., Yusuff, S., Moore, J. C., Siekmann, A. F., Lawson, N. and Leach, S. D.** (2009). Notch-responsive cells initiate the secondary transition in larval zebrafish pancreas. *Mech Dev* **126**, 898.
- Patterson, L. J., Gering, M. and Patient, R.** (2005). Scl is required for dorsal aorta as well as blood formation in zebrafish embryos. *Blood* **105**, 3502-11.
- Pendeville, H., Winandy, M., Manfroid, I., Nivelles, O., Motte, P., Pasque, V., Peers, B., Struman, I., Martial, J. A. and Voz, M. L.** (2008). Zebrafish Sox7 and Sox18 function together to control arterial-venous identity. *Dev Biol* **317**, 405-16.
- Pennisi, D., Gardner, J., Chambers, D., Hosking, B., Peters, J., Muscat, G., Abbott, C. and Koopman, P.** (2000). Mutations in Sox18 underlie cardiovascular and hair follicle defects in ragged mice. *Nat Genet* **24**, 434-7.
- Petrova, T. V., Bono, P., Holthoner, W., Chesnes, J., Pytowski, B., Sihto, H., Laakkonen, P., Heikkila, P., Joensuu, H. and Alitalo, K.** (2008). VEGFR-3 expression is restricted to blood and lymphatic vessels in solid tumors. *Cancer Cell* **13**, 554-6.
- Petrova, T. V., Makinen, T., Makela, T. P., Saarela, J., Virtanen, I., Ferrell, R. E., Finegold, D. N., Kerjaschki, D., Yla-Herttuala, S. and Alitalo, K.** (2002). Lymphatic endothelial reprogramming of vascular endothelial cells by the Prox-1 homeobox transcription factor. *Embo J* **21**, 4593.
- Pham, V. N., Lawson, N. D., Mugford, J. W., Dye, L., Castranova, D., Lo, B. and Weinstein, B. M.** (2007). Combinatorial function of ETS transcription factors in the developing vasculature. *Dev Biol* **303**, 772-83.
- Phng, L. K. and Gerhardt, H.** (2009). Angiogenesis: a team effort coordinated by notch. *Dev Cell* **16**, 196-208.
- Risau, W.** (1997). Mechanisms of angiogenesis. *Nature* **386**, 671-4.
- Risau, W. and Flamme, I.** (1995). Vasculogenesis. *Annu Rev Cell Dev Biol* **11**, 73-91.
- Roca, C. and Adams, R. H.** (2007). Regulation of vascular morphogenesis by Notch signaling. *Genes Dev* **21**, 2511-24.
- Roman, B. L., Pham, V. N., Lawson, N. D., Kulik, M., Childs, S., Lekven, A. C., Garrity, D. M., Moon, R. T., Fishman, M. C., Lechleider, R. J. et al.** (2002). Disruption of *acvr1l1* increases endothelial cell number in zebrafish cranial vessels. *Development* **129**, 3009-19.
- Roman, B. L. and Weinstein, B. M.** (2000). Building the vertebrate vasculature: research is going swimmingly. *Bioessays* **22**, 882-93.
- Ross, R.** (1993). The pathogenesis of atherosclerosis: a perspective for the 1990s. *Nature* **362**, 801-9.
- Saharinen, P., Ekman, N., Sarvas, K., Parker, P., Alitalo, K. and Silvennoinen, O.** (1997). The Bmx tyrosine kinase induces activation of the Stat signaling pathway, which is specifically inhibited by protein kinase Cdelta. *Blood* **90**, 4341-53.
- Sainson, R. C. A. and Harris, A. L.** (2007). Anti-Dll4 therapy: can we block tumour growth by increasing angiogenesis? *Trends Mol Med* **13**, 389.
- Sakamoto, Y., Hara, K., Kanai-Azuma, M., Matsui, T., Miura, Y., Tsunekawa, N., Kurohmaru, M., Saijoh, Y., Koopman, P. and Kanai, Y.** (2007). Redundant roles of

- Sox17 and Sox18 in early cardiovascular development of mouse embryos. *Biochem Biophys Res Commun* **360**, 539-44.
- Santoro, M. M., Pesce, G. and Stainier, D. Y.** (2009). Characterization of vascular mural cells during zebrafish development. *Mech Dev* **126**, 638-49.
- Sasaki, A. T. and Firtel, R. A.** (2006). Regulation of chemotaxis by the orchestrated activation of Ras, PI3K, and TOR. *Eur J Cell Biol* **85**, 873-95.
- Schonbeck, U., Sukhova, G. K., Shimizu, K., Mach, F. and Libby, P.** (2000). Inhibition of CD40 signaling limits evolution of established atherosclerosis in mice. *Proc Natl Acad Sci U S A* **97**, 7458-63.
- Schweisguth, F.** (2004). Regulation of notch signaling activity. *Curr Biol* **14**, R129-38.
- Scott, I. C., Masri, B., D'Amico, L. A., Jin, S. W., Jungblut, B., Wehman, A. M., Baier, H., Audigier, Y. and Stainier, D. Y.** (2007). The g protein-coupled receptor agr1b regulates early development of myocardial progenitors. *Dev Cell* **12**, 403-13.
- Sehnert, A. J., Huq, A., Weinstein, B. M., Walker, C., Fishman, M. and Stainier, D. Y.** (2002). Cardiac troponin T is essential in sarcomere assembly and cardiac contractility. *Nat Genet* **31**, 106-10.
- Selkoe, D. and Kopan, R.** (2003). Notch and Presenilin: regulated intramembrane proteolysis links development and degeneration. *Annu Rev Neurosci* **26**, 565-97.
- Seo, S., Fujita, H., Nakano, A., Kang, M., Duarte, A. and Kume, T.** (2006). The forkhead transcription factors, Foxc1 and Foxc2, are required for arterial specification and lymphatic sprouting during vascular development. *Dev Biol* **294**, 458-70.
- Servant, G., Weiner, O. D., Herzmark, P., Balla, T., Sedat, J. W. and Bourne, H. R.** (2000). Polarization of chemoattractant receptor signaling during neutrophil chemotaxis. *Science* **287**, 1037-40.
- Shalaby, F., Ho, J., Stanford, W. L., Fischer, K. D., Schuh, A. C., Schwartz, L., Bernstein, A. and Rossant, J.** (1997). A requirement for Flk1 in primitive and definitive hematopoiesis and vasculogenesis. *Cell* **89**, 981-90.
- Shawber, C. J., Funahashi, Y., Francisco, E., Vorontchikhina, M., Kitamura, Y., Stowell, S. A., Borisenko, V., Feirt, N., Podgrabska, S., Shiraishi, K. et al.** (2007). Notch alters VEGF responsiveness in human and murine endothelial cells by direct regulation of VEGFR-3 expression. *J Clin Invest* **117**, 3369.
- Shawber, C. J. and Kitajewski, J.** (2008). Arterial regulators taken up by lymphatics. *Lymphat Res Biol* **6**, 139.
- Shibuya, M.** (2006). Differential roles of vascular endothelial growth factor receptor-1 and receptor-2 in angiogenesis. *J Biochem Mol Biol* **39**, 469-78.
- Shiojima, I. and Walsh, K.** (2002). Role of Akt signaling in vascular homeostasis and angiogenesis. *Circ Res* **90**, 1243-50.
- Siekman, A. F. and Lawson, N. D.** (2007). Notch signalling limits angiogenic cell behaviour in developing zebrafish arteries. *Nature* **445**, 781-4.
- Simard, A., Di Pietro, E., Young, C. R., Plaza, S. and Ryan, A. K.** (2006). Alterations in heart looping induced by overexpression of the tight junction protein Claudin-1 are dependent on its C-terminal cytoplasmic tail. *Mech Dev* **123**, 210-27.
- Smithers, L., Haddon, C., Jiang, Y. J. and Lewis, J.** (2000). Sequence and embryonic expression of deltaC in the zebrafish. *Mech Dev* **90**, 119-23.
- Soker, S., Takashima, S., Miao, H. Q., Neufeld, G. and Klagsbrun, M.** (1998). Neuropilin-1 is expressed by endothelial and tumor cells as an isoform-specific receptor for vascular endothelial growth factor. *Cell* **92**, 735-45.
- Song, H.-D., Sun, X.-J., Deng, M., Zhang, G.-W., Zhou, Y., Wu, X.-Y., Sheng, Y., Chen, Y., Ruan, Z., Jiang, C.-L. et al.** (2004). Hematopoietic gene expression profile in zebrafish kidney marrow. *Proc Natl Acad Sci U S A* **101**, 16240.
- Sorensen, L. K., Brooke, B. S., Li, D. Y. and Urness, L. D.** (2003). Loss of distinct arterial and venous boundaries in mice lacking endoglin, a vascular-specific TGFbeta coreceptor. *Dev Biol* **261**, 235-50.
- Sorli, S. C., Le Gonidec, S., Knibiehler, B. and Audigier, Y.** (2007). Apelin is a potent activator of tumour neoangiogenesis. *Oncogene* **26**, 7692-9.
- Sorli, S. C., van den Berghe, L., Masri, B., Knibiehler, B. and Audigier, Y.** (2006). Therapeutic potential of interfering with apelin signalling. *Drug Discov Today* **11**, 1100-6.
- Stainier, D. Y., Weinstein, B. M., Detrich, H. W., 3rd, Zon, L. I. and Fishman, M. C.** (1995). Cloche, an early acting zebrafish gene, is required by both the endothelial and hematopoietic lineages. *Development* **121**, 3141-50.
- Suchting, S., Freitas, C., le Noble, F., Benedito, R., Breant, C., Duarte, A. and Eichmann, A.** (2007).

- The Notch ligand Delta-like 4 negatively regulates endothelial tip cell formation and vessel branching. *Proc Natl Acad Sci U S A* **104**, 3225-30.
- Sumanas, S., Gomez, G., Zhao, Y., Park, C., Choi, K. and Lin, S.** (2008). Interplay among Etsrp/ER71, Scl, and Alk8 signaling controls endothelial and myeloid cell formation. *Blood* **111**, 4500-10.
- Sumanas, S., Joraniak, T. and Lin, S.** (2005). Identification of novel vascular endothelial-specific genes by the microarray analysis of the zebrafish cloche mutants. *Blood* **106**, 534-41.
- Sumanas, S. and Lin, S.** (2006). Ets1-related protein is a key regulator of vasculogenesis in zebrafish. *PLoS Biol* **4**, e10.
- Suri, C., Jones, P. F., Patan, S., Bartunkova, S., Maisonpierre, P. C., Davis, S., Sato, T. N. and Yancopoulos, G. D.** (1996). Requisite role of angiopoietin-1, a ligand for the TIE2 receptor, during embryonic angiogenesis. *Cell* **87**, 1171-80.
- Swift, M. R. and Weinstein, B. M.** (2009). Arterial-venous specification during development. *Circ Res* **104**, 576-88.
- Szeto, D. P., Griffin, K. J. P. and Kimelman, D.** (2002). HrT is required for cardiovascular development in zebrafish. *Development* **129**, 5093.
- Tammela, T., Saaristo, A., Lohela, M., Morisada, T., Tornberg, J., Norrmen, C., Oike, Y., Pajusola, K., Thurston, G., Suda, T. et al.** (2005). Angiopoietin-1 promotes lymphatic sprouting and hyperplasia. *Blood* **105**, 4642.
- Tammela, T., Zarkada, G., Wallgard, E., Murtomaki, A., Suchting, S., Wirzenius, M., Waltari, M., Hellstrom, M., Schomber, T., Peltonen, R. et al.** (2008). Blocking VEGFR-3 suppresses angiogenic sprouting and vascular network formation. *Nature* **454**, 656-60.
- Theodosiou, A., Arhondakis, S., Baumann, M. and Kossida, S.** (2009). Evolutionary scenarios of Notch proteins. *Mol Biol Evol* **26**, 1631.
- Thisse, B., Pflumio, S., Fürthauer, M., Loppin, B., Heyer, V., Degrave, A., Woehl, R., Lux, A., Steffan, T., Charbonnier, X.Q., et al.** (2001). Expression of the zebrafish genome during embryogenesis. In *ZFIN Direct Data Submission* (<http://zfin.org>), (ed).
- Thisse, C. and Thisse, B.** (2008). High-resolution in situ hybridization to whole-mount zebrafish embryos. *Nat Protoc* **3**, 59-69.
- Thisse, C. and Zon, L. I.** (2002). Organogenesis--heart and blood formation from the zebrafish point of view. *Science* **295**, 457-62.
- Thomas, M. and Augustin, H. G.** (2009). The role of the Angiopoietins in vascular morphogenesis. *Angiogenesis* **12**, 125-37.
- Thompson, M. A., Ransom, D. G., Pratt, S. J., MacLennan, H., Kieran, M. W., Detrich, H. W., 3rd, Vail, B., Huber, T. L., Paw, B., Brownlie, A. J. et al.** (1998). The cloche and spadetail genes differentially affect hematopoiesis and vasculogenesis. *Dev Biol* **197**, 248-69.
- Thurston, G.** (2003). Role of Angiopoietins and Tie receptor tyrosine kinases in angiogenesis and lymphangiogenesis. *Cell Tissue Res* **314**, 61-8.
- Thurston, G., Noguera-Troise, I. and Yancopoulos, G. D.** (2007). The Delta paradox: DLL4 blockade leads to more tumour vessels but less tumour growth. *Nat Rev Cancer* **7**, 327-31.
- Thurston, G. and Yancopoulos, G. D.** (2001). Gridlock in the blood. *Nature* **414**, 163-4.
- Torres-Vazquez, J., Gitler, A. D., Fraser, S. D., Berk, J. D., Van, N. P., Fishman, M. C., Childs, S., Epstein, J. A. and Weinstein, B. M.** (2004). Semaphorin-plexin signaling guides patterning of the developing vasculature. *Dev Cell* **7**, 117-23.
- Trinh, L. A. and Stainier, D. Y.** (2004). Fibronectin regulates epithelial organization during myocardial migration in zebrafish. *Dev Cell* **6**, 371-82.
- Tucker, B., Hepperle, C., Kortschak, D., Rainbird, B., Wells, S., Oates, A. C. and Lardelli, M.** (2007). Zebrafish Angiotensin II Receptor-like 1a (agtr1a) is expressed in migrating hypoblast, vasculature, and in multiple embryonic epithelia. *Gene Expr Patterns* **7**, 258-65.
- Urness, L. D., Sorensen, L. K. and Li, D. Y.** (2000). Arteriovenous malformations in mice lacking activin receptor-like kinase-1. *Nat Genet* **26**, 328-31.
- van Nieuw Amerongen, G. P. and van Hinsbergh, V. W.** (2001). Cytoskeletal effects of rho-like small guanine nucleotide-binding proteins in the vascular system. *Arterioscler Thromb Vasc Biol* **21**, 300-11.
- Veikkola, T., Jussila, L., Makinen, T., Karpanen, T., Jeltsch, M., Petrova, T. V., Kubo, H., Thurston, G., McDonald, D. M., Achen, M. G. et al.** (2001). Signalling via vascular endothelial growth factor receptor-3 is sufficient for lymphangiogenesis in transgenic mice. *Embo J* **20**, 1223-31.
- Visvader, J. E., Fujiwara, Y. and Orkin, S. H.** (1998). Unsuspected role for the T-cell leukemia protein SCL/tal-1 in vascular development. *Genes Dev* **12**, 473-9.

- Vogeli, K. M., Jin, S. W., Martin, G. R. and Stainier, D. Y.** (2006). A common progenitor for haematopoietic and endothelial lineages in the zebrafish gastrula. *Nature* **443**, 337-9.
- Weber, G. J., Choe, S. E., Dooley, K. A., Paffett-Lugassy, N. N., Zhou, Y. and Zon, L. I.** (2005). Mutant-specific gene programs in the zebrafish. *Blood* **106**, 521-30.
- Weinmaster, G.** (2000). Notch signal transduction: a real rip and more. *Curr Opin Genet Dev* **10**, 363-9.
- Weinstein, B. M., Stemple, D. L., Driever, W. and Fishman, M. C.** (1995). Gridlock, a localized heritable vascular patterning defect in the zebrafish. *Nat Med* **1**, 1143-7.
- Wick, N., Saharinen, P., Saharinen, J., Gurnhofer, E., Steiner, C. W., Raab, I., Stokic, D., Giovanoli, P., Buchsbaum, S., Burchard, A. et al.** (2007). Transcriptomal comparison of human dermal lymphatic endothelial cells ex vivo and in vitro. *Physiol Genomics* **28**, 179.
- Wienholds, E., Schulte-Merker, S., Walderich, B. and Plasterk, R. H.** (2002). Target-selected inactivation of the zebrafish rag1 gene. *Science* **297**, 99-102.
- Wigle, J. T., Harvey, N., Detmar, M., Lagutina, I., Grosveld, G., Gunn, M. D., Jackson, D. G. and Oliver, G.** (2002). An essential role for Prox1 in the induction of the lymphatic endothelial cell phenotype. *Embo J* **21**, 1505-13.
- Williams, C. K., Li, J.-L., Murga, M., Harris, A. L. and Tosato, G.** (2006). Up-regulation of the Notch ligand Delta-like 4 inhibits VEGF-induced endothelial cell function. *Blood* **107**, 931.
- Wolfe, M. S., Xia, W., Ostaszewski, B. L., Diehl, T. S., Kimberly, W. T. and Selkoe, D. J.** (1999). Two transmembrane aspartates in presenilin-1 required for presenilin endoproteolysis and gamma-secretase activity. *Nature* **398**, 513.
- Wong, K. S., Proulx, K., Rost, M. S. and Sumanas, S.** (2009). Identification of vasculature-specific genes by microarray analysis of Etsrp/Etv2 overexpressing zebrafish embryos. *Dev Dyn* **238**, 1836-50.
- Yamashita, J., Itoh, H., Hirashima, M., Ogawa, M., Nishikawa, S., Yurugi, T., Naito, M., Nakao, K. and Nishikawa, S.** (2000). Flk1-positive cells derived from embryonic stem cells serve as vascular progenitors. *Nature* **408**, 92-6.
- Yamazaki, T., Yoshimatsu, Y., Morishita, Y., Miyazono, K. and Watabe, T.** (2009). COUP-TFII regulates the functions of Prox1 in lymphatic endothelial cells through direct interaction. *Genes Cells* **14**, 425.
- Yancopoulos, G. D., Klagsbrun, M. and Folkman, J.** (1998). Vasculogenesis, angiogenesis, and growth factors: ephrins enter the fray at the border. *Cell* **93**, 661-4.
- Yang, X. Y., Yao, J. H., Cheng, L., Wei, D. W., Xue, J. L. and Lu, D. R.** (2003). Molecular cloning and expression of a smooth muscle-specific gene SM22alpha in zebrafish. *Biochem Biophys Res Commun* **312**, 741-6.
- Yaniv, K., Isogai, S., Castranova, D., Dye, L., Hitomi, J. and Weinstein, B. M.** (2006). Live imaging of lymphatic development in the zebrafish. *Nat Med* **12**, 711-6.
- You, L. R., Lin, F. J., Lee, C. T., DeMayo, F. J., Tsai, M. J. and Tsai, S. Y.** (2005). Suppression of Notch signalling by the COUP-TFII transcription factor regulates vein identity. *Nature* **435**, 98-104.
- Young, N., Hahn, C. N., Poh, A., Dong, C., Wilhelm, D., Olsson, J., Muscat, G. E., Parsons, P., Gamble, J. R. and Koopman, P.** (2006). Effect of disrupted SOX18 transcription factor function on tumor growth, vascularization, and endothelial development. *J Natl Cancer Inst* **98**, 1060-7.
- Zeng, X. X., Wilm, T. P., Sepich, D. S. and Solnica-Krezel, L.** (2007). Apelin and its receptor control heart field formation during zebrafish gastrulation. *Dev Cell* **12**, 391-402.
- Zhang, C., Basta, T. and Klymkowsky, M. W.** (2005). SOX7 and SOX18 are essential for cardiogenesis in Xenopus. *Dev Dyn* **234**, 878-91.
- Zhong, T. P., Rosenberg, M., Mohideen, M. A., Weinstein, B. and Fishman, M. C.** (2000). gridlock, an HLH gene required for assembly of the aorta in zebrafish. *Science* **287**, 1820-4.

Samenvatting in het Nederlands

Hart- en vaatziekten vormen naast kanker de belangrijkste doodsoorzaak in de westerse wereld. Om deze ziektes beter te kunnen bestrijden is het van belang om beter te begrijpen hoe zulke ziektes ontstaan. Hiertoe wordt veel onderzoek gedaan naar de normale functie van hart- en bloedvaten, maar ook naar wat er mis kan gaan, zoals tijdens aderverkalking. Binnen dit onderzoek hebben we de vraag hoe bloedvaten ontstaan centraal gesteld. Meer specifiek hebben we gekeken welk deel van het erfelijk materiaal betrokken is bij de aanmaak van nieuwe bloedvaten, en wat de functie van specifieke delen van dit erfelijk materiaal binnen dit proces is.

Elk levend organisme bestaat uit cellen, die erfelijke informatie bevatten, opgeslagen in het DNA. Het DNA is het genetisch materiaal wat nodig is voor de aanmaak van eiwitten. Elk eiwit wordt afgeleid van een specifiek deel van aaneengesloten DNA, ook wel een gen genoemd. Naar schatting bevat het menselijke DNA zo'n 25.000 genen. Niet al deze genen zijn tegelijkertijd actief binnen één cel. Zo wordt het onderscheid tussen bijvoorbeeld een zenuwcel, een bloedcel en een huidcel bepaald door welke combinatie van genen actief is binnen deze cellen. Voor heel veel eiwitten, en dus ook genen, kan een gelijkwaardige kopie worden gevonden wanneer de mens met soortgelijke organismen wordt vergeleken. Zo delen zebrafissen ongeveer 75% van het erfelijk materiaal met mensen, terwijl onze gemeenschappelijke voorouders alweer zo'n 300 miljoen jaar geleden leefden. Dit komt omdat essentiële levensprocessen, zoals de aanleg van het hart- en bloedvaten systeem, zo belangrijk zijn dat de genen betrokken bij dit proces bewaard zijn gebleven gedurende de evolutie. Gezien de grote genetische overeenkomsten tussen verschillende organismen kunnen sommige soorten worden ingezet als modelorganisme voor de mens in wetenschappelijk onderzoek, zoals ook de zebrafis. Een volwassen zebrafis wordt ongeveer 3 à 4 cm groot en wordt gekenmerkt door het typische strepenpatroon dat over zijn lijf loopt. Gezien de geringe grootte van de zebrafis is het mogelijk om tegen relatief lage kosten grote aantallen te houden. Zebrafissen worden geslachtsrijp na 2 à 3 maanden en een volwassen zebrafis vrouwtje kan tot soms wel 1000 eitjes per legsel produceren. Het feit dat deze eitjes zich buiten de moeder ontwikkelen, tezamen met de transparantie van de zebrafisembryo maakt het tot een ideaal systeem voor de visualisatie van verschillende ontwikkelingsprocessen. Daarnaast ontwikkelt een zebrafisembryo zich razendsnel; al een dag na bevruchting van de eicel heeft het embryo een kloppend hart en circuleert er bloed door de bloedvaten. Dankzij deze redenen is sinds drie decennia de zebrafis in zwang als klein modelorganisme voor wetenschappelijk onderzoek. Binnen dit onderzoek zetten wij de zebrafis in voor de bestudering van de genetische regulatie van de ontwikkeling van bloedvaten.

In **hoofdstuk 2** beschrijven we een nieuwe methode voor het ontdekken en beschrijven van onbekende genen die een rol spelen in de ontwikkeling van het bloedvatstelsel. Hiertoe hebben we cellen uit de bloedvatwand van muizenembryo's geïsoleerd, om vervolgens te analyseren welke genen actief zijn (tot expressie komen) in deze cellen. Voor deze genen hebben we bekeken of ze ook actief zijn in de vaatwand van de zebrafis. Zodra we vonden

dat dit het geval was, gingen we over tot de functionele karakterisatie van het betreffende gen. Dit hebben we gedaan door deze genen één voor één uit te schakelen. De defecten die ontstaan in de vorming van het bloedvatstelsel nadat een gen wordt uitgeschakeld geven een aanwijzing over de functie van dit gen in de natuurlijke situatie.

In **hoofdstuk 3** wordt de functie van de genen *sox7* en *sox18* bestudeerd. Deze twee genen behoren tot dezelfde klasse van genen en zijn beide actief op eenzelfde locatie binnen het bloedvatenstelsel. Simultane uitschakeling van deze genen in zebrafisembryo's heeft tot gevolg dat er haast geen circulatie van bloed meer tot stand komt. Dit ondanks het feit dat er normale hoeveelheden bloed worden gevormd en dat het hart normale contractiliteit vertoont. Tegelijkertijd hebben we kunnen aantonen dat deze embryo's fusies van de aders en slagaders vertonen (zogenaamde *shunts*), wat verklaart waarom het bloed vroegtijdig richting het hart terugvloeit of zelfs helemaal niet in circulatie komt. Analyse van een aantal genen dat betrokken is bij de segregatie van aders en slagaders (zogenaamde *arterioveneuze differentiatie*) toonde aan dat de expressie van arteriële genen binnen de aorta na uitschakeling van *sox7* en *sox18* sterk gereduceerd was. Anderzijds bleek de expressie van veneuze genen nu ook aanwezig te zijn binnen de aorta. Hiermee hebben we kunnen aantonen dat *sox7* en *sox18* een essentiële rol vervullen in het aansturen van de expressie van genen die de arterioveneuze differentiatie van bloedvaten controleren. In zowel muizen als mensen leiden defecten in *Sox18* functie tot vergelijkbare vasculaire afwijkingen. Zo heeft men elders aangetoond dat *hypotrichosis-lymphedema-telangiectasia* (HLT), een ziektebeeld gekenmerkt door haarverlies, lymfe- en bloedvatdefecten, wordt veroorzaakt door defecten in *SOX18*. Onze bevindingen tonen aan dat een defect in de arterioveneuze differentiatie van de bloedvaten een mogelijke oorzaak vormt voor de vorming van de telangiectasias in patiënten met HLT.

In **hoofdstuk 4** gaan we in op de uitgroei van de vertakkingen van het bloedvatenstelsel en welke rol het gen *agtr1b* hierin speelt. In onze studie hebben we gevonden dat de vertakkende vaten die normaliter uit de hoofdslagader worden gevormd onvoldoende uitgroeien wanneer *agtr1b* wordt uitgeschakeld. Eerder heeft men al aangetoond dat *agtr1b* wordt aangetrokken door *apelin* als een kompas naald die naar het noorden wordt aangetrokken. Dit *apelin* wordt geproduceerd op de locatie waar de vertakkende vaten naartoe groeien. Wat wij hebben kunnen aantonen is dat de hoeveelheid cellen in deze vertakkende vaten hetzelfde is in vissen waarin *agtr1b* is uitgeschakeld in vergelijking met normale vissen. Het werkelijke defect van deze cellen zit hem in de mate waarin deze zich voortbewegen; zij bewegen veel minder en vertonen ook minder karakteristieken die typerend zijn voor migrerende cellen.

In **hoofdstuk 5** bestuderen we de rol van het gen *dll4* in de aanmaak van lymfevaten. Wat we hebben kunnen aantonen is dat wanneer *dll4* wordt uitgeschakeld, er geen enkel lymfevat wordt aangemaakt. Van lymfevaten is bekend dat ze oorspronkelijk ontstaan vanuit de hoofdader. Wij hebben kunnen aantonen dat de cellen die uit deze hoofdader ontstaan zich niet meer gedragen als lymf cellen, maar juist als bloedvat cellen wanneer *dll4* wordt uitgeschakeld. Als een consequentie van het veranderde karakter van deze oorspronkelijke lymf cellen worden er middels een complex proces van herverbindingen van bloedvaten méér veneuze vaten gevormd ten kosten van het aantal arteriële vaten. Dat lijkt in eerste

instantie een onschuldig iets, maar aangezien we ook voor het eerst hebben aangetoond dat lymfevaten zich consequent langs een arterieel vat vormen, heeft dit desastreuze gevolgen. De geijkte paden waarlangs deze lymfevaten zich normaal zouden vormen zijn dus niet, of in lagere aantallen, aanwezig, waardoor eventuele cellen die zich wel als lymf cel gedragen geen normaal lymfevat meer kunnen vormen. Lymfevaten vormen een belangrijke route waarlangs tumoren zich verspreiden (zogenaamde *metastaseringen*). Een manier om de spreiding van tumoren tegen te gaan is dan ook door de groei van lymfevaten te blokkeren. *Dll4* functie wordt al in soortgelijke behandelingen geblokkeerd om de bloedvatgroei naar tumoren te remmen. Onze bevindingen suggereren dat *Dll4* ook een aantrekkelijke kandidaat vormt om lymfvat groei naar tumoren te blokkeren.

Tenslotte beschrijven we in **hoofdstuk 6** hoe het gen *dll4* een rol speelt bij de regulering van *flt4/vegfc* signalering in arteriën. Het feit dat één en hetzelfde gen (*dll4* in dit geval) meerdere functies kan vervullen vormt een mooie illustratie van hoe de natuur effectief met haar middelen omspringt. *Flt4* is een gen dat specifiek een rol speelt in de bloedvatwand. *Flt4* kan echter pas normaal functioneren nadat het geactiveerd is, door in dit geval *vegfc*, dat specifiek bindt aan *flt4*. Wanneer bepaalde cellen *vegfc* uitscheiden, zullen de bloedvaten hierop reageren via *flt4* (ook wel *flt4/vegfc* signalering genoemd). Wat we hebben kunnen aantonen is dat de wildgroei van bloedvaten die plaatsvindt wanneer *dll4* is uitgeschakeld wordt opgeheven zodra ook *flt4/vegfc* signalering wordt onderdrukt. Wanneer we *vegfc* voortijdig introduceren terwijl *dll4* is uitgeschakeld vinden we dat de arteriële bloedvaten hierop reageren door extra materiaal te produceren. De arteriële bloedvaten zijn dus als ware gevoelig geworden voor *vegfc* wanneer *dll4* afwezig is. Hieruit hebben we kunnen concluderen dat een van de functies van *dll4* is om *flt4/vegfc* signalering in arteriën te onderdrukken. Deze bevinding biedt interessante perspectieven voor de bestrijding van tumoren. Zo scheiden tumoren stoffen uit (o.a. *Vegfc*) die de groei van bloed- en lymfevaten naar de tumor bevorderen, wat de groei en spreiding van de tumor weer bevordert. Sinds enige jaren probeert men de groei van tumoren te remmen door de groei van bloedvaten naar de tumor te verhinderen. *Dll4* is een geschikte kandidaat gebleken om de bloedvatgroei te remmen. Onze bevindingen suggereren dat tumoren die *Vegfc* uitscheiden een verhoogde gevoeligheid zullen vertonen wanneer een tumor wordt behandeld met *Dll4* remmers.

Dit onderzoek heeft een sterk fundamenteel karakter, dat er aanvankelijk op uit is de kennis en begripsvorming rondom de aanleg van het cardiovasculaire stelsel te vergroten. Zulk soort fundamenteel onderzoek vormt soms een directe basis voor verder geneeskundig onderzoek. Zo is bijvoorbeeld het erfelijkheidsonderzoek erop gericht om te bepalen of iemand een erfelijke aanleg heeft voor een ziekte en of die aanleg ook bij andere familieleden voorkomt. Genetisch onderzoek zoals dat beschreven is in dit proefschrift kan leiden tot de ontdekking van nieuwe genen die, wanneer er fouten in optreden, de oorzaak vormen voor het ontstaan van erfelijke cardiovasculaire ziektes. Tevens biedt dergelijk onderzoek een basis voor de bestrijding van bepaalde tumoren, door hun groei en verspreiding tegen te gaan. Anderzijds kan de kennis over de groei van bloedvaten worden ingezet om bloedvatvorming te stimuleren. Zo zouden mensen erbij gebaat zijn als na hartfalen de doorbloeding van de hartspier gestimuleerd zou worden, zodat de hartspierfunctie weer genormaliseerd wordt.

Dankwoord / Acknowledgements

Promoveren doe je niet alleen, en zonder de hulp van een groot aantal mensen was het waarschijnlijk ook niet zo soepel verlopen. Ik wil iedereen die geholpen heeft bij de totstandkoming van dit werk bedanken, maar een aantal mensen wil ik hier in het bijzonder noemen.

Als eerste wil ik graag mijn (co-)promotoren bedanken. Prof.dr. Duncker, ik wil u graag bedanken voor alle hulp en ondersteuning bij het gereed komen van mijn proefschrift. Zeer veel dank gaat natuurlijk uit naar jou, Eric. Je hebt me vier jaar geleden dit project toevertrouwd en daar ben ik je zeer erkentelijk voor. Jouw brede oriëntatie op het wetenschappelijke vlak plus de durf om zaken in een groter perspectief te plaatsen heb ik altijd zeer inspirerend gevonden. De fysieke afstand tussen Rotterdam en Utrecht mocht dan soms beperkingen opleveren, desondanks hebben we er een aantal mooie publicaties uit weten te slepen! Stefan, I would also like to express my sincere gratitude towards you for enabling me to pursue my PhD in your lab. I've learned a lot about politics and effective leadership from you. Moreover, your enthusiasm and extensive knowledge on a broad range of subjects has been invaluable to me in finishing my PhD.

Tijdens de vier jaren die ik op het Hubrecht Instituut heb doorgebracht heb ik ook veel steun van en aangename momenten met mijn labgenoten gehad, in het bijzonder met mijn (oud)-kamergenoten Kirsten, Frank, Jeroen en Ben. Kirsten, ik kon me natuurlijk geen betere collega wensen dan jij om naast te zitten. Bedankt voor al je vrolijkheid, het is zo nu en dan zeker op me overgesprongen! Frank, samen op zoek naar ES-tags en clones, maar ook samen de piste af tijdens Keystone, ik vond het in ieder geval fantastisch. Succes met het afronden van jouw onderzoek. Jeroen, jouw plezier in en kennis van de biologie in zijn geheel waren soms jaloersmakend, maar vooral heb je er heel veel mensen mee weten te helpen, waaronder ondergetekende. Het ga je goed in Münster. Ben, you've been a great pal and an awesome colleague during my PhD. I've really enjoyed your enthusiasm, useful discussions and all the help you gave me with all the various projects. I wish you all the best for your own lab!

Bedankt aan alle andere (ex-)collega's van het Schulte-Merker lab: Josi voor allerlei praktische hulp en het leren van nieuwe technieken; Evisa for all the excitement at the bench; Ellen & Ive haast onafscheidelijk, maar wat een team; bone people, Chrissy, Leonie and Jo, you're all off to a splendid future; Merlijn, bedankt voor al je hulp bij immuno's en wat niet meer; Joëlle, je was een geweldige student, succes bij Ben; en alle anderen, bedankt voor alle hulp en de aangename sfeer binnen en buiten het lab. Hetzelfde geldt natuurlijk voor alle collega's van het lab Experimentele Cardiologie te Rotterdam, bedankt voor de prettige samenwerking!

In het bijzonder wil ik Esther hier graag noemen, zonder wiens werk en hulp dit project niet zomaar van start had kunnen gaan.

Menig ander persoon binnen het Hubrecht wil ik ook graag bedanken, Jeroen Korving voor alle prachtige coupes. Erma, Mark, Rob, Mark en Bert voor het toezien op het welzijn van al die vissen. De dames en een eventuele herder van het Bakkers-lab en Tijsterman-lab voor allerlei uiteenlopende zaken. Mensen van het Cuppen-lab voor alle hulp met sequencing en TILLING, maar vooral voor het dragen van de vrijdagmiddag borrel.

Alle vrienden en familie die buiten het lab voor de nodige niet-wetenschappelijke ondersteuning hebben gezorgd wil ik ook graag bedanken. Het is een verademing om af en toe de dagelijkse sleur te ontsnappen en de nodige relativering te ervaren. Alle vrienden uit Sittard, inmiddels zijn we allen uitgewaaid naar andere oorden, maar om nog steeds een hechte groep vrienden te hebben die naar mijn praatjes over vissen in de blender wil luisteren is fantastisch! Vrienden uit Wageningen bedankt voor alle feestjes, bokbier momenten en andere activiteiten. Mensen uit Utrecht, Anne, Wanda, Erik, Saskia, Jerome, Ellen, Kelly en Ben, bedankt voor alle avonden, etentjes, lange gesprekken aan de toog, feestjes, Movember, ritjes naar Duitsland, vakanties en luie zondagmiddagen! Gwen, kleine chicka, jij mag hier uiteraard ook niet ontbreken :P Tenslotte Jo, Marianne en Bram, lieve ouders en broer, bedankt voor alle steun en toeverlaat en het eindeloze vertrouwen en geduld dat jullie in me stellen!

En als laatste wil ik mijn paranimfen, Anne en Erik bedanken voor het delen van de vier jaar van mijn promotietijd. Supertof dat jullie mijn paranimfen willen zijn, en ik beschouw het dan ook als een grote eer om jullie er aan het einde bij te mogen hebben. Over het welslagen van het feestje hoef ik me in ieder geval geen zorgen te maken!

-Robert-

Curriculum Vitae

Robert Herpers is geboren op 5 juni 1980 te Urmond. In 1998 behaalde hij zijn Gymnasium diploma aan het College te Sittard. Van 1998 tot 2005 studeerde hij Bioprocestechnologie aan de Universiteit van Wageningen. Tijdens zijn studie liep hij stage bij de vakgroep organische chemie onder leiding van Prof.dr. E.J. Sudholter en bij de vakgroep moleculaire biologie onder leiding van Prof.dr. T. Bisseling. Daarnaast liep hij stage bij de genetica afdeling van DSM Delft Food Specialties en de afdeling Plant Pathology van de Universiteit van Californië, Davis (USA) onder leiding van Prof. D. Cook. In november 2005 begon hij met het onderzoek beschreven in dit proefschrift aan het Hubrecht Instituut onder begeleiding van Prof.dr. S. Schulte-Merker en Dr. H.J. Duckers van het Erasmus Medisch Centrum.

Robert Herpers was born on June 5 1980 in Urmond. In 1998 he passed his Gymnasium exam at the College in Sittard. From 1998 to 2005 he was a Bioprocestechnology student at the University of Wageningen. During this time he completed rotations at the department of organic chemistry led by Prof.dr. E.J. Sudholter and the department of molecular biology led by Prof.dr. T. Bisseling. He then successfully completed internships at DSM Delft Food Specialties and the department of Plant Pathology at the University of California, Davis (USA) led by Prof. D. Cook. In November 2005 he initiated the work described in this thesis at the Hubrecht Institute under the supervision of Prof.dr. S. Schulte-Merker and Dr. H.J. Duckers of the Erasmus Medical Centre.

List of Publications

Herpers, R., van de Kamp, E., Duckers*, H. J. and Schulte-Merker*, S. (2008). Redundant roles for sox7 and sox18 in arteriovenous specification in zebrafish. *Circ Res* **102**, 12-5.

Herpers*, R., Hogan*, B. M., Witte, M., Helotera, H., Alitalo, K., Duckers, H. J. and Schulte-Merker, S. (2009). Vegfc/Flt4 signalling is suppressed by Dll4 in developing zebrafish intersegmental arteries. *Development* **136**, 4001.

Herpers*, R., Geudens*, I., Hermans*, K., Segura, I., Ruiz de Almodovar, C., Hogan, B.M., De Smet, F., Vandeveld, W., Bussmann, J., Siekmann, A., Claes, F., Moore, J., Pistocchi, A.S., Loges, S., Mazzone, M., Mariggi, G., Bruyère, F., Cotelli, F., Kerjaschki, D., Noël, A., Foidart, J-M., Gerhardt, H., Ny, A., Langenberg, T., Lawson, N., Duckers, H.J., Schulte-Merker*, S., Carmeliet*, P., and Dewerchin*, M. (2009). Role of Dll4 / Notch in the formation and wiring of the lymphatic network in zebrafish. *Under Review*.

Weijers, C. A., Meeuwse, P., **Herpers, R.**, Franssen, M. C. and Sudholter, E. J. (2005). Stereoselectivity and substrate specificity in the kinetic resolution of methyl-substituted 1-oxaspiro[2.5]octanes by Rhodotorula glutinis epoxide hydrolase. *J Org Chem* **70**, 6639-46.

*Equal contribution

PhD Portfolio

Summary of PhD training and teaching

Name PhD student: **Robert Herpers**
Erasmus MC Department: **Cardiology**
Research School: **COEUR and CGDB (former OOB)**

PhD period: **2005 - 2010**
Promotor(s): **Prof.dr. D.J.G.M. Duncker**
Prof.dr. S. Schulte-Merker
Supervisor: **Dr. H.J. Duckers**

1. PhD training

	Year	Workload (Hours/ ECTS)
General courses		
- Introductory Course CGDB	2006	1.5 ECTS
- Zebrafish in Development, Organogenesis and Disease CGDB	2006	1.5 ECTS
- Introduction to Bioinformatics CGDB	2006	1.5 ECTS
- Molecular biology in cardiovascular research COEUR	2007	1.5 ECTS
- Photoshop Course CGDB	2007	1.0 ECTS
- Developmental Vascular Biology Workshop III CGDB	2008	1.0 ECTS
Seminars and workshops		
- Various COEUR and CGDB research seminars	2005 – 2010	6 ECTS
- PhD Masterclass CGDB	2005 – 2008	2 ECTS
- PhD Retreat CGDB	2006 – 2008	3 ECTS
- PhD training Nederlandse Hartstichting – Vascular Biology	2006	1.5 ECTS
Presentations		
- CGDB seminars – Lunchmeetings	2005 – 2009	2.4 ECTS
- NAI meeting - COEUR	2007	0.6 ECTS
- Keystone Symposium – Angiogenesis and Hypoxia	2007	0.6 ECTS
- Keystone Symposium – Angiogenesis and Lymphangiogenesis in Cancer	2009	0.2 ECTS
- 7 th International Symposium on the Biology of Endothelial Cells	2009	0.6 ECTS
(Inter)national conferences		
- 5 th European Zebrafish Genetics and Development meeting	2007	1 ECTS
- Keystone Symposium – Angiogenesis and Hypoxia	2008	1.5 ECTS
- 2 nd Dutch Zebrafish Meeting	2008	1 ECTS
- Keystone Symposium – Angiogenesis and Lymphangiogenesis in Cancer	2009	1.5 ECTS
- 7 th International Symposium on the Biology of Endothelial Cells	2009	1.5 ECTS

2. Teaching

	Year	Workload (Hours/ ECTS)
Lecturing		
- Molecular biology in cardiovascular research	2007	0.2 ECTS
- COEUR Research Seminar - Neo-Angiogenesis as a treatment of myocardial ischemia	2009	0.2 ECTS
Supervising Master's theses		
- Master's Student	2005-2006	1.5 ECTS
- Master's Student	2009	3.0 ECTS